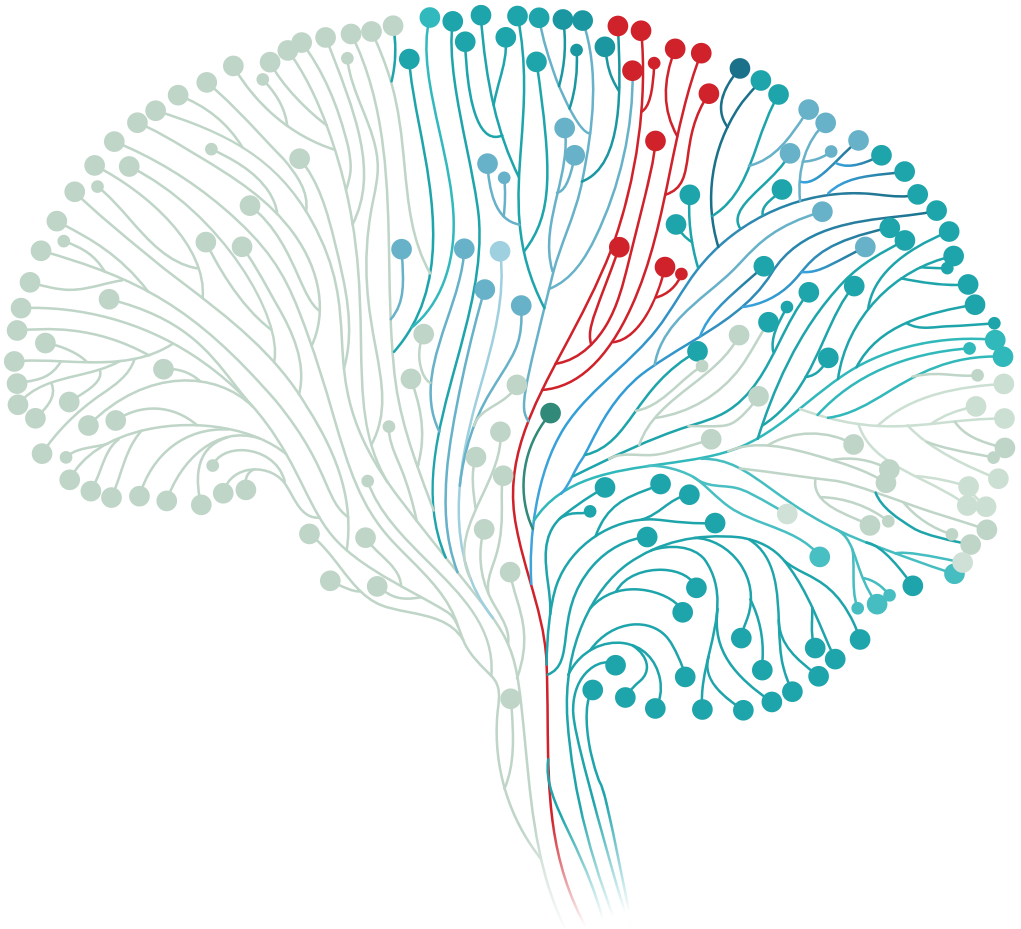


PROGNOSIS IN GLIOBLASTOMA

A clinical and translational approach



UMC Utrecht Brain Center

Sharon Berendsen

PROGNOSIS IN GLIOBLASTOMA

A clinical and translational approach

Sharon Berendsen

Cover image adapted from Shutterstock

Layout and design by Joppe Klein, persoonlijkproefschrift.nl

Printed by Ipskamp Printing, proefschriften.net

ISBN: 978-94-028-1854-3

© 2019 Sharon Berendsen

The research in this thesis was financially supported by the T. & P. Bohnenn fund for neuro-oncological research, Stichting StopHersentumoren.nl, the Belgian Ministry of Health, FNRS Belgium, the Belgian foundation against cancer, The National Cancer Institute (USA).

The printing of this thesis was financially supported by the UMC Utrecht Brain Center and Chipsoft B.V.

Prognosis in glioblastoma

A clinical and translational approach

Prognose van glioblastomen

Een klinisch en translationeel onderzoek

(met een samenvatting in het Nederlands)

Proefschrift

ter verkrijging van de graad van doctor aan de Universiteit Utrecht
op gezag van de rector magnificus, prof.dr. H.R.B.M. Kummeling,
ingevolge het besluit van het college voor promoties in het openbaar te
verdedigen op dinsdag 14 januari 2020 des middags te 4.15 uur

door

Sharon Berendsen

geboren op 22 maart 1988
te Rheden

Promotor: Prof. dr. P.A.J.T. Robe

Copromotor: Dr. T.J. Snijders

TABLE OF CONTENTS

Chapter 1.	General introduction & thesis outline	7
Chapter 2.	Valproic acid for the treatment of malignant gliomas: review of the preclinical rationale and published clinical results	23
Chapter 3.	Effects of valproic acid on HDAC inhibition <i>in vitro</i> and in glioblastoma patient samples	75
Chapter 4.	Prognostic relevance of epilepsy at presentation in glioblastoma patients	93
Chapter 5.	Epilepsy associates with decreased HIF-1 α /STAT5b signaling in glioblastoma	121
Chapter 6.	Adverse prognosis of glioblastoma contacting the subventricular zone: biological correlates	141
Chapter 7.	Glioblastomas within the subventricular zone are region-specific enriched for mesenchymal transition markers: an intratumoral gene expression analysis	173
Chapter 8.	Fractal structure correlates with oxidative metabolic pathway gene expression signature in glioblastoma	197
Chapter 9.	General discussion & Recommendations	217
Appendices.	Nederlandse samenvatting	232
	Curriculum vitae	238
	List of publications	239
	Dankwoord	241





CHAPTER 1

General introduction & thesis outline

Sharon Berendsen, Tom J. Snijders & Pierre A. Robe

Glioblastoma (World Health Organization (WHO) grade IV) is the most common and most malignant primary brain tumor. It still remains an incurable disease with a poor prognosis, despite an extensive treatment regimen [1]. Although the prognosis remains poor, a minority of the patients survives for several years. Others survive no more than a few months and do not seem to benefit from the extensive treatment. The identification of patients with a relatively longer or shorter prognosis would be very helpful in clinical decision making, individualized patient information and treatment. To this end, several prognostic factors have been explored in recent years. In addition, prognostic associations might shed light on specific underlying tumor biological mechanisms, which could result in new therapeutic approaches.

The aim of this thesis is to identify clinical and radiological prognostic factors in glioblastoma patients and to explore associations with tumor biology. These associations might provide explanations for the observed prognostic effects and might provide new directions for treatment development.

In this chapter, I introduce the current clinical aspects of diagnosis and treatment in glioblastoma. For this introduction, I follow the sequence of events that characterize the glioblastoma patient's journey: starting at epidemiology and first symptoms and ending in treatment and prognosis. Subsequently, the outline of this thesis is presented.

Epidemiology

Glioblastoma is the most common and most malignant primary brain tumor with an incidence of 2.5 per 100,000 persons in the Netherlands [2]. The disease occurs slightly more in men compared to women (incidence rates 3.2 versus 1.9 per 100,000), and the median age at diagnosis is 61 years [2].

Glioblastomas, and other adult diffuse gliomas (WHO grades II – IV), are progressive tumors of the brain that are characterized by diffuse infiltrative growth into healthy brain tissue. Despite many scientific efforts, these tumors exhibit a high degree of resistance to available antitumor treatments. Glioblastomas still remain incurable, and come with a poor prognosis. The median overall survival of glioblastoma patients approximates 12-16 months, despite extensive treatment with surgery, chemotherapy and radiotherapy [1, 3]. After this combined treatment, approximately 25-30% of patients survives beyond 2 years, and less than 10% survives for more than 5 years [1, 2].

Clinical symptoms

A glioblastoma has an enormous impact on the lives of patients and their relatives. Not only is a glioblastoma an oncological disease, it is also a disease of the brain, resulting in specific neurological symptoms. Based on the location of the tumor, patients can

experience several focal neurological deficits, such as paresis, or dysphasia. In addition, many patients suffer from cognitive deficits or behavioral alterations. During the course of the disease, approximately 30-60% of glioblastoma patients will experience one or more epileptic seizures [4]. Glioblastomas are tumors that are mostly fast-growing and generally develop within several weeks or months. This aggressive behavior can result in symptoms of elevated intracranial pressure, such as headache, vomiting, and/or visual disturbances.

Glioma-associated epilepsy

In 30-40% of patients, an epileptic seizure is a first symptom of the underlying glioblastoma [5-7]. In patients with lower grade gliomas, epileptic seizures are even more prevalent. In the case of glioma patients, seizures are a symptom of underlying brain disease, and most often of focal onset, sometimes with impairment of consciousness and sometimes with involvement to a bilateral tonic-clonic seizure. Glioma-associated epilepsy presents an extra burden on the quality of life of patients, as reports suggest that the prevalence of drug-resistant epilepsy is high in glioma patients, with estimates between 24% to 87% depending on the study population and study type [8-10], in comparison to an estimated 20% of patients who become pharmacoresistant across all types of epilepsy [11]. Other clinical observations further distinguish glioma-associated epilepsy from other types of epilepsy. In low grade glioma patients, seizure recurrence after initial seizure control has been associated with tumor progression [12]. Some patients with epilepsy experience a status epilepticus, which is defined as an ongoing seizure for more than 30 minutes (in case of a generalized tonic-clonic seizure) [13]. In patients with brain tumors (including gliomas), status epilepticus is associated with higher mortality, longer durations and a higher rate of neurological deficits [14].

Several factors may contribute to seizures in glioma patients. Alterations in tumor biology, such as altered expression of drug targets or resistance proteins, are suggested to increase pharmacoresistance to anti-epileptic drugs [15]. In glioma-associated epilepsy, effective tumor treatment – regardless of treatment modality – may contribute to seizure control. In these patients, tumor treatment is also epilepsy treatment [16, 17]. Specifically, surgery contributes to seizure control in many patients [12], however, the epileptogenic zone may extend beyond the tumor boundaries in about 1/3 of patients [18].

Several hypotheses on epileptogenesis in brain tumors have been suggested, but the exact mechanisms remain unclear and are probably multifactorial, as reviewed by De Groot [15]. In high-grade tumors, abrupt tissue damage leading to necrosis and hemosiderin deposition are thought to contribute to epileptogenicity [19]. In lower grade tumors functional alterations in gap junction proteins, ion channels and transporters and receptors are associated with the development of seizures [15]. Although in low grade gliomas, mutations of isocitrate dehydrogenase 1 or 2 (IDH1 or IDH2) are associated with higher

rates of glioma-associated seizures [20], this association was not found in higher-grade gliomas [21]. Mutant IDH leads to an excess of the oncometabolite 2-hydroxyglutarate (2HG), which is structurally similar to the neurotransmitter glutamate [22]. Excess release of glutamate by gliomas can induce epilepsy. Furthermore, changes in the perilesional neuronal network as well as whole brain connectivity have been linked to glioma-associated epilepsy [15].

It has been hypothesized that glioma patients with seizures may have a more favorable prognosis [23], but this was contradicted by others [24-27] and the potential mechanisms that would explain such a survival advantage remain speculative. Interestingly, one of the possible explanations of this effect was thought to result from the treatment of glioblastoma patients with anti-epileptic drugs. In several *in vitro* studies and retrospective clinical studies, a potential survival benefit by the anti-epileptic drug valproic acid (VPA) has been suggested. It has been shown that VPA can inhibit tumor cell growth and alter resistance to treatment *in vitro*, presumably through inhibition of histone deacetylases (HDAC) and alteration of expression of several key transcription factors, such as NF- κ B, STAT3/5, p53, and TCF/ β -catenin [28-32]. In retrospective clinical series, a correlation between VPA and survival in glioblastoma patients has been suggested [6, 33, 34].

Radiological findings in glioblastoma

Magnetic resonance imaging (MRI) is the principal radiological technique for diagnosis and follow-up in glioblastoma. These tumors show a radiologically heterogeneous appearance, with geographically irregular tumor margins and central necrotic or cystic areas. A key radiological feature of glioblastomas is contrast enhancement as a sign of contrast leakage from the damaged blood-brain barrier vessels.

Glioblastomas mostly arise in the supratentorial brain, and can involve all areas and lobes [35, 36]. Some studies suggest that glioblastomas show a predominance in regions close to the subventricular zone (SVZ, Figure 1) [35]. This region, which lines the lateral ventricles in the brain, has been shown to harbor neural stem cells [37], and has gained increasing attention in glioblastoma research. The SVZ region has been suggested to be the region of origin of glioblastomas [38, 39], and the place where tumor cells can escape treatment and favor tumor recurrence [40, 41]. Several studies have implied that glioblastomas contacting the SVZ are associated with a worse prognosis [42, 43].

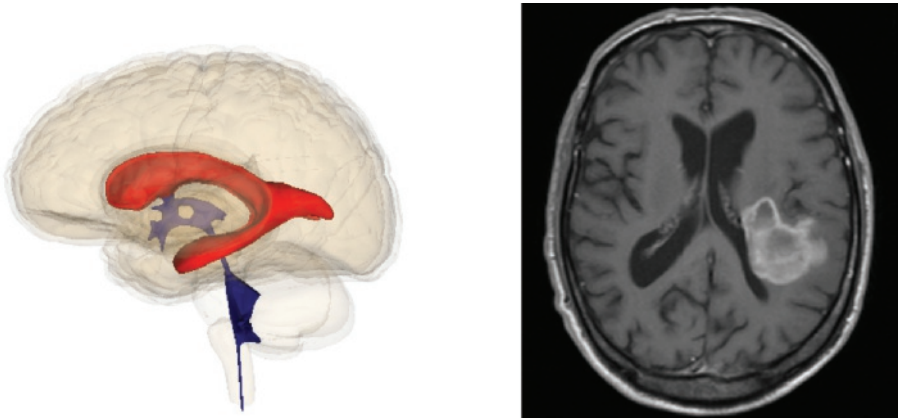


Figure 1 – A. The subventricular zone (SVZ) lines the lateral ventricles (red) of the brain. Image obtained and adapted from Anatomography Life Science Databases under the Creative Commons Attribution share alike 2.1 Japan licence.
B. Contrast-enhancing region of glioblastoma on T1 weighted MRI scan contacts the SVZ.

Tissue is the issue: pathology and classification of diffuse gliomas

The histopathological examination is the golden standard for the diagnosis of glioblastoma. The World Health Organization (WHO) initiated an international classification system for human tumors in 1956, as an objective to uniformly classify and grade tumors worldwide. Clearly defined histopathological and clinical diagnostic criteria obviously contribute to optimal patient care worldwide, but are also of paramount importance for the conduction of research at an international level. Since the publication of the first classification criteria for tumors of the nervous system in 1979, regular updates have followed that incorporated the newest scientific insights. For decades, the histopathological characteristics of the tumor were decisive for its classification. Diffuse gliomas were categorized based on their phenotype, as either astrocytic, oligodendroglial or mixed (oligoastrocytic) [44]. In addition, a grading system was applied based on morphological features of a more aggressive behavior, such as increased cellularity, marked cytological atypia, high mitotic activity, microvascular proliferation and necrosis. It was already noted that most glioblastomas develop without any evidence of a less aggressive precursor tumor (primary glioblastomas), and some originate from a lower grade glioma (secondary glioblastomas). In earlier WHO classifications, it was also already introduced that some histological phenotypes are associated with specific tumor-associated genetic alterations. For instance, oligodendroglial tumors were known to show loss of the short arm on chromosome 1 (1p), and the long arm of chromosome 19 (19q), and became the first brain tumors for which routine molecular genetic analysis was performed in clinical practice [45].

In 2016, the latest update of the WHO classification system of Tumors of the Central Nervous System was published [46]. In this version, recent advances in knowledge on

the genetic basis of the tumorigenesis in the diffuse glioma subgroups [47, 48] has led to the development of a layered diagnostic approach in which both histopathological and genotypic parameters are integrated in the classification of the tumor. This resulted in a major restructuring of the classification system and glioma classes that were used until then. For instance, the categories of gliomatosis cerebri and oligoastrocytic tumors have been abandoned. The developments in the WHO classification system in the past decade are shown in figure 2.

For the classification of glioblastoma, WHO grade IV, the most important development is the introduction of the routine analysis of the mutation status of isocitrate dehydrogenase 1 or 2 (IDH1 or IDH2). Approximately 90% of glioblastomas have an IDH-wildtype genotype, which highly corresponds to a *de novo*, or primary glioblastoma. Mutation of IDH1 or IDH2, which occurs in almost 10% of cases and most often involves the IDH1 R132H mutation, is highly associated with a secondary glioblastoma with a history of prior lower grade glioma [46]. A distinctive and nearly invariable feature of IDH mutant gliomas is the glioma CpG island methylator phenotype (G-CIMP) [49]. Mutation of IDH and the G-CIMP phenotype are strong favorable prognostic factors in glioblastoma [49-51].

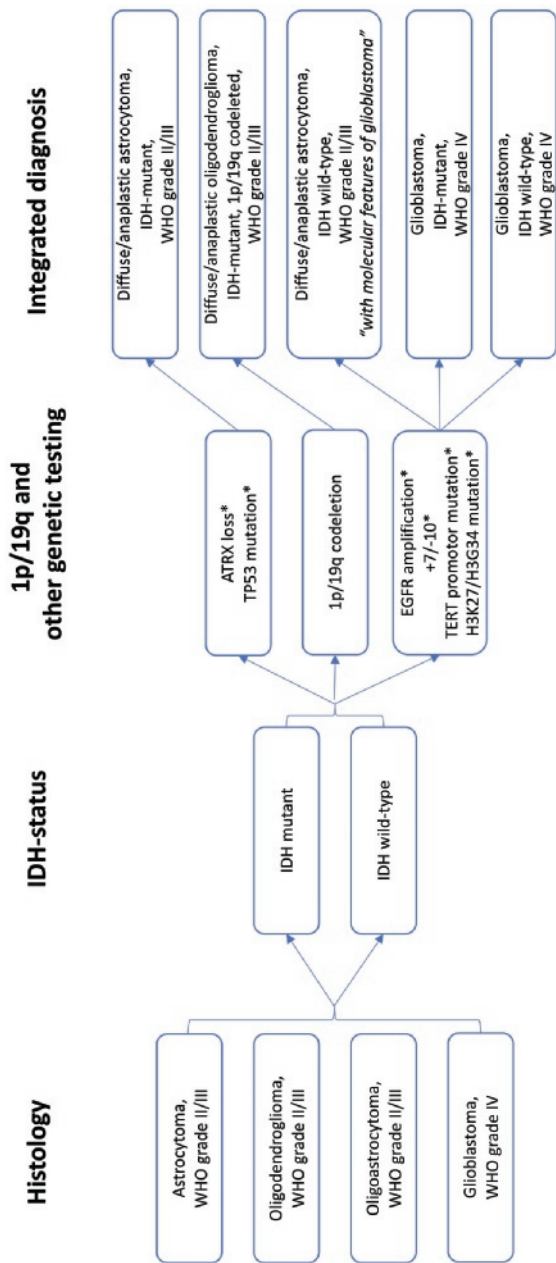


Figure 2 – Incorporation of histologic and genetic tumor features results in an integrated diagnosis of gliomas. According to the WHO 2016 classification of central nervous system tumors (Louis), histology is combined with genetic characteristics of the tumor to form an integrated diagnosis. The diagnostic process starts with histology, and combined with IDH- and 1p/19q-status gliomas can be classified. Some genetic alterations (marked with *) are not required for the diagnosis but contribute to a specific classification. In some cases when molecular testing is not available or inconclusive, gliomas are classified based on their histological appearance and termed 'Not otherwise specified (NOS)'.

It has been shown that some tumors that are histologically graded as diffuse (WHO grade II) or anaplastic astrocytoma (WHO grade III) also present an IDH-wildtype genotype. In several studies, these IDH-wildtype astrocytomas were associated with similar (poor) prognoses as IDH-wildtype glioblastomas [52]. However, other glial tumor types, such as ganglioglioma, pilocytic astrocytoma, pleomorphic xanthoastrocytoma, are also IDH-wildtype and present a more favorable prognosis. Therefore, additional molecular analyses are advised to correctly identify IDH-wildtype diffuse or anaplastic gliomas that will behave similar to an IDH-wildtype glioblastoma [52]. The presence of EGFR amplification, combined gain of chromosome 7 and loss of chromosome 10 or TERT promoter mutation in IDH-wildtype diffuse astrocytic gliomas of WHO grade II or III are associated with significantly shorter patient survival compared to patients with other WHO grade II or III gliomas, and clinical outcomes comparable to patients with IDH-wildtype glioblastoma [53-55]. These tumors are now termed diffuse astrocytic glioma, IDH-wildtype, with molecular features of glioblastoma, WHO grade IV [52].

Common transcriptomic alterations in glioblastoma

Glioblastomas are characterized by multiple heterogeneous genomic and transcriptomic alterations, as was extensively detailed by Brennan et al. [48], after multidimensional analyses of more than 500 glioblastoma samples from The Tumor Genome Atlas (TCGA). Pathways that are typically altered in glioblastoma include the Rb pathway, the p53 pathway and the PI3K pathway. EGFR signaling is usually altered by various alterations at the DNA and RNA level [48]. Specific gene expression patterns in glioblastoma were previously categorized into distinct transcriptomic molecular subclasses (proneural, neural, classical and mesenchymal) [56]. Later, tumor methylation profiles were linked to these subclasses as well, and the glioma CpG island methylator phenotype (G-CIMP) was associated with an increased rate of the proneural subtype and better prognosis [48, 49].

Current glioblastoma treatment strategies

Surgery is a key element of the treatment of glioblastoma, and necessary for the tissue diagnosis. Although large-scale randomized studies on the effects of surgery are lacking, gross total resection is associated with a longer overall survival [57-59]. For decades, radiotherapy has been the standard of care in glioblastoma treatment, which has significantly prolonged patient survival [60].

A randomized phase III trial by the European Organisation for Research and Treatment of Cancer (EORTC) and National Cancer Institute of Canada Clinical Trials Group (NCIC) showed an increase in overall survival for glioblastoma patients treated with concomitant and adjuvant temozolomide combined with radiotherapy, compared to radiotherapy alone. This combined treatment regimen is still the only treatment for glioblastoma that has proven such an undisputed survival benefit [1] and has since then been standard of care

for most patients with a newly diagnosed glioblastoma aged under 70 and with a good clinical performance status [61].

In a phase III-trial, addition of tumor-treating fields (TTF) to adjuvant TMZ in patients with a *de novo* glioblastoma increased PFS and OS by several months [62]. The incorporation of this treatment modality in clinical practice has been hampered by its high costs as well as the absence of confirmatory trial results [63-66].

Older patients that are not considered eligible for the combined modality treatment, are generally treated with either hypofractionated radiotherapy or temozolomide monotherapy. This treatment decision is based on the methylation status of the O6-methylguanine DNA methyltransferase (MGMT) promotor. This gene encodes a DNA repair gene with resistance to alkylating chemotherapy. Methylation of the MGMT promotor region in the tumor tissue has been shown to predict response to temozolomide and was associated with improved survival compared to glioblastoma patients with MGMT promotor methylated tumors treated with radiotherapy alone [67, 68].

After the diagnosis: outlook on glioblastoma prognosis

As described above, glioblastoma is an incurable disease. Although the median overall survival ranges between 12-16 months from diagnosis [1, 3], about 25-30% of patients survives for more than 2 years, with a minority surviving past 5 years, as described above. The variability in the prognosis of glioblastoma patients makes it difficult for the clinician to inform patients about their individual prognosis. The identification of patients with a relatively longer or shorter prognosis would be very helpful in clinical counseling. To this end, several prognostic factors have been explored in recent years. In addition, although prognostic research only shows associations, and does not imply etiology, prognostic factors might shed light on specific underlying oncogenic mechanisms, which could result in new therapeutic approaches.

A comprehensive prognostic analysis by Gorlia et al. in the cohort of 573 patients with a newly diagnosed glioblastoma from the randomized trial that compared treatment with either radiotherapy alone or combined temozolomide and radiotherapy [1] led to the development of a prognosis nomogram for patients with newly diagnosed glioblastoma [69]. In this study, several clinical prognostic factors in glioblastoma patients were established: combined temozolomide and radiotherapy treatment, extent of surgery, age, WHO performance status, corticosteroids at randomization, MMSE score, tumor location (unilobar or central/multilobar) and MGMT promotor hypermethylation status [69]. In other studies, other survival prediction models were developed, and included among others Karnofsky Performance Status (KPS), preoperative motor or language deficits, periventricular location (SVZ), IDH mutation and gender [70-74]. Currently, none of

these models is extensively used in clinical practice, as comparative studies have shown that the current models are not exceptionally specific or accurate yet [75, 76].

THESIS OUTLINE

In this thesis, I investigate associations between clinical and radiological factors and prognosis in glioblastoma patients. Subsequently, correlations between tumor biological mechanisms and each of these factors are explored, which could aid in further understanding of the biology of glioblastomas and may offer new treatment directions.

This thesis starts with an exploration of the prognostic role of epileptic seizures and the use of anti-epileptic drugs at diagnosis in glioblastoma. A review of the literature providing preclinical and clinical support for the antitumor effects of the anti-epileptic drugs valproic acid (VPA) is provided in **chapter 2**. Following earlier reports, *in vitro* effects of VPA on inhibition of histone deacetylase are confirmed in **chapter 3**. In this chapter, the effects of VPA on histone acetylation are also explored in tumor samples from patients who were treated with VPA. Following these observations, in **chapter 4** I describe the results of a retrospective prognostic cohort study, which focuses on the prognostic roles of epileptic seizures at presentation of a glioblastoma as well as treatment with VPA. The scientific discussion that resulted from this paper is reflected in a subsequent Reply to a Letter to the editor, which is included as well. In **chapter 5**, the gene and protein expression signatures that correlate with epileptic seizures at presentation in glioblastoma are explored.

From **chapter 6** onwards, the focus lies on radiological factors, and their correlation with prognosis and tumor biology in glioblastoma. The independent prognostic role of contact of the glioblastoma to the SVZ is explored in **chapter 6**, and this prognostic effect is further analyzed by correlations with several patient- and tumor-related factors, such as tumor volume, postoperative complications, and gene and protein expression patterns. In addition to this chapter, the association between intratumoral gene expression patterns and the SVZ microenvironment in glioblastomas that contact the SVZ is explored in **chapter 7**.

In **chapter 8**, the fractal structure of volumetric contrast enhancement pattern in glioblastoma is analyzed, and correlated to the tumor's metabolism.

Chapter 9 contains a general discussion, in which the results and coherence of the several chapters is detailed. I conclude by providing recommendations for investigators and clinicians, based on the work described in this thesis.

REFERENCES

1. Stupp, R., et al., Effects of radiotherapy with concomitant and adjuvant temozolomide versus radiotherapy alone on survival in glioblastoma in a randomised phase III study: 5-year analysis of the EORTC-NCIC trial. *Lancet Oncol*, 2009. 10(5): p. 459-66.
2. Ho, V.K., et al., Changing incidence and improved survival of gliomas. *European journal of cancer (Oxford, England : 1990)*, 2014. 50(13): p. 2309-2318.
3. Ostrom, Q.T., et al., CBTRUS Statistical Report: Primary Brain and Other Central Nervous System Tumors Diagnosed in the United States in 2011-2015. *Neuro Oncol*, 2018. 20(suppl_4): p. iv1-iv86.
4. Ijzerman-Korenvaa, M., et al., Prevalence of symptoms in glioma patients throughout the disease trajectory: a systematic review. *J Neurooncol*, 2018. 140(3): p. 485-496.
5. van Breemen, M.S., E.B. Wilms, and C.J. Vecht, Epilepsy in patients with brain tumours: epidemiology, mechanisms, and management. *Lancet Neurol*, 2007. 6(5): p. 421-30.
6. Kerkhof, M., et al., Effect of valproic acid on seizure control and on survival in patients with glioblastoma multiforme. *Neuro-oncology*, 2013. 15(7): p. 961-967.
7. Snijders, T.J., et al., Glioma-associated epilepsy: toward mechanism-based treatment. *Translational Cancer Research*, 2017. 6(S2): p. S337-S341.
8. Hildebrand, J., et al., Epileptic seizures during follow-up of patients treated for primary brain tumors. *Neurology*, 2005. 65(2): p. 212-5.
9. Neal, A., et al., Postoperative seizure control in patients with tumor-associated epilepsy. *Epilepsia*, 2016. 57(11): p. 1779-1788.
10. You, G., et al., Seizure characteristics and outcomes in 508 Chinese adult patients undergoing primary resection of low-grade gliomas: a clinicopathological study. *Neuro Oncol*, 2012. 14(2): p. 230-41.
11. Picot, M.C., et al., The prevalence of epilepsy and pharmacoresistant epilepsy in adults: a population-based study in a Western European country. *Epilepsia*, 2008. 49(7): p. 1230-8.
12. Chang, E.F., et al., Seizure characteristics and control following resection in 332 patients with low-grade gliomas. *J Neurosurg*, 2008. 108(2): p. 227-35.
13. Trinka, E., et al., A definition and classification of status epilepticus--Report of the ILAE Task Force on Classification of Status Epilepticus. *Epilepsia*, 2015. 56(10): p. 1515-23.
14. Arik, Y., et al., Prognosis and therapy of tumor-related versus non-tumor-related status epilepticus: a systematic review and meta-analysis. *BMC Neurol*, 2014. 14: p. 152.
15. de Groot, M., et al., Epilepsy in patients with a brain tumour: focal epilepsy requires focused treatment. *Brain*, 2012. 135(Pt 4): p. 1002-16.
16. van den Bent, M.J., et al., Long-term efficacy of early versus delayed radiotherapy for low-grade astrocytoma and oligodendroglioma in adults: the EORTC 22845 randomised trial. *Lancet*, 2005. 366(9490): p. 985-90.
17. Koekkoek, J.A., et al., Seizure reduction in a low-grade glioma: more than a beneficial side effect of temozolomide. *J Neurol Neurosurg Psychiatry*, 2015. 86(4): p. 366-73.
18. Gilmore, R., et al., Mirror focus: function of seizure frequency and influence on outcome after surgery. *Epilepsia*, 1994. 35(2): p. 258-63.
19. Riva, M., Brain tumoral epilepsy: a review. *Neurol Sci*, 2005. 26 Suppl 1: p. S40-2.
20. Liubinas, S.V., et al., IDH1 mutation is associated with seizures and protoplasmic subtype in patients with low-grade gliomas. *Epilepsia*, 2014. 55(9): p. 1438-1443.

21. Phan, K., et al., Association Between IDH1 and IDH2 Mutations and Preoperative Seizures in Patients with Low-Grade Versus High-Grade Glioma: A Systematic Review and Meta-Analysis. *World Neurosurg*, 2018. 111: p. e539-e545.
22. Neal, A., et al., IDH1 and IDH2 mutations in postoperative diffuse glioma-associated epilepsy. *Epilepsy Behav*, 2018. 78: p. 30-36.
23. Lote, K., et al., Prevalence and prognostic significance of epilepsy in patients with gliomas. *European journal of cancer (Oxford, England : 1990)*, 1998. 34(1): p. 98-102.
24. Kilpatrick, C., et al., Epilepsy and primary cerebral tumours. *Journal of clinical neuroscience : official journal of the Neurosurgical Society of Australasia*, 1994. 1(3): p. 178-181.
25. Mineo, J.F., et al., Prognosis factors of survival time in patients with glioblastoma multiforme: a multivariate analysis of 340 patients. *Acta Neurochirurgica*, 2007. 149(3): p. 245-52; discussion 252-3.
26. Stark, A.M., et al., Glioblastoma: clinical characteristics, prognostic factors and survival in 492 patients. *Clinical neurology and neurosurgery*, 2012. 114(7): p. 840-845.
27. Rosati, A., et al., Glutamine synthetase expression as a valuable marker of epilepsy and longer survival in newly diagnosed glioblastoma multiforme. *Neuro-oncology*, 2013. 15(5): p. 618-625.
28. Ichiyama, T., et al., Sodium valproate inhibits production of TNF-alpha and IL-6 and activation of NF-kappaB. *Brain research*, 2000. 857(1-2): p. 246-251.
29. Alvarez-Breckenridge, C.A., et al., The histone deacetylase inhibitor valproic acid lessens NK cell action against oncolytic virus-infected glioblastoma cells by inhibition of STAT5/T-BET signaling and generation of gamma interferon. *J Virol*, 2012. 86(8): p. 4566-77.
30. Ni, L., et al., The histone deacetylase inhibitor valproic acid inhibits NKG2D expression in natural killer cells through suppression of STAT3 and HDAC3. *Sci Rep*, 2017. 7: p. 45266.
31. Chen, C.H., et al., Enhancement of temozolomide-induced apoptosis by valproic acid in human glioma cell lines through redox regulation. *J Mol Med (Berl)*, 2011. 89(3): p. 303-15.
32. Jung, G.A., et al., Valproic acid induces differentiation and inhibition of proliferation in neural progenitor cells via the beta-catenin-Ras-ERK-p21Cip/WAF1 pathway. *BMC Cell Biol*, 2008. 9: p. 66.
33. Weller, M., et al., Prolonged survival with valproic acid use in the EORTC/NCIC temozolomide trial for glioblastoma. *Neurology*, 2011. 77(12): p. 1156-1164.
34. Barker, C.A., et al., Valproic acid use during radiation therapy for glioblastoma associated with improved survival. *International journal of radiation oncology, biology, physics*, 2013. 86(3): p. 504-509.
35. Steed, T.C., et al., Differential localization of glioblastoma subtype: implications on glioblastoma pathogenesis. *Oncotarget*, 2016. 7(18): p. 24899-24907.
36. Bohman, L.E., et al., Magnetic resonance imaging characteristics of glioblastoma multiforme: implications for understanding glioma ontogeny. *Neurosurgery*, 2010. 67(5): p. 1319-27; discussion 1327-8.
37. Sanai, N., et al., Unique astrocyte ribbon in adult human brain contains neural stem cells but lacks chain migration. *Nature*, 2004. 427(6976): p. 740-4.
38. Sanai, N., A. Alvarez-Buylla, and M.S. Berger, Neural stem cells and the origin of gliomas. *The New England journal of medicine*, 2005. 353(8): p. 811-822.
39. Lee, J.H., et al., Human glioblastoma arises from subventricular zone cells with low-level driver mutations. *Nature*, 2018. 560(7717): p. 243-247.

40. Goffart, N., et al., CXCL12 mediates glioblastoma resistance to radiotherapy in the subventricular zone. *Neuro Oncol*, 2017. 19(1): p. 66-77.
41. Chen, L., et al., Glioblastoma recurrence patterns near neural stem cell regions. *Radiotherapy and oncology : journal of the European Society for Therapeutic Radiology and Oncology*, 2015. 116(2): p. 294-300.
42. Chaichana, K.L., et al., Relationship of glioblastoma multiforme to the lateral ventricles predicts survival following tumor resection. *J Neurooncol*, 2008. 89(2): p. 219-24.
43. Jungk, C., et al., Location-Dependent Patient Outcome and Recurrence Patterns in IDH1-Wildtype Glioblastoma. *Cancers (Basel)*, 2019. 11(1).
44. Louis, D.N., et al., The 2007 WHO classification of tumours of the central nervous system. *Acta Neuropathol*, 2007. 114(2): p. 97-109.
45. Kleihues, P., et al., The WHO classification of tumors of the nervous system. *J Neuropathol Exp Neurol*, 2002. 61(3): p. 215-25; discussion 226-9.
46. Louis, D.N., et al., The 2016 World Health Organization Classification of Tumors of the Central Nervous System: a summary. *Acta Neuropathol*, 2016. 131(6): p. 803-20.
47. Eckel-Passow, J.E., et al., Glioma Groups Based on 1p/19q, IDH, and TERT Promoter Mutations in Tumors. *N Engl J Med*, 2015. 372(26): p. 2499-508.
48. Brennan, C.W., et al., The somatic genomic landscape of glioblastoma. *Cell*, 2013. 155(2): p. 462-477.
49. Noshmehr, H., et al., Identification of a CpG island methylator phenotype that defines a distinct subgroup of glioma. *Cancer Cell*, 2010. 17(5): p. 510-22.
50. Turcan, S., et al., IDH1 mutation is sufficient to establish the glioma hypermethylator phenotype. *Nature*, 2012. 483(7390): p. 479-83.
51. Baysan, M., et al., G-cimp status prediction of glioblastoma samples using mRNA expression data. *PLoS One*, 2012. 7(11): p. e47839.
52. Brat, D.J., et al., cIMPACT-NOW update 3: recommended diagnostic criteria for "Diffuse astrocytic glioma, IDH-wildtype, with molecular features of glioblastoma, WHO grade IV". *Acta Neuropathol*, 2018. 136(5): p. 805-810.
53. Brat, D.J., et al., Comprehensive, Integrative Genomic Analysis of Diffuse Lower-Grade Gliomas. *N Engl J Med*, 2015. 372(26): p. 2481-98.
54. Aoki, K., et al., Prognostic relevance of genetic alterations in diffuse lower-grade gliomas. *Neuro Oncol*, 2018. 20(1): p. 66-77.
55. Aibaidula, A., et al., Adult IDH wild-type lower-grade gliomas should be further stratified. *Neuro Oncol*, 2017. 19(10): p. 1327-1337.
56. Verhaak, R.G., et al., Integrated genomic analysis identifies clinically relevant subtypes of glioblastoma characterized by abnormalities in PDGFRA, IDH1, EGFR, and NF1. *Cancer cell*, 2010. 17(1): p. 98-110.
57. Sanai, N., et al., An extent of resection threshold for newly diagnosed glioblastomas. *Journal of neurosurgery*, 2011. 115(1): p. 3-8.
58. Vuorinen, V., et al., Debulking or biopsy of malignant glioma in elderly people - a randomised study. *Acta Neurochirurgica*, 2003. 145(1): p. 5-10.
59. Kreth, F.W., et al., Gross total but not incomplete resection of glioblastoma prolongs survival in the era of radiochemotherapy. *Ann Oncol*, 2013. 24(12): p. 3117-23.
60. Laperriere, N., L. Zuraw, and G. Cairncross, Radiotherapy for newly diagnosed malignant glioma in adults: a systematic review. *Radiother Oncol*, 2002. 64(3): p. 259-73.

61. Weller, M., et al., European Association for Neuro-Oncology (EANO) guideline on the diagnosis and treatment of adult astrocytic and oligodendroglial gliomas. *Lancet Oncol*, 2017. 18(6): p. e315-e329.
62. Stupp, R., et al., Effect of Tumor-Treating Fields Plus Maintenance Temozolomide vs Maintenance Temozolomide Alone on Survival in Patients With Glioblastoma: A Randomized Clinical Trial. *Jama*, 2017. 318(23): p. 2306-2316.
63. Sampson, J.H., Alternating Electric Fields for the Treatment of Glioblastoma. *Jama*, 2015. 314(23): p. 2511-3.
64. Chamberlain, M.C., Treatment for Patients With Newly Diagnosed Glioblastoma. *Jama*, 2016. 315(21): p. 2348.
65. Mehta, M., et al., Critical review of the addition of tumor treating fields (TTFields) to the existing standard of care for newly diagnosed glioblastoma patients. *Crit Rev Oncol Hematol*, 2017. 111: p. 60-65.
66. Bernard-Arnoux, F., et al., The cost-effectiveness of tumor-treating fields therapy in patients with newly diagnosed glioblastoma. *Neuro Oncol*, 2016. 18(8): p. 1129-36.
67. Wick, W., et al., Temozolomide chemotherapy alone versus radiotherapy alone for malignant astrocytoma in the elderly: the NOA-08 randomised, phase 3 trial. *Lancet Oncol*, 2012. 13(7): p. 707-15.
68. Malmstrom, A., et al., Temozolomide versus standard 6-week radiotherapy versus hypofractionated radiotherapy in patients older than 60 years with glioblastoma: the Nordic randomised, phase 3 trial. *Lancet Oncol*, 2012. 13(9): p. 916-26.
69. Gorlia, T., et al., Nomograms for predicting survival of patients with newly diagnosed glioblastoma: prognostic factor analysis of EORTC and NCIC trial 26981-22981/CE.3. *Lancet Oncol*, 2008. 9(1): p. 29-38.
70. Li, J., et al., Validation and simplification of the Radiation Therapy Oncology Group recursive partitioning analysis classification for glioblastoma. *Int J Radiat Oncol Biol Phys*, 2011. 81(3): p. 623-30.
71. Wee, C.W., et al., Novel recursive partitioning analysis classification for newly diagnosed glioblastoma: A multi-institutional study highlighting the MGMT promoter methylation and IDH1 gene mutation status. *Radiother Oncol*, 2017. 123(1): p. 106-111.
72. Chaichana, K., et al., A proposed classification system that projects outcomes based on preoperative variables for adult patients with glioblastoma multiforme. *J Neurosurg*, 2010. 112(5): p. 997-1004.
73. Yang, F., et al., Stratification according to recursive partitioning analysis predicts outcome in newly diagnosed glioblastomas. *Oncotarget*, 2017. 8(26): p. 42974-42982.
74. Gittleman, H., et al., An independently validated nomogram for individualized estimation of survival among patients with newly diagnosed glioblastoma: NRG Oncology RTOG 0525 and 0825. *Neuro Oncol*, 2017. 19(5): p. 669-677.
75. Woo, P., et al., A Comparative Analysis of the Usefulness of Survival Prediction Models for Patients with Glioblastoma in the Temozolomide Era: The Importance of Methylguanine Methyltransferase Promoter Methylation, Extent of Resection, and Subventricular Zone Location. *World Neurosurg*, 2018. 115: p. e375-e385.
76. Parks, C., et al., Can the prognosis of individual patients with glioblastoma be predicted using an online calculator? *Neuro Oncol*, 2013. 15(8): p. 1074-8.





CHAPTER 2

Valproic acid for the treatment of malignant gliomas: review of the preclinical rationale and published clinical results

Sharon Berendsen, Marike L. Broekman, Tatjana Seute, Tom J. Snijders,
Corine A. van Es, Filip Y. de Vos, Luca Regli, Pierre A. Robe.

Published in: Expert Opinion on Investigational Drugs. 2012 Sep;21(9):1391-415.

ABSTRACT

Introduction: Glioblastoma is the most common and aggressive primary brain tumor. Valproate has been used as an anti-epileptic drug and mood stabilizer for decades. Recently, it was found to inhibit the proliferation of various cancers including glioblastoma.

Areas covered: We provide a comprehensive review of the mechanisms of action of valproate in gliomas, of its potential side effects and of the published clinical results obtained with this drug in glioblastomas. Valproate inhibits a subset of histone deacetylases and cellular kinases, and affects gene transcription through histone hyperacetylation, DNA hypomethylation and the modulation of several transcription factors. As a result, VPA induces differentiation of glioma cells, can prevent their invasion in surrounding tissues and may inhibit tumor angiogenesis. VPA can also inhibit DNA repair, thereby potentiating cytotoxic treatments such as chemotherapies or radiation therapy. Based on these mechanisms and case reports of glioblastoma remissions following VPA treatment, several clinical studies currently assess the therapeutic potential of VPA in glioma therapy.

Expert opinion: The combination of VPA treatment with chemotherapy and radiotherapy in glioblastoma appears a rational option that deserves well-designed prospective clinical trials that assess the efficacy and the molecular characteristics of the responding tumors in these patients.

INTRODUCTION

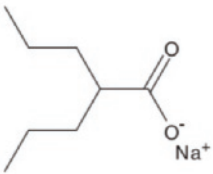
Valproic acid or its salt, sodium valproate (VPA) (Box 1), is an established anticonvulsant drug and mood stabilizer. Among other mechanisms of action, valproate enhances the inhibitory effects of the neurotransmitter GABA, blocks voltage-gated sodium channels and T-type calcium channels, alters the firing frequency of neurons and attenuates NMDA-mediated excitation (see Drug Summary box) [1]. This short-branched fatty acid easily penetrates the blood-brain barrier and can be safely administered chronically both in adult and in pediatric patients [2]. During pregnancy, however, VPA can induce neural tube defects in the fetus. In attempts to find the mechanism responsible for this latter toxicity, VPA was found to potently inhibit a specific subset of histone deacetylase (HDAC) isoforms [3,4].

HDACs are a family of enzymes capable of removing acetyl groups from histones and a range of other target proteins. This action increases the positive charge of histone tails, favors chromatin condensation and reduces the recruitment of transcriptional activators. This results in repression of gene expression [5]. HDACs also deacetylate several transcription factors (e.g., STAT3, NF- κ B, p53), thus regulating their function, promoter selectivity and differential gene expression [6-8]. They contribute to the regulation of intracellular signaling cascades via the formation of quaternary signaling complexes and interaction with protein-phosphatase complexes [9,10]. All of these actions contribute to the control of cell proliferation. HDAC inhibitors have consistently been found to inhibit the growth of a variety of tumor cell types in experimental conditions as well as in some preliminary clinical trials [11].

Glioblastoma is the most common and aggressive form of primary brain tumors. Despite advances in surgical, radiological and chemotherapeutic treatments, prognosis is poor with a mean survival duration of 15 months, at best [12]. Although highly heterogeneous, glioblastomas present common alterations of several key homeostasis pathways. These include tyrosine kinase receptor signaling, MAP kinase cascades, p53, Rb and NF- κ B signaling pathways. Several genetic (e.g., mutations, deletions, recombinations, amplifications) and epigenetic (e.g., DNA methylation, histone acetylation) events underlie these deregulations [13-15].

The expression of several HDAC subtypes was arguably reported to vary with tumor grade in gliomas [16]. HDAC inhibitors were shown to restore the expression of cell cycle inhibitors (e.g., p21) [17] and tumor suppressors [18], and to decrease Akt-dependent signaling [9]. They subsequently reduce cell proliferation and invasion, and can induce apoptosis in these tumors. Moreover, they act as radiosensitizing and chemosensitizing agents in gliomas [19-21].

Given its HDAC inhibitory and cell signaling modulating properties, VPA has become an experimental drug for the treatment of pediatric malignant gliomas [22]. This paper reviews the physiopathological, pharmacodynamic, pharmacokinetic, preclinical and clinical evidence that supports the further development of valproate-based clinical trials against high-grade gliomas, both in pediatric and in adult patients.

Box 1. Drug summary.	
Drug name	Valproic acid
Phase	Malignant glioma
Indication	Off-label indication
Pharmacology description	Histone deacetylase inhibitor
Route of administration	Intravenous, oral
Chemical structure	 <p>pentanoic acid, 2-propyl-, sodium salt [CAS] [195,22,204]</p>
Pivotal trial(s)	
Pharmaprojects – copyright to Citeline Drug Intelligence (an Informa business). Readers are referred to Pipeline (http://informa-pipeline.citeline.com) and Citeline (http://informa.citeline.com).	

2. PHARMACODYNAMIC PROPERTIES OF VPA: RELEVANT TARGETS IN GLIOMAS

2.1 VPA as an HDAC inhibitor

2.1.1 Histone deacetylases and glioblastoma

The dynamic packaging of DNA into the dynamic structure of chromatin controls the accessibility of transcription factors to DNA regulatory sequences. Chromatin consists of nucleosomes, which comprise 146 base pairs of DNA wrapped around histone proteins (H2A, H2B, H3 or H4). The N-terminal tails of histone proteins are prone to post-translational modifications, such as acetylation, methylation, ubiquitination and phosphorylation [1]. These modifications alter both the tridimensional aspect and the electric charge of the histones, which in turn regulates the intensity of chromatin condensation.

Histone acetylation depends on the balance between the effects of histone acetyl transferases (HATs) and HDACs. HATs transfer acetyl groups from acetyl-CoA to the ϵ -amino group of lysine residues of histone proteins, resulting in chromatin decondensation and a better access of transcription factors and of the translation machinery to DNA. The reverse reaction, involving the deacetylation of acetylated lysine residues, is mediated by HDACs and enhances the condensation of chromatin [23].

HDACs are categorized into four classes (I - IV). Class I (HDAC 1, 2, 3 and 8), class IIA (HDAC 4, 5, 7 and 9), class IIB (HDAC 6 and 10) and class IV (HDAC 11), all contain a structurally conserved catalytic domain that contains an essential zinc cation [24]. They, however, have defined partners, specific functions, for instance during the embryologic development [25], and sensibility to pharmacological inhibitors. Class III HDAC enzymes are homologues of the yeast Sir2 protein and are, therefore, termed sirtuins. They are structurally distinct from classes I, II and IV in that their action is NAD dependent and these enzymes do not have a zinc cation in their active site. Sirtuins are, therefore, insensitive to conventional HDAC inhibitors that target the zinc pocket of other classes [13,23,26].

Like HATs, HDACs do not directly bind to DNA but are recruited in quaternary complexes, with transcription factor proteins, cell signaling proteins and/or regulators of histone methylation [27,28]. Class I HDACs are for instance found in four types of histone demethylase-containing multiprotein complexes (Sin3, CoREST, NCoR-SMRT and NuRD). These complexes contain class I HDACs, zinc-finger proteins able to bind the DNA helix, protein switches and histone demethylases. They participate in the integration of cell signaling cascades into various gene transcription programs and are involved in DNA repair, energy production, cell-cycle control, cell invasion, astroglial differentiation and self-renewal of stem and progenitor cells [29].

Transcription factor complexes can also recruit HDAC 1 and HDAC 2 at specific sites, where these HDACs inhibit the action of the transcription factor complexes through histone hyperacetylation. This mechanism participates in the general repression of pro-apoptotic genes [30] and of YKL-40 in glioblastoma cells [31] by transcription factor nuclear factor-kappa B (NF- κ B). HDAC 1 also associates in glioblastomas with Bcl-2 interacting protein BNIP3 to repress the expression of apoptosis-inducing factor (AIF) and increase resistance to apoptosis [32].

Additionally, class II HDACs, some sirtuins and to a lesser extent HDAC 1 and 3 can shuttle between the cytoplasm and the nucleus [33]. Indeed, lysine acetylation does not only occur on histone tails, but also participates in the regulation of more than 1700 intracellular proteins in mammals. These range from transcription factors (e.g., NF- κ B

p65, c-myc, p53, SMAD2, β -catenin, GATA-1), protein kinases (e.g., CDK2, DNAPK, CK2), chaperone proteins (e.g., HSP90), ribosomal proteins (e.g., EIF4A1), cytoskeleton and endo/exocytosis components (e.g., tubulin), nuclear trafficking proteins (e.g., CRM1; 14-3-3) and a variety of DNA and RNA-modifying enzymes (e.g., helicases, ATM) [34,35].

These targets are of particular relevance in glioblastomas. For instance, NF- κ B p65, which also plays a major role in the growth, therapeutic resistance and invasion of malignant gliomas [14,36], is also inactivated by acetylation, a process that can be reversed by class I HDACs [37].

Interestingly, malignant gliomas present altered levels of HDACs. The intensity and patterns of histones H3 and H4 acetylation vary with tumor grade and may be associated with differential prognosis for tumors of similar histological grade [38]. The expression of class II and IV HDAC mRNAs is downregulated in glioblastomas compared with low-grade gliomas and normal brain tissue, and translates in reduced HDAC 9 protein levels [27]. On the other hand, HDAC 1 and 2 are overexpressed in high-grade tumors, whereas the level of expression of HDAC 3 remains a matter of debate. The expression of HDAC 1 further increases in recurrent tumors and that of HDAC 2 correlates with tumor progression toward more malignant grades [16]. Sequencing of HDAC-encoding genes has also revealed mutations in HDACs 2 and 9 in glioblastoma [13,39], and the subcellular localization of some HDACs (e.g., HDAC 3) may be altered in these tumors [16].

Class III HDACs, or sirtuins (SIRT), are also aberrantly expressed in gliomas. SIRT1 [40] and SIRT2 are downregulated in glioblastoma, as a consequence of histone deacetylation of the SIRT2 5' untranslated region and because of 19q13.2 deletions. SIRT2 acts as a mitotic checkpoint regulator that blocks chromosome condensation in response to mitotic stress and is thought to inhibit glioma proliferation [41].

2.1.2 VPA and HDAC inhibition: specificity and reversibility

VPA (di-n-propylacetic acid or 2-propylpentanoic acid) is a small branched fatty acid with a molecular weight of 144.21 U. VPA is highly soluble in organic acids, slightly soluble in water and is stable at room temperature.

VPA interacts in cells with several proteins, among which HDACs [3,4], T-type Ca^{2+} channels [42], voltage-gated sodium channels [1], succinic amide dehydrogenase (SSA-DH) [43] and glycogen synthase kinase-3 β (GSK-3 β) (Figure 1) [44,45]. While little is known about the structural relationship of VPA with these latter four targets, the interaction of VPA and HDAC is well characterized. Although HDAC inhibitors are structurally different, most of them contain a metal-binding domain that interacts with the zinc pocket, a surface recognition site and a linker domain. The walls of the narrow, deep pocket of

the HDAC enzyme are covered with hydrophobic and aromatic residues, allowing Van der Waals bonding and π - π stacking with HDAC inhibitors. It is thought that the HDAC inhibitory capacity of different inhibitors is partially dependent on the interactions of the aliphatic chain of the HDAC inhibitor with the walls of the zinc pocket at the catalytic site [24]. In the case of valproate, however, *in silico* data suggest that the hydrophobic affinity with the walls of the catalytic site is low. Instead, valproate appears to bind to the zinc ion and some hydrophilic residues in its vicinity. VPA also independently forms hydrophobic bonds between its aliphatic chain and hydrophobic residues situated in the so-called hydrophobic active site channel, where acetyl moieties are normally released after acetylation [46].

Several groups have analyzed the specificity of VPA against the various subclasses of HDACs (Table 1). Valproate was shown to inhibit class I HDAC 1 - 3 and to stimulate the ubiquitination and subsequent proteasomal degradation of HDAC 2 at submillimolar concentrations [3,4,47-49]. Inhibition of HDAC 4, 5, 7 and 8 by VPA has also been inconsistently reported. However, the half-maximal inhibitory concentration (IC_{50}) values for these subclasses were over the millimolar range and well over the safe therapeutic concentrations that can be achieved in human plasma and CSF (see below) [47,49]. Finally, the expression of HDAC 9 and 11 seems to be upregulated by treatment with VPA [50].

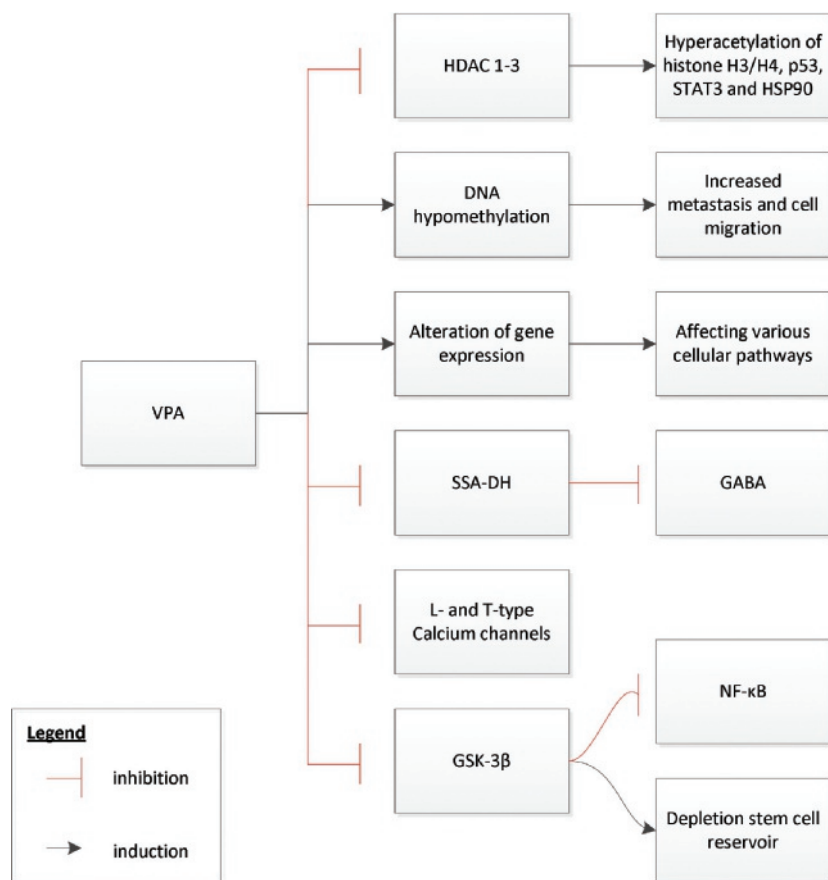


Figure 1 - Targets of VPA. VPA has been shown to inhibit histone deacetylase (HDAC) 1 - 3 at submillimolar concentrations [3,4,47-49]. In addition, VPA treatment results in DNA hypomethylation, which might lead to increased metastasis and cell migration [60,61]. Exposure to VPA has also been shown to result in the alteration of the expression of several genes, affecting various cellular pathways [65-68]. The anti-epileptic activity of VPA stems from its capacity to inhibit succinic amide dehydrogenase (SSA-DH), resulting in increased gamma-butyric acid (GABA) levels [43]. VPA has been shown to inhibit L- and T-type calcium channels; however, the clinical relevance of this effect has to be further investigated [42,74-76]. Submillimolar concentrations of VPA result in direct inhibition of GSK-3 β [44,45], which is believed to mediate anti-tumor effects in glioblastoma through NF- κ B inhibition [82] and depletion of the stem cell reservoir [83].

Abbreviations: DNA: Deoxyribonucleic acid; GABA: Gamma-butyric acid; GSK-3 β : Glycogen synthase kinase-3 β ; HDAC: Histone deacetylase; HSP90: Heat shock protein 90; NF- κ B: Nuclear factor- κ B; SSA-DH: Succinic amide dehydrogenase; STAT3: Signal transducer and activator of transcription 3; VPA: Valproic acid.

As a consequence of its HDAC inhibitory properties, VPA has been shown to cause hyperacetylation of the N-terminal tails of histones H3 and H4 in glioma cell lines [51-53]. These effects are reversible, as histone acetylation status almost returns to control levels

3h after removal of VPA [51]. Similarly, VPA treatment results in the hyperacetylation of several non-histone proteins, such as p53 in neuroblastoma cells [54].

There are several classes of HDAC inhibitor compounds, for example, hydroxamic acids (TSA, vorinostat), short chain fatty acids (VPA, sodium butyrate), benzamides (MS-275) and cyclic peptides (depsipeptide) [1,28]. Compared with these other compounds, VPA is a relatively weak HDAC inhibitor; however, it is shown to inhibit HDAC 1 and 2 well within clinically relevant concentrations [4,48]. There are limited published clinical trials using HDAC inhibitors other than VPA in glioblastoma treatment. Other than the results from VPA studies (see below), the results of these trials show modest (vorinostat - [55]) or no anti-tumor effects (depsipeptide - [56]) in the treatment of recurrent malignant glioma.

Table 1 – Overview of histone deacetylase (HDAC) classification and inhibition of HDACs by VPA

HDAC Classes	Inhibition by VPA	Reference
Class I		
HDAC 1	++	[4, 47-49]
HDAC 2	++	[3, 4, 47-49]
HDAC 3	++	[4, 47-49]
HDAC 8	+	[4, 47, 48]
Class IIA		
HDAC 4	+	[47, 49]
HDAC 5	+/-	[3, 48, 49]
HDAC 7	+/-	[48, 48, 49]
HDAC 9	-	[48, 50]
Class IIB		
HDAC 6	+/-	[3, 48, 49]
HDAC 10	-	[49]
Class III		
SIRT 1	-	[23]
SIRT 2	-	[23]
SIRT 3	-	[23]
SIRT 4	-	[23]
SIRT 5	-	[23]
SIRT 6	-	[23]
SIRT 7	-	[23]
Class IV		
HDAC 11	-	[50]

Level of HDAC inhibition by VPA: IC₅₀ in submillimolar range (++); IC₅₀ over millimolar range (+); inconsistent reporting (+/-); no inhibition by VPA (-). Abbreviations: HDAC, histone deacetylase; VPA, valproic acid; SIRT, sirtuin.

2.2 VPA and DNA methylation

DNA methylation results from the action of DNA methyl-transferases (DNMTs) that add methyl groups on the fifth carbon of cytosine at CpG sites. The epigenetic information generated by these enzymes results in a durable and heritable, yet regulated and reversible, repression of gene transcription. This mechanism plays a role in the sequential transcriptional program of embryogenesis, the maintenance of cell lineage-specific gene expression patterns, the inactivation of the X-chromosome and the phenomenon of imprinting [57]. DNA methylation patterns are induced on both strands of DNA by DNMT 3A and DNMT 3B, or de novo DNMTs. Maintenance of DNA methylation after cell division results from the action of DNMT 1, which uses the mother strand of DNA to duplicate its pattern of methylation on the newly formed DNA strand. Inhibition or inactivation of DNMT 1 thus results in a progressive, passive loss of DNA methylation patterns over subsequent cell mitoses. Although still a matter of controversy and depending on ill-defined mechanisms, active genome-wide and stimulus-regulated, gene-specific DNA demethylation events could also result from the replacement of methylated C bases by unmethylated C bases on DNA molecules [57].

Global DNA hypomethylation occurs in approximately 80% of primary glioblastomas, and the most severe globally hypomethylated primary malignant gliomas are the most proliferative, notably via the transcriptional activation of the oncogene melanoma antigen A1 (MAGEA1). In contrast to global hypomethylation, locus-specific hypermethylation is also common in glioblastoma, especially at CpG island promoters. Hypermethylation often occurs at the level of tumor suppressor genes such as those that control the p53, PI3K or Rb pathways [13,52].

Glioma cells often present an upregulation of DNMTs 1 and 3 with respect to normal brain tissue. Inhibition of these enzymes may result in the upregulation of several tumor suppressor and apoptosis inducer transcripts such as p21, p27, PTEN or Bax. This occurs not only via direct demethylation of certain gene promoters, but also via intricate interactions among DNMTs, histone acetylation and overall chromatin accessibility [58,59]. Of note, DNMT silencing failed to inhibit cell proliferation and colony formation in vitro in these experiments [59].

Although yet poorly characterized and indirect, these DNA-demethylation properties of VPA are important, as they have the potential to either promote or inhibit tumor growth. Of relevance for this review, VPA was indeed shown to induce DNA hypomethylation in rat astrocytes. This process appears reversible, is independent of DNMT 1 [60] and might involve its chromatin remodeling properties and improved access of the active demethylation machinery to promoter regions [61].

In agreement with the above-mentioned mixed effects of DNA methylation on the expression of cancer-related genes, VPA-induced promoter demethylation was found to upregulate proteins associated with metastasis and cell migration, such as the gelatinases MMP2 and MMP9, bone matrix protein lumican and the melanoma antigen B2 gene (MAGEB2) in human embryonic kidney (HEK293) cells [61], but not in gliomas [62]. In human glioblastomas, VPA treatment also increases the expression of O-6-methylguanine-DNA methyltransferase (MGMT) mRNA, but not of its protein. MGMT is a DNA repair enzyme known to modulate the response of these tumors to alkylating agents and the expression of which is tightly controlled by promoter methylation [63,64].

2.3 VPA-mediated effects on gene expression

Microarray analysis of rat brain gene expression after chronic VPA administration (200 mg/kg) has demonstrated the downregulation of 87 genes and upregulation of 34 genes. The affected genes are involved in various cellular pathways, including synaptic transmission, ion channels and transport, G-protein signaling, lipid, glucose and amino acid metabolism, transcriptional and translational regulation, phosphoinositol cycle, protein kinases and phosphatases, and apoptosis. A subset of genes and proteins affected by VPA are listed in Table 2 and described below [65]. Chronic VPA administration has also been shown to induce downregulation of the GluK2 kainate receptor and cPLA₂ in mouse astrocytes [66].

Another microarray analysis of chronic lymphocytic leukemia B cells after treatment with 1 mM VPA revealed that VPA induced apoptosis by upregulating several pro-apoptotic genes and downregulating anti-apoptotic genes and thus disturbing the balance between pro-apoptotic and anti-apoptotic genes (Table 2) [67]. Similar VPA-induced effects on gene expression have been described in several other tumor types, such as cervical carcinoma [68], but have not yet been described in glioblastomas.

Table 2 – VPA-mediated effects on gene and protein expression.

Target gene/protein	VPA-mediated up/ downregulation	Cell type	Reference
Cell proliferation			
p21	↑	Glioblastoma	[52]
p53	↑	Prostate cancer	[90]
GSK-3	↓	Neural progenitor cell	[103]
Wnt 1, 2	↑	Mouse brain cell	[77]
Cyclin D3	↑	Rat C6 glioma	[89]

Table 2 (continued) – VPA-mediated effects on gene and protein expression.

Target gene/protein	VPA-mediated up/ downregulation	Cell type	Reference
Cell differentiation			
GFAP	↑/↓	Rat C6 glioma	[51, 52, 106]
GDNF	↓	Rat C6 glioma	[51]
BDNF	↑	Rat C6 glioma	[51]
β3-tubulin	↑	Rat C6 glioma	[51]
CD133	↑	Glioblastoma	[108]
CD44	↓	Glioblastoma	[85]
Cell death			
p53	↑	Prostate cancer	[90]
Bim	↑	Leukemia	[111]
TRAIL DR-5	↑	Leukemia	[110]
Bax	↑	Glioblastoma	[62]
Chk1	↓	Non-small cell lung cancer	[112]
Survivin	↓	Gastric cancer/leukemia	[109, 110]
Bcl-2	↓	Glioblastoma	[62]
ROS	↑	Glioblastoma	[88]
GSH	↑	Glioblastoma	[88]
Angiogenesis			
VEGF	↓	Glioblastoma	[122]
Tumor invasion			
MMP2	↓	Glioblastoma	[62]
MMP9	↓/↑	Glioblastoma	[62, 132]
TIMP1	↑	Glioblastoma	[62]
IL-6	↓	Glioblastoma	[94]
NF-κB	↓	Glioblastoma	[94]
Resistance to VPA			
Clusterin	↑	Neuroblastoma	[71]

VPA-mediated upregulation (↑); VPA-mediated downregulation (↓). Abbreviations: VPA, valproic acid; GSK-3, glycogen synthase kinase-3; GFAP, glial fibrillary acidic protein; GDNF, glial cell line-derived neurotrophic factor; BDNF, brain-derived neurotrophic factor; CD133, cluster determinant 133; CD44, cluster determinant 44; TRAIL DR5, TNF-related apoptosis-inducing ligand death receptor 5; Chk1, checkpoint kinase 1; bcl-2, B-cell lymphoma-2; ROS, reactive oxygen species; GSH, glutathione; VEGF, vascular endothelial growth factor; MMP2, matrix metalloprotease 2; MMP9, matrix metalloprotease 9; TIMP1, TIMP metalloprotease inhibitor 1; IL-6, interleukin 6; NF-κB, nuclear factor-κB.

2.4 VPA and GABA

The anti-epileptic properties of valproate notably stem from its action on GABAergic neurotransmission. Although VPA does not interfere with GABA receptor binding or GABA uptake mechanisms, it has been shown to inhibit succinic amide dehydrogenase (SSA-DH) within minutes of administration. This enzyme of the tricarboxylic acid (TCA) cycle mediates the transformation of succinate semialdehyde (SSA), a derivative of GABA that stems from the action of GABA-transaminase, into succinate. SSA-DH inhibition thus increases cellular levels of SSA, resulting in a negative feedback on GABA-transaminase and preventing the degradation of GABA [43].

Gliomas synthesize GABA and express a functional GABA receptor, albeit with an expression level that seems to decrease with histological grade [69]. GABA was shown to reduce the secretion of IL-6 [70], a cytokine involved in tumor invasion in glioma [71]. Whether VPA-mediated GABA-increase plays a role in the anti-tumor effects of this drug remains to be elucidated.

Succinate itself is a stabilizer of HIF-1 α , a transcription factor that participates in the proliferation, aggressiveness and cell resistance of glioma cells [72]. Whether valproate-induced SSA-DH inhibition results in significantly decreased intracellular levels of succinate and inhibition of the HIF-1 α pathway is, however, not yet known.

2.5 VPA and calcium channels

VPA inhibits L- and T-type calcium channels – in a dose-dependent manner – starting at micromolar concentrations [42]. Gliomas express specific splice variants of T-type calcium channels [73] that have been correlated with the proliferative phenotype of glioma cell lines. Although this issue remains controversial and needs to be investigated further [74–76], the existing evidence suggests that the interaction between VPA and calcium channels probably plays a minor role in its anti-tumor properties.

2.6 GSK-3

Although the structural relationship between VPA and glycogen synthase kinase-3 β (GSK-3 β) remains unclear, submillimolar concentrations of VPA directly inhibit GSK-3 β [44,45].

This inhibition has several effects. Among others, it stimulates Wnt/ β -catenin signaling and can result in cell differentiation in neuroblastoma cells [44]. Additional mechanisms might be involved in the upregulation of VPA-mediated Wnt signaling. For example, demethylation of Wnt 1 and 2 gene promoters, increased expression of these proteins and enhanced Wnt/ β -catenin activity have been observed in the brain of pups born from VPA-fed pregnant mice [77]. In normal neural progenitor cells with normal cell cycle checkpoints, VPA-enhanced β -catenin transcription seems to provoke a sustained

activation of the ERK pathway and results in p21 overexpression and cell-cycle arrest [44]. In gliomas, however, β -catenin activation is known to promote glioma cell migration [78], angiogenesis [79], tumorigenesis [80] and radioresistance [81].

GSK-3 β inhibition, however, also reduces NF- κ B activation [82] and depletes the glioma stem cell reservoir [83]. As a result, it is believed that GSK-3 β mediates global anti-tumor effects in glioblastomas [84].

3. PRECLINICAL DATA

3.1 Anti-proliferative effect of VPA

VPA inhibits the proliferation of various human glioma cell lines (Figure 2), albeit in a cell-type, dose- and time-dependent profile. The half-maximal inhibitory concentration (IC_{50}) of human glioma cell lines may thus vary from as low as 0.1 to up to 7 mM [1,85], and VPA treatment preferentially elicits a G_0/G_1 or a G_2/M arrest pending on the wild type or mutated p53 status of the glioma cell line considered [1,52,53,86-88].

VPA was shown to upregulate and favor nuclear shuttling of cyclin D3 in C6 glioma cells during mid- G_1 phase and does not reduce the expression of cyclin D1, a key regulator of the progression of the G_1 phase of the cell cycle and a frequent downstream target of mitotic stimuli in glioma cells [89]. Although cyclins are generally considered to be pro-mitotic proteins, this deregulated activation of cyclin D3 was ultimately considered as a potential contributor to cell cycle arrest [89].

More importantly, VPA induces the expression of CDK inhibitor p21^{CIP} through epigenetic mechanisms [52] and via the direct acetylation of the transcription factor p53 [54,90]. P21^{CIP} preferentially inactivates cyclin E/Cdk2 complexes, thereby blocking the inactivating phosphorylation of pRb, which represses genes important for S-phase entry. The p21 protein also binds to proliferating cell nuclear antigen (PCNA) and thereby blocks DNA synthesis [91]. In normal cells, however, p21 is necessary to allow the progression of the G_2/M phase, after phosphorylation and interaction with the Cdc2/ cyclin B complex [92]. This suggests that additional factors than a mere overexpression of p21 might contribute to the VPA-induced G_2/M arrest in p53-deficient cells. For instance, HDAC inhibitors also cause an accumulation of reactive oxygen species (ROS) in transformed cells (see below). This may harm their DNA and lead to a G_2/M arrest, mediated by a blockade of the interaction of Cdc25C with PCNA by p21^{CIP1} [93].

Additionally, HDAC inhibition disrupts the pericentric heterochromatin and is associated with chromosomal segregation defects. HDAC 3 also associates with the mitotic kinase

Aurora B during mitosis and is involved in microtubule-kinetochore attachment. HDAC inhibition also leads to spindle assembly checkpoint dysfunction [23].

HDACs also regulate the activity of several transcription factors and intracellular signaling pathways, which may contribute to the anti-proliferative properties of VPA. Aberrant transcriptional activity of nuclear factor-kappaB (NF- κ B) is for instance a hallmark of malignant gliomas and significantly contributes to their proliferation and treatment resistance [14,21]. VPA, at submillimolar concentrations, inhibits NF- κ B DNA-binding activity in human glioma cells [31,94]. Similar effects of VPA on NF- κ B transcriptional activity have also been observed on other cancer cell types, such as pancreatic cancer [95] or leukemia cells [31,94]. The mechanisms of VPA-driven NF- κ B inhibition are not yet demonstrated. These mechanisms might, however, involve the HDAC 1- and 2-dependent regulation of p65 activity by acetylation [6], alteration of the activity of HDAC co-effectors recruited by NF- κ B at promoter sites [31,94] or yet transcriptional or translational regulation of NF- κ B subunits. In support of this latter mechanism, chronic administration of VPA to mice was shown to reduce p50 protein expression and p50/p65-binding activity in frontal cortex astrocytes [96].

The signal transducer and activator of transcription (STAT) proteins are latent self-signaling transcription factors in the cytoplasm, which are used by most cytokine receptors to rapidly turn on gene expression in the nucleus. The expression of STAT3 is required for transcriptional activity of several genes involved in cell cycle progression, such as cyclin D3 or c-myc [7]. The STAT3 protein is constitutively activated in various primary tumors [10]. In glioblastoma, however, STAT3 may either promote or suppress oncogenesis pending on the PTEN and EGFR mutational profile of the tumor [97] and acts as a tumor suppressor in PTEN-deficient tumor cells. The activation of STAT3 is induced by histone acetyltransferase p300-mediated acetylation of lysine 685 and phosphorylation of serine 727 in the transcriptional activation domain. HDAC3 regulates both the acetylation and the phosphorylation of the STAT3 protein [7,10].

Although treatment with several HDAC inhibitors results in the activation of STAT3 in various cell types [7,10], the effect of VPA on STAT proteins in glioblastoma is poorly investigated and might require supra-therapeutic drug concentrations (5 mM) [98].

STAT5b, one of the other STAT proteins, has also been reported to play a role in glioblastoma cell growth, cell cycle progression, invasion and migration [99]. The activation of STAT5b in glioblastoma is induced by EGFRvIII [100], and STAT5b can modulate gene expression of among others Bcl-2, p21^{WAF1/CIP1} and vascular endothelial growth factor (VEGF) [99]. VPA has recently been shown to inhibit STAT5 in natural killer cells, resulting in a decrease in interferon γ (IFN- γ) expression in these cells. In this

study, treatment of NK cells with 5 mM VPA was reported to reduce NK-mediated cell killing of oncolytic virus-infected glioblastoma cells [101]. However, to date, the effect of VPA on the expression of STAT5 in glioblastoma is still unknown.

Even though tumor cells are on average more sensitive to the cytotoxic effects of HDAC inhibition than normal cells, the *in vitro* effects of VPA on the proliferation of glioma cells remain generally weak and are cell line and context dependent [52]. Submillimolar concentrations of valproate have, however, recently been reported to enhance the proliferation of a line of glioma cells *in vitro* [102]. This may be explained by several factors. First, as mentioned previously, the nature of p21- and STAT3-dependent anti-proliferative effects of HDAC inhibition may depend on the p53, EGFR and PTEN status of the cells. Second, the growth-suppressive effects of NF- κ B inhibition by HDAC inhibitors may be annihilated in some tumors, as NF- κ B-mediated repression of YKL-40, an important glioma cell proliferation and radiation resistance protein, is HDAC 1 and 2 dependent (see above) [31]. Third, VPA directly and indirectly inhibits regulating kinase GSK-3 [44,45,103,104] and thereby enhances Wnt/ β -catenin signaling (see above).

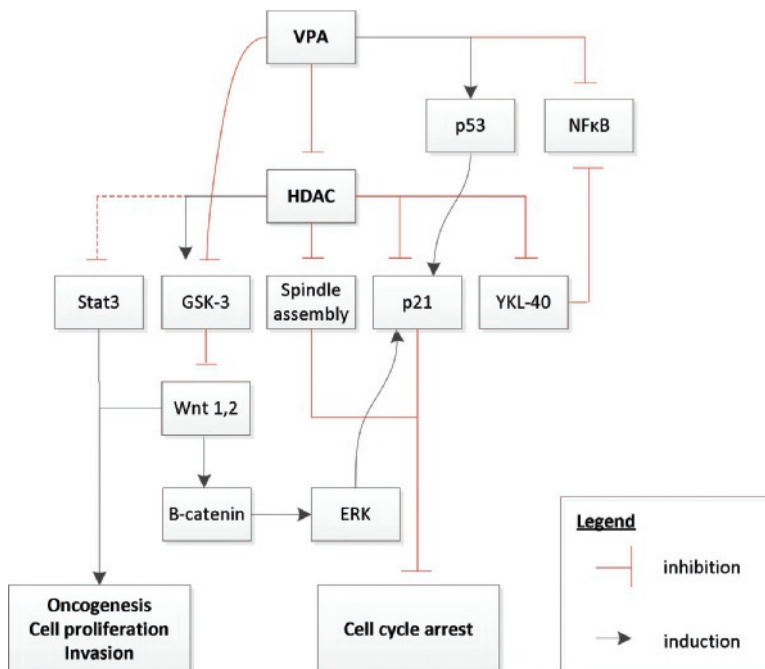


Figure 2 - Anti-proliferative effects of VPA. VPA has several contradictory effects on tumor cell proliferation, both through histone deacetylase (HDAC) inhibition and direct effects. VPA possibly directly alters the acetylation status of p53 [90] and inhibits nuclear factor- κ B (NF- κ B), possibly through HDAC inhibition. NF- κ B may also be inhibited by VPA-mediated HDAC inhibition and subsequent increased expression of YKL-40, which is an inhibitor of NF- κ B [6,31,94]. VPA-mediated

Figure 2 - Anti-proliferative effects of VPA (continued). cell cycle arrest is induced through increased p21 expression by HDAC inhibition [52] and p53 acetylation [54,90], and spindle assembly defects through HDAC inhibition [23]. Through direct and indirect inhibition of GSK-3 β , both tumor proliferation and cell cycle arrest [44] have been described. β -catenin expression is enhanced by direct and indirect inhibition of GSK-3 β [44,82,103,104]. Stat3 can also induce oncogenesis depending on the epidermal growth factor receptor and phosphatase and tensin homologue mutant status of the tumor [97].

EGFR: Epidermal growth factor receptor; ERK: Extracellular signal-regulated kinase; GSK-3 β : Glycogen synthase kinase-3 β ; HDAC: Histone deacetylase; NF- κ B: Nuclear factor- κ B; PTEN: Phosphatase and tensin homologue; Stat3: Signal transducer and activator of transcription 3; VPA: Valproic acid; YKL-40: Cartilage glycoprotein-39.

3.2 Effect of VPA on glioma cell differentiation

Although its true significance remains to be elucidated, the experimental morphological differentiation of glioma cells toward astrocytic or even neuronal phenotypes seems to correlate with reduced cell proliferation and tumor aggressiveness. In human gliomas, recent literature has provided some support to this view. Indeed, tumors with an mRNA expression profile enriched in neuronal markers seem to present a less dismal prognosis as those expressing more stem cell-like gene-expression patterns [105].

At clinically relevant concentrations (1 - 1.5 mM), VPA simultaneously induces neuronal differentiation and reduces proliferation *in vitro* and *in vivo* of basic fibroblast growth factor (bFGF)-treated rat neural progenitor cells. These effects were shown to be mediated by β -catenin signaling and the subsequent activation of the Raf/MEK/ERK pathway and induction of p21^{CIP/WAF1} [44].

Higher concentrations (1.5 - 2 mM) of VPA have been shown to enhance the expression of glial fibrillary acidic protein (GFAP) and to promote the adoption of a glial phenotype in rat C6 glioma cells while reducing their proliferation and migration [106,107]. At yet higher concentrations and after several days of culture, VPA decreased GFAP expression and other glial marker proteins (e.g., GDNF). However, it stimulated the expression of neuronal genes (e.g., BDNF, β 3-tubulin). A retraction of the cell borders and growth of long neurite-like and cone-like structures at the end of projections occurs in parallel in a subpopulation of C6 glioma cells [51].

In human glioma cell lines and *in vitro*, valproate (1.5 mM) has also been shown to induce GFAP expression and to alter cell morphology toward a flattened and stellate shape while increasing p21 and hyper-acetylating histone H4 [52]. Lower doses of the drug (0.1 - 1 mM) can simultaneously reduce the proliferation of a panel of human glioma cell lines and to decrease their expression of the stem cell marker CD44 [85]. However, and of potential concern for therapeutic trials in humans, VPA was also recently shown to enhance the expression of CD133, another stem cell marker, in some glioblastoma cell lines [108].

3.3 Effects of VPA on cell death

Valproate experimentally induces cell death in malignant cells through multiple and cell-type-specific, p53-related and -unrelated and dose-dependent mechanisms (Figure 3) (e.g., [109]). VPA alters the balance of pro- and anti-apoptotic factors at therapeutically relevant concentrations (0.5 - 1 mM). At these concentrations, valproate for instance alters the phosphorylation status of p53 in prostate carcinoma cells [90], decreases the expression of anti-apoptotic proteins such as survivin or bcl-2 in gastric cancers [109] and leukemias [110] and increases the expression of pro-apoptotic protein Bim in acute myeloid leukemias [111]. It also increases the expression of TRAIL death receptor DR5 in leukemias, among others [110]. VPA even downregulates the expression of checkpoint kinase (Chk1) in non-small cell lung cancer cells, provoking an aberrant entry in mitosis and subsequent apoptosis [112]. In malignant gliomas, it was likewise shown to induce Bax and decrease Bcl-2 expression [62].

Clinically relevant concentrations (0.25 mM) of valproate (monotherapy) were also reported to increase the intracellular concentration of ROS. Even though this phenomenon can be partially compensated by a concomitant increase in glutathione (GSH) in some lines [88], VPA-induced ROS provoke an oxidation of bases from the DNA strands. Oxidized bases are normally removed by glycosylases, leaving abasic sites in the DNA molecule. These are recognized by an AP-endonuclease, which generates single-strand breaks (SSBs). These SSBs are normally efficiently repaired to prevent their conversion into lethal double-strand breaks (DSBs) during DNA replication or transcription [23], a mechanism that is, however, often deficient in tumor cells and is further inhibited by HDAC inhibitors, leading to cell death [113,114]. VPA has often proven a weak inducer of apoptosis in human glioma cell lines when used alone and in the submillimolar range [52,88,115]. In several glioma cell lines indeed, the VPA-dependent increase in ROS enhances the activity of the ERK1/2 MAPK kinases. Although the ERK/MAPK pathway is anti-apoptotic in essence, its activation by ROS seems to promote autophagy, which appears to be the main cause of cell death instead of apoptosis in glioma cell lines following VPA treatment alone [87].

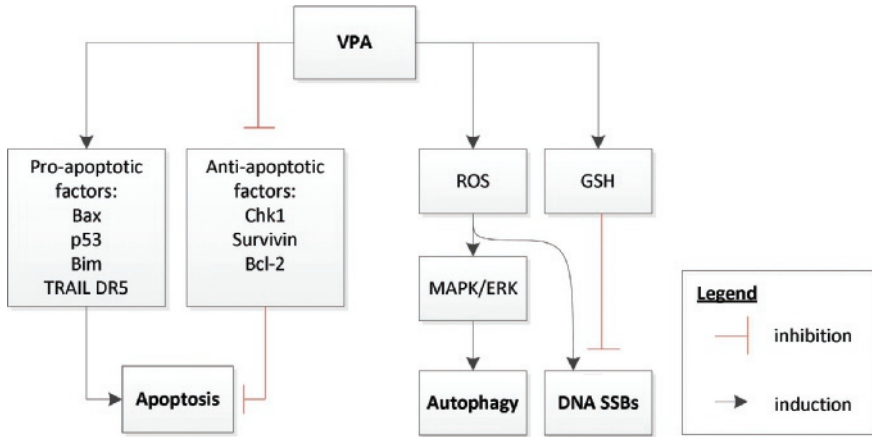


Figure 3 - VPA-mediated effects on cell death. VPA leads to the upregulation of several pro-apoptotic and anti-apoptotic factors [62,90,109-112]. Also VPA treatment results in increased formation of reactive oxygen species (ROS) [88]. ROS lead to autophagy and DNA single-strand breaks (SSBs). The effects of ROS are opposed by VPA-mediated increased expression of glutathione (GSH) [88]. Abbreviations: Bcl-2: B-cell lymphoma 2; Chk1: Checkpoint kinase 1; DNA: Deoxyribonucleic acid; ERK: Extracellular signal-regulated kinase; GSH: Glutathione; MAPK: Mitogen-activated protein kinase; ROS: Reactive oxygen species; SSBs: Single-strand breaks; TRAIL DR5: TNF-related apoptosis-inducing ligand death receptor 5; VPA: Valproic acid.

3.4 Anti-angiogenic effects of VPA

Valproate is a potent inhibitor of endothelial cell proliferation, migration and endothelial tube formation *in vitro* at submillimolar doses. Moreover, VPA was shown to inhibit angiogenesis in chick chorio-allantoic membrane assays and matrigel plug assays *in vivo* [116,117]. These results may prove important in the context of tumors in general, and specifically in glial tumors, where angiogenesis is key to tumor growth [118]. Like other HDAC inhibitors, VPA was shown to decrease the expression of VEGF, a potent inducer of angiogenesis, in several cancer cell types among which are prostate and colon carcinomas [119-121] and malignant gliomas [122]. Accordingly, VPA was also reported to inhibit angiogenesis in an *in vivo* model of rodent glioma [122].

The activity of another major determinant of tumoral angiogenesis, the hypoxia-inducible factor-1 α (HIF-1 α) transcription factor, is also directly and indirectly regulated by HDACs. Acetylation of transcriptional cofactor CBP/300 inactivates association with HIF-1 α . On the other hand, HIF-1 α also associates with several HDACs, among which 1 and 3, that regulate both its stability and its activity [123]. This interaction could be cell type specific and has to date not been studied in gliomas [124] where HIF-1 α emerges as a critical determinant of tumor progression, angiogenesis and stem cell maintenance [125,126].

3.5 VPA-mediated effects on tumor invasion

Diffuse brain invasion is a hallmark of malignant gliomas and contributes to their morbidity, recurrences and resistance to treatment [127-129]. Cell migration and invasion in glioblastomas depend on the activation of several signaling pathways, such as the PI3K/Akt, NF- κ B or Rho/ROCK signaling cascades [127,128]. Glioblastoma progression is also associated with altered expression of cell membrane receptors and changes in the composition of the central nervous system extracellular matrix [130,131].

HDAC inhibitors impede glioma cell migration and invasion in experimental models [132,133]. Several mechanisms play a role and include the overexpression of various integrins, downregulation of normal extracellular matrix components and changes in matrix metalloproteases 2 and 9 (MMP2 and MMP9) expression [132].

VPA impairs the mobility and invasion of malignant glioma cells in vitro at millimolar concentrations [102,134]. It decreases the expression and activity of MMP2 and MMP9, and strongly increases the expression of their inhibitor TIMP-1 [62]. At similar concentrations, VPA also represses interleukin 6 (IL-6) secretion and the activity of the NF- κ B pathway in gliomas [94], which are both significantly involved in the invasion of these tumors [71,127].

As for its cytostatic properties, the invasion-inhibitory effects of valproate, however, appear to vary with cell line, and pro-invasive properties of VPA have even been reported in one glioma cell line [134].

3.6 Modulation of the peri-tumoral environment by VPA

Aside from the neovascularization that both nourishes the tumor and creates niches where tumor progenitor cells can hide and become resistant to treatments [135], the brain tumor microenvironment has recently gained interest as a modulator of tumor growth and invasion. Several cell types are either attracted to the site of glioma growth or interact with them as tumors develop [136]. Microglial cells and macrophages adopt a specific non-inflammatory phenotype as they become attracted to glioblastomas. Endothelial precursor cells, fibroblasts and pericytes are also recruited to the tumor bed. Astrocytes in the vicinity of tumor cells are activated and the composition of the extracellular matrix progressively drifts. All these changes help reduce the immunogenicity of glioma cells, favor cell invasion through the secretion of matrix metalloproteases, chemoattractants and the activation of surface receptors [136,137] and may participate to the paracrine signaling cascades that enhance glioma growth [136]. Neural precursor cells are also attracted to tumor cells and may inhibit their proliferation [138,139], an effect that is thought to subside with age as neurogenesis decreases [136].

Interestingly, valproate was shown to modulate gene expression, phenotype and survival of several of these cell populations. It may for instance induce apoptosis in microglial cells at submillimolar concentrations [140]. VPA also inhibits neural progenitor cell death *in vivo* in developing rat pups [141], but may induce their differentiation and suppress their proliferation *in vitro* [44]. At higher doses (4 mM), it may also modulate the expression of several chemoattractants and interleukins in astrocytes [142]. In addition, VPA was reported to significantly alter the general pattern of gene expression in the brain when used chronically, as shown in rodent experiments [65].

Overall, however, the global contribution of all these emerging effects of valproate, as well as their potential action on the immune system and on the control of glioma proliferation still, remains to be elucidated.

3.7 Resistance to VPA

VPA is a substrate of neither members of the multidrug resistance family of proteins MDR1 and 2, nor the efflux-transporter P-glycoprotein [143-145]. Therefore, cell resistance to VPA seems to result from several other mechanisms. These were observed in several tumor cells, but have not yet been studied in gliomas [146].

VPA and other HDAC inhibitors for instance induce a reversible overexpression of the cytoprotective chaperone clusterin in neuroblastoma cells. The accumulation of clusterin suppresses VPA-induced growth arrest, as this protein binds to the pro-apoptotic protein Bax in the mitochondria and prevents Bax-mediated cytochrome C release and apoptosis [147].

In colon cancer cells, resistance to high-dose valproate (2 mM) may stem from mutations of the adenomatous polyposis coli (APC) protein. In wild-type APC-expressing cells, this supra-therapeutic concentration of valproate increases GSK-3 β . This leads to the phosphorylation and proteasome-mediated degradation of β -catenin and a reduced transcription of the anti-apoptotic factor survivin [148]. Mutant APC-expressing cells are unable to translate the VPA-induced GSK-3 β expression into a degradation of β -catenin and a downregulation of survivin.

Resistance may also develop in colon cancer cells treated with increasing concentrations of VPA. The resistance then remains irreversible after cessation of the treatment. Also cross-resistance to other HDAC inhibitors may develop. The mechanism that underlies this resistance is not yet completely understood, but does not seem to depend on an increased HDAC expression or on a general desensitization of cells to cytotoxic treatments [149,150]. Whether an influence of the mutL homologue 1 (MHL1) protein of the mismatch

repair complex or mutations of HDAC genes are involved in this irreversible resistance, as described for other HDAC inhibitors, is not yet known [150].

4. VPA AND COMBINATION THERAPY

As mentioned in the previous section, the effects of VPA on proliferation, death and migration/invasion of glioma cells are variable and weak when the drug is used alone. Valproate does, however, induce changes in the level of expression and activity of several key regulators of cell death and increases the production of reactive oxygen species. It also remodels the chromatin and increases its accessibility to potential DNA-damaging agents. The maintenance of the heterochromatin – a more compact form of DNA that may be less sensitive to DNA-damaging agents [151,152] – appears to depend mainly on HDAC 2. This HDAC is a primary target of VPA and is frequently overexpressed in glioblastomas [4,16,25]. Based on these arguments, several groups have assessed the cytotoxicity of combinations of chemotherapies, DNA-damaging drugs and radiation therapy with valproate in gliomas.

4.1 Chemotherapy and VPA

HDAC inhibitors effectively enhance the cytotoxicity of DNA-damaging drugs and cytotoxic chemotherapies in a variety of tumor types in experimental conditions [21,153,154]. In gliomas specifically, *in vitro* studies showed that VPA synergizes with the topoisomerase-II poison, anti-proliferative and DNA-damaging agent etoposide [52]. In these experiments, the combination of high doses of VPA (1.5 mM) and etoposide synergically increased the fraction of cells in G₂/M arrest and induced prominent apoptosis, independent of the p53 status of the tumors. Mechanisms underlying this synergy are thought to involve increased access of topoisomerase inhibitors to the DNA molecule and machinery through increased histone H3 and H4 acetylation, and VPA-induced alteration of the expression of several key heterochromatin maintenance genes [25]. Anecdotally, VPA induced the expression of both the α - and β -isoforms of topoisomerase-II in these cells, and the increased protein level of the alpha isoform seemed to correlate with more resistance to etoposide cytotoxicity in one tested cell line [52].

Lower doses of VPA (0.375 mM) failed to produce any synergy between VPA and etoposide [52]. Another *in vitro* study also failed to observe any enhancement of cytotoxic or cytostatic effect by 0.25 mM VPA combined with bis-chloroethylnitrosourea (BCNU), cytarabine, teniposide, vincristine, cisplatin or doxorubicin in glioma cells [155]. At a concentration of 1 mM, however, VPA can sensitize glioma cells *in vitro* and *in vivo* to the alkylating agent BCNU [115] and enhances the efficacy of autophagy-inducing agents, such as the PI3K inhibitor Ly294002 or the mTOR blocker rapamycin [87].

These results might raise the possibility that VPA only enhances the effect of cytotoxic drugs at concentrations at least equal to 1 mM. However, valproate was still recently shown to potentiate the apoptotic effect of alkylating agent temozolomide in glioma cells at submillimolar concentrations (0.25 mM) in a ROS- and Nrf-2 translocation-dependent fashion [88].

4.2 Radiation therapy and VPA

HDAC inhibitors are studied as radiosensitizing agents, since hyperacetylation of the core histones of chromosomes leads to a decondensed chromatin structure. This mimicks euchromatin, alters gene expression and may affect the distribution of tumor cells in the cell cycle [156-158]. These factors are believed to influence the efficacy of radiation therapy. Although still a matter of debate [157], euchromatin has been reported to be more sensitive to radiation therapy than heterochromatin. The efficacy of DNA repair mechanisms might also differ between these two forms of DNA [151,152]. In agreement with those hypotheses, VPA enhances radiosensitivity of glioma cells *in vitro* and *in vivo* at concentrations of 0.5 - 2 mM (Figure 4), and this effect remains when radiation therapy is combined with temozolomide therapy [159]. The amplitude of core histone hyperacetylation correlates with radiosensitivity [53,86,160].

Non-core histones are, however, also probably involved in the synergy between radiation therapy and valproate treatment. DNA DSBs are regarded as one of the most important radiation-induced lesions that lead to cell death – often by apoptosis or mitotic catastrophe – or to cell senescence. The repair of DNA DSBs is critical in determining radiosensitivity [161]. Most DNA DSBs are repaired by non-homologous end joining (NHEJ) during the G1 phase of the cell cycle. This mechanism involves the phosphorylation of histone H2Ax and its recruitment to DNA DSBs and subsequent recruitment of several DNA repair enzymes. The availability of a sister chromatid following DNA replication allows homologous recombination (HR) in G2 and S phases [162,163]. It has been observed that VPA treatment induces a persistence of phospho-H2Ax foci beyond their time of normal disappearance following irradiation, and it is suspected that VPA induced a defect in DNA repair mechanism [53,160]. In agreement with this finding, others have observed that valproate also sensitized glioma cells to the effect of radiation therapy when given after radiation exposure. This phenomenon was also accompanied by delayed dispersal of phospho-H2Ax foci and acetylation of H2Ax [86,160].

Interestingly, using COMET assays, it was recently observed that the persistence of DNA repair complexes at sites of initial DNA damage did not correspond to the persistence of DNA DSBs. Instead, the DNA repair machinery was not able to dissociate from the DNA molecule. It was then suggested that the increased acetylation of histone H2Ax following VPA treatment impaired the dephosphorylation of this protein. This would prevent the

dispersal of the entire complex. Subsequently, this would prevent blocking cell mitosis during subsequent divisions and provoke a mitotic catastrophe [164] (<http://videocast.nih.gov/Summary.asp?File=15828>).

As seen in other cell types and models, several other mechanisms might contribute to VPA-induced radiosensitization and alteration of DNA repair mechanisms. Examples include alteration of p53 acetylation [165] or, as shown for other HDAC inhibitors, acetylation of Ku70, a key NHEJ component, and altered expression of genes encoding HR components [23,86,160]. In p53-WT colon carcinoma cells, VPA exposure leads to radiation-induced expression of mitochondrial Bax, cytochrome C release and mitochondrial membrane depolarization, resulting in increased apoptosis [26].

Interestingly, on the contrary to what has been reported in other cancer types, where the radiosensitizing effect by VPA differs between wild-type and mutant p53-dependent cells [26], the radiosensitizing effects of VPA have been observed in both p53 WT and p53-mutant glioma cells [53,160].

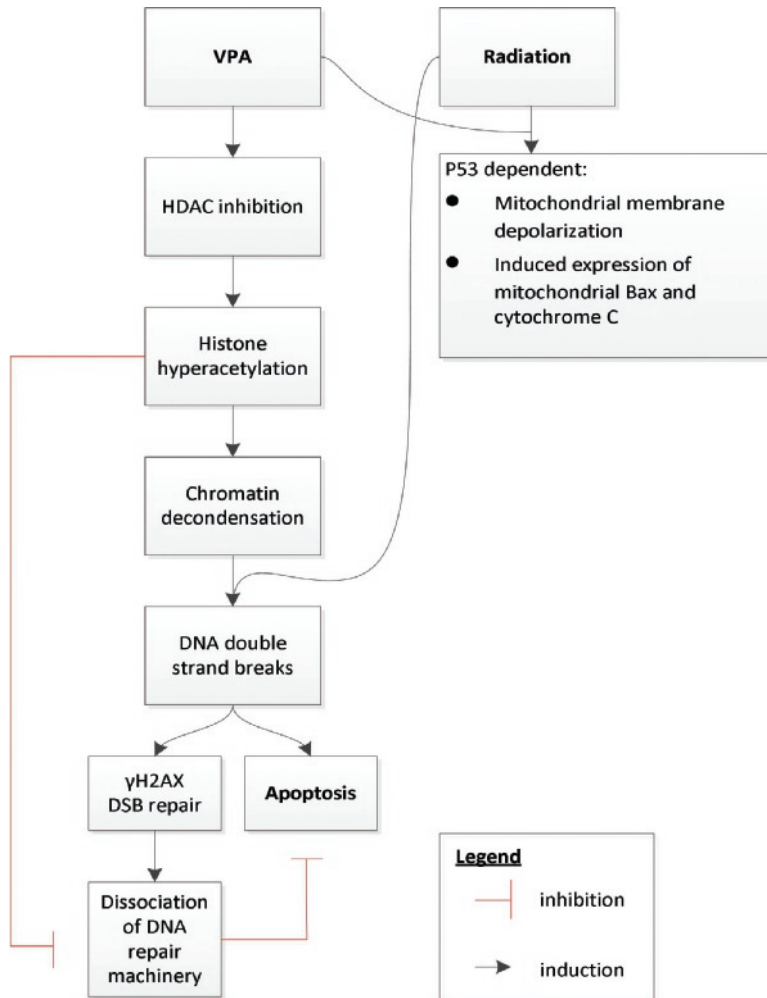


Figure 4 - Proposed mechanism for radiosensitization of glioma cells by VPA. VPA leads to histone hyperacetylation (including H2Ax) in glioma cells through HDAC inhibition [53,160]. Histone hyperacetylation leads to chromatin decondensation, which sensitizes the DNA to radiation therapy. Radiation causes DNA double-strand breaks (DSBs), which in combination with VPA exposure results in the phosphorylation of histone H2AX (γ H2AX). The dispersion of γ H2AX is associated with DNA DSB repair [53,86,160]. DNA DSBs initiate apoptotic cell death, unless efficiently repaired [26]. VPA-mediated histone H2Ax hyperacetylation possibly inhibits the dissociation of the DNA repair machinery from the DNA after DSB repair. This may lead to apoptosis [164]. In p53-WT colon carcinoma cells, VPA exposure leads to radiation-induced expression of mitochondrial Bax, cytochrome C release and mitochondrial membrane depolarization, resulting in increased apoptosis [26]. Abbreviations: DNA: Deoxyribonucleic acid; DSB: double-strand break; HDAC: Histone deacetylase; VPA: Valproic acid.

4.3 Valproate and miscellaneous experimental therapies

Aside from radiation therapy and targeted and anti-mitotic chemotherapies, several novel strategies are currently being developed in the treatment of gliomas. Among these, VPA was shown to increase the propagation and glioma cell killing induced by herpes-based oncolytic virus, albeit at high doses (5 - 30 mM) [166]. We found N-butyrate, an HDAC inhibitor with a pharmacological profile similar to that of valproate, to enhance the bystander effect of HSV-TK/ganciclovir gene therapy in gliomas [21]. Valproate was shown to increase the efficacy of this treatment in head and neck carcinomas [167]. It was also shown to increase caspase 8 expression in medulloblastoma cells deficient for this protein and thereby to restore TRAIL killing [168].

There is to date no report on the influence of VPA on other novel therapies, such as dendritic cell vaccination, targeted cytotoxin delivery or photodynamic therapy.

5. CLINICAL USE OF VALPROATE

5.1 Pharmacokinetic data

5.1.1 Absorption and distribution

VPA exists in a dissociated form in aqueous solutions and can be delivered to organisms and cells in the form of magnesium or sodium salts. These salts are bioequivalent [169] and can be administered orally or intravenously. When administered as uncoated tablets containing sodium valproate, the drug rapidly dissociates in the stomach to the corresponding acid. The oral bioavailability is almost complete, but the time to reach the maximum plasma concentration and the maximum concentration achieved depends on the pharmaceutical preparation. Maximum concentrations usually occur within 2 - 3 h for syrup, capsules and uncoated tablets; between 3 and 5 h for enteric-coated tablets; and between 5 and 10 h for sustained release preparations [2].

Serum and plasma levels of valproate are routinely measured by commercial reagent-based immunoassay techniques [170]. Other techniques include gas chromatography [171] and high-performance liquid chromatography [172]. The target range of plasma VPA concentration is 40 - 100 mg/l for epilepsy (0.28 - 0.7 mM) [173], although earlier reports showed serum ranges of 60 - 120 mg/l (0.42 - 0.84 mM) to be safe and effective [174]

The starting dosage in adults, when used for the treatment of epilepsy, is usually 500 mg twice daily, which is then increased at intervals of 2 - 3 days according to the clinical response. The usual effective dosage when used as an anti-epileptic drug is 500 - 2500 mg/day in two or three divided doses with conventional formulations or two divided daily doses with sustained release formulations. In children, treatment may be initiated with

10 - 15 mg/kg/day and increased, if necessary, by 10 - 15 mg/kg/day in 2-week intervals according to the clinical response. If dosages above 40 mg/kg/day are required, clinical chemistry and hematological parameters should be monitored with special care as they carry a higher risk of hematological toxicity (see below) [2,175].

VPA is extensively bound to plasma proteins (> 90%), mainly to plasma albumin. The extent of binding decreases with increasing drug concentration and varies between 85 and 94%. The distribution of sodium valproate is mostly restricted to the circulation and rapidly exchangeable water, with an apparent volume of distribution of 0.13 - 0.19 l/kg [2]. Valproate can, however, distribute to other compartments, including breast milk where concentrations of up to 15% of total plasma levels can be found [176]. Valproate also crosses the blood-brain barrier effectively and rapidly. Mechanisms involve both passive diffusion and bidirectional carrier-mediated transport via an anion exchanger at the brain capillary endothelium. As a result, cerebrospinal fluid (CSF) concentrations vary between 1 and 10% of total plasma concentrations, while the ratio between CSF and unbound plasma concentrations ranges between 0.6 and 1.0 [2]. Active transport mediates the uptake of VPA into neuronal and glial cells, which results in intracellular concentrations that are higher than interstitial fluid concentrations [2,177]. This transport notably depends on monocarboxylate transporter 1 (MCT1) [178], a membrane protein that is overexpressed in gliomas in correlation with histological grade [[179] and personal, unpublished observation].

5.1.2 Metabolism and plasmatic half-life

VPA is metabolized primarily in the liver, notably via microsomal glucuronide conjugation, mitochondrial β -oxidation and cytochrome P450-dependent oxygenation involving the CYP2C9, CYP2A6, CYP2B6 and CYP2C19 isoforms of this enzyme [2,180]. Only a small fraction of unchanged VPA is excreted in the urine, together with its metabolites. A small portion of the drug is also excreted via the feces [2].

5.1.3 Drug interactions

VPA is categorized as a non-enzyme-inducing anti-epileptic drug (non-EI-AED) and slightly inhibits cytochrome P450 isoenzymes CYP2C9, CYP2C19, CYP2D6, CYP3A4 and the UDP glucuronosyltransferases UGT1A4 and UGT1A1. VPA, however, slightly induces CYP2A6 and it can significantly displace drugs from plasma proteins. These effects result in several pharmacological interactions (Table 3). For instance, VPA-mediated inhibition of drug metabolism leads to increased plasma concentration of anticonvulsant drugs phenobarbital and lamotrigine [181]. It can also displace anticoagulants as warfarin from plasma proteins and induce significant INR changes [182].

On the other hand, enzyme-inducing drugs such as several other anti-epileptic drugs (e.g., carbamazepine or phenytoin) stimulate VPA metabolism and increase its clearance. Likewise, several non-steroidal anti-inflammatory drugs displace VPA from plasma proteins and may compete with VPA for mitochondrial oxidation in the liver [2].

In the setting of glioma chemotherapies, VPA does not interact with imatinib or irinotecan and its metabolite SN-38 [183]. Through CYP inhibition, however, it is suspected to decrease the rate of metabolism of 1-(2-chloroethyl)-3-cyclohexyl-1-nitrosourea (CCNU), which may lead to elevated drug concentrations and increased hematological toxicity [184,185], and was shown to decrease the clearance of temozolomide by approximately 5% (source: NHS evidence, UK). In addition, VPA interacts with cisplatin for binding of plasma proteins and is associated with an increased risk for hematological toxicities due to higher levels of this chemotherapy [186]. Finally, sorafenib inhibits cytochrome p450 isoforms, such as CYP2B6, and might influence the plasma levels of VPA [186].

Of lesser relevance in the context of gliomas, the use of methotrexate lowers the plasma levels of VPA, which could be due to damage to the intestinal mucosa and impaired absorption. Finally, the anticancer drug vorinostat also inhibits the activity of the class I and II HDACs and has been reported to cause thrombocytopenia and gastrointestinal bleeding when used in combination with other HDAC inhibitors, such as VPA [186].

Table 3 – Reported drug interactions with VPA

Drug interactions with VPA	Reference
VPA increases drug plasma concentration:	
AEDs: Phenobarbital, lamotrigine	[181]
Warfarin	[182]
CCNU	[184, 185]
Temozolomide	NHS evidence, UK
Cisplatin	[186]
Drug increases VPA plasma concentration:	
NSAIDs	[2]
Sorafenib	[186]
Drug decreases VPA plasma concentration:	
EI-AEDs: carbamazepine, phenytoin	[2]
Methotrexate	[186]
Other drug interactions with VPA:	
Vorinostat	[186]

Abbreviations: VPA, valproic acid; AEDs, anti-epileptic drugs; CCNU, 1-(2-chloroethyl)-3-cyclohexyl-1-nitrosourea; NSAIDs, non-steroidal anti-inflammatory drugs; EI-AEDs, enzyme-inducing anti-epileptic drugs.

5.2 Side effects of VPA

VPA is generally well tolerated. Neurological side effects such as sedation, dizziness and tremor, as well as mild gastrointestinal toxicities may, however, be reported early during treatment (Table 4) [187]. Chronic use of VPA can result in body weight gain, hyperinsulinism, hypothyroidism and hair loss or changes in hair texture. Some also consider VPA a possible cause of polycystic ovarian syndrome or hyperandrogenism, but this remains a topic of discussion [188,189]. Hyperammonemia is reported in up to 50% of patients treated with VPA and especially in those who concurrently take enzyme-inducing anti-epileptic drugs (EI-AEDs). Although usually asymptomatic, hyperammonemia due to valproate can result in a mild to severe encephalopathy [190]. A VPA-induced decrease in plasma carnitine levels has also been reported and might play a role in several other side effects of the drug, including hyperammonemia and liver deficiency [2,175].

Valproate was reported to alter the production and plasma levels of several coagulation factors, notably factor 13. This results in an increased risk of bruising, epistaxis or, theoretically, surgical bleeding for craniotomy patients [191,192]. It is the authors' personal experience, however, that valproate treatment does not lead to increased preoperative or postoperative bleeds during craniotomies for tumor removal. This fact is confirmed by

several independent studies that did not report any increased bleeding complications in valproate-treated patients undergoing neurosurgery [193,194].

Hematological toxicity occurs in 1 - 32% of patients using VPA and results mainly in asymptomatic, dose-dependent thrombocytopenia, but neutropenia and more severe forms of bone marrow toxicity have also been reported [195,196]. As a result of combined toxicity and metabolic interaction, bone marrow toxicity is more frequent when valproate is used in combination with chemotherapy [184,185].

Of note, the use of VPA in combination with EI-AEDs is associated with an increased risk of procarbazine hypersensitivity reactions, possibly through formation of a reactive intermediate generated by CYP3A isoform induction. It is, however, not yet known whether VPA alone is also associated with an increased risk of procarbazine hypersensitivity reactions [197].

Severe idiosyncratic reactions to VPA may also occur. Acute valproate-induced pancreatitis is unusual, but may be fatal and its mechanism remains unknown [198]. Acute liver failure occurs at an incidence of 5/100,000 and is more frequent in patients with mitochondrial, metabolic or pre-existing liver disease as well as in pediatric patients under the age of 2 [2]. Early signs include apathy, anorexia, nausea and jaundice and should always lead to assessment of liver function, discontinuation of the treatment and, possibly, carnitine therapy [199].

Finally, VPA is teratogenic in humans and administration of VPA during pregnancy can result in major malformations, dysmorphic syndromes and a risk of neural tube defects of 1 - 3% [200].

Table 4 – Reported adverse effects due to VPA treatment

Adverse effects due to VPA treatment	Reference
Neurological adverse effects:	
Sedation	[187]
Dizziness	[187]
Tremor	[187]
Encephalopathy	[190]
Gastrointestinal adverse effects:	
Mild gastrointestinal toxicity	[187]
Liver deficiency / acute liver failure	[2, 175, 199]
Acute pancreatitis	[198]

Table 4 (continued) – Reported adverse effects due to VPA treatment

Adverse effects due to VPA treatment	Reference
Hematological adverse effects:	
Bruising, epistaxis, surgical bleeding	[191, 192]
Trombocytopenia	[195, 196]
Neutropenia	[195, 196]
Bone marrow toxicity	[195, 196]
Endocrine adverse effects:	
Body weight gain	[188, 189]
Hyperinsulinism	[188, 189]
Hypothyroidism	[188, 189]
PCOS / hyperandrogenism	[188, 189]
Teratogenic effects:	
Malformations, dysmorphic syndromes	[200]
Neural tube defects	[200]
Other adverse effects:	
Hair loss / change in hair texture	[188, 189]
Procarbazine toxicity (in combination with EI-AED)	[197]

Abbreviations: VPA, valproic acid; PCOS, polycystic ovarian syndrome; EI-AED, enzyme-inducing anti-epileptic drug.

5.3 Clinical experience in the context of glioma treatment

5.3.1 Case reports and retrospective clinical studies in gliomas

In 2004, a case report was published about a 10-year-old male with a glioblastoma who was initially treated with partial surgical resection and radiochemotherapy with etoposide, vincristine and procarbazine [195,201]. After 20 weeks, the chemotherapy was switched to topotecan due to adverse effects. The clinical condition of the patient kept worsening and the topotecan treatment was discontinued after 10 weeks. The patient was then started on oral VPA (plasma levels > 1 mmol/l or 140 mg/l). Following this treatment, the clinical situation improved and the patient was able to attend school again. After 14 weeks, tumor size decreased and after 10 months MRI scans showed complete remission. However, the patient reduced the dosage of VPA treatment himself, because of drug-related drowsiness, and the tumor relapsed 16 months after the onset of VPA therapy [201].

Rokes et al. subsequently reported a case of a 10-month-old female with a spinal glioblastoma. After disease progression using an intensified chemotherapy regimen [195], a combination of daily sorafenib, daily VPA (100 - 150 mg/l), daily hyperbaric oxygen and monthly temozolomide was used and resulted in a clinical and radiological improvement in the patient that lasted at least 12 months after initial presentation [202].

A retrospective patient study reported the effects of EI-AEDs or non-EI-AEDs (mainly sodium valproate) in 168 patients with glioblastomas treated with surgery, radiation therapy and chemotherapy (CCNU or temozolomide) on survival and hematotoxicity. A median survival of 11.7 months was observed in the group of patients not receiving any AED ($n = 88$). The median survival was 10.8 months in the group receiving EI-AEDs ($n = 43$), but reached 13.9 months for those taking non-EI-AEDs ($n = 37$). Although the survival differences between patients taking either type of AEDs and those not taking any did not reach statistical significance, it did between the group receiving EI-AEDs and the group receiving non-EI-AEDs ($p = 0.042$). Of note, however, increased hematotoxicity (grades 2 and 3 events) was seen in the group receiving non-EI-AEDs in comparison with patients treated with EI-AEDs [185].

Another study explored the effects of anti-epileptic drugs in patients with gliomas and seizures and also compared the survival of glioma patients with and without VPA [203]. The authors noted a positive trend of VPA on the outcome of glioblastoma patients ($n = 56$): median survival reached 20 months in patients using VPA (with or without other AEDs) versus 15 months in the group of patients who did not use VPA despite a younger median age in this latter group. This difference did, however, not reach statistical significance (log rank $p=0.460$), possibly due to the small number glioblastoma patients without VPA [203].

More recently, Weller et al. performed a subgroup analysis of the survival of patients included in EORTC 26981-22981/ NCIC CE.3, based on the nature of their concomitant intake of anti-epileptic drugs. A total of 573 patients was identified, of which 97 patients received VPA only. No difference in overall survival was found between patients receiving either VPA, enzyme-inducing anti-epileptic drugs or no anti-epileptic drugs and treated with postoperative radiation only. The survival benefit of adding temozolomide to radiation therapy tended, however, to be higher in patients receiving valproate than in patients receiving EI-AEDs ($p = 0.042$) or none at all (trend, $p = 0.09$). Whether the additional benefit of VPA in patients treated with chemotherapy and radiation therapy results from a potentiation of this therapy or from increased bioavailability of the chemotherapy (temozolomide) could not be assessed from this study. Moreover, patients on valproate and temozolomide experienced significantly more thrombocytopenia and leucopenia events than those with EI-AED. There was, however, no difference between the three epilepsy treatment subgroups with respect to grade 3 or 4 adverse hematological events [204].

Recently, a retrospective study was published in which the effect of VPA treatment on overall survival of glioblastoma patients was investigated. A total number of 102 patients was identified, of whom 33 had received VPA treatment, with a serum target level of 50 - 100 mg/l (0.35 - 0.69 mM). In uni-variate analysis, VPA appeared to have a significant effect on overall survival ($p = 0.035$) in univariate analysis. However, no significant effect

was seen in multivariate analysis taking additional patient characteristics into account. Notably, patients receiving VPA treatment also tended to be in the temozolomide group, which might explain the survival benefit of VPA found in the univariate analysis. However, in the temozolomide chemotherapy group, the hazard ratio (HR) of the patients who received VPA within 1 week after surgery was lower than that of the patient group that had not received VPA (HR = 0.607). This was not the case in the group that did not receive temozolomide [205]. These results corroborate the study published by Weller et al., which was mentioned above [204].

The authors also assessed the level of VPA-induced histone hyperacetylation in seven patients of which they had received pre- and post-VPA treatment surgical samples. Of these seven surgical samples, four displayed increased acetyl-H3K9 staining. These results indicate that VPA (0.5 mM) can induce histone hyperacetylation in a subset of glioblastoma patients [205].

Finally, a large single center retrospective study reviewed the incidence of radiation necrosis in a series of 439 consecutive patients irradiated for a glioma with conventional doses and fractions between 1996 and 2003. In the 426 patients who could be analyzed, 21 developed proven radiation necrosis after being followed up until death or a minimum 3 years for surviving patients. Although the incidence of radiation necrosis was not influenced by treatment with VPA at the time of irradiation, the onset of the radionecrosis was significantly delayed in those patients ($p = 0.013$) [206].

5.3.2 Prospective clinical trials in gliomas

A recently published multicenter Phase I study of VPA in solid tumors including CNS tumors enrolled 26 pediatric patients, of which 16 were evaluable for treatment toxicity. Ten out of these sixteen evaluable patients reached target VPA levels of 100 - 150 mg/l (cohort 1), three patients experienced dose-limiting toxicities in the form of grade 3 excessive somnolence ($n = 2$) and one patient with lung metastases from synovial sarcoma experienced a lethal hemothorax (grade 5). In contrast, no severe adverse event was noted in those six patients with serum VPA levels of 75 - 100 mg/l (cohort 0). One partial response (PR) was reported in a patient with thalamic glioblastoma from cohort 0 and treated for 7 months, and one minor response in a brainstem glioma treated for 5 months in cohort 1. Several pharmacokinetic measurements were also performed during this study, showing that the unbound fraction of VPA increased from 20% up to 125 mg/l of total serum concentration, but rose sharply to more than 40% beyond this concentration [207]. Finally, 50% of patients showed increased acetylation of histones H3 and H4 in their peripheral blood mononuclear cells with respect to pre-treatment values. Although this increase did not correlate well with the serum levels of VPA, the most dramatic increase in

acetylation status of histones H3 and H4 was observed in the patient with a glioblastoma who experienced PR after treatment with VPA for 7 months [207].

The HIT-GBM[®] treatment protocol is a prospective, multicenter, Phase II cohort comparison study performed in pediatric patients (aged 3 - 18 years) suffering from diffuse intra-pontine or high-grade (WHO grade 3 or 4) gliomas and treated following several treatment protocols [208]. In the HIT-GBM-C cohort, patients were treated with standard fractionated radiation and concomitant chemotherapy. Radiation was started within 14 days after diagnosis and was given to the tumor and a 2-cm margin in 5 1.8-Gy fractions a week, up to a total of 54 Gy for patients 6 years and younger, as well as to brain stem localizations. A total dose of 59.4 Gy was given to older patients with tumors in other locations. Chemotherapy started during the first week of radiation and the first cycle consisted of cisplatin 20 mg/m² 5 days, etoposide 100 mg/m² 3 days and vincristine 1.5 mg/m² on day 5 (PEV cycle). This was followed by weekly vincristine and, during the last week of radiation therapy, one PEIV cycle (consisting of PEV plus ifosfamide 1.5 g/m² / day on days 1 - 5). Chemotherapy then continued for a maximum of eight monthly cycles of PEIV preceded by vincristine 1 week before. Oral VPA was introduced as a single maintenance treatment after at least four intensive chemotherapy cycles with stable disease or completion of the eight cycles, or as a rescue treatment in patients progressing/ relapsing under chemotherapy. Doses of VPA were progressively increased to attempt to reach target levels of 100 - 150 mg/l in the serum [195]. In an initial report, adverse events and early tumor response 6 weeks after the introduction of VPA were assessed using unidimensional measurements of MRI tumor volume in 44 patients not otherwise treated with VPA (i.e., for epilepsy) [106]. The mean serum level of VPA was 99 ± 26 mg/l. While the authors did not report any serious adverse events, minor toxic reactions (grade I or II somnolence (three counts) and one count of each with difficulties in concentrating, increased sensitivity to light, enuresis thrombocytopenia and anemia) occurred and were paradoxically more frequent in patients with lower serum levels of VPA. Among 22 patients who started VPA treatment after completion of the HIT-GBM-C protocol, 19 remained stable after 6 weeks and 3 developed progressive disease. Fourteen of the remaining twenty-two patients, who received VPA treatment as a relapse therapy, could be evaluated for tumor response. Of those patients, one experienced a partial response (i.e., more than 50% decrease in tumor diameter), seven had stable disease and six further progressed. Outcomes did not correlate with VPA serum levels in all these patients [106].

A more recent evaluation of a larger number of patients included in the HIT-GBM-C protocol compared the outcome of the patients included in this study with cohorts of patients with similar tumors but enrolled in other treatment protocols (HIT-GBM-A and B) that notably did not include VPA in the treatment [195]. The overall survival rates of all 97 patients treated according to the HIT-GBM-C protocol were 91% at 6 months, 56%

at 12 months, 30% at 24 months and 19% after 60 months. Patients with pontine tumors fared the worse while patients with completely resected tumors had better survival than others. For patients with pontine tumors or residual tumor after surgery outside the pons, no significant effect was found on median overall survival duration for the treatment group in comparison with the historical control group. On the contrary, patients with completely resected tumors in the HIT-GBM-C treatment group had a far better outcome and had not yet reached the median overall survival, as compared with those of cohorts B and A, who together had a median overall survival of 1,85 years (± 0.6 ; 95% CI: 0.78 - 4.4) [195]. The specific benefit of VPA with respect to other chemotherapies included in the treatment protocol of cohort C was not specifically evaluated however.

5.3.3 Active clinical trials

As of the date of writing this manuscript, and to the best of our knowledge, there are only two clinical trials using VPA in glioma therapy and opened for accrual (www.clinicaltrials.gov, Table 5). The first study is a multi-institutional Phase II trial opened in March 2006 with VPA in combination with radiation therapy and temozolomide (Stupp protocol, [12]) as the first line of treatment of adult patients with glioblastoma. The study aims to enroll 41 patients and VPA therapy is started 1 week before radiation therapy and is given twice a day until completion of the combined phase of chemotherapy and radiation therapy. Clinical and imaging follow-up is planned 1 month after the completion of therapy, then every 3 months for 2 years and then every 6 months for 3 years. No study results have been published yet (www.clinicaltrials.gov; NCT00302159).

The second study is a pediatric, non-randomized Phase II study of VPA and radiation, followed by maintenance therapy of VPA and bevacizumab. The study will enroll 56 patients between 3 and 21 years old, with newly diagnosed high-grade gliomas or brain stem gliomas. Patients receive radiation therapy in a total dose between 54.0 and 59.4 Gy pending on their age, in 30 - 33 fractions over 6 - 7 weeks. After radiation therapy, patients receive bevacizumab (10 mg/kg i.v.) every 2 weeks for a maximal duration of therapy of 24 months. Oral VPA is administered daily during radiation and bevacizumab therapy. Target concentrations are 85 - 115 mg/l. No study results have been published yet (www.clinicaltrials.gov; NCT00879437).

Table 5 - Published and active clinical trials using VPA in glioma treatment.

Published results				
Study type	Patients (no.; age)	VPA schedule; dose	Combination therapy	Outcome
Case report [201]	GBM (1; 10 years)	> 1 mmol/L	-	CR after 10 months, relapse after 16 months after lowering VPA dosage.
Case report [202]	Spinal GBM (1; 10 months)	100-150 mg/L	Sorafenib (50 mg 2/day) Monthly TMZ Bevacizumab Daily hyperbaric oxygen	Clinical and radiological improvement during at least 12 months.
Retrospective [185]	GBM (168; adults)	Daily; 900 mg	CCNU (100 mg/m ²) or TMZ (150 mg/m ²)	Patients receiving non-EI-AEDs showed higher OS than patients receiving EI-AEDs.
Subgroup analysis [203]	Brain tumor (140; adults)	VPA as AED	Surgery, radiation and/or chemotherapy. Other AEDs.	No significant positive effect of VPA on OS in GBM patients.
Retrospective [204]	GBM (573; adults; 97 receiving VPA only)	VPA as AED	RT alone or RT+TMZ	Survival benefit of adding TMZ to treatment regimen is higher for patients receiving VPA.
Retrospective [205]	GBM (102 adults)	VPA as AED	Surgery, RT and/or chemotherapy	Survival benefit in patients receiving VPA in univariate analysis. Lower HR in patients receiving VPA + TMZ than in patients receiving TMZ alone. Histone hyperacetylation in a subset of patients.
Retrospective [206]	Glioma (426)	VPA as AED	RT	21 patients developed radiation necrosis. Significant delay of onset radiation necrosis in patients receiving VPA during RT.

Table 5 (continued) - Published and active clinical trials using VPA in glioma treatment.

Published results				
Study type	Patients (no.; age)	VPA schedule; dose	Combination therapy	Outcome
Phase I [207] NCT00107458	Refractory solid or CNS tumors (16; children)	Daily; 100-150 mg/L and 75-100 mg/L	-	100-150 mg/L: DLTs 75-100 mg/L: 1 PR, 1 MR and 1 unconfirmed MR. Increased histone acetylation in PBMN cells in 50%.
Phase II [106]	HGG (44; children)	Maintenance after HIT-GBM-C protocol or relapse; daily; 100-150 mg/L	HIT-GBM-C protocol	After HIT-GBM-C protocol: 19 SD, 3 PD. After relapse: 1 PR, 7 SD, 6 PD.
Phase II [195]	HGG and DIPG (97; children)	Daily after radiation therapy; 100-150 mg/L	Radiotherapy (54-59,4 Gy) Chemotherapy (PEV, vincristine, PEI)	Higher OS for patients with completely resected tumors then for patients with residual tumor (median OS not reached vs. 1.85 (± 0.6) years).
Active clinical trials				
Study type	Patients (no.; age)	VPA schedule; dose	Combination therapy	Primary outcome measures
Phase II NCT00302159	GBM (41; adults)	Twice a day during radiation and chemotherapy	Radiation therapy Temozolomide	Progression free survival and overall survival
Phase II NCT00879437	HGG or brain stem glioma (56; 3-21 years)	Daily, 85-115 mg/L	Radiation therapy (54-59,4 Gy) Maintenance: bevacizumab	Event free survival

Abbreviations: VPA, valproic acid; GBM, glioblastoma multiforme; HGG, high-grade glioma; DIPG, diffuse intrinsic pontine glioma; CNS, central nervous system; mmol, millimole; L, liter; mg, milligram; m, meter; TMZ, temozolomide; CCNU, 1-(2-chloroethyl)-3-cyclohexyl-1-nitrosourea; AEDs, anti-epileptic drugs; EI-AEDs, enzyme-inducing anti-epileptic drugs; RT, radiotherapy; HIT-GBM-C, hirtumor-glioblastoma multiforme-C; CR, complete response; PR, partial response; MR, minor response; SD, stable disease; PD, progressive disease; OS, overall survival; HR, hazard ratio; DLT, dose-limiting toxicity; PBMN, peripheral blood mononuclear.

6. EXPERT OPINION

VPA is a drug that has been used in humans for more than 50 years for the treatment of epilepsy and as a mood stabilizer. Although it presents a safe clinical profile, this drug is also a potent teratogenic agent during pregnancy, which led to uncover its HDAC inhibitor properties. At doses that can be reached in human serum and in the CSF, this drug was shown to alter the expression and/or function of several regulators of tumor cell growth, migration and death. Of particular importance in the scope of glial tumors, valproate is notably a modulator of GSK-3 β -, NF- κ B-, STAT3- and β -catenin-dependent signaling and inhibits angiogenesis and may decrease cell invasion. Preclinical evidence also demonstrates the DNA repair inhibitory properties of VPA, which contribute to its potentiating effect on cytotoxic treatments such as chemotherapies (e.g., temozolomide and etoposide) or radiation therapy.

Based on these abundant preclinical *in vitro* and *in vivo* data, as well as on reports of efficacy in the treatment of human hematological malignancies, valproate is slowly entering the clinical field of glioma treatment, both in pediatric and in adult populations, and the results of a few Phase I and Phase II clinical studies have been published and show promising results.

The effects of valproate on glioma cells may, however, vary in relation with the molecular characteristics of given tumors, and the mechanisms of resistance of tumor cells to VPA are not yet completely understood. As a result, the effects of VPA may remain weak when used as a single agent in malignant glioma therapy. The combination of VPA treatment with chemotherapy and/or radiotherapy thus appears a rational option that deserves well-designed prospective clinical trials that assess the safety, the efficacy and the molecular characteristics of the responding tumors in these patients.

REFERENCES

1. Duenas-Gonzalez A, Candelaria M, Perez-Plascencia C, Perez-Cardenas E, de la Cruz-Hernandez E, Herrera LA. Valproic acid as epigenetic cancer drug: Preclinical, clinical and transcriptional effects on solid tumors. *Cancer Treat Rev.* 2008 May;34(3):206-22.
2. Perucca E. Pharmacological and therapeutic properties of valproate: A summary after 35 years of clinical experience. *CNS Drugs.* 2002;16(10):695-714.
3. Gottlicher M, Minucci S, Zhu P, Kramer OH, Schimpf A, Giavara S, et al. Valproic acid defines a novel class of HDAC inhibitors inducing differentiation of transformed cells. *EMBO J.* 2001 Dec 17;20(24):6969-78.
4. Bradner JE, Mak R, Tanguturi SK, Mazitschek R, Haggarty SJ, Ross K, et al. Chemical genetic strategy identifies histone deacetylase 1 (HDAC1) and HDAC2 as therapeutic targets in sickle cell disease. *Proc Natl Acad Sci U S A.* 2010 Jul 13;107(28):12617-22.
5. Haberland M, Montgomery RL, Olson EN. The many roles of histone deacetylases in development and physiology: Implications for disease and therapy. *Nat Rev Genet.* 2009 Jan;10(1):32-42.
6. Chen Y, Wang H, Yoon SO, Xu X, Hottiger MO, Svaren J, et al. HDAC-mediated deacetylation of NF-kappaB is critical for schwann cell myelination. *Nat Neurosci.* 2011 Apr;14(4):437-41.
7. Yuan ZL, Guan YJ, Chatterjee D, Chin YE. Stat3 dimerization regulated by reversible acetylation of a single lysine residue. *Science.* 2005 Jan 14;307(5707):269-73.
8. Buerki C, Rothgiesser KM, Valovka T, Owen HR, Rehrauer H, Fey M, et al. Functional relevance of novel p300-mediated lysine 314 and 315 acetylation of RelA/p65. *Nucleic Acids Res.* 2008 Mar;36(5):1665-80.
9. Chen CS, Weng SC, Tseng PH, Lin HP, Chen CS. Histone acetylation-independent effect of histone deacetylase inhibitors on akt through the reshuffling of protein phosphatase 1 complexes. *J Biol Chem.* 2005 Nov 18;280(46):38879-87.
10. Togi S, Kamitani S, Kawakami S, Ikeda O, Muromoto R, Nanbo A, et al. HDAC3 influences phosphorylation of STAT3 at serine 727 by interacting with PP2A. *Biochem Biophys Res Commun.* 2009 Feb 6;379(2):616-20.
11. Wagner JM, Hackanson B, Lubbert M, Jung M. Histone deacetylase (HDAC) inhibitors in recent clinical trials for cancer therapy. *Clin Epigenetics.* 2010 Dec;1(3-4):117-36.
12. Stupp R, Mason WP, van den Bent MJ, Weller M, Fisher B, Taphoorn MJ, et al. Radiotherapy plus concomitant and adjuvant temozolomide for glioblastoma. *N Engl J Med.* 2005 Mar 10;352(10):987-96.
13. Nagarajan RP, Costello JF. Epigenetic mechanisms in glioblastoma multiforme. *Semin Cancer Biol.* 2009 Jun;19(3):188-97.
14. Bredel M, Scholtens DM, Yadav AK, Alvarez AA, Renfrow JJ, Chandler JP, et al. NFKBIA deletion in glioblastomas. *N Engl J Med.* 2011 Feb 17;364(7):627-37.
15. Cancer Genome Atlas Research Network. Comprehensive genomic characterization defines human glioblastoma genes and core pathways. *Nature.* 2008 Oct 23;455(7216):1061-8.
16. Campos B, Bermejo JL, Han L, Felsberg J, Ahmadi R, Grabe N, et al. Expression of nuclear receptor corepressors and class I histone deacetylases in astrocytic gliomas. *Cancer Sci.* 2011 Feb;102(2):387-92.
17. Sharma V, Koul N, Joseph C, Dixit D, Ghosh S, Sen E. HDAC inhibitor, scriptaid, induces glioma cell apoptosis through JNK activation and inhibits telomerase activity. *J Cell Mol Med.* 2010 Aug;14(8):2151-61.

18. Gensert JM, Baranova OV, Weinstein DE, Ratan RR. CD81, a cell cycle regulator, is a novel target for histone deacetylase inhibition in glioma cells. *Neurobiol Dis.* 2007 Jun;26(3):671-80.
19. Sarcar B, Kahali S, Chinnaiyan P. Vorinostat enhances the cytotoxic effects of the topoisomerase I inhibitor SN38 in glioblastoma cell lines. *J Neurooncol.* 2010 Sep;99(2):201-7.
20. Chinnaiyan P, Vallabhaneni G, Armstrong E, Huang SM, Harari PM. Modulation of radiation response by histone deacetylase inhibition. *Int J Radiat Oncol Biol Phys.* 2005 May 1;62(1):223-9.
21. Robe PA, Jolais O, N'Guyen M, Princen F, Malgrange B, Merville MP, et al. Modulation of the HSV-TK/ganciclovir bystander effect by n-butyrate in glioblastoma: Correlation with gap-junction intercellular communication. *Int J Oncol.* 2004 Jul;25(1):187-92.
22. Su JM, Li XN, Thompson P, Ou CN, Ingle AM, Russell H, et al. Phase 1 study of valproic acid in pediatric patients with refractory solid or CNS tumors: A children's oncology group report. *Clin Cancer Res.* 2011 Feb 1;17(3):589-97.
23. Eot-Houllier G, Fulcrand G, Magnaghi-Jaulin L, Jaulin C. Histone deacetylase inhibitors and genomic instability. *Cancer Lett.* 2009 Feb 18;274(2):169-76.
24. Bertrand P. Inside HDAC with HDAC inhibitors. *Eur J Med Chem.* 2010 Jun;45(6):2095-116.
25. Marchion DC, Bicaku E, Turner JG, Schmitt ML, Morelli DR, Munster PN. HDAC2 regulates chromatin plasticity and enhances DNA vulnerability. *Mol Cancer Ther.* 2009 Apr;8(4):794-801.
26. Chen X, Wong P, Radany E, Wong JY. HDAC inhibitor, valproic acid, induces p53-dependent radiosensitization of colon cancer cells. *Cancer Biother Radiopharm.* 2009 Dec;24(6):689-99.
27. Lucio-Eterovic AK, Cortez MA, Valera ET, Motta FJ, Queiroz RG, Machado HR, et al. Differential expression of 12 histone deacetylase (HDAC) genes in astrocytomas and normal brain tissue: Class II and IV are hypoexpressed in glioblastomas. *BMC Cancer.* 2008 Aug 19;8:243.
28. Mehnert JM, Kelly WK. Histone deacetylase inhibitors: Biology and mechanism of action. *Cancer J.* 2007 Jan-Feb;13(1):23-9.
29. Hayakawa T, Nakayama J. Physiological roles of class I HDAC complex and histone demethylase. *J Biomed Biotechnol.* 2011;2011:129383.
30. Campbell KJ, Rocha S, Perkins ND. Active repression of antiapoptotic gene expression by RelA(p65) NF-kappa B. *Mol Cell.* 2004 Mar 26;13(6):853-65.
31. Bhat KP, Pelloski CE, Zhang Y, Kim SH, deLaCruz C, Rehli M, et al. Selective repression of YKL-40 by NF-kappaB in glioma cell lines involves recruitment of histone deacetylase-1 and -2. *FEBS Lett.* 2008 Sep 22;582(21-22):3193-200.
32. Burton TR, Eisenstat DD, Gibson SB. BNIP3 (bcl-2 19 kDa interacting protein) acts as transcriptional repressor of apoptosis-inducing factor expression preventing cell death in human malignant gliomas. *J Neurosci.* 2009 Apr 1;29(13):4189-99.
33. Sadoul K, Wang J, Diagouraga B, Khochbin S. The tale of protein lysine acetylation in the cytoplasm. *J Biomed Biotechnol.* 2011;2011:970382.
34. Choudhary C, Kumar C, Gnäd F, Nielsen ML, Rehman M, Walther TC, et al. Lysine acetylation targets protein complexes and co-regulates major cellular functions. *Science.* 2009 Aug 14;325(5942):834-40.
35. Glozak MA, Sengupta N, Zhang X, Seto E. Acetylation and deacetylation of non-histone proteins. *Gene.* 2005 Dec 19;363:15-23.

36. Li L, Gondi CS, Dinh DH, Olivero WC, Gujrati M, Rao JS. Transfection with anti-p65 intrabody suppresses invasion and angiogenesis in glioma cells by blocking nuclear factor-kappaB transcriptional activity. *Clin Cancer Res.* 2007 Apr 1;13(7):2178-90.
37. Kiernan R, Bres V, Ng RW, Coudart MP, El Messaoudi S, Sardet C, et al. Post-activation turn-off of NF-kappa B-dependent transcription is regulated by acetylation of p65. *J Biol Chem.* 2003 Jan 24;278(4):2758-66.
38. Liu BL, Cheng JX, Zhang X, Wang R, Zhang W, Lin H, et al. Global histone modification patterns as prognostic markers to classify glioma patients. *Cancer Epidemiol Biomarkers Prev.* 2010 Nov;19(11):2888-96.
39. Parsons DW, Jones S, Zhang X, Lin JC, Leary RJ, Angenendt P, et al. An integrated genomic analysis of human glioblastoma multiforme. *Science.* 2008 Sep 26;321(5897):1807-12.
40. Chang CJ, Hsu CC, Yung MC, Chen KY, Tzao C, Wu WF, et al. Enhanced radiosensitivity and radiation-induced apoptosis in glioma CD133-positive cells by knockdown of SirT1 expression. *Biochem Biophys Res Commun.* 2009 Mar 6;380(2):236-42.
41. Inoue T, Hiratsuka M, Osaki M, Yamada H, Kishimoto I, Yamaguchi S, et al. SIRT2, a tubulin deacetylase, acts to block the entry to chromosome condensation in response to mitotic stress. *Oncogene.* 2007 Feb 15;26(7):945-57.
42. Kito M, Maehara M, Watanabe K. Antiepileptic drugs--calcium current interaction in cultured human neuroblastoma cells. *Seizure.* 1994 Jun;3(2):141-9.
43. Johannessen CU. Mechanisms of action of valproate: A commentary. *Neurochem Int.* 2000 Aug-Sep;37(2-3):103-10.
44. Jung GA, Yoon JY, Moon BS, Yang DH, Kim HY, Lee SH, et al. Valproic acid induces differentiation and inhibition of proliferation in neural progenitor cells via the beta-catenin-ras-ERK-p21Cip/WAF1 pathway. *BMC Cell Biol.* 2008 Dec 9;9:66.
45. Chen G, Huang LD, Jiang YM, Manji HK. The mood-stabilizing agent valproate inhibits the activity of glycogen synthase kinase-3. *J Neurochem.* 1999 Mar;72(3):1327-30.
46. Bermudez-Lugo JA, Perez-Gonzalez O, Rosales-Hernandez MC, Ilizaliturri-Flores I, Trujillo-Ferrara J, Correa-Basurto J. Exploration of the valproic acid binding site on histone deacetylase 8 using docking and molecular dynamic simulations. *J Mol Model.* 2011 Oct 4.
47. Phiel CJ, Zhang F, Huang EY, Guenther MG, Lazar MA, Klein PS. Histone deacetylase is a direct target of valproic acid, a potent anticonvulsant, mood stabilizer, and teratogen. *J Biol Chem.* 2001 Sep 28;276(39):36734-41.
48. Khan N, Jeffers M, Kumar S, Hackett C, Boldog F, Khramtsov N, et al. Determination of the class and isoform selectivity of small-molecule histone deacetylase inhibitors. *Biochem J.* 2008 Jan 15;409(2):581-9.
49. Gurvich N, Tsygankova OM, Meinkoth JL, Klein PS. Histone deacetylase is a target of valproic acid-mediated cellular differentiation. *Cancer Res.* 2004 Feb 1;64(3):1079-86.
50. Bradbury CA, Khanim FL, Hayden R, Bunce CM, White DA, Drayson MT, et al. Histone deacetylases in acute myeloid leukaemia show a distinctive pattern of expression that changes selectively in response to deacetylase inhibitors. *Leukemia.* 2005 Oct;19(10):1751-9.
51. Benitez JA, Arregui L, Cabrera G, Segovia J. Valproic acid induces polarization, neuronal-like differentiation of a subpopulation of C6 glioma cells and selectively regulates transgene expression. *Neuroscience.* 2008 Oct 28;156(4):911-20.

52. Das CM, Aguilera D, Vasquez H, Prasad P, Zhang M, Wolff JE, et al. Valproic acid induces p21 and topoisomerase-II (alpha/beta) expression and synergistically enhances etoposide cytotoxicity in human glioblastoma cell lines. *J Neurooncol.* 2007 Nov;85(2):159-70.
53. Camphausen K, Cerna D, Scott T, Sproull M, Burgan WE, Cerra MA, et al. Enhancement of in vitro and in vivo tumor cell radiosensitivity by valproic acid. *Int J Cancer.* 2005 Apr 10;114(3):380-6.
54. Condorelli F, Gnemmi I, Vallario A, Genazzani AA, Canonico PL. Inhibitors of histone deacetylase (HDAC) restore the p53 pathway in neuroblastoma cells. *Br J Pharmacol.* 2008 Feb;153(4):657-68.
55. Galanis E, Jaeckle KA, Maurer MJ, Reid JM, Ames MM, Hardwick JS, et al. Phase II trial of vorinostat in recurrent glioblastoma multiforme: A north central cancer treatment group study. *J Clin Oncol.* 2009 Apr 20;27(12):2052-8.
56. Iwamoto FM, Lamborn KR, Kuhn JG, Wen PY, Yung WK, Gilbert MR, et al. A phase I/II trial of the histone deacetylase inhibitor romidepsin for adults with recurrent malignant glioma: North american brain tumor consortium study 03-03. *Neuro Oncol.* 2011 May;13(5):509-16.
57. Wu SC, Zhang Y. Active DNA demethylation: Many roads lead to rome. *Nat Rev Mol Cell Biol.* 2010 Sep;11(9):607-20.
58. Rajendran G, Shanmuganandam K, Bendre A, Mujumdar D, Goel A, Shiras A. Epigenetic regulation of DNA methyltransferases: DNMT1 and DNMT3B in gliomas. *J Neurooncol.* 2011 Jan 13.
59. Foltz G, Yoon JG, Lee H, Ryken TC, Sibenaller Z, Ehrich M, et al. DNA methyltransferase-mediated transcriptional silencing in malignant glioma: A combined whole-genome microarray and promoter array analysis. *Oncogene.* 2009 Jul 23;28(29):2667-77.
60. Perisic T, Zimmermann N, Kirmeier T, Asmus M, Tuorto F, Uhr M, et al. Valproate and amitriptyline exert common and divergent influences on global and gene promoter-specific chromatin modifications in rat primary astrocytes. *Neuropsychopharmacology.* 2010 Feb;35(3):792-805.
61. Milutinovic S, D'Alessio AC, Detich N, Szyf M. Valproate induces widespread epigenetic reprogramming which involves demethylation of specific genes. *Carcinogenesis.* 2007 Mar;28(3):560-71.
62. Papi A, Ferreri AM, Rocchi P, Guerra F, Orlandi M. Epigenetic modifiers as anticancer drugs: Effectiveness of valproic acid in neural crest-derived tumor cells. *Anticancer Res.* 2010 Feb;30(2):535-40.
63. Sasai K, Akagi T, Aoyanagi E, Tabu K, Kaneko S, Tanaka S. O6-methylguanine-DNA methyltransferase is downregulated in transformed astrocyte cells: Implications for anti-glioma therapies. *Mol Cancer.* 2007 Jun 5;6:36.
64. Hegi ME, Diserens AC, Gorlia T, Hamou MF, de Tribolet N, Weller M, et al. MGMT gene silencing and benefit from temozolomide in glioblastoma. *N Engl J Med.* 2005 Mar 10;352(10):997-1003.
65. Bosetti F, Bell JM, Manickam P. Microarray analysis of rat brain gene expression after chronic administration of sodium valproate. *Brain Res Bull.* 2005 Apr 30;65(4):331-8.
66. Li B, Zhang S, Li M, Zhang H, Hertz L, Peng L. Down-regulation of GluK2 kainate receptor expression by chronic treatment with mood-stabilizing anti-convulsants or lithium in cultured astrocytes and brain, but not in neurons. *Neuropharmacology.* 2009 Sep;57(4):375-85.
67. Stamatopoulos B, Meuleman N, De Bruyn C, Mineur P, Martiat P, Bron D, et al. Antileukemic activity of valproic acid in chronic lymphocytic leukemia B cells defined by microarray analysis. *Leukemia.* 2009 Dec;23(12):2281-9.

68. De la Cruz-Hernandez E, Perez-Plasencia C, Perez-Cardenas E, Gonzalez-Fierro A, Trejo-Becerril C, Chavez-Blanco A, et al. Transcriptional changes induced by epigenetic therapy with hydralazine and magnesium valproate in cervical carcinoma. *Oncol Rep.* 2011 Feb;25(2):399-407.
69. Frattola L, Ferrarese C, Canal N, Gaini SM, Galluso R, Piolti R, et al. Characterization of the gamma-aminobutyric acid receptor system in human brain gliomas. *Cancer Res.* 1985 Sep;45(9):4495-8.
70. Roach JD, Jr, Aguinaldo GT, Jonnalagadda K, Hughes FM, Jr, Spangelo BL. Gamma-aminobutyric acid inhibits synergistic interleukin-6 release but not transcriptional activation in astrocytoma cells. *Neuroimmunomodulation.* 2008;15(2):117-24.
71. Liu Q, Li G, Li R, Shen J, He Q, Deng L, et al. IL-6 promotion of glioblastoma cell invasion and angiogenesis in U251 and T98G cell lines. *J Neurooncol.* 2010 Nov;100(2):165-76.
72. Thompson CB. Metabolic enzymes as oncogenes or tumor suppressors. *N Engl J Med.* 2009 Feb 19;360(8):813-5.
73. Latour I, Louw DF, Beedle AM, Hamid J, Sutherland GR, Zamponi GW. Expression of T-type calcium channel splice variants in human glioma. *Glia.* 2004 Nov 1;48(2):112-9.
74. Lu F, Chen H, Zhou C, Wu S. Is there a role for T-type Ca²⁺ channel in glioma cell proliferation? *Cell Calcium.* 2005 Dec;38(6):593,5; author reply 597.
75. Panner A, Cribbs LL, Zainelli GM, Origitano TC, Singh S, Wurster RD. Variation of T-type calcium channel protein expression affects cell division of cultured tumor cells. *Cell Calcium.* 2005 Feb;37(2):105-19.
76. Bertolesi GE, Shi C, Elbaum L, Jollimore C, Rozenberg G, Barnes S, et al. The ca(2+) channel antagonists mibefradil and pimozide inhibit cell growth via different cytotoxic mechanisms. *Mol Pharmacol.* 2002 Aug;62(2):210-9.
77. Wang Z, Xu L, Zhu X, Cui W, Sun Y, Nishijo H, et al. Demethylation of specific Wnt/beta-catenin pathway genes and its upregulation in rat brain induced by prenatal valproate exposure. *Anat Rec (Hoboken).* 2010 Nov;293(11):1947-53.
78. Zhang X, Chen T, Zhang J, Mao Q, Li S, Xiong W, et al. Notch1 promotes glioma cell migration and invasion by stimulating beta-catenin and NF-kappaB signaling via AKT activation. *Cancer Sci.* 2011 Nov 17.
79. Williams SP, Nowicki MO, Liu F, Press R, Godlewski J, Abdel-Rasoul M, et al. Indirubins decrease glioma invasion by blocking migratory phenotypes in both the tumor and stromal endothelial cell compartments. *Cancer Res.* 2011 Aug 15;71(16):5374-80.
80. Bowman A, Nusse R. Location, location, location: FoxM1 mediates beta-catenin nuclear translocation and promotes glioma tumorigenesis. *Cancer Cell.* 2011 Oct 18;20(4):415-6.
81. Kim Y, Kim KH, Lee J, Lee YA, Kim M, Lee SJ, et al. Wnt activation is implicated in glioblastoma radioresistance. *Lab Invest.* 2011 Nov 14.
82. Kotliarova S, Pastorino S, Kovell LC, Kotliarov Y, Song H, Zhang W, et al. Glycogen synthase kinase-3 inhibition induces glioma cell death through c-MYC, nuclear factor-kappaB, and glucose regulation. *Cancer Res.* 2008 Aug 15;68(16):6643-51.
83. Korur S, Huber RM, Sivasankaran B, Petrich M, Morin P, Jr, Hemmings BA, et al. GSK3beta regulates differentiation and growth arrest in glioblastoma. *PLoS One.* 2009 Oct 13;4(10):e7443.
84. Miyashita K, Kawakami K, Nakada M, Mai W, Shakoori A, Fujisawa H, et al. Potential therapeutic effect of glycogen synthase kinase 3beta inhibition against human glioblastoma. *Clin Cancer Res.* 2009 Feb 1;15(3):887-97.

85. Knupfer MM, Hernaiz-Driever P, Poppenborg H, Wolff JE, Cinatl J. Valproic acid inhibits proliferation and changes expression of CD44 and CD56 of malignant glioma cells in vitro. *Anticancer Res.* 1998 Sep-Oct;18(5A):3585-9.
86. Chinnaiyan P, Cerna D, Burgan WE, Beam K, Williams ES, Camphausen K, et al. Postradiation sensitization of the histone deacetylase inhibitor valproic acid. *Clin Cancer Res.* 2008 Sep 1;14(17):5410-5.
87. Fu J, Shao CJ, Chen FR, Ng HK, Chen ZP. Autophagy induced by valproic acid is associated with oxidative stress in glioma cell lines. *Neuro Oncol.* 2010 Apr;12(4):328-40.
88. Chen CH, Chang YJ, Ku MS, Chung KT, Yang JT. Enhancement of temozolomide-induced apoptosis by valproic acid in human glioma cell lines through redox regulation. *J Mol Med.* 2011 Mar;89(3):303-15.
89. Bacon CL, Gallagher HC, Haughey JC, Regan CM. Antiproliferative action of valproate is associated with aberrant expression and nuclear translocation of cyclin D3 during the G6 glioma G1 phase. *J Neurochem.* 2002 Oct;83(1):12-9.
90. Fortson WS, Kayarthodi S, Fujimura Y, Xu H, Matthews R, Grizzle WE, et al. Histone deacetylase inhibitors, valproic acid and trichostatin-A induce apoptosis and affect acetylation status of p53 in ERG-positive prostate cancer cells. *Int J Oncol.* 2011 Jul;39(1):111-9.
91. Simboeck E, Sawicka A, Zupkovitz G, Senese S, Winter S, Dequiedt F, et al. A phosphorylation switch regulates the transcriptional activation of cell cycle regulator p21 by histone deacetylase inhibitors. *J Biol Chem.* 2010 Dec 24;285(52):41062-73.
92. Dash BC, El-Deiry WS. Phosphorylation of p21 in G2/M promotes cyclin B-Cdc2 kinase activity. *Mol Cell Biol.* 2005 Apr;25(8):3364-87.
93. Ando T, Kawabe T, Ohara H, Ducommun B, Itoh M, Okamoto T. Involvement of the interaction between p21 and proliferating cell nuclear antigen for the maintenance of G2/M arrest after DNA damage. *J Biol Chem.* 2001 Nov 16;276(46):42971-7.
94. Ichiyama T, Okada K, Lipton JM, Matsubara T, Hayashi T, Furukawa S. Sodium valproate inhibits production of TNF-alpha and IL-6 and activation of NF-kappaB. *Brain Res.* 2000 Feb 28;857(1-2):246-51.
95. Lehmann A, Denkert C, Budczies J, Buckendahl AC, Darb-Esfahani S, Noske A, et al. High class I HDAC activity and expression are associated with RelA/p65 activation in pancreatic cancer in vitro and in vivo. *BMC Cancer.* 2009 Nov 13;9:395.
96. Rao JS, Bazinet RP, Rapoport SI, Lee HJ. Chronic treatment of rats with sodium valproate downregulates frontal cortex NF-kappaB DNA binding activity and COX-2 mRNA. *Bipolar Disord.* 2007 Aug;9(5):513-20.
97. de la Iglesia N, Konopka G, Puram SV, Chan JA, Bachoo RM, You MJ, et al. Identification of a PTEN-regulated STAT3 brain tumor suppressor pathway. *Genes Dev.* 2008 Feb 15;22(4):449-62.
98. Chen Q, Ouyang DY, Geng M, Xu LH, Zhang YT, Wang FP, et al. Valproic acid exhibits biphasic effects on apoptotic cell death of activated lymphocytes through differential modulation of multiple signaling pathways. *J Immunotoxicol.* 2011 Apr 4.
99. Liang QC, Xiong H, Zhao ZW, Jia D, Li WX, Qin HZ, et al. Inhibition of transcription factor STAT5b suppresses proliferation, induces G1 cell cycle arrest and reduces tumor cell invasion in human glioblastoma multiforme cells. *Cancer Lett.* 2009 Jan 8;273(1):164-71.
100. Hu J, Jo M, Cavenee WK, Furnari F, VandenBerg SR, Gonias SL. Crosstalk between the urokinase-type plasminogen activator receptor and EGF receptor variant III supports survival and growth of glioblastoma cells. *Proc Natl Acad Sci U S A.* 2011 Sep 20;108(38):15984-9.

101. Alvarez-Breckenridge CA, Yu J, Price R, Wei M, Wang Y, Nowicki MO, et al. The HDAC inhibitor valproic acid lessens NK cell action against oncolytic virus-infected glioblastoma cells with inhibition of STAT5/T-BET signaling and IFN γ generation. *J Virol*. 2012 Feb 8.
102. Gotfryd K, Skladchikova G, Lepekhn EA, Berezin V, Bock E, Walmod PS. Cell type-specific anti-cancer properties of valproic acid: Independent effects on HDAC activity and Erk1/2 phosphorylation. *BMC Cancer*. 2010 Jul 21;10:383.
103. Lange C, Mix E, Frahm J, Glass A, Muller J, Schmitt O, et al. Small molecule GSK-3 inhibitors increase neurogenesis of human neural progenitor cells. *Neurosci Lett*. 2011 Jan 13;488(1):36-40.
104. Jonathan Ryves W, Dalton EC, Harwood AJ, Williams RS. GSK-3 activity in neocortical cells is inhibited by lithium but not carbamazepine or valproic acid. *Bipolar Disord*. 2005 Jun;7(3):260-5.
105. Phillips HS, Kharbanda S, Chen R, Forrest WF, Soriano RH, Wu TD, et al. Molecular subclasses of high-grade glioma predict prognosis, delineate a pattern of disease progression, and resemble stages in neurogenesis. *Cancer Cell*. 2006 Mar;9(3):157-73.
106. Wolff JE, Kramm C, Kortmann RD, Pietsch T, Rutkowski S, Jorch N, et al. Valproic acid was well tolerated in heavily pretreated pediatric patients with high-grade glioma. *J Neurooncol*. 2008 Dec;90(3):309-14.
107. Morita K, Gotohda T, Arimochi H, Lee MS, Her S. Histone deacetylase inhibitors promote neurosteroid-mediated cell differentiation and enhance serotonin-stimulated brain-derived neurotrophic factor gene expression in rat C6 glioma cells. *J Neurosci Res*. 2009 Aug 15;87(11):2608-14.
108. Tabu K, Sasai K, Kimura T, Wang L, Aoyanagi E, Kohsaka S, et al. Promoter hypomethylation regulates CD133 expression in human gliomas. *Cell Res*. 2008 Oct;18(10):1037-46.
109. Yagi Y, Fushida S, Harada S, Kinoshita J, Makino I, Oyama K, et al. Effects of valproic acid on the cell cycle and apoptosis through acetylation of histone and tubulin in a scirrhous gastric cancer cell line. *J Exp Clin Cancer Res*. 2010 Nov 17;29:149.
110. Iacomino G, Medici MC, Russo GL. Valproic acid sensitizes K562 erythroleukemia cells to TRAIL/Apo2L-induced apoptosis. *Anticancer Res*. 2008 Mar-Apr;28(2A):855-64.
111. Xie C, Edwards H, Xu X, Zhou H, Buck SA, Stout ML, et al. Mechanisms of synergistic antileukemic interactions between valproic acid and cytarabine in pediatric acute myeloid leukemia. *Clin Cancer Res*. 2010 Nov 15;16(22):5499-510.
112. Brazelle W, Krehling JM, Gemmer J, Ma Y, Cress WD, Haura E, et al. Histone deacetylase inhibitors downregulate checkpoint kinase 1 expression to induce cell death in non-small cell lung cancer cells. *PLoS One*. 2010 Dec 14;5(12):e14335.
113. Chai G, Li L, Zhou W, Wu L, Zhao Y, Wang D, et al. HDAC inhibitors act with 5-aza-2'-deoxycytidine to inhibit cell proliferation by suppressing removal of incorporated abases in lung cancer cells. *PLoS One*. 2008 Jun 18;3(6):e2445.
114. Lee JH, Choy ML, Ngo L, Foster SS, Marks PA. Histone deacetylase inhibitor induces DNA damage, which normal but not transformed cells can repair. *Proc Natl Acad Sci U S A*. 2010 Aug 17;107(33):14639-44.
115. Ciusani E, Balzarotti M, Calatozzolo C, de Grazia U, Boiardi A, Salmaggi A, et al. Valproic acid increases the in vitro effects of nitrosureas on human glioma cell lines. *Oncol Res*. 2007;16(10):453-63.
116. Blaheta RA, Michaelis M, Driever PH, Cinatl Jr. J. Evolving anticancer drug valproic acid: Insights into the mechanism and clinical studies. *Med Res Rev*. 2005 ;25(4):383-97.
117. Michaelis M, Michaelis UR, Fleming I, Suhan T, Cinatl J, Blaheta RA, et al. Valproic acid inhibits angiogenesis in vitro and in vivo. *Mol Pharmacol*. 2004 Mar;65(3):520-7.

118. Norden AD, Drappatz J, Wen PY. Antiangiogenic therapies for high-grade glioma. *Nat Rev Neurol*. 2009 Nov;5(11):610-20.
119. Zgouras D, Becker U, Loitsch S, Stein J. Modulation of angiogenesis-related protein synthesis by valproic acid. *Biochem Biophys Res Commun*. 2004 Apr 9;316(3):693-7.
120. Gao D, Xia Q, Lv J, Zhang H. Chronic administration of valproic acid inhibits PC3 cell growth by suppressing tumor angiogenesis in vivo. *Int J Urol*. 2007 Sep;14(9):838-45.
121. Deroanne CF, Bonjean K, Servotte S, Devy L, Colige A, Clausse N, et al. Histone deacetylases inhibitors as anti-angiogenic agents altering vascular endothelial growth factor signaling. *Oncogene*. 2002 Jan 17;21(3):427-36.
122. Osuka S, Takano S, Yamamoto T, Ishikawa E, Matsumura A. Histone deacetylase inhibitor, valproic acid inhibits glioma angiogenesis in vitro and in vivo in the brain. *Neuro-oncology*. 2009;11(6):962.
123. Kim SH, Jeong JW, Park JA, Lee JW, Seo JH, Jung BK, et al. Regulation of the HIF-1 α stability by histone deacetylases. *Oncol Rep*. 2007 Mar;17(3):647-51.
124. Ellis L, Hammers H, Pili R. Targeting tumor angiogenesis with histone deacetylase inhibitors. *Cancer Lett*. 2009 Aug 8;280(2):145-53.
125. Kaur B, Khwaja FW, Severson EA, Matheny SL, Brat DJ, Van Meir EG. Hypoxia and the hypoxia-inducible-factor pathway in glioma growth and angiogenesis. *Neuro Oncol*. 2005 Apr;7(2):134-53.
126. Qiang L, Wu T, Zhang HW, Lu N, Hu R, Wang YJ, et al. HIF-1 α is critical for hypoxia-mediated maintenance of glioblastoma stem cells by activating notch signaling pathway. *Cell Death Differ*. 2011 Aug 5.
127. Lefranc F, Brotchi J, Kiss R. Possible future issues in the treatment of glioblastomas: Special emphasis on cell migration and the resistance of migrating glioblastoma cells to apoptosis. *J Clin Oncol*. 2005 Apr 1;23(10):2411-22.
128. Zhai GG, Malhotra R, Delaney M, Latham D, Nestler U, Zhang M, et al. Radiation enhances the invasive potential of primary glioblastoma cells via activation of the rho signaling pathway. *J Neurooncol*. 2006 Feb;76(3):227-37.
129. Kroonen J, Nassen J, Boulanger YG, Provenzano F, Capraro V, Bours V, et al. Human glioblastoma-initiating cells invade specifically the subventricular zones and olfactory bulbs of mice after striatal injection. *Int J Cancer*. 2011 Aug 1;129(3):574-85.
130. Teodorczyk M, Martin-Villalba A. Sensing invasion: Cell surface receptors driving spreading of glioblastoma. *J Cell Physiol*. 2010 Jan;222(1):1-10.
131. Zamecnik J. The extracellular space and matrix of gliomas. *Acta Neuropathol*. 2005 Nov;110(5):435-42.
132. An Z, Gluck CB, Choy ML, Kaufman LJ. Suberoylanilide hydroxamic acid limits migration and invasion of glioma cells in two and three dimensional culture. *Cancer Lett*. 2010 Jun 28;292(2):215-27.
133. Eyupoglu IY, Hahnen E, Trankle C, Savaskan NE, Siebzehnruhl FA, Buslei R, et al. Experimental therapy of malignant gliomas using the inhibitor of histone deacetylase MS-275. *Mol Cancer Ther*. 2006 May;5(5):1248-55.
134. Knupfer MM, Pulzer F, Schindler I, Hernaiz Driever P, Knupfer H, Keller E. Different effects of valproic acid on proliferation and migration of malignant glioma cells in vitro. *Anticancer Res*. 2001 Jan-Feb;21(1A):347-51.
135. Gilbertson RJ, Rich JN. Making a tumour's bed: Glioblastoma stem cells and the vascular niche. *Nat Rev Cancer*. 2007 Oct;7(10):733-6.

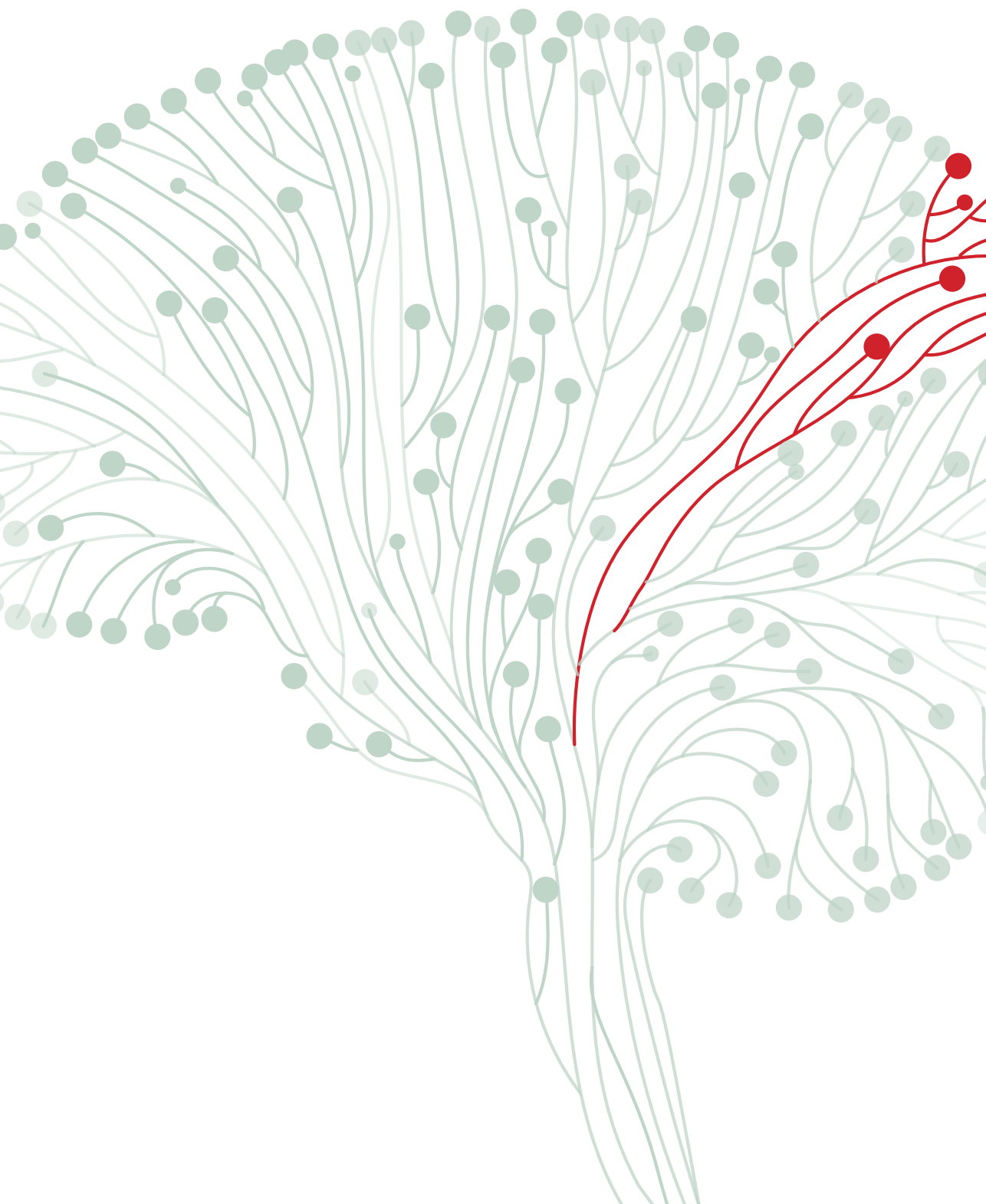
136. Charles NA, Holland EC, Gilbertson R, Glass R, Kettenmann H. The brain tumor microenvironment. *Glia*. 2011 Aug;59(8):1169-80.
137. Markovic DS, Glass R, Synowitz M, Rooijen N, Kettenmann H. Microglia stimulate the invasiveness of glioma cells by increasing the activity of metalloprotease-2. *J Neuropathol Exp Neurol*. 2005 Sep;64(9):754-62.
138. Chen FX, Ren WW, Yang Y, Shen D, Zong Y, Xu S, et al. Reciprocal effects of conditioned medium on cultured glioma cells and neural stem cells. *J Clin Neurosci*. 2009 Dec;16(12):1619-23.
139. Chirasani SR, Sternjak A, Wend P, Momma S, Campos B, Herrmann IM, et al. Bone morphogenetic protein-7 release from endogenous neural precursor cells suppresses the tumorigenicity of stem-like glioblastoma cells. *Brain*. 2010 Jul;133(Pt 7):1961-72.
140. Chen PS, Wang CC, Bortner CD, Peng GS, Wu X, Pang H, et al. Valproic acid and other histone deacetylase inhibitors induce microglial apoptosis and attenuate lipopolysaccharide-induced dopaminergic neurotoxicity. *Neuroscience*. 2007 Oct 12;149(1):203-12.
141. Go HS, Seo JE, Kim KC, Han SM, Kim P, Kang YS, et al. Valproic acid inhibits neural progenitor cell death by activation of NF-kappaB signaling pathway and up-regulation of bcl-XL. *J Biomed Sci*. 2011 Jul 4;18(1):48.
142. Suh HS, Choi S, Khattar P, Choi N, Lee SC. Histone deacetylase inhibitors suppress the expression of inflammatory and innate immune response genes in human microglia and astrocytes. *J Neuroimmune Pharmacol*. 2010 Dec;5(4):521-32.
143. Baltes S, Fedrowitz M, Tortos CL, Potschka H, Loscher W. Valproic acid is not a substrate for P-glycoprotein or multidrug resistance proteins 1 and 2 in a number of in vitro and in vivo transport assays. *J Pharmacol Exp Ther*. 2007 Jan;320(1):331-43.
144. Rivers F, O'Brien TJ, Callaghan R. Exploring the possible interaction between anti-epilepsy drugs and multidrug efflux pumps; in vitro observations. *Eur J Pharmacol*. 2008 Nov 19;598(1-3):1-8.
145. Tang R, Faussat AM, Majdak P, Perrot JY, Chaoui D, Legrand O, et al. Valproic acid inhibits proliferation and induces apoptosis in acute myeloid leukemia cells expressing P-gp and MRP1. *Leukemia*. 2004 Jul;18(7):1246-51.
146. Kortenhorst MS, Zahurak M, Shabbeer S, Kachhap S, Galloway N, Parmigiani G, et al. A multiple-loop, double-cube microarray design applied to prostate cancer cell lines with variable sensitivity to histone deacetylase inhibitors. *Clin Cancer Res*. 2008 Nov 1;14(21):6886-94.
147. Liu T, Liu PY, Tee AE, Haber M, Norris MD, Gleave ME, et al. Overexpression of clusterin is a resistance factor to the anti-cancer effect of histone deacetylase inhibitors. *Eur J Cancer*. 2009 Jul;45(10):1846-54.
148. Huang X, Guo B. Adenomatous polyposis coli determines sensitivity to histone deacetylase inhibitor-induced apoptosis in colon cancer cells. *Cancer Res*. 2006 Sep 15;66(18):9245-51.
149. Fedier A, Dedes KJ, Imesch P, Von Bueren AO, Fink D. The histone deacetylase inhibitors suberoylanilide hydroxamic (vorinostat) and valproic acid induce irreversible and MDR1-independent resistance in human colon cancer cells. *Int J Oncol*. 2007 Sep;31(3):633-41.
150. Imesch P, Dedes KJ, Furlato M, Fink D, Fedier A. MLH1 protects from resistance acquisition by the histone deacetylase inhibitor trichostatin A in colon tumor cells. *Int J Oncol*. 2009 Sep;35(3):631-40.
151. Cowell IG, Sunter NJ, Singh PB, Austin CA, Durkacz BW, Tilby MJ. gammaH2AX foci form preferentially in euchromatin after ionising-radiation. *PLoS One*. 2007 Oct 24;2(10):e1057.

152. Goodarzi AA, Jeggo P, Lobrich M. The influence of heterochromatin on DNA double strand break repair: Getting the strong, silent type to relax. *DNA Repair (Amst)*. 2010 Dec 10;9(12):1273-82.
153. Green SR, Choudhary AK, Fleming IN. Combination of sapacitabine and HDAC inhibitors stimulates cell death in AML and other tumour types. *Br J Cancer*. 2010 Oct 26;103(9):1391-9.
154. Sato A, Asano T, Horiguchi A, Ito K, Sumitomo M, Asano T. Antitumor effect of suberoylanilide hydroxamic acid and topotecan in renal cancer cells. *Oncol Res*. 2011;19(5):217-23.
155. Stander M, Dichgans J, Weller M. Anticonvulsant drugs fail to modulate chemotherapy-induced cytotoxicity and growth inhibition of human malignant glioma cells. *J Neurooncol*. 1998 May;37(3):191-8.
156. Camphausen K, Burgan W, Cerra M, Oswald KA, Trepel JB, Lee MJ, et al. Enhanced radiation-induced cell killing and prolongation of gammaH2AX foci expression by the histone deacetylase inhibitor MS-275. *Cancer Res*. 2004 Jan 1;64(1):316-21.
157. Puerto S, Ramirez MJ, Marcos R, Creus A, Surrallés J. Radiation-induced chromosome aberrations in human euchromatic (17cen-p53) and heterochromatic (1cen-1q12) regions. *Mutagenesis*. 2001 Jul;16(4):291-6.
158. Pawlik TM, Keyomarsi K. Role of cell cycle in mediating sensitivity to radiotherapy. *Int J Radiat Oncol Biol Phys*. 2004 Jul 15;59(4):928-42.
159. Van Niftrik KA, Van den Berg J, Slotman BJ, Lafleur MV, Sminia P, Stalpers LJ. Valproic acid sensitizes human glioma cells for temozolomide and gamma-radiation. *J Neurooncol*. 2012 Mar;107(1):61-7.
160. Camphausen K, Tofilon PJ. Inhibition of histone deacetylation: A strategy for tumor radiosensitization. *J Clin Oncol*. 2007 Sep 10;25(26):4051-6.
161. Thoms J, Bristow RG. DNA repair targeting and radiotherapy: A focus on the therapeutic ratio. *Semin Radiat Oncol*. 2010 Oct;20(4):217-22.
162. Mahaney BL, Meek K, Lees-Miller SP. Repair of ionizing radiation-induced DNA double-strand breaks by non-homologous end-joining. *Biochem J*. 2009 Feb 1;417(3):639-50.
163. Shrivastav M, De Haro LP, Nickoloff JA. Regulation of DNA double-strand break repair pathway choice. *Cell Res*. 2008 Jan;18(1):134-47.
164. Shabason JE, Tofilon PJ, Camphausen K. Grand rounds at the national institutes of health: HDAC inhibitors as radiation modifiers, from bench to clinic. *J Cell Mol Med*. 2011 Mar 1.
165. Kawano T, Akiyama M, Agawa-Ohta M, Mikami-Terao Y, Iwase S, Yanagisawa T, et al. Histone deacetylase inhibitors valproic acid and depsipeptide sensitize retinoblastoma cells to radiotherapy by increasing H2AX phosphorylation and p53 acetylation-phosphorylation. *Int J Oncol*. 2010 Oct;37(4):787-95.
166. Otsuki A, Patel A, Kasai K, Suzuki M, Kurozumi K, Chiocca EA, et al. Histone deacetylase inhibitors augment antitumor efficacy of herpes-based oncolytic viruses. *Mol Ther*. 2008 Sep;16(9):1546-55.
167. Kothari V, Joshi G, Nama S, Somasundaram K, Mulherkar R. HDAC inhibitor valproic acid enhances tumor cell kill in adenovirus-HSVtk mediated suicide gene therapy in HNSCC xenograft mouse model. *Int J Cancer*. 2010 Feb 1;126(3):733-42.
168. Hacker S, Dittrich A, Mohr A, Schweitzer T, Rutkowski S, Krauss J, et al. Histone deacetylase inhibitors cooperate with IFN-gamma to restore caspase-8 expression and overcome TRAIL resistance in cancers with silencing of caspase-8. *Oncogene*. 2009 Sep 3;28(35):3097-110.
169. Balbi A, Sottofattori E, Mazzei M, Sannita WG. Study of bioequivalence of magnesium and sodium valproates. *J Pharm Biomed Anal*. 1991;9(4):317-21.

170. Patsalos PN, Berry DJ, Bourgeois BF, Cloyd JC, Glauser TA, Johannessen SI, et al. Antiepileptic drugs--best practice guidelines for therapeutic drug monitoring: A position paper by the subcommission on therapeutic drug monitoring, ILAE commission on therapeutic strategies. *Epilepsia*. 2008 Jul;49(7):1239-76.
171. Lundberg B, Nergardh A, Boreus LO. Plasma concentrations of valproate during maintenance therapy in epileptic children. *J Neurol*. 1982;228(2):133-41.
172. Moody JP, Allan SM. Measurement of valproic acid in serum as the 4-bromophenacyl ester by high performance liquid chromatography. *Clin Chim Acta*. 1983 Jan 24;127(2):263-9.
173. Tomson T, Dahl ML, Kimland E. Therapeutic monitoring of antiepileptic drugs for epilepsy. *Cochrane Database Syst Rev*. 2007 Jan 24;(1)(1):CD002216.
174. Covanis A, Gupta AK, Jeavons PM. Sodium valproate: Monotherapy and polytherapy. *Epilepsia*. 1982 Dec;23(6):693-720.
175. Perrott J, Murphy NG, Zed PJ. L-carnitine for acute valproic acid overdose: A systematic review of published cases. *Ann Pharmacother*. 2010 Jul-Aug;44(7-8):1287-93.
176. Hagg S, Spigset O. Anticonvulsant use during lactation. *Drug Saf*. 2000 Jun;22(6):425-40.
177. Wieser HG. Comparison of valproate concentrations in human plasma, CSF and brain tissue after administration of different formulations of valproate or valpromide. *Epilepsy Res*. 1991 Jul;9(2):154-9.
178. Fischer W, Praetor K, Metzner L, Neubert RH, Brandsch M. Transport of valproate at intestinal epithelial (caco-2) and brain endothelial (RBE4) cells: Mechanism and substrate specificity. *Eur J Pharm Biopharm*. 2008 Oct;70(2):486-92.
179. Froberg MK, Gerhart DZ, Enerson BE, Manivel C, Guzman-Paz M, Seacotte N, et al. Expression of monocarboxylate transporter MCT1 in normal and neoplastic human CNS tissues. *Neuroreport*. 2001 Mar 26;12(4):761-5.
180. Kiang TK, Ho PC, Anari MR, Tong V, Abbott FS, Chang TK. Contribution of CYP2C9, CYP2A6, and CYP2B6 to valproic acid metabolism in hepatic microsomes from individuals with the CYP2C9*1/*1 genotype. *Toxicol Sci*. 2006 Dec;94(2):261-71.
181. Patsalos PN, Perucca E. Clinically important drug interactions in epilepsy: General features and interactions between antiepileptic drugs. *Lancet Neurol*. 2003 Jun;2(6):347-56.
182. Yoon HW, Giraldo EA, Wijidicks EF. Valproic acid and warfarin: An underrecognized drug interaction. *Neurocrit Care*. 2011 Aug;15(1):182-5.
183. Pursche S, Schleyer E, von Bonin M, Ehninger G, Said SM, Prondzinsky R, et al. Influence of enzyme-inducing antiepileptic drugs on trough level of imatinib in glioblastoma patients. *Curr Clin Pharmacol*. 2008 Sep;3(3):198-203.
184. Bourg V, Lebrun C, Chichmanian RM, Thomas P, Frenay M. Nitroso-urea-cisplatin-based chemotherapy associated with valproate: Increase of haematologic toxicity. *Ann Oncol*. 2001 Feb;12(2):217-9.
185. Oberndorfer S, Piribauer M, Marosi C, Lahrmann H, Hitzengerger P, Grisold W. P450 enzyme inducing and non-enzyme inducing antiepileptics in glioblastoma patients treated with standard chemotherapy. *J Neurooncol*. 2005 May;72(3):255-60.
186. Yap KY, Chui WK, Chan A. Drug interactions between chemotherapeutic regimens and antiepileptics. *Clin Ther*. 2008 Aug;30(8):1385-407.

187. Atmaca A, Al-Batran SE, Maurer A, Neumann A, Heinzel T, Hentsch B, et al. Valproic acid (VPA) in patients with refractory advanced cancer: A dose escalating phase I clinical trial. *Br J Cancer*. 2007 Jul 16;97(2):177-82.
188. Isojarvi JI, Laatikainen TJ, Pakarinen AJ, Juntunen KT, Myllylä VV. Polycystic ovaries and hyperandrogenism in women taking valproate for epilepsy. *N Engl J Med*. 1993 Nov 4;329(19):1383-8.
189. Verrotti A, D'Egidio C, Mohn A, Coppola G, Parisi P, Chiarelli F. Antiepileptic drugs, sex hormones, and PCOS. *Epilepsia*. 2011 Feb;52(2):199-211.
190. Davis R, Peters DH, McTavish D. Valproic acid. A reappraisal of its pharmacological properties and clinical efficacy in epilepsy. *Drugs*. 1994 Feb;47(2):332-72.
191. Koenig S, Gerstner T, Keller A, Teich M, Longin E, Dempfle CE. High incidence of valproate-induced coagulation disorders in children receiving valproic acid: A prospective study. *Blood Coagul Fibrinolysis*. 2008 Jul;19(5):375-82.
192. Manohar C, Avitsian R, Lozano S, Gonzalez-Martinez J, Cata JP. The effect of antiepileptic drugs on coagulation and bleeding in the perioperative period of epilepsy surgery: The Cleveland clinic experience. *J Clin Neurosci*. 2011 Sep;18(9):1180-4.
193. Anderson GD, Lin YX, Berge C, Ojemann GA. Absence of bleeding complications in patients undergoing cortical surgery while receiving valproate treatment. *J Neurosurg*. 1997 Aug;87(2):252-6.
194. Psaras T, Will BE, Schoeber W, Rona S, Mittelbronn M, Honegger JB. Quantitative assessment of postoperative blood collection in brain tumor surgery under valproate medication. *Zentralbl Neurochir*. 2008 Nov;69(4):165-9.
195. Wolff JE, Driever PH, Erdlenbruch B, Kortmann RD, Rutkowski S, Pietsch T, et al. Intensive chemotherapy improves survival in pediatric high-grade glioma after gross total resection: Results of the HIT-GBM-C protocol. *Cancer*. 2010 Feb 1;116(3):705-12.
196. Acharya S, Bussell JB. Hematologic toxicity of sodium valproate. *J Pediatr Hematol Oncol*. 2000 Jan-Feb;22(1):62-5.
197. Lehmann DF, Hurteau TE, Newman N, Coyle TE. Anticonvulsant usage is associated with an increased risk of procarbazine hypersensitivity reactions in patients with brain tumors. *Clin Pharmacol Ther*. 1997 Aug;62(2):225-9.
198. Chapman SA, Wacksman GP, Patterson BD. Pancreatitis associated with valproic acid: A review of the literature. *Pharmacotherapy*. 2001 Dec;21(12):1549-60.
199. Bohan TP, Helton E, McDonald I, Konig S, Gazitt S, Sugimoto T, et al. Effect of L-carnitine treatment for valproate-induced hepatotoxicity. *Neurology*. 2001 May 22;56(10):1405-9.
200. Samren EB, van Duijn CM, Koch S, Hiilesmaa VK, Klepel H, Bardy AH, et al. Maternal use of antiepileptic drugs and the risk of major congenital malformations: A joint European prospective study of human teratogenesis associated with maternal epilepsy. *Epilepsia*. 1997 Sep;38(9):981-90.
201. Witt O, Schweigerer L, Driever PH, Wolff J, Pekrun A. Valproic acid treatment of glioblastoma multiforme in a child. *Pediatr Blood Cancer*. 2004 Aug;43(2):181.
202. Rokes CA, Remke M, Guha-Thakurta N, Witt O, Korshunov A, Pfister S, et al. Sorafenib plus valproic acid for infant spinal glioblastoma. *J Pediatr Hematol Oncol*. 2010 Aug;32(6):511-4.
203. van Breemen MS, Rijsman RM, Taphoorn MJ, Walchenbach R, Zwinkels H, Vecht CJ. Efficacy of anti-epileptic drugs in patients with gliomas and seizures. *J Neurol*. 2009 Sep;256(9):1519-26.

204. Weller M, Gorlia T, Cairncross JG, van den Bent MJ, Mason W, Belanger K, et al. Prolonged survival with valproic acid use in the EORTC/NCIC temozolomide trial for glioblastoma. *Neurology*. 2011 Sep 20;77(12):1156-64.
205. Tsai HC, Wei KC, Tsai CN, Huang YC, Chen PY, Chen SM, et al. Effect of valproic acid on the outcome of glioblastoma multiforme. *Br J Neurosurg*. 2011 Dec 15.
206. Ruben JD, Dally M, Bailey M, Smith R, McLean CA, Fedele P. Cerebral radiation necrosis: Incidence, outcomes, and risk factors with emphasis on radiation parameters and chemotherapy. *Int J Radiat Oncol Biol Phys*. 2006 Jun 1;65(2):499-508.
207. Su JM, Li XN, Thompson P, Ou CN, Ingle AM, Russell HV, et al. Phase 1 study of valproic acid in pediatric patients with refractory solid or CNS tumors: A children's oncology group report. *Clin Cancer Res*. 2010 Nov 29.
208. Wolff JE, Boos J, Kuhl J. HIT-GBM: Multicenter study of treatment of children with malignant glioma. *Klin Padiatr*. 1996 Jul-Aug;208(4):193-6.





CHAPTER 3

Effects of valproic acid on HDAC inhibition *in vitro* and in glioblastoma patient samples

Sharon Berendsen, Elselien Frijlink, Jèrôme Kroonen, Wim G.M. Spliet,
Wim van Hecke, Tatjana Seute, Tom J. Snijders, Pierre A. Robe

Published in: Neuro-Oncology Advances. 2019 May-December;1(1).

ABSTRACT

Background: The anti-epileptic drug valproic acid (VPA) inhibits histone deacetylase in glioblastoma cells *in vitro*, which influences several oncogenic pathways and decreases glioma cell proliferation. The clinical relevance of these observations remains unclear, as VPA does not seem to affect glioblastoma patient survival. In this study, we analyzed whether the *in vitro* effects of VPA treatment on histone acetylation are also observed in tumor tissues of glioblastoma patients.

Methods: The *in vitro* effects of VPA treatment on histone acetylation were assessed with immunofluorescence and western blotting. On tissue microarrays and in fresh frozen glioblastoma tissues we investigated the histone acetylation patterns of patients who were either treated with VPA or did not receive anti-epileptic drugs at the time of their surgery. We also performed mRNA expression-based and gene set enrichment analyses on these tissues.

Results: VPA increased the expression levels of acetylated histones H3 and H4 *in vitro*, in agreement with previous reports. In tumor samples obtained from glioblastoma patients however, VPA treatment affected neither gene (set) expression nor histone acetylation.

Conclusions: The *in vitro* effects of VPA on histone acetylation status in glioblastoma cells could not be confirmed in clinical tumor samples of glioblastoma patients using anti-epileptic doses of VPA, which reflects the lack of effect of VPA on the clinical outcome of glioblastoma patients.

INTRODUCTION

Glioblastoma is the most aggressive primary brain tumor, and confers a dismal prognosis with a median survival of 15-20 months [1], despite extensive treatment. Genetic and epigenetic events condition the deregulation of growth, invasion and therapeutic resistance pathways in glioblastoma [2, 3].

Valproic acid (VPA) is a potent inhibitor of histone deacetylase (HDAC) and modulator of epigenetic events that has been used for several decades as an antiepileptic drug and mood-stabilizer[4]. VPA is also reported to elicit various anti-tumor effects in glioma cells *in vitro* [5-8]. Through the inhibition of a subset of histone deacetylases (HDACs) [4, 9] and cellular kinases (e.g., GSK-3 β) [10, 11], it decreases the activity of several transcription factors and signaling cascades, for instance NF- κ B, STAT3, p53, p21 and Wnt/ β -catenin signaling. In addition, in experimental gliomas, VPA reduces angiogenesis and inhibits tumor invasion, inhibits DNA repair and potentiates the effect of chemotherapies (e.g., temozolomide and etoposide) and radiation therapy (for a review, see [5]).

The study of large cohorts of patients with glioblastomas did however not find any favorable effect of VPA on glioblastoma patient survival [12, 13], especially when taking into account that epilepsy at diagnosis is a favorable independent prognostic factor, irrespective of anti-epileptic drug use, in these tumors [13]. This raises the question whether the clinical doses of VPA are able to elicit antitumor effects in glioblastomas in the clinical setting.

In order to answer this question, we compared the histone acetylation and RNA expression profiles of patient-derived glioblastoma tissue samples obtained from patients treated or not with this drug.

METHODS

Ethical statement

This study was conducted following approval by the ethical committee, biobank and institutional review board of the University Medical Center Utrecht (protocols 09-420, 14-225 and WARB2011/25).

Patient selection

Fresh frozen glioblastoma tissue was obtained from surgery, after written informed consent of the patients. Seventy-six fresh-frozen surgical samples of *de novo* glioblastomas were prospectively collected between 2010 and 2015, as reported previously [14]. From these patients, we selected all patients that were treated with VPA for epileptic seizures at the

time of surgery (n=12). As a control group, we selected all patients that had experienced tumor related epileptic seizures, but were not treated with any anti-epileptic drug at the time of surgery (n=7), since epileptogenic glioblastomas are biologically different from glioblastomas that do not cause epilepsy [14-17]. These fresh frozen samples were used for mRNA expression analyses and Western blotting, as described below.

Archival fresh frozen paraffin embedded glioblastoma tumor tissues from a consecutive cohort of 286 patients treated in the University Medical Center of Utrecht between 2009 and 2013 were included on tissue microarrays (TMA's) as described previously [13]. Among these patients, we selected all patients receiving VPA for epilepsy at the time of their surgery. The control group consisted of all consecutive glioblastoma patients with epilepsy who did not receive anti-epileptic treatment at the time of their surgery.

The median VPA treatment duration until surgery was 33 days (range 13-196). In 11 patients, VPA treatment duration could not be verified. All patients on VPA continued the use of VPA in the peri-operative timeframe.

IDH1 mutational status was not yet routinely determined in clinical practice at our center, but was available for 41/43 patients from a post-hoc analysis from another study [13]

mRNA expression analysis

RNA was extracted with the Nucleospin® TriPrep (Macherey-Nagel) and the QIASymphony RNA (Qiagen) kits according to the manufacturers' instructions. Affymetrix HG U133 plus 2.0 arrays were prepared and scanned according to the manufacturer's protocol and as reported previously[18].

Differential gene expression analyses and exploratory Gene Set Enrichment Analyses (GSEA) were performed after RMA-normalization [19] and batch correction, with the Partek® Genomics suite platform (v6.6). Analyses were performed with the Broad Institute MySig libraries of curated gene sets C1 – C7 version 5.0 [20], 1000 permutations and default additional parameters. An FDR threshold of 0.1 was applied.

Class prediction

Molecular subclassification (proneural, neural, classical, mesenchymal) was determined by hierarchical clustering[21]. Microarray normalization, data filtering and analysis of inter-array homogeneity were performed as reported previously[21, 22]. Affymetrix HG U133 plus 2.0 probesets were matched to 840 genes originally published for the classification of glioblastomas (http://tcga-data.nci.nih.gov/docs/publications/gbm_exp/). Relative gene expression values were calculated. Genes were then excluded for a median absolute deviation below 0.5[21]. After filtering, 768 genes were used for the class prediction. The

hierarchical clustering of samples was performed with cluster3 software [23] with the agglomerative average linkage for the structure and 1 minus the Pearson's correlation for the distance metric[21]. Classes could be assigned to 17/19 samples.

Cell culture

Primary cell culture GM3 was obtained by mincing fresh surgical tumor samples as described previously[24]. The U87 cell line was obtained from ATCC. Cells were maintained at low passages and cultivated in Dulbecco's modified Eagle's medium supplemented with 10% fetal bovine serum and 1% sodium pyruvate.

Cell survival assay

To assess acute cell toxicity due to VPA treatment, cell survival in response to VPA treatment was assayed using an MTS test (One Solution Cell Proliferation Assay, Promega). Cell line U87 and primary cell cultures GM3 were treated with different concentrations of VPA (0 mM, 0.1 mM, 0.5 mM, 1 mM, 2.5 mM, 5 mM and 10 mM) for 24 hours before performing the MTS assays. The MTS assays were performed as recommended by the manufacturer's protocol.

Western blotting

Cells were treated once daily with VPA (0 – 1 mM) for 48 hours. We performed protein extraction with RIPA buffer (Sigma-Aldrich) or a nuclear extraction kit (Active Motif) and proteins were separated by means of 10% polyacrylamide gel electrophoresis. Membrane transfer was performed with the Trans-Blot® Turbo™ Transfer System (Bio-Rad). After blocking of aspecific sites, membranes incubated overnight at 4°C in the presence of primary antibody directed against anti-histone H4 (acetyl K8) (rabbit polyclonal, Abcam), anti-histone H3 (acetyl K9) (rabbit polyclonal, Abcam), GAPDH (Rabbit, Sigma). An HRP-coupled secondary antibody was subsequently incubated, and the signal was developed with ECL and the Super Signal West Femto Chemiluminescent substrate (Thermo Fisher Scientific) and the ImageQuant LAS 4000 Biomolecular Imager (GE Healthcare). Western blots were performed at least three independent times. We quantified the images with the gel analysis tool of ImageJ software (Rasband W.S., National Institutes of Health, Bethesda, Maryland, USA).

Immunocytochemistry

Immunocytochemistry was performed as described previously [25]. Cells were treated once daily for 48 hours with 0 – 1 mM VPA. Primary antibody incubation (anti-histone H3 (acetyl K9) (rabbit polyclonal, Abcam) and anti-histone H4 (acetyl K8) (rabbit polyclonal, Abcam)) was performed overnight at 4°C. RRX- and FITC-conjugated (Jackson ImmunoResearch Laboratories) were used as secondary antibodies. Omission of primary antibodies resulted in a complete loss of detectable signal.

Imaging was performed with use of a laser-scanning confocal microscope (Olympus Fluoview 1000). Microscope setting were kept constant across the experimental conditions. We quantified the fluorescence signal intensity per cell with ImageJ.

Tissue microarrays and immunohistochemistry

A senior clinical neuropathologist reviewed histology of each specimen and performed marking on H&E stained sections. We reported details on tissue microarray construction and immunohistochemical staining previously [13]. The following primary antibodies were used: anti-histone H4 (acetyl K8) (Rabbit polyclonal, Abcam) and anti-histone H3 (acetyl K9) (Rabbit polyclonal, Abcam). The signal was developed with 3,3'-diaminobenzidine (DAB). Nuclei were counterstained with hematoxylin.

Researchers were blinded to the clinical data during evaluation of the protein expression. The percentage of nuclear staining and/or cytoplasmatic staining was scored as: 0, no positive staining; 1, 1-25% positive staining; 2, 26-50% positive staining; 3, 51-75% positive staining and 4, 76-100% positive staining. A mean staining score was computed for each patient.

Western blotting fresh frozen tissues

Fresh frozen glioblastoma tissue from 14 patients (VPA: n=8, no AED: n=6) was available for Western blotting. Protein extraction was performed with RIPA buffer containing protease and phosphatase inhibitors. 50 ng of protein lysate was used for Western blotting, which was performed as described above. We used the following primary antibodies: anti-histone H4 (acetyl K8) (rabbit polyclonal, Abcam), anti-histone H3 (acetyl K9) (rabbit polyclonal, Abcam), GAPDH (Rabbit, Sigma).

Statistical analysis

Statistical analyses were performed with Graphpad Prism 7 software. We checked the data distribution graphically with boxplots. The MTS test was analyzed compared to the control condition with one-way ANOVA with Dunnet's post-hoc test. The immunofluorescence data was analyzed compared to the control condition with a one-sample t-test. Western blots with multiple dosages of VPA were analyzed with a 2-sided ANOVA to control for interexperimental variation. The Western blotting experiment containing patient material and immunohistochemistry results were analyzed with a Mann-Whitney U test. Two-sided p-values < 0.05 were considered significant.

RESULTS

VPA treatment increases expression of acetylated histone H3 and H4 in glioblastoma cells *in vitro*.

In U87 cells, we confirmed with western blotting and immunocytochemistry that VPA, starting at a concentration of 0.6mM, can increase histone H3 and H4 acetylation (Figure 1). In GM3 primary glioblastoma cells we repeatedly observed a similar trend, although these results did not reach statistical significance (Figure 1 and S1). Acute cell toxicity by VPA treatment for 48 hours was only observed with a dosage of 10 mM (Figure 1E).

VPA does not increase histone acetylation activity in tumor tissue from glioblastoma patients.

Among the 286 patients of our TMA, 29 patients were treated with VPA for epilepsy at the time of their surgery. The control group consisted of 14 glioblastoma patients with epilepsy who did not receive anti-epileptic treatment. Staining could not be analyzed for 1 (histone H3) and 2 (histone H4) patients from the VPA group, due to insufficient tissue quality on the TMA. The baseline characteristics of these patients are summarized in table S1.

There was no difference in the acetylation patterns on TMAs of histone H3 and H4 in the patients treated with VPA as compared to the patients with epilepsy but without any AED (figure 2A, Mann Whitney U test, $p=0.41$ and 0.46 respectively). Additionally, we analyzed acetyl-H3 and acetyl-H4 levels in 14 fresh frozen glioblastoma samples with Western blotting, which might be more sensitive to pick up a difference in histone acetylation levels. Again, there was no difference in acetylated histone H3 and H4 expression between patients that were treated with VPA ($n=8$) and those that had epileptic seizures, but were not treated with any AED at the time of surgery ($n=6$, figure 2B-C, Mann Whitney U test, $p=0.8$ for both experiments).

VPA does not alter mRNA or gene set expression in glioblastoma tissue.

Affymetrix U133 plus 2.0 RNA expression data were obtained for 12 glioblastoma patients who were treated with VPA at the time of their surgery and for 7 glioblastoma patients who experienced seizures at presentation of the disease, but were not treated with any AED at the time of surgery. Baseline characteristics of these patients are summarized in table S2. Distribution of the molecular subtypes (according to Verhaak [21]) did not differ between the subgroups (Figure 2D, Fisher exact test, $p=1.0$). There was no significant mRNA expression difference between in the VPA group compared to the patients without any AED after correction for multiple testing (ANOVA, cutoff $p<0.05$, FDR <0.05). Exploratory gene set enrichment analyses (GSEA) likewise did not show any association between VPA and gene set expression with cutoff $p<0.05$ and FDR < 0.1 . We did observe an isolated

higher expression of the BIOCARTA_AHSP_PATHWAY in the VPA group as compared to patients without any AED ($p < 0.0001$), but with higher FDR (0.12).

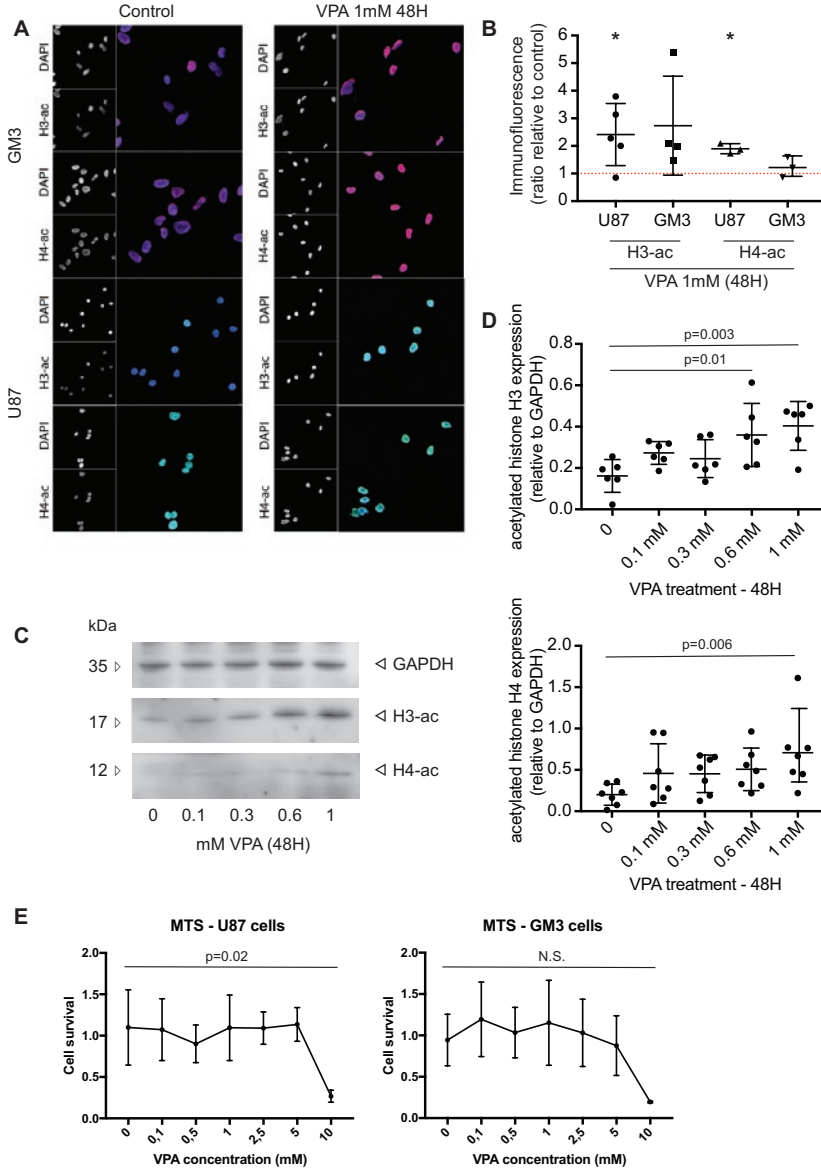


Figure 1 - Increased expression of acetylated histone H3 and H4 in glioblastoma cells after VPA treatment.

(A) Immunofluorescent stainings of acetylated histone H3K9 and H4K8 in GM3 (upper panels) and U87 cells (lower panels). Cells were treated with VPA 1 mM or control during 48 hours. (B) Quantification of immunofluorescence experiments shown in A. Results are shown as ratio compared

Figure 1 - Increased expression of acetylated histone H3 and H4 in glioblastoma cells after VPA treatment (continued). to control. Bars represent mean \pm SD. n=3-5. Results were analyzed by one-sample t-tests. *: $p < 0.05$. (C) Western blot results for acetylated histone H3K9 (upper panels) and H4K8 (lower panels) and GAPDH (loading control) in U87 cells. Cells were treated with 0, 0.1, 0.3, 0.6 and 1 mM VPA during 48 hours. (D) Quantification of Western blot results for acetylated histone H3K9 and H4K8, relative to GAPDH expression, in U87 cells. N=6-7. Bars represent mean \pm SD. Results were analyzed by two-way ANOVA controlling for interexperimental variation. (E) Cell survival assay (MTS test). The proportion of surviving cells after treatment with VPA with increasing dosages (0, 0.1, 0.5, 1, 2.5, 5, 10 mM) for 48 hours is plotted. N=3. Bars represent mean \pm SD. Results were analyzed with one-way ANOVA with Dunnet's posthoc test.

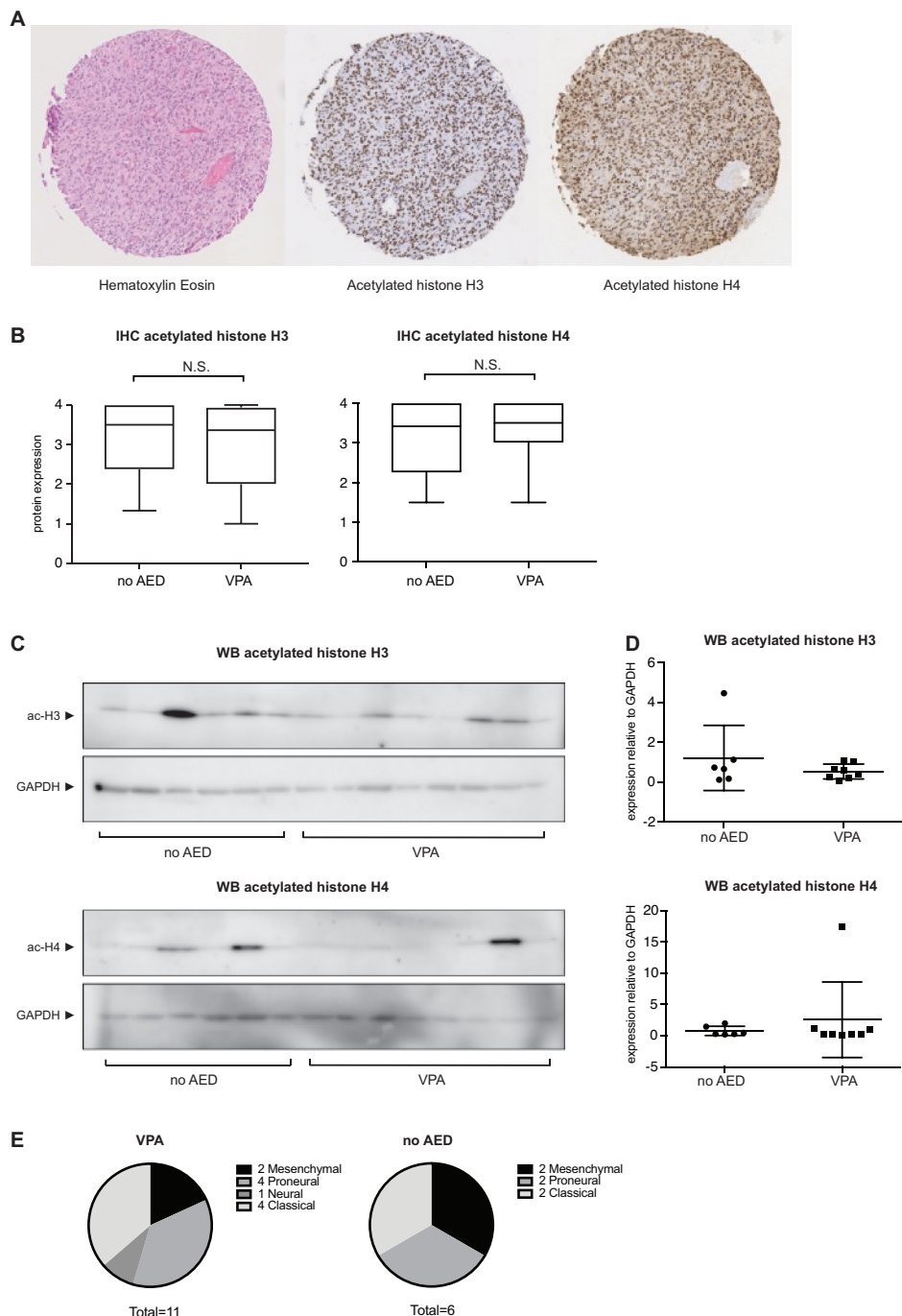


Figure 2 - VPA does not increase histone acetylation activity in tumor tissue from glioblastoma patients. (A) Examples of immunohistochemical staining of glioblastoma sample on tissue microarray. The left panel displays hematoxylin eosin staining, the middle panel shows immunostaining of

Figure 2 - VPA does not increase histone acetylation activity in tumor tissue from glioblastoma patients (continued). acetylated histone H3 and the right panel displays immunostaining of acetylated histone H4 in the same patient. (B) Quantification of immunohistochemical staining on tissue microarrays (TMA's) containing tumor tissue from glioblastoma patients. TMA's were stained for acetylated histone H3K9 and H4K8. Boxes represent median and quartiles, whiskers represent data range. Results were analyzed by Mann Whitney U test. (C) Quantification of western blot results for acetylated histone H3K9 and H4K8, relative to GAPDH expression, in fresh-frozen patient-derived glioblastoma tissue. Bars represent mean \pm SD. VPA: patients that were treated with VPA for epileptic seizures, n=8. No AED: patients had tumor-associated seizures but were not treated with any AED at the time of surgery, n=6. Results were analyzed by Mann Whitney U test. (D) Western blot results for acetylated histone H3K9 and H4K8 and GAPDH (loading control) in fresh-frozen glioblastoma tissues. (E) Molecular subtype distribution in the patients with VPA and patients with epilepsy but without anti-epileptic drugs treatment. Fisher exact test, p=1.0.

DISCUSSION

Our *in vitro* observation that VPA increases histone H3 and H4 acetylation in glioblastoma (primary) cells at concentrations above 0.6 mM after treatment for 48 hours confirms a wealth of previous reports [4, 7, 9, 26, 27] that have triggered the study of use of VPA as an adjunct for the treatment of glioblastoma patients. Both the resulting clinical trials and several retrospective cohort analyses have however failed to show any survival benefit of this drug for glioblastoma patients [12, 13].

In order to assess whether VPA has relevant antitumor effects in clinical conditions, we compared the histone acetylation and RNA expression profiles of patient-derived glioblastoma tissue samples obtained from patients treated or not with this drug.

Since epileptogenic tumors differ biologically from those that do not elicit epilepsy [14-17], we only included glioblastoma patients in our analyses who had epileptic seizures at presentation of the disease. Some other anti-epileptic drugs, e.g. topiramate and a major metabolite of levetiracetam, have been reported to influence HDAC expression and function as well [28, 29]. Therefore, in order to avoid any confounding effect, we only included patients in the control group who experienced one or more epileptic seizures but who were not yet treated with any AED prior to their surgery. Although Dutch guidelines recommend treatment with AED for focal tumor-related epilepsy as a rule, the option of withholding AED, e.g. after a single seizure, is mentioned as a matter of shared decision making with the patient. Therefore, we could include a (small) control group of patients with epilepsy who did not receive any AED.

In these comparisons, the level of H3 and H4 acetylation did not differ between glioblastoma tissue obtained from patients with seizures that were treated with valproic

acid at the time of their surgery. Likewise, there was no difference of gene expression between these tumors.

A likely explanation for these observations stems from the pharmacokinetics of VPA. Indeed, while serum VPA concentration of 0.7-1.4 mM can be attained with standard clinical dosages of 900-1000 mg VPA twice daily, VPA concentrations in organ tissues, including brain tissue, are 8-9x lower [30]. Tissue concentrations are likely to be higher in glioblastomas as they are characterized by disruption of the blood-brain barrier [31], but are unlikely to be equal to those of the serum, and superior to the *in vitro* threshold of 0.6 mM.

Another potential explanation for the discrepancy between experimental and clinical results is that long term treatment (30 days) has been shown to induce resistance of glioblastoma cells to VPA [32]. In our study, the median duration of VPA treatment was 33 days, and resistance to glioblastoma cells could not be excluded. This duration of treatment possibly results from the time to referral to our tertiary center. Unfortunately, as a limitation of our retrospective study design, the serum and tissue concentrations of VPA were not available.

In line with the lack of clinical effect of VPA on histone acetylation in glioblastomas, GSEA showed no associations of VPA on gene set expression in all analyses, except for an isolated higher expression of the BIOCARTA_AHSP_PATHWAY in the VPA group as compared to patients without any AED ($p < 0.0001$), but with higher FDR (0.12). VPA and other HDACs have been investigated for effects on hemoglobinopathies in the past and a recent preclinical study showed that 0.5 mM VPA treatment could increase AHSP expression in a human erythroleukemia cell line [33].

A limitation to our study is that in order to exclude confounding by biological effects due to the presence of epilepsy itself or that of other anti-epileptic drugs, despite a large surgical load at our institution, we could only include a relatively low number of patients. While larger studies may be necessary to prove the lack of any subtle effect of VPA on the gene expression in tumor tissue in glioblastoma patients, we believe that our findings can seal the discussion on the lack of effect of VPA on the histone acetylation of glioblastoma in the clinic at common dosages [12, 13].

This discrepancy between experimental results and effects in patient samples might explain the lack of effect of VPA on survival of glioblastoma patients. Supraclinical dosages might be necessary to reach the anti-tumor effects that have been shown *in vitro*. Alternatively, other methods of HDAC inhibition may prove more relevant.

REFERENCES

1. Stupp R, Taillibert S, Kanner AA, et al. Maintenance Therapy With Tumor-Treating Fields Plus Temozolomide vs Temozolomide Alone for Glioblastoma: A Randomized Clinical Trial. *Jama*. 2015; 314(23):2535-2543.
2. Brennan CW, Verhaak RG, McKenna A, et al. The somatic genomic landscape of glioblastoma. *Cell*. 2013; 155(2):462-477.
3. Bredel M, Scholtens DM, Yadav AK, et al. NFKBIA deletion in glioblastomas. *The New England journal of medicine*. 2011; 364(7):627-637.
4. Phiel CJ, Zhang F, Huang EY, Guenther MG, Lazar MA, Klein PS. Histone deacetylase is a direct target of valproic acid, a potent anticonvulsant, mood stabilizer, and teratogen. *J Biol Chem*. 2001; 276(39):36734-36741.
5. Berendsen S, Broekman M, Seute T, et al. Valproic acid for the treatment of malignant gliomas: review of the preclinical rationale and published clinical results. *Expert opinion on investigational drugs*. 2012; 21(9):1391-1415.
6. Hosein AN, Lim YC, Day B, et al. The effect of valproic acid in combination with irradiation and temozolomide on primary human glioblastoma cells. *J Neurooncol*. 2015; 122(2):263-271.
7. Das CM, Aguilera D, Vasquez H, et al. Valproic acid induces p21 and topoisomerase-II (alpha/beta) expression and synergistically enhances etoposide cytotoxicity in human glioblastoma cell lines. *J Neurooncol*. 2007; 85(2):159-170.
8. Cornago M, Garcia-Alberich C, Blasco-Angulo N, et al. Histone deacetylase inhibitors promote glioma cell death by G2 checkpoint abrogation leading to mitotic catastrophe. *Cell Death Dis*. 2014; 5:e1435.
9. Gurvich, N. et al., Histone Deacetylase Is a Target of Valproic Acid-Mediated Cellular Differentiation. *Cancer Research*, 2004. 64: p. 1079–1086.
10. Chen, G., et al., The Mood-Stabilizing Agent Valproate Inhibits the Activity of Glycogen Synthase Kinase-3. *J. Neurochem*, 1999. 72: p. 1327–1330.
11. Zhang C, Liu S, Yuan X, et al. Valproic Acid Promotes Human Glioma U87 Cells Apoptosis and Inhibits Glycogen Synthase Kinase-3beta Through ERK/Akt Signaling. *Cell Physiol Biochem*. 2016; 39(6):2173-2185.
12. Happpold C, Gorlia T, Chinot O, et al. Does Valproic Acid or Levetiracetam Improve Survival in Glioblastoma? A Pooled Analysis of Prospective Clinical Trials in Newly Diagnosed Glioblastoma. *J Clin Oncol*. 2016; 34(7):731-739.
13. Berendsen S, Varkila M, Kroonen J, et al. Prognostic relevance of epilepsy at presentation in glioblastoma patients. *Neuro Oncol*. 2016; 18(5):700-706.
14. Berendsen S, Spliet WGM, Geurts M, et al. Epilepsy Associates with Decreased HIF-1alpha/STAT5b Signaling in Glioblastoma. *Cancers*. 2019; 11(1); 41.
15. Rosati A, Marconi S, Pollo B, et al. Epilepsy in glioblastoma multiforme: correlation with glutamine synthetase levels. *Journal of neuro-oncology*. 2009; 93(3):319-324.
16. Rosati A, Poliani PL, Todeschini A, et al. Glutamine synthetase expression as a valuable marker of epilepsy and longer survival in newly diagnosed glioblastoma multiforme. *Neuro-oncology*. 2013; 15(5):618-625.
17. Yuan Y, Xiang W, Yanhui L, et al. Ki-67 overexpression in WHO grade II gliomas is associated with poor postoperative seizure control. *Seizure*. 2013; 22(10):877-881.
18. Turkheimer FE, Roncaroli F, Hennuy B, et al. Chromosomal patterns of gene expression from microarray data: methodology, validation and clinical relevance in gliomas. *BMC bioinformatics*. 2006; 7:526.

19. Subramanian A, Tamayo P, Mootha VK, et al. Gene set enrichment analysis: a knowledge-based approach for interpreting genome-wide expression profiles. *Proceedings of the National Academy of Sciences of the United States of America*. 2005; 102(43):15545-15550.
20. Reich M, Liefeld T, Gould J, Lerner J, Tamayo P, Mesirov JP. GenePattern 2.0. *Nature genetics*. 2006; 38(5):500-501.
21. Verhaak RG, Hoadley KA, Purdom E, et al. Integrated genomic analysis identifies clinically relevant subtypes of glioblastoma characterized by abnormalities in PDGFRA, IDH1, EGFR, and NF1. *Cancer cell*. 2010; 17(1):98-110.
22. Wislet-Gendebien S, Poulet C, Neirinckx V, et al. In vivo tumorigenesis was observed after injection of in vitro expanded neural crest stem cells isolated from adult bone marrow. *PloS one*. 2012; 7(10):e46425.
23. Eisen MB, Spellman PT, Brown PO, Botstein D. Cluster analysis and display of genome-wide expression patterns. *Proceedings of the National Academy of Sciences of the United States of America*. 1998; 95(25):14863-14868.
24. Robe PA, Bentires-Alj M, Bonif M, et al. In vitro and in vivo activity of the nuclear factor-kappaB inhibitor sulfasalazine in human glioblastomas. *Clinical cancer research : an official journal of the American Association for Cancer Research*. 2004; 10(16):5595-5603.
25. Kroonen J, Nassen J, Boulanger YG, et al. Human glioblastoma-initiating cells invade specifically the subventricular zones and olfactory bulbs of mice after striatal injection. *International journal of cancer. Journal international du cancer*. 2011; 129(3):574-585.
26. Gottlicher, M. et al., Valproic acid defines a novel class of HDAC inhibitors inducing differentiation of transformed cells. *The EMBO Journal*, 2001. 24: p. 6969-6978.
27. Benitez JA, Arregui L, Cabrera G, Segovia J. Valproic acid induces polarization, neuronal-like differentiation of a subpopulation of C6 glioma cells and selectively regulates transgene expression. *Neuroscience*. 2008; 156(4):911-920.
28. Eyal S, Yagen B, Sobol E, Altschuler Y, Shmuel M, Bialer M. The activity of antiepileptic drugs as histone deacetylase inhibitors. *Epilepsia*. 2004; 45(7):737-744.
29. Ookubo M, Kanai H, Aoki H, Yamada N. Antidepressants and mood stabilizers effects on histone deacetylase expression in C57BL/6 mice: Brain region specific changes. *Journal of psychiatric research*. 2013; 47(9):1204-1214.
30. Ogungbenro K, Aarons L, Cresim, Epi CPG. A physiologically based pharmacokinetic model for Valproic acid in adults and children. *Eur J Pharm Sci*. 2014; 63:45-52.
31. Dubois LG, Campanati L, Righy C, et al. Gliomas and the vascular fragility of the blood brain barrier. *Front Cell Neurosci*. 2014; 8:418.
32. Riva M, Salmaggi A, Marchioni E, et al. Tumour-associated epilepsy: clinical impact and the role of referring centres in a cohort of glioblastoma patients. A multicentre study from the Lombardia Neurooncology Group. *Neurological sciences : official journal of the Italian Neurological Society and of the Italian Society of Clinical Neurophysiology*. 2006; 27(5):345-351.
33. Okhovat MA, Ziari K, Ranjbaran R, Nikouyan N. The effect of histone deacetylase inhibitors on AHSP expression. *PLoS One*. 2018; 13(2):e0189267.

SUPPLEMENTARY FILES

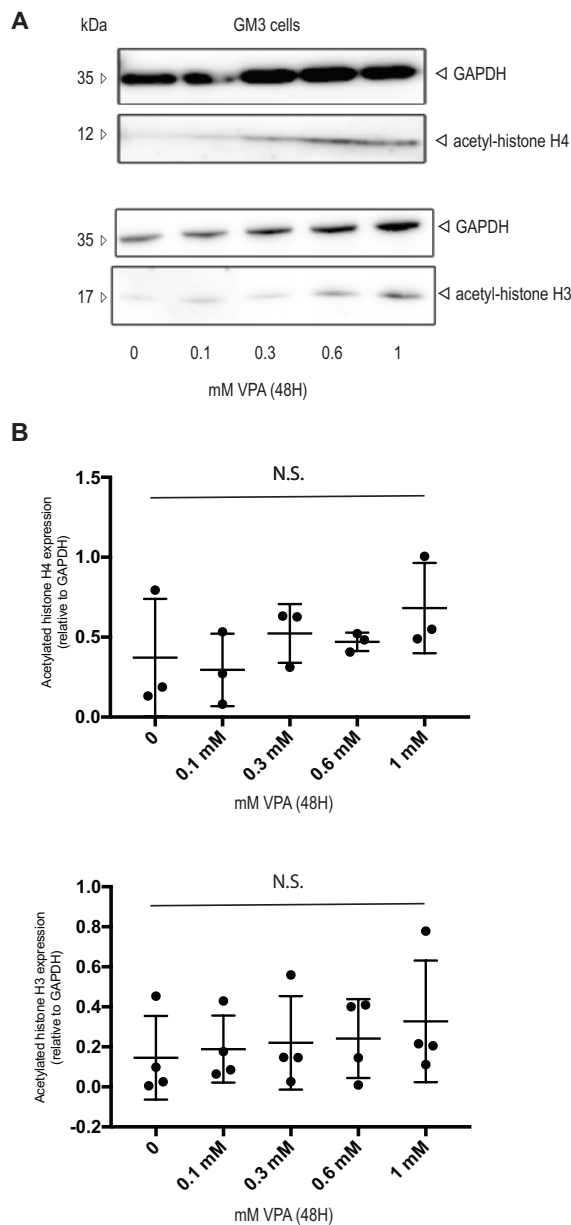


Figure S1 – Effect of VPA on histone acetylation in GM3 cells. (A) Western blot results for acetylated histone H3K9 and H4K8 and GAPDH (loading control) in GM3 cells. Cells were treated with 0, 0.1, 0.3, 0.6 and 1 mM VPA during 48 hours. (B) Quantification of western blot results for acetylated histone H3K9 and H4K8, relative to GAPDH expression, in GM3 cells. Bars represent mean \pm SD. N=3-4. Results were analyzed by two-way ANOVA controlling for interexperimental variation.

Table S1 – Baseline table TMA analyses

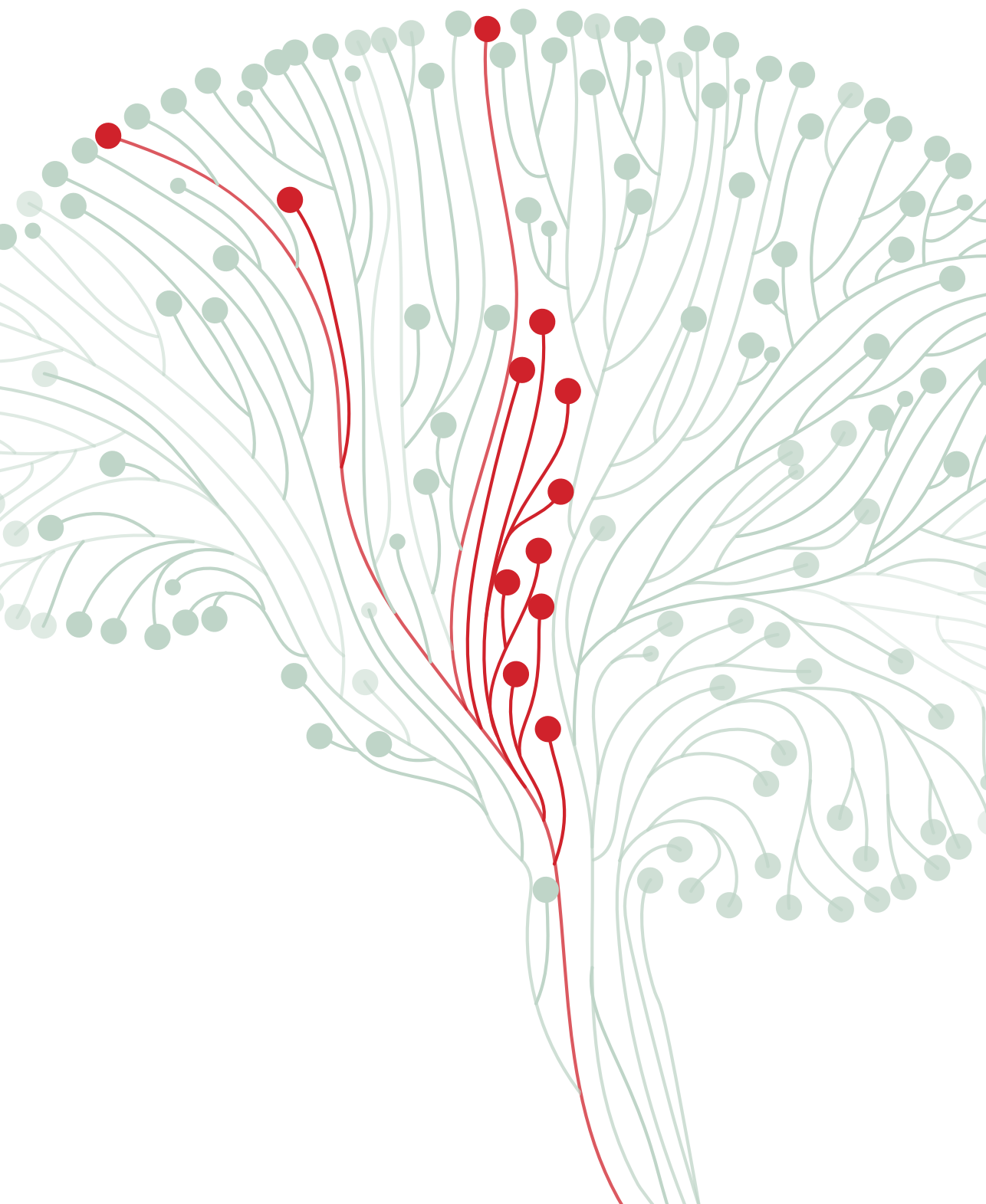
Patient characteristics <i>n</i> (%)	Epilepsy without AED 14 (32.6)	VPA 29 (67.4)
Age (<i>mean ± SD</i>)	61.1 ± 14.8	57.2 ± 12.9
Gender (% <i>male</i>)	64.2	58.6
KPS <i>n</i> (%)		
< 70	4 (28.6)	8 (27.6)
≥ 70	9 (64.3)	21 (72.4)
	Missing: 1 (7.1)	
Tumor volume <i>cm</i> ³ (<i>median (range)</i>)	37.4 (2.5-85.3)	32.0 (3.1-155.7) Missing: 3 (3.2)
Extent of surgery <i>n</i> (%)		
Biopsy	0	2 (6.9)
Debulking	14 (100)	27 (93.1)
Post-surgical treatment <i>n</i> (%)		
None	2 (14.3)	2 (6.9)
Monotherapy RT or TMZ	2 (14.3)	4 (13.8)
RT + TMZ	10 (71.4)	23 (79.3)
Epilepsy at presentation <i>n</i> (%)	14 (100)	29 (100)
AED treatment <i>n</i> (%)		
VPA	-	29 (100)
LEV	-	4 (13.8)
CBZ	-	2 (6.9)
PHN	-	2 (6.9)
Other	-	1 (3.4)
Duration VPA treatment - <i>days</i> (<i>median (range)</i>)	-	33 (13-196) Missing 10 (34.5)
IDH1 mutational status <i>n</i> (%)		
Wildtype	14 (100)	24 (82.8)
IDH1 R132H mutation	0	3 (10.3)
		Missing: 2 (6.9)

Abbreviations: VPA: valproic acid; LEV: levetiracetam; CBZ: carbamazepine; PHN: phenytoin; AED: anti-epileptic drugs; KPS: Karnofsky performance score; IQR: interquartile range; RT: radiotherapy; TMZ: temozolomide

Table S2 – Baseline table GSEA samples

Patient characteristics <i>n</i> (%)	Epilepsy without AED 7 (36.8)	VPA 12 (63.2)
Age (<i>mean ± SD</i>)	58.7 ± 14.6	58.6 ± 10.4
Gender (% <i>male</i>)	71.4	75
KPS <i>n</i> (%)		
< 70	0	2 (27.6)
≥ 70	7 (100)	10 (72.4)
Extent of surgery <i>n</i> (%)		
Biopsy	0	0
Debulking	7 (100)	12 (100)
Post-surgical treatment <i>n</i> (%)		
None	0	1 (8.3)
Monotherapy RT or TMZ	1 (14.3)	1 (8.3)
RT + TMZ	6 (85.7)	10 (83.3)
Epilepsy at presentation <i>n</i> (%)	7 (100)	12 (100)
Duration VPA treatment - <i>days</i> (<i>median (range)</i>)	-	33 (13-146) <i>Missing: 2</i>
IDH1 mutational status <i>n</i> (%)		
Wildtype	5 (71.4)	5 (41.7)
IDH1 R132H mutation	0 <i>Missing: 2 (28.6)</i>	1 (8.3) <i>Missing: 6 (50)</i>

Abbreviations: VPA: valproic acid; AED: anti-epileptic drugs; KPS: Karnofsky performance score; RT: radiotherapy; TMZ: temozolomide





CHAPTER 4

Prognostic relevance of epilepsy at presentation in glioblastoma patients

Based on:

Prognostic relevance of epilepsy at presentation in glioblastoma patients

Sharon Berendsen, Meri Varkila, Jérôme Kroonen, Tatjana Seute, Tom J. Snijders, Frans Kauw, Wim G.M. Spliet, Marie Willems, Christophe Poulet, Marike L. Broekman, Vincent Bours, and Pierre A. Robe

Published in: Neuro-Oncology. 2016 May;18(5):700-6.

And:

Response to: “Prognostic relevance of epilepsy at presentation in lower-grade gliomas”

Sharon Berendsen, Tom J. Snijders, Pierre A. Robe.

Published in: Neuro-Oncology. 2016 Sep;18(9):1327-8.

ABSTRACT

Background. Epileptogenic glioblastomas are thought to convey a favorable prognosis, either due to early diagnosis or potential antitumor effects of antiepileptic drugs. We investigated the relationship between survival and epilepsy at presentation, early diagnosis, and antiepileptic drug therapy in glioblastoma patients.

Methods. Multivariable Cox regression was applied to survival data of 647 consecutive patients diagnosed with *de novo* glioblastoma between 2005 and 2013 in order to investigate the association between epilepsy and survival in glioblastoma patients. In addition, we quantified the association between survival and valproic acid (VPA) treatment.

Results. Epilepsy correlated positively with survival (HR: 0.75 (95% CI: 0.61 – 0.92), $P < .01$). This effect is independent of age, sex, performance status, type of surgery, adjuvant therapy, tumor location, and tumor volume, suggesting that this positive correlation cannot be attributed solely to early diagnosis. For patients who presented with epilepsy, the use of the antiepileptic drug VPA did not associate with survival when compared with patients who did not receive VPA treatment.

Conclusion. Epilepsy is an independent prognostic factor for longer survival in glioblastoma patients. This prognostic effect is not solely explained by early diagnosis, and survival is not associated with VPA treatment.

INTRODUCTION

Glioblastoma is the most malignant form of primary brain tumors, and 30% – 40% of glioblastoma patients initially present with epileptic seizures [1,2]. It has been hypothesized that seizures may convey a more favorable prognosis [3], although this latter assertion remains controversial [4 – 7] and potential mechanisms that would underlie a survival advantage remain speculative. At the most trivial level, seizures could trigger earlier presentation for care, thus accelerating diagnosis and initiating earlier treatment of smaller glioblastomas [8]. Epileptogenic glioblastomas may have distinct biological characteristics, such as a higher expression of glutamate and the $X_{(c)(-)}$ -system [9] and lower contents of glutamine synthetase [7,10], which have been proposed to be oncogenic [11,12]. In addition, the IDH1 R132H mutation is frequently identified in proneural glioblastomas [13] and is reported to be associated with epilepsy in low-grade glioma [14] and be a favorable prognostic factor in glioblastoma patients [15,16]. However, the correlation between these biological differences reported for epileptogenic glioblastomas and patient survival still awaits demonstration.

In vitro data suggest that antiepileptic drugs (AEDs) such as valproic acid (VPA) can alter glioma tumor growth and treatment resistance. VPA is believed to slow tumor growth through inhibition of a subset of histone deacetylases and modulation of the expression and activity of key transcription factors and cell-cycle regulators such as NF- κ B, STAT3, p53, p21 and TCF/ β -catenin. VPA was further shown to reduce angiogenesis, tumor invasion, and DNA repair caused by chemotherapies (e.g., temozolomide and etoposide) or radiation therapy (reviewed in [17]). Consistent with these *in vitro* data, some retrospective studies suggest a correlation between VPA and the overall survival of glioblastoma patients [1,18,19]. These studies, however, fail to differentiate the proper role of epilepsy from that of its treatment, and others do not observe this effect [20]. In this study, we assessed the prognostic relevance of epileptic onset and subsequent VPA treatment in a cohort of 647 consecutive *de novo* glioblastoma patients.

MATERIALS AND METHODS

Patient cohort

All adult patients (n=647) with histologically confirmed *de novo* supratentorial glioblastoma (WHO grade IV) diagnosed at the University Medical Center Utrecht between 2005 and 2013 were retrospectively included in this study. Hospital records of all patients were screened for the presence of at least one *de novo* epileptic seizure at symptom onset (i.e., prior to the surgery that obtained tissue for histological diagnosis), resulting in subgroups of patients with and without epilepsy at presentation. In addition, all patients were screened

for treatment with AEDs at the time of surgery. For analysis of the effect of AEDs on patient survival, we included patients who continued to use the specific AED for at least 2 months or until death. Other characteristics such as age, sex, KPS, tumor volume, type of surgery (biopsy or resection), the contrast-enhancing lesion on the presurgical MRI scan (T1 weighted + gadolinium) with use of OsiriX version 4.1.2 (Pixmeo). These scans were also used to determine the location of the contrast-enhancing lesion.

Ethics statement

This study was conducted following approval by the ethical committee and institutional review board of the University Medical Center Utrecht (protocols 09-420 and 14-225).

Tissue microarrays, immunohistochemistry, and scoring

Archival formalin-fixed, paraffin-embedded tumor tissue was available and collected retrospectively for 360 of the 647 glioblastoma patients treated in the University Medical Center Utrecht between 2005 and 2013. The histology of each specimen was reviewed by a senior clinical neuropathologist and marked on hematoxylin-and-eosin stained sections. For each patient, 2–3 tissue cores were placed on recipient arrayed paraffin blocks using a manual arrayer (Beecher Instruments). Immunohistochemical staining was performed on 4 mm sectioned TMA slides, which were deparaffinated in xylene and rehydrated with graded alcohol solutions. After peroxidase blocking, antigen retrieval was achieved by incubation in citrate buffer (pH 6) for 12 minutes at 126°C. Slides were incubated with anti-IDH1 R132H (Immunologic) for 1 hour at room temperature. Protein expression evaluation was blinded to the clinical data and scored as negative (0% of cells expressing IDH1 R132H) or positive (>0% of cells expressing IDH1 R132H).

Statistical analysis

Statistical analyses were performed with the use of SPSS 22.0 (IBM). P-values <.05 were considered significant. Differences in baseline characteristics were analyzed with chi-square tests or Fisher exact tests and independent t-tests or Mann-Whitney U tests, according to the distribution of data. We analyzed differences in IDH1 R132H expression between subgroups using the chi-square test. Kaplan-Meier curves were analyzed with use of the log-rank test. Cox regression was used for the survival analyses. Since the Cox model assumes that survival curves of 2 strata follow hazard functions that are proportional over time, this proportional hazards (PH) assumption was checked for each variable in the model with log-minus-log plots and time-dependent variables and did not hold for the variables KPS and tumor volume. Extension of the model with time-dependent variables for KPS and tumor volume resulted in a significantly better model fit, and these time-dependent variables (KPS*time and tumor volume*time) were therefore included in the final model. These time-dependent variables represent the changing association of the variable as time progresses.

The PH assumption held for the epilepsy variable for patients with survival up to 1000 days after surgery but was not valid after this point. Therefore, in addition to performing the survival analyses with the unadjusted follow-up time, the analyses were restricted to a maximal follow-up time of 1000 days after surgery. All patients who survived beyond this point were censored at 1000 days.

Univariable Cox regression was performed to assess the effect of epilepsy on glioblastoma patient survival. Next, multivariable Cox regression was performed, including other prognostic factors and baseline variables that differed across the subgroups. The following variables were included in the multivariable model: epilepsy, age at diagnosis, KPS, tumor volume, KPS*time, tumor volume*time, type of surgery, postsurgical treatment, tumor location, and sex.

Next, we evaluated the effect of VPA treatment compared with treatment with other AEDs on patient survival using Kaplan-Meier curves and univariate analysis. The effect was also corrected for age at diagnosis, KPS, KPS*time, tumor volume, tumor volume*time, type of surgery, surgery*time, post-surgical treatment, tumor location, and sex.

RESULTS

Epilepsy and survival in glioblastoma patients: univariable analysis

All adult patients with de novo supratentorial glioblastoma diagnosed at the University Medical Center Utrecht between 2005 and 2013 (n=647) were retrospectively included in this study. Baseline characteristics of the subgroups are described in Table 1.

The median overall survival in the total cohort of patients was 9.9 months (range: 0 ->103 mo) from surgery. One hundred twenty-three patients were still alive and censored at the time of analysis. A total of 212 glioblastoma patients presented with epileptic seizures, of which 191 received AED treatment. Twenty-one patients with epileptic seizures were not treated with an AED. One patient without epilepsy at presentation received carbamazepine for treatment of neuropathic pain. None of the patients without epilepsy received prophylactic AED treatment. Epilepsy was significantly associated with longer overall survival, with a median survival in the epilepsy group of 13.2 months (95% CI: 11.4 – 14.9) versus 8.4 months for patients without epilepsy (95% CI: 7.4 – 9.5; log-rank $P<.0001$) (Supplementary Fig. S1). As mentioned above, the PH assumption of the Cox model did not hold for the entire range of the follow-up period. The analysis was thus restricted to the period of time when this assumption was valid by censoring all survival data that surpassed 1000 days. Epileptic glioblastoma presentation remained significantly associated with an increased overall survival compared with glioblastoma patients without

epilepsy, as tested both with the log-rank test (median: 13.2; 95% CI: 11.4–14.9; versus median: 8.4; 95% CI: 7.4 – 9.5; $P < .00005$; Fig. 1A) as well as with univariable Cox regression (crude HR: 0.68; 95% CI: 0.56–0.82; $P < .001$; Table 2).

Epilepsy and survival in glioblastoma patients: multivariable analysis

The epilepsy and nonepilepsy subgroups showed evident differences with respect to age, sex, KPS, type of surgery, and post-surgical treatment. Lobar involvement differed notably, with left occipital, right frontal, and bilateral tumor locations observed more in the nonepilepsy subgroup (Table 1). These locations were therefore included in the multivariable model. We also found epileptogenic glioblastomas to be significantly smaller than nonepileptogenic ones (17.8 cm³ [0.1–201.6] vs 40.9 cm³ [0.4 – 204.2]; Mann-Whitney U test; $P < .0005$), which has been reported by others as well [21].

Despite these differences, epilepsy remained significantly associated with survival of glioblastoma patients (HR: 0.75 [95% CI: 0.61 – 0.92]; $P < .01$) after correcting for age, sex, type of surgery, postsurgical treatment, tumor volume, affected lobes, bilateral tumor involvement, and KPS (Table 2). Mutation of the IDH1 R132H allele was observed in 8 of 136 patients in the epilepsy subgroup, compared with 13 of 224 for the patients without epilepsy (difference not significant; chi-square test; $P = .98$). The baseline characteristics for the patients included in this analysis are described in Supplementary Table S1.

Prognostic relevance of valproic acid in glioblastoma patients

Although several previous studies have suggested a favorable effect of the AED VPA on the overall survival of glioblastoma patients [1,18,19], we did not find evidence for this. Within the epileptic glioblastoma group, the survival of patients who received VPA ($n=55$; median survival: 13.8 mo; 95% CI: 10.1 – 17.4) did not differ significantly from those with seizures who did not receive VPA ($n=157$; median survival: 12.7 mo; 95% CI: 10.6 – 14.8; log-rank test; $P = .55$; crude HR: 0.90; 95% CI: 0.62 – 1.29; $P = .55$; Fig. 1B, Supplementary Table S2). Baseline characteristics of these subgroups are described in Table 1. In multivariable analysis, the association between VPA treatment and survival remained nonsignificant (adjusted HR: 0.99; 95% CI: 0.65–1.50; $P = .95$, Supplementary Table S2).

Table 1 - Baseline characteristics of total cohort and subgroups analyzed in this study

Patient characteristics <i>n</i> (%)	Total cohort 647 (100)	Epilepsy 212 (32.9)	No epilepsy 435 (67.1)	VPA 55 (8.5)	Epilepsy, not treated with VPA 157 (24.3)
Age (<i>mean</i> \pm <i>SD</i>)	61.5 \pm 12.3	59.3 \pm 12.8	62.5 \pm 11.9	57.9 \pm 13.7	59.7 \pm 12.5
Gender (% <i>male</i>)	59.8	68.4	55.6	61.8	70.7
KPS <i>n</i> (%)					
< 70	182 (28.1)	47 (22.2)	135 (31.0)		35 (22.3)
\geq 70	461 (71.3)	163 (76.9)	298 (68.5)	12 (21.8)	120 (76.4)
	Missing: 4 (0.6)	Missing: 2 (0.9)	Missing: 2 (0.5)	43 (78.2)	Missing: 2 (1.3)
Tumor volume <i>cm</i> ³ (<i>median</i> (<i>range</i>))	34.3 (0.1-204.2)	17.8 (0.1-201.6)	40.7 (0.4-204.2)	17.0 (0.8-201.6)	18.6 (0.1-111.8)
	Missing: 19 (2.9)	Missing: 9 (4.2)	Missing: 10 (2.3)	Missing: 3 (5.5)	Missing: 6 (3.8)
Tumor location <i>n</i> (%) †					
Left					
frontal	106 (16.4)	37 (17.5)	69 (15.9)	11 (20.0)	26 (16.6)
parietal	93 (14.4)	27 (12.7)	66 (15.2)	3 (5.5)	24 (15.3)
temporal	124 (19.2)	43 (20.3)	81 (18.6)	14 (25.5)	29 (18.5)
occipital	46 (7.1)	7 (3.3)	39 (9.0)	1 (1.8)	6 (3.8)
Right					
frontal	113 (17.5)	51 (24.1)	62 (14.3)	11 (20.0)	40 (25.5)
parietal	125 (19.3)	49 (23.1)	76 (17.5)	12 (21.8)	37 (23.6)
temporal	168 (26.0)	54 (25.5)	114 (26.2)	13 (23.6)	41 (26.1)
occipital	61 (9.4)	15 (7.1)	46 (10.6)	0 (0)	15 (9.6)
Bilateral	109 (16.8)	16 (7.5)	93 (21.4)	3 (5.5)	13 (8.3)
	Missing: 11 (1.7)	Missing: 3 (0.5)	Missing: 8 (1.8)	Missing: 1 (1.8)	Missing: 2 (1.3)
Extent of surgery <i>n</i> (%)					
Biopsy	223 (34.5)	59 (27.8)	164 (37.7)	16 (29.1)	43 (27.4)
Debulking	424 (65.5)	153 (72.2)	271 (62.3)	39 (70.9)	114 (72.6)

Table 1 (continued) - Baseline characteristics of total cohort and subgroups analyzed in this study

Patient characteristics <i>n</i> (%)	Total cohort 647 (100)	Epilepsy 212 (32.9)	No epilepsy 435 (67.1)	VPA 55 (8.5)	Epilepsy, not treated with VPA 157 (24.3)
Post-surgical treatment					
<i>n</i> (%)	147 (22.7)	30 (14.2)	117 (26.9)	6 (10.9)	24 (15.3)
None	163 (25.2)	44 (20.8)	119 (27.4)	9 (16.4)	35 (22.3)
Monotherapy(RT/TMZ)	332 (51.3)	136 (64.2)	196 (45.1)	40 (72.7)	96 (61.1)
RT + TMZ	Missing: 5 (0.8)	Missing: 2 (0.9)	Missing: 3 (0.7)		Missing: 2 (1.3)
Treatment with AED					
<i>n</i> (%) †	455 (70.3)	21 (9.9)	433 (99.8)	-	21 (13.4)
None	55 (8.5)	55 (25.9)	-	55 (100)	-
Valproic acid	92 (14.2)	92 (43.4)	-	9 (16.4)	83 (52.9)
Levetiracetam	26 (4.0)	25 (11.8)	1 (0.2)	2 (3.6)	23 (14.6)
Carbamazepine	37 (5.7)	37 (17.5)	-	2 (3.6)	35 (22.3)
Phenytoin	3 (0.5)	3 (1.4)	-	1 (1.8)	2 (1.3)
Other	21 (3.2)	21 (9.9)	-	14 (25.5)	7 (4.5)
Combination of AEDs					

Abbreviations: AED: antiepileptic drug; RT: radiotherapy, TMZ: temozolomide; VPA, valproic acid.

†Percentages do not add up to 100% for these variables due to possible multilobar tumor locations and multiple AED treatments per patient.

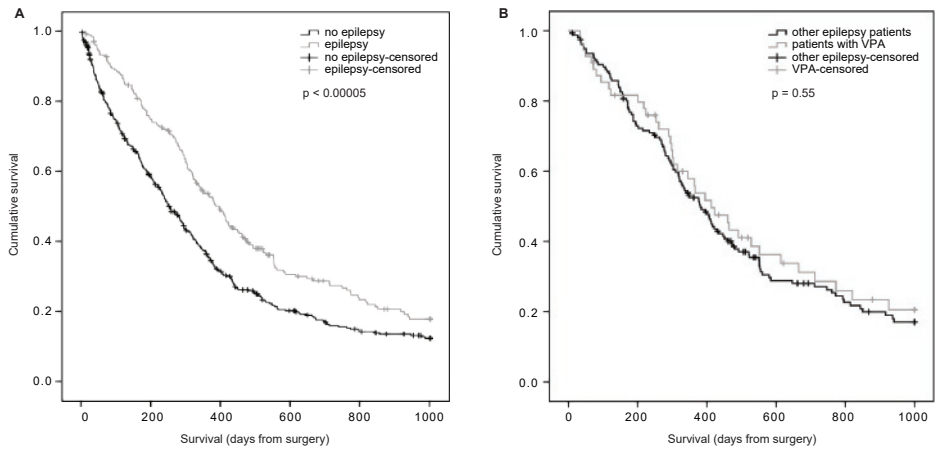


Figure 1 – Effect of epilepsy and valproic acid (VPA) on glioblastoma patient survival. (A) Kaplan-Meier plot of patients with (grey, n=212) and without epilepsy (black, n=435). Patients with survival >1000 days from surgery were censored. Survival was significantly different between the 2 groups (log-rank test, $P < 0.00005$). (B) Kaplan-Meier plot of glioblastoma patients treated with VPA (grey, n=55) or all other patients with epilepsy (black, n=157). Patients with survival >1000 days from surgery were censored. Survival was not significantly different between the 2 groups (log-rank test, $P = 0.55$).

Table 2 - Univariable and multivariable Cox proportional hazard regression analysis

Variable	Crude HR (95% CI)	p-value	Adjusted HR (95% CI)	p-value
Epilepsy	0.68 (0.56-0.82)	< 0.001	0.75 (0.61-0.92)	< 0.01
Gender (male)	1.05 (0.88-1.26)	0.57	0.93 (0.82-1.20)	0.94
Age	1.03 (1.03-1.04)	< 0.0005	1.011 (1.002-1.019)	< 0.05
KPS < 70	1.00	< 0.0005	1.00	< 0.01
KPS ≥ 70	0.24 (0.17-0.32)	< 0.0005	0.61 (0.43-0.86)	< 0.005
KPS * time	1.003 (1.002-1.004)		1.002 (1.001-1.003)	
Biopsy	1.00	< 0.005	1.00	< 0.005
Resection	0.40 (0.33-0.48)		0.71 (0.57-0.89)	
Postoperative treatment				
None	1.00		1.00	
RT only	0.17 (0.13-0.22)	< 0.0005	0.20 (0.15-0.27)	< 0.0005
RT + TMZ	0.06 (0.05-0.08)	< 0.0005	0.08 (0.06-0.12)	< 0.0005
Tumor location				
Left occipital	1.03 (0.74-1.43)	0.46	1.7 (0.75-1.51)	0.72
Right frontal	0.73 (0.57-0.93)	< 0.05	0.80 (0.61-1.03)	0.09
Bilateral	2.54 (2.02-3.18)	< 0.0005	1.62 (1.23-2.14)	< 0.005
Tumor volume	1.006 (1.002-1.011)	< 0.005	1.003 (0.999-1.007)	0.11
Tumor volume * time	1.000 (1.000-1.000)	< 0.005	1.000 (1.000-1.000)	< 0.005

Abbreviations: CI, confidence interval; HR, hazard ratio; RT, radiotherapy, TMZ, temozolomide. Epilepsy remains significantly associated with survival of glioblastoma patients in multivariable analysis. Time-dependent variables (KPS * time and tumor volume * time) are included to correct for violation of the proportional hazards assumption and represent changes in the association between the variable and survival over time.

DISCUSSION

Our study demonstrates a favorable association between epilepsy at presentation and prolonged survival of glioblastoma patients in the largest consecutive cohort studied to this end so far (n=647). With a hazard ratio of 0.75 in multivariable Cox regression (95% CI: 0.61 – 0.92; P<.01), our results build upon existing smaller studies [5 – 7] to firmly establish this correlation. Furthermore, we show that the improved prognosis of patients with epileptic glioblastomas is independent of the age, sex, or performance status of the patients as well as the location of their tumors or the surgical and adjuvant treatments they received. Consistent with previous observations [21], the volume of epileptogenic tumors was significantly smaller than that of nonepileptogenic ones. However, epilepsy remained a significant prognostic factor independent of tumor size in multivariable analysis, suggesting that mechanisms other than early detection may also contribute to the better outcome of epileptogenic tumors.

AEDs have been postulated to alter the outcome of epileptic glioblastoma patients. An analysis of the survival of nonepileptic glioblastoma patients treated prophylactically with non-enzyme-inducing AEDs pointed to a survival advantage for these patients [22]. VPA treatment was also reported to enhance survival in a few retrospective studies of high-grade glioma patients [1,19,23] and in a post-hoc analysis of the EORTC 26981/NCIC 3.E trial [18]. The actual therapeutic benefit is still being debated [20,24], and the anti-tumoral mechanisms of therapeutic doses of VPA in glioblastomas have yet to be demonstrated in patients. In our retrospective cohort, however, VPA usage at the time of glioblastoma diagnosis was not associated with any survival advantage when compared with all other patients with epileptic seizures.

Previous studies have examined the effect of VPA on survival by including only glioblastoma patients treated with radiotherapy [19] or chemoradiation [1,18], whereas our analysis also included patients who did not receive any adjuvant treatment. When we restricted our comparison to epileptic glioblastoma patients treated with chemoradiation, there was no survival difference among those who received VPA (n=40) and those who did not (n=96; log-rank test; $P=.88$). Similarly, for epileptic glioblastoma patients who received radiotherapy (with or without chemotherapy), there was no difference in survival between patients treated with VPA (n=49) and those who did not receive VPA (n=131; log-rank test; $P=.76$). However, the limited statistical power of these latter subanalyses (due to fewer patients contributing to the measure) should be taken into consideration, since small but meaningful differences might become apparent in larger cohorts.

Detangling the independent relationship between AED use and presence of seizures is problematic because no patients received prophylactic AEDs in the absence of clinical seizures, and few patients with seizures did not receive AEDs. Since there are no patients without epilepsy who received prophylactic AED treatment in this study, we cannot completely rule out an association of VPA with survival of glioblastoma patients, which might be overshadowed by the more profound prognostic effect of epilepsy per se. To be solved, this question would likely require a randomized prospective trial with AED administration to patients both with and without epilepsy.

Even though VPA has received the most attention in literature for its possible antitumor effects, some studies have investigated the effects of other AEDs. For instance, levetiracetam has been reported to chemosensitize glioma cells to temozolomide treatment, possibly by inhibition of MGMT expression [25]. A recent study reported a survival benefit for glioblastoma patients receiving chemoradiation therapy and treatment with levetiracetam compared with those who were not treated with levetiracetam. However, the majority of patients in that study received seizure prophylaxis and did not present with epilepsy at diagnosis [26]. Guthrie *et al* reported a survival benefit for glioblastoma patients receiving

carbamazepine or phenytoin compared with patients receiving no AED treatment [27]. However, the epilepsy status was not included in the multivariable analyses in both studies. In our cohort, we analyzed the survival of patients who presented with epilepsy and were treated with levetiracetam, carbamazepine, or phenytoin to the survival of other patients who presented with epilepsy. The baseline characteristics of the analyzed subgroups were comparable (Supplementary Tables S3 – S5), and we did not observe any association between specific AED use and survival using Kaplan-Meier analysis (Supplementary Fig. S2A–C) and univariable Cox regression (Supplementary Table S6).

A potential limitation of this study remains its retrospective nature. As a result, medical imaging to assess the extent of resection was incomplete for patients diagnosed in the first years of the cohort. This presents a challenge because the surgeon's perception of the estimated extent of resection does not always correspond strictly to quantitative radiological assessment of the pre- and postoperative tumor burden [28]. Furthermore, surgical resection of >78% of the tumor volume can provide a survival benefit compared with biopsy alone, with further significant increments for additional tumor debulking [29]. Despite this, the differentiation between biopsy and resection (whether for debulking or gross-total resection) has been proven to have a significant effect on prognosis [30], and we used this for our survival analyses.

The observed prognostic effect might result from distinct biological features of epileptogenic tumors. For instance, the IDH1 R132H mutation has been reported to occur frequently in proneural glioblastomas [13] to correlate with epilepsy in low-grade glioma patients [14], and to confer a more favorable prognosis in glioblastoma patients [15,16]. In our series, however, the IDH1 mutational status did not correlate with epilepsy status at all (chi-square test; $P=0.98$). This finding should, however, be nuanced. Indeed, the subset of patients included in our histochemical IDH1 analysis was enriched in patients who underwent debulking rather than biopsy due to tissue availability constraints. They likewise presented a higher average age, a larger median tumor volume, more involvement of the right hemisphere and less bilateral tumor location, and involved more patients treated with chemoradiation and more patients presenting with epilepsy than our complete patient population (Supplementary Table S1).

Previous reports also suggested some gene expression alterations in epileptogenic gliomas such as higher expression of glutamate and the $X_{(c)(-)}$ -system [9] and lower expression of glutamine synthetase [7,10]. Our laboratory is currently investigating whether such biological differences are indeed present in our cohort of patients.

Collectively, our results show that epilepsy at presentation is associated with prolonged survival of glioblastoma patients independent of age, sex, performance status, type of

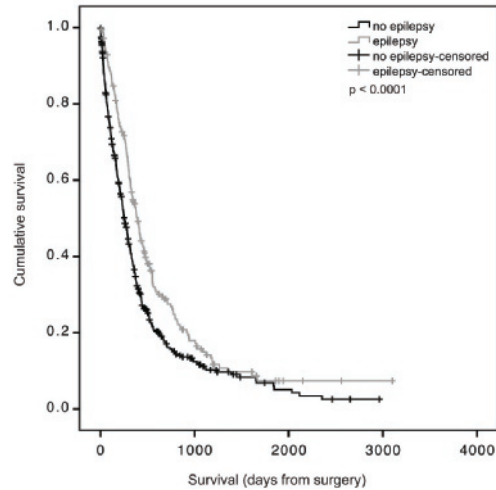
surgery, postsurgical treatment, and tumor volume and location. This prognostic effect cannot be solely explained by early diagnosis, and survival was not associated with VPA treatment.

REFERENCES

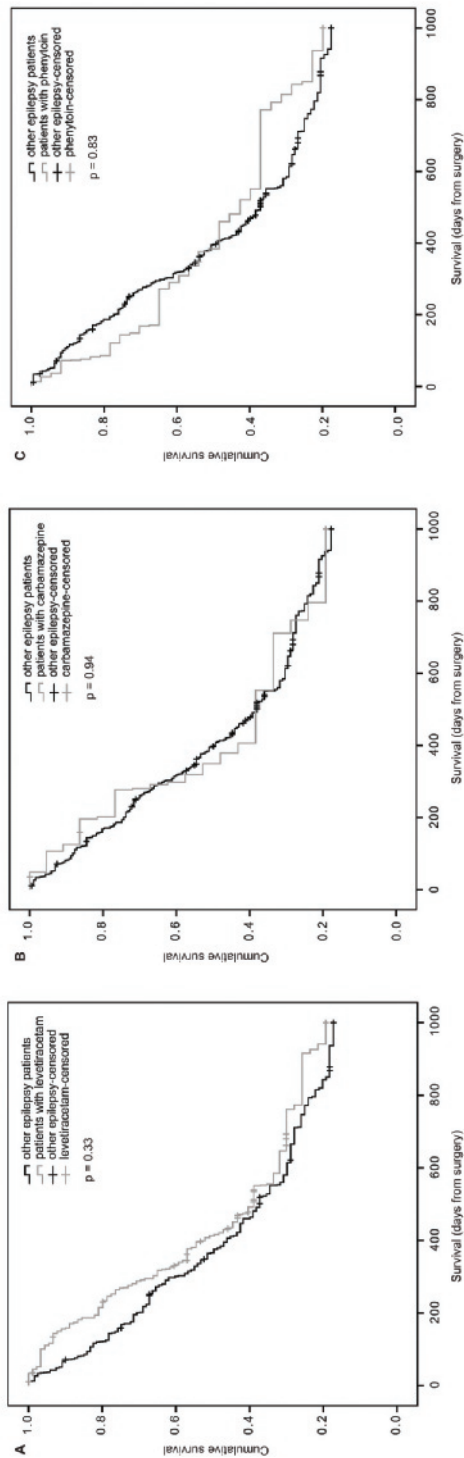
1. Kerkhof M, Dielemans JC, van Breemen MS, et al. Effect of valproic acid on seizure control and on survival in patients with glioblastoma multiforme. *Neuro Oncol*. 2013;15(7):961–967.
2. Beaumont A, Whittle IR. The pathogenesis of tumour associated epilepsy. *Acta Neurochir (Wien)*. 2000;142(1):1 – 15.
3. Lote K, Stenwig AE, Skullerud K, Hirschberg H. Prevalence and prognostic significance of epilepsy in patients with gliomas. *Eur J Cancer*. 1998;34(1):98 – 102.
4. Kilpatrick C, Kaye A, Dohrmann P, Gonzales M, Hopper J. Epilepsy and primary cerebral tumours. *J Clin Neurosci*. 1994;1(3): 178 – 181.
5. Mineo JF, Bordron A, Baroncini M, et al. Prognosis factors of survival time in patients with glioblastoma multiforme: A multivariate analysis of 340 patients. *Acta Neurochir (Wien)*. 2007;149(3): 245 – 252.
6. Stark AM, van de Bergh J, Hedderich J, Mehdorn HM, Nabavi A. Glioblastoma: Clinical characteristics, prognostic factors and survival in 492 patients. *Clin Neurol Neurosurg*. 2012;114(7): 840 – 845.
7. Rosati A, Poliani PL, Todeschini A, et al. Glutamine synthetase expression as a valuable marker of epilepsy and longer survival in newly diagnosed glioblastoma multiforme. *Neuro Oncol*. 2013;15(5):618 – 625.
8. Yuile P, Dent O, Cook R, Biggs M, Little N. Survival of glioblastoma patients related to presenting symptoms, brain site and treatment variables. *J Clin Neurosci*. 2006;13(7):747 – 751.
9. Yuen TI, Morokoff AP, Bjorksten A, et al. Glutamate is associated with a higher risk of seizures in patients with gliomas. *Neurology*. 2012;79(9):883 – 889.
10. Rosati A, Marconi S, Pollo B, et al. Epilepsy in glioblastoma multiforme: Correlation with glutamine synthetase levels. *J Neurooncol*. 2009;93(3):319–324.
11. Robert SM, Sontheimer H. Glutamate transporters in the biology of malignant gliomas. *Cell Mol Life Sci*. 2014;71(10):1839–1854.
12. Lyons SA, Chung WJ, Weaver AK, Ogunrinu T, Sontheimer H. Autocrine glutamate signaling promotes glioma cell invasion. *Cancer Res*. 2007;67(19):9463–9471.
13. Verhaak RG, Hoadley KA, Purdom E, et al. Integrated genomic analysis identifies clinically relevant subtypes of glioblastoma characterized by abnormalities in PDGFRA, IDH1, EGFR, and NF1. *Cancer Cell*. 2010;17(1):98–110.
14. Liubinas SV, D’Abaco GM, Moffat BM, et al. IDH1 mutation is associated with seizures and protoplasmic subtype in patients with low-grade gliomas. *Epilepsia*. 2014;55(9):1438–1443.
15. Gerber NK, Goenka A, Turcan S, et al. Transcriptional diversity of long-term glioblastoma survivors. *Neuro Oncol*. 2014;16(9): 1186 – 1195.
16. Hartmann C, Hentschel B, Simon M, et al. Long-term survival in primary glioblastoma with versus without isocitrate dehydrogenase mutations. *Clin Cancer Res*. 2013;19(18): 5146 – 5157.
17. Berendsen S, Broekman M, Seute T, et al. Valproic acid for the treatment of malignant gliomas: Review of the preclinical rationale and published clinical results. *Expert Opin Investig Drugs*. 2012;21(9):1391–1415.
18. Weller M, Gorlia T, Cairncross JG, et al. Prolonged survival with valproic acid use in the EORTC/NCIC temozolomide trial for glioblastoma. *Neurology*. 2011;77(12):1156–1164.
19. Barker CA, Bishop AJ, Chang M, Beal K, Chan TA. Valproic acid use during radiation therapy for glioblastoma associated with improved survival. *Int J Radiat Oncol Biol Phys*. 2013;86(3): 504 – 509.

20. van Breemen MS, Rijsman RM, Taphoorn MJ, Walchenbach R, Zwinkels H, Vecht CJ. Efficacy of anti-epileptic drugs in patients with gliomas and seizures. *J Neurol.* 2009;256(9):1519–1526.
21. Lee JW, Wen PY, Hurwitz S, et al. Morphological characteristics of brain tumors causing seizures. *Arch Neurol.* 2010;67(3):336 – 342.
22. Jaeckle KA, Ballman K, Furth A, Buckner JC. Correlation of enzyme-inducing anticonvulsant use with outcome of patients with glioblastoma. *Neurology.* 2009;73(15):1207–1213.
23. Oberndorfer S, Piribauer M, Marosi C, Lahrmann H, Hitzemberger P, Grisold W. P450 enzyme inducing and non-enzyme inducing antiepileptics in glioblastoma patients treated with standard chemotherapy. *J Neurooncol.* 2005;72(3):255 – 260.
24. Tsai HC, Wei KC, Tsai CN, et al. Effect of valproic acid on the outcome of glioblastoma multiforme. *Br J Neurosurg.* 2012; 26(3):347 – 354.
25. Bobustuc GC, Baker CH, Limaye A, et al. Levetiracetam enhances p53-mediated MGMT inhibition and sensitizes glioblastoma cells to temozolomide. *Neuro Oncol.* 2010;12(9):917–927.
26. Kim YH, Kim T, Joo JD, et al. Survival benefit of levetiracetam in patients treated with concomitant chemoradiotherapy and adjuvant chemotherapy with temozolomide for glioblastoma multiforme. *Cancer.* 2015;121(17):2926–2932.
27. Guthrie GD, Eljamel S. Impact of particular antiepileptic drugs on the survival of patients with glioblastoma multiforme. *J Neurosurg.* 2013;118(4):859–865.
28. Orringer D, Lau D, Khatri S, et al. Extent of resection in patients with glioblastoma: Limiting factors, perception of resectability, and effect on survival. *J Neurosurg.* 2012;117(5):851–859.
29. Sanai N, Polley MY, McDermott MW, Parsa AT, Berger MS. An extent of resection threshold for newly diagnosed glioblastomas. *J Neurosurg.* 2011;115(1):3 – 8.
30. Vuorinen V, Hinkka S, Farkkila M, Jaaskelainen J. Debulking or biopsy of malignant glioma in elderly people - a randomised study. *Acta Neurochir (Wien).* 2003;145(1):5–10.

SUPPLEMENTARY FILES



Supplementary figure S1 - Effect of epilepsy on unadjusted glioblastoma patient survival. Kaplan Meier plot of glioblastoma patients with (grey, n=212) and without epilepsy (black, n=435) using unadjusted survival data. Survival is measured in days from surgery. Survival is significantly different between the two groups (log-rank test, $p < 0.0001$).



Supplementary figure S2 - Effect of anti-epileptic drug treatment on glioblastoma patient survival. Patients with survival over 1000 days from surgery were censored. (A) Kaplan-Meier plot of glioblastoma patients treated with levetiracetam (grey, n=92) and all other patients with epilepsy (black, n=120). There were no significant differences in survival between the two groups (log-rank test, $p=0.33$). (B) Kaplan-Meier plot of glioblastoma patients treated with carbamazepine (grey, n=23) and all other patients with epilepsy (black, n=189). There were no significant differences in survival between the two groups (log-rank test, $p=0.94$). (C) Kaplan-Meier plot of glioblastoma patients treated with phenytoin (grey, n=37) and all other patients with epilepsy (black, n=175). There were no significant differences in survival between the two groups (log-rank test, $p=0.83$).

Supplementary table S1 – Baseline characteristics of total cohort and the subgroup studied for IDH1 R132H expression.

Patient characteristics <i>n</i> (%)	Patients included in IDH1 expression analysis 360 (55.6)	Patients not included in IDH1 expression analysis 287 (44.4)
Age (<i>mean ± SD</i>)	60.4 ± 12.6	62.8 ± 11.8 *
Gender (% <i>male</i>)	59.4	60.3
KPS <i>n</i> (%)		
< 70	95 (26.4)	87 (30.3)
≥ 70	262 (72.8) <i>Missing: 3 (0.8)</i>	199 (69.3) <i>Missing: 1 (0.3)</i>
Tumor volume <i>cm</i> ³ (<i>median (range)</i>)	40.4 (0.1-204.2) <i>Missing: 9 (2.5)</i>	28.3 (0.2-201.6) *** <i>Missing: 10 (3.5)</i>
Tumor location <i>n</i> (%) †		
Left		
frontal	56 (15.6)	49 (17.1)
parietal	47 (13.1)	44 (15.3)
temporal	68 (18.9)	58 (20.2)
occipital	27 (7.5)	21 (7.3)
Right		
frontal	76 (21.1)	48 (16.7)
parietal	88 (24.4)	44 (15.3) *
temporal	116 (32.2)	55 (19.2) **
occipital	45 (12.5)	18 (6.3) *
Bilateral	33 (9.2) <i>Missing: 6 (1.7)</i>	66 (23.0) *** <i>Missing: 3 (1)</i>
Type of surgery <i>n</i> (%)		
Biopsy	30 (8.3)	193 (67.2) ***
Debulking	330 (91.7)	94 (32.8)
Post-surgical treatment <i>n</i> (%)		
None	60 (16.9)	87 (30.3) ***
Monotherapy RT or TMZ	78 (21.9)	85 (29.6)
RT + TMZ	218 (60.6) <i>Missing: 4 (1.1)</i>	114 (39.7) <i>Missing: 1 (0.3)</i>
Epilepsy at presentation <i>n</i> (%)	136 (37.8)	76 (26.5) **
Treatment with AED <i>n</i> (%) †		
None	240 (66.7)	215 (74.9)
Valproic acid	33 (9.2)	22 (7.7)
Levetiracetam	61 (16.9)	29 (10.1)
Carbamazepine	15 (4.2)	9 (3.1)
Phenytoin	24 (6.7)	11 (3.8)
Other	2 (0.6)	1 (0.3)
Combination of AEDs	15 (4.2)	6 (2.1)

† Percentages do not add up to 100% for these variables, due to possible multilobar tumor locations and multiple AED treatments per patient. Significant differences between subgroups: * $p < 0.05$, ** $p < 0.01$, *** $p < 0.0005$. KPS: Karnofsky performance status, RT: radiotherapy, TMZ: temozolomide, AED: anti-epileptic drug.

Supplementary table S2 – Univariable and multivariable Cox proportional hazard regression.

Variable	Crude HR (95% CI)	p-value	Adjusted HR (95% CI)	p-value
Other epilepsy (no VPA)	1.00		1.00	
VPA	0.90 (0.62-1.29)	0.55	0.99 (0.65-1.50)	0.95
Gender (male)	0.98 (0.70-1.38)	0.91	1.08 (0.75-1.56)	0.68
Age	1.03 (1.02-1.05)	< 0.0005	1.02 (1.002-1.032)	< 0.05
KPS < 70	1.00		1.00	
KPS ≥ 70	0.16 (0.08-0.31)	< 0.005	0.34 (0.15-0.73)	< 0.01
KPS * time	1.003 (1.001-1.005)	< 0.0005	1.003 (1.001-1.006)	< 0.05
Biopsy	1.00		1.00	
Resection	0.46 (0.33-0.65)	< 0.005	0.48 (0.25-0.95)	< 0.05
Surgery * time			1.002 (1.000-1.003)	0.12
Postoperative treatment				
None	1.00		1.00	
Monotherapy RT or TMZ	0.12 (0.09-0.17)	< 0.0005	0.27 (0.14-0.51)	< 0.0005
RT + TMZ	0.02 (0.01-0.04)	< 0.0005	0.15 (0.08-0.30)	< 0.0005
Right occipital location	0.76 (0.41-1.41)	0.39	0.78 (0.39-1.54)	0.47
Tumor volume	1.006 (0.998-1.014)	0.31	0.999 (0.991-1.006)	0.75
Tumor volume * time	1.000 (1.000-1.000)	0.15	1.000 (1.000-1.000)	0.69

Treatment with valproic acid is not significantly associated with survival of glioblastoma patients in univariable and multivariable analysis, as compared to other epileptic patients. Time-dependent variables (KPS*time, tumor volume*time and surgery*time) are included to correct for violation of the proportional hazards assumption and represent changes in the association between the variable and survival over time.

VPA: valproic acid, HR: hazard ratio, KPS: Karnofsky performance status, RT: radiotherapy, TMZ: temozolomide.

Supplementary table S3 – Baseline characteristics of glioblastoma patients treated with levetiracetam and all other patients with epilepsy at presentation.

Patient characteristics <i>n</i> (%)	Levetiracetam 92 (43.4)	Epilepsy, no levetiracetam treatment 120 (56.6)
Age (<i>mean ± SD</i>)	59.0 ± 12.5	59.4 ± 13.1
Gender (% <i>male</i>)	70.7	66.7
KPS <i>n</i> (%)		
< 70	17 (18.5)	30 (24.8)
≥ 70	75 (81.5)	89 (73.6)
		Missing: 2 (1.7)
Tumor volume <i>cm</i> ³ (<i>median (range)</i>)	16.0 (0.1-111.8) Missing: 4 (4.3)	21.0 (0.8-201.6) Missing: 5 (4.2)
Tumor location <i>n</i> (%)†		
Left		
frontal	17 (18.5)	21 (17.5)
parietal	14 (15.2)	15 (12.5)
temporal	23 (25.0)	22 (18.3)
occipital	7 (7.6)	5 (4.2)
Right		
frontal	18 (19.6)	31 (25.8)
parietal	19 (20.7)	29 (24.2)
temporal	21 (22.8)	26 (21.5)
occipital	6 (6.5)	11 (9.2)
Bilateral	7 (7.6)	12 (10.0)
	Missing: 1 (1.1)	Missing: 2 (1.7)
Type of surgery <i>n</i> (%)		
Biopsy	23 (25.0)	36 (30.0)
Debulking	69 (75.0)	84 (70.0)
Post-surgical treatment <i>n</i> (%)		
None	8 (8.7)	22 (18.3)
Monotherapy RT or TMZ	18 (19.6)	26 (21.7)
RT + TMZ	66 (71.7)	70 (58.3)
		Missing: 2 (1.7)
Treatment with AED <i>n</i> (%)†		
None	-	21 (17.5)
Valproic acid	9 (9.8)	46 (38.3)
Levetiracetam	92 (100)	-
Carbamazepine	3 (3.3)	22 (18.3)
Phenytoin	2 (2.2)	35 (29.2)
Other	-	3 (2.5)
Combination of AEDs	14 (15.2)	7 (5.8)

† Percentages do not add up to 100% for these variables, due to possible multilobar tumor locations and multiple AED treatments per patient. KPS: Karnofsky performance status, RT: radiotherapy, TMZ: temozolomide, AED: anti-epileptic drug.

Supplementary table S4 – Baseline characteristics of glioblastoma patients treated with carbamazepine and all other patients with epilepsy at presentation.

Patient characteristics <i>n</i> (%)	Carbamazepine 23 (10.8)	Epilepsy, no carbamazepine treatment 189 (89.2)
Age (<i>mean ± SD</i>)	57.5 ± 13.3	59.5 ± 12.8
Gender (% <i>male</i>)	52.2	70.4
KPS <i>n</i> (%)		
< 70	6 (26.1)	41 (21.7)
≥ 70	17 (73.9)	146 (77.2)
		Missing: 2 (1.1)
Tumor volume <i>cm</i> ³ (<i>median (range)</i>)	11.0 (1.7-91.1)	18.4 (0.1-201.6)
		Missing: 9 (4.8)
Tumor location <i>n</i> (%)†		
Left		
frontal	5 (21.7)	33 (17.5)
parietal	3 (13.0)	26 (13.8)
temporal	3 (13.0)	42 (22.2)
occipital	0 (0)	12 (6.3)
Right		
frontal	5 (21.7)	44 (23.3)
parietal	4 (17.4)	44 (23.3)
temporal	7 (30.4)	40 (21.2)
occipital	1 (4.3)	16 (8.5)
Bilateral	2 (8.7)	17 (9.0)
		Missing: 3 (1.6)
Type of surgery <i>n</i> (%)		
Biopsy	7 (30.4)	52 (27.5)
Debulking	16 (69.6)	137 (72.5)
Post-surgical treatment <i>n</i> (%)		
None	3 (13.0)	27 (14.3)
Monotherapy RT or TMZ	7 (30.4)	37 (19.6)
RT + TMZ	11 (47.8)	125 (66.1)
	Missing 2 (8.7)	
Treatment with AED <i>n</i> (%)†		
None	-	21 (11.1)
Valproic acid	2 (8.7)	53 (28.0)
Levetiracetam	3 (13.0)	89 (47.1)
Carbamazepine	23 (100)	-
Phenytoin	-	35 (18.5)
Other	-	3 (1.6)
Combination of AEDs	5 (21.7)	16 (8.5)

† Percentages do not add up to 100% for these variables, due to possible multilobar tumor locations and multiple AED treatments per patient. KPS: Karnofsky performance status, RT: radiotherapy, TMZ: temozolomide, AED: anti-epileptic drug.

Supplementary table S5 – Baseline characteristics of glioblastoma patients treated with phenytoin and all other patients with epilepsy at presentation.

Patient characteristics <i>n</i> (%)	Phenytoin 37 (17.5)	Epilepsy, no phenytoin treatment 175 (82.5)
Age (<i>mean ± SD</i>)	58.5 ± 13.0	59.4 ± 12.8
Gender (% <i>male</i>)	78.4	66.3
KPS <i>n</i> (%)		
< 70	8 (21.6)	39 (22.3)
≥ 70	29 (78.4)	134 (76.6)
		<i>Missing: 2 (1.1)</i>
Tumor volume <i>cm</i> ³ (<i>median (range)</i>)	19.8 (1.1-84.6) <i>Missing: 1 (2.7)</i>	17.8 (0.1-201.6) <i>Missing: 8 (4.6)</i>
Tumor location <i>n</i> (%)†		
Left		
frontal	6 (16.2)	32 (18.3)
parietal	5 (13.5)	24 (13.7)
temporal	7 (18.9)	38 (21.7)
occipital	3 (8.1)	9 (5.1)
Right		
frontal	9 (24.3)	40 (22.9)
parietal	10 (27.0)	38 (21.7)
temporal	6 (16.2)	41 (23.4)
occipital	4 (10.8)	13 (7.4)
Bilateral	4 (10.8)	15 (8.6)
	<i>Missing: 1 (2.7)</i>	<i>Missing: 2 (1.1)</i>
Type of surgery <i>n</i> (%)		
Biopsy	10 (27.0)	49 (28.0)
Debulking	27 (73.0)	127 (72.0)
Post-surgical treatment <i>n</i> (%)		
None	9 (24.3)	21 (12.0)
Monotherapy RT or TMZ	9 (24.3)	35 (20.0)
RT + TMZ	19 (51.4)	117 (66.9)
		<i>Missing 2 (1.1)</i>
Treatment with AED <i>n</i> (%)†		
None	-	21 (12.0)
Valproic acid	2 (5.4)	53 (30.2)
Levetiracetam	2 (5.4)	90 (51.4)
Carbamazepine	2 (5.4)	22 (12.6)
Phenytoin	37 (100)	-
Other	-	3 (1.7)
Combination of AEDs	6 (16.2)	15 (8.6)

† Percentages do not add up to 100% for these variables, due to possible multilobar tumor locations and multiple AED treatments per patient. KPS: Karnofsky performance status, RT: radiotherapy, TMZ: temozolomide, AED: anti-epileptic drug.

Supplementary table S6

Variable	Crude HR (95% CI)	p-value
Other epilepsy (no levetiracetam)	1.00	0.33
Levetiracetam	0.85 (0.62-1.18)	
Other epilepsy (no carbamazepine)	1.00	0.94
Carbamazepine	0.98 (0.59-1.62)	
Other epilepsy (no phenytoin)	1.00	0.83
Phenytoin	0.96 (0.64-1.44)	

Univariable Cox proportional hazard regression analysis on the association between levetiracetam, carbamazepine or phenytoin treatment and survival of glioblastoma patients, compared to other patients with epilepsy. HR: hazard ratio.

REPLY TO LETTER

Response to: Zhou, H. et al, Prognostic relevance of epilepsy at presentation in lower-grade gliomas, Neuro Oncol. 2016 Sep; 18(9): 1326–1327.

We thank Zhou et al. for their interest and comments regarding our article [1].

We acknowledge the theoretical interest of taking the IDH1 mutational status of tumors into account in the multivariable survival analysis of glioblastoma patients presenting with or without epilepsy. We also agree that the inclusion of IDH1 status in this analysis should not depend on its mere correlation with epilepsy, and have indeed not proceeded in such a way in our analysis. As discussed in our article, tissue to determine IDH1 status was only available for 360 of the 647 glioblastoma patients, a limitation of our retrospective study. However, restricting our analysis to these patients would have led to selection bias. Indeed, and as stated in our manuscript, these 360 patients showed significant differences with respect to age, tumor location, resection and postoperative treatment, and proportion of patients presenting with epilepsy, as compared to our complete patient cohort [1]. Moreover, these patients showed significantly longer survival (median OS: 376.0 days from surgery, 95%CI: 337.4–414.6) compared to patients not included in the IDH1 analysis (median OS: 196.0, 95%CI: 159.2–232.8, log-rank test, $P < 0.0005$). Of note as well, IDH1 mutation was only observed in 21 of 360 patients (5.8%). Since IDH1 status did not correlate to epilepsy at presentation (χ^2 -test, $P = 0.98$), it is unlikely that IDH1 mutation is the underlying factor that explains the prognostic effect of epilepsy at presentation in glioblastoma patients.

We also thank Zhou et al. for sharing their preliminary analysis on the prognostic relevance of epilepsy at presentation in an institutional cohort of 113 lower grade gliomas and in 477 patients from the The Cancer Genome Atlas (tumor grade undescribed). With use of a univariable log-rank test, they did not observe a significant association between survival and epilepsy at presentation in their institutional cohort ($P = 0.131$). In the TCGA dataset, a history of seizures was associated to survival in univariable analysis ($P = 0.048$), but not after correction for age, KPS, tumor location, WHO grade, histological classification, radiotherapy, chemotherapy ($P = 0.682$). This analysis of Zhou et al. in fact addresses a different research question than that investigated in our paper, as they report on the prognostic relevance of epilepsy in lower grade gliomas. In order to interpret the results of this analysis however, more information regarding baseline characteristics of the patients included in their study is needed, in particular regarding the distribution of grade II and grade III patients in their cohorts. Indeed, the median follow-up of their institutional cohort (37 months) seems very short for LGG patients as compared to the published median survival of grade II glioma patients [2], suggesting either an overrepresentation of grade III

astrocytic tumors or immature follow-up data. Additionally, it would be very interesting for Zhou et al. to address their own question on the role of IDH1 mutational status, which is more frequently found in lower grade tumors [3]. We are looking forward to reading a future report of their analyses, and in particular the results of a multivariable analysis of their matured institutional data.

REFERENCES

1. Berendsen S, Varkila M, Kroonen J, et al. Prognostic relevance of epilepsy at presentation in glioblastoma patients. *Neuro Oncol.* 2015; Sep 29. pii: nov238. [Epub ahead of print].
2. Gorlia T, Wu W, Wang M, et al. New validated prognostic models and prognostic calculators in patients with low-grade gliomas diagnosed by central pathology review: a pooled analysis of EORTC/ RTOG/NCCTG phase III clinical trials. *Neuro Oncol.* 2013; 15(11):1568–1579.
3. Eckel-Passow JE, Lachance DH, Molinaro AM, et al. Glioma Groups Based on 1p/19q, IDH, and TERT Promoter Mutations in Tumors. *N Engl J Med.* 2015; 372(26):2499-508.





CHAPTER 5

Epilepsy associates with decreased HIF-1 α /STAT5b
signaling in glioblastoma

Sharon Berendsen, Wim G.M. Spliet, Marjolein Geurts, Wim Van
Hecke, Tatjana Seute, Tom J. Snijders, Vincent Bours, Erica H. Bell,
Arnab Chakravarti and Pierre A. Robe.

Published in: Cancers (Basel). 2019 Jan 4;11(1). pii: E41.

ABSTRACT

Introduction: Epilepsy at presentation is an independent favorable prognostic factor in glioblastoma. In this study, we analyze the oncologic signaling pathways that associate with epilepsy in human glioblastomas, and that can underlie this prognostic effect.

Methods: Following ethical approval and patient consent, fresh frozen glioblastoma tissue was obtained from 76 patient surgeries. Hospital records were screened for the presence of seizures at presentation of the disease. mRNA and miRNA expression-based and gene set enrichment analyses were performed on these tissues, to uncover candidate oncologic pathways that associate with epilepsy. We performed qPCR experiments and immunohistochemistry on tissue microarrays containing 286 glioblastomas to further explore the association of these candidate pathways and of markers of mesenchymal transformation (NF- κ B, CEBP- β , STAT3, STAT5b, VEGFA, SRF) with epilepsy.

Results: Gene sets involved in hypoxia/HIF-1 α , STAT5, CEBP- β and epithelial-mesenchymal transformation signaling were significantly downregulated in epileptogenic glioblastomas. On confirmatory protein expression analyses, epileptogenic tumors were characterized by a significant downregulation of phospho-STAT5b, a target of HIF-1 α . Epilepsy status did not associate with molecular subclassification or miRNA expression patterns of the tumors.

Conclusion: Epileptogenic glioblastomas correlate with decreased hypoxia/HIF-1 α /STAT5b signaling compared to glioblastomas that do not present with epilepsy.

INTRODUCTION

Glioblastoma is the most malignant primary brain tumor with a dismal prognosis. Median patient survival in those who can undergo aggressive therapy is 15–20 months from diagnosis [1]. Genetic and epigenetic (e.g., DNA methylation, histone acetylation) events condition the deregulation of key signaling pathways in glioblastoma and hence, its growth, invasion and therapeutic resistance [2]. Specific molecular characteristics provide distinct molecular glioblastoma subtypes, of which the mesenchymal subtype has been linked to a more aggressive and invasive tumor phenotype [3] and is driven by alterations in master transcription factors such as STAT3, CEBP- β and NF- κ B [4, 5].

The disease presents itself with epileptic seizures in 30–40% of the cases [6, 7], and we previously showed that epilepsy at presentation is an independent favorable prognostic factor for overall survival in glioblastoma patients [7]. This prognostic effect could not be explained by treatment with specific anti-epileptic drugs [7, 8], a smaller tumor volume at presentation, due to an earlier detection of the tumor, or IDH1 mutations [7]. The mechanisms underlying this prognostic effect in glioblastoma thus remain to be elucidated.

Glioma-associated epilepsy is (in part) mediated by tumor specific biological changes. Most studies have however been performed in low grade gliomas (LGGs), since these tumors more often present with epilepsy compared to glioblastomas [9].

Tumor-associated epilepsy results, at least in part, from a local neuronal excitation/inhibition disbalance. For instance, the release of D-2-hydroxyglutarate (D2HG), a substance structurally similar to glutamate, in the tumor microenvironment was associated with epilepsy [10]. NR2B, a predominantly extrasynaptic NMDA glutamate receptor, is highly phosphorylated in peritumoral mouse brain tissue, and increases Ca²⁺ influx in the cells, leading to a self-activating circle and overexcitation of neurons [11, 12]. Another proposed mechanism of tumor-associated seizures is mediated by the glutamate release pathway cystine/glutamate transporter System _{xc-} (SXC), which expression is elevated in a subset of glioblastoma tissues, and in peritumoral tissues. Higher glutamate concentrations and lower glutamine synthetase expression in the tumors and peritumoral tissues were also linked to glioma-related seizures [13–15].

Some studies have also linked glioma-associated epilepsy with IDH1 mutation [16–18]. We have shown that such mutations cannot solely explain the favorable prognosis of epileptogenic glioblastomas [7]. A lower expression of OLIG2, linked to the proneural glioblastoma subtype [3], was also related to an increased risk of tumor-associated seizures [19]. How this could relate to the prognosis is however unknown.

The mechanisms underlying the prognostic effect of epilepsy at presentation on overall survival in glioblastoma patients have thus not yet been investigated. Therefore, in this study, we focus on the oncogenic signaling pathways that associate with epilepsy in human glioblastomas, in search for the mechanisms that underlie this prognostic effect.

MATERIALS AND METHODS

Ethics Statement

This study was conducted following approval by the local ethical committee, and institutional review board (protocols 09-420, 16-229, 16-348).

Clinical data and Tumor Tissues

Following ethical approval and written patient consent, fresh frozen glioblastoma tissue was prospectively obtained from 76 patients at first surgery for their disease between 2010–2015. Hospital records were screened for the presence of seizures at diagnosis.

mRNA Expression Analysis

Seventy-six fresh-frozen surgical samples of *de novo* glioblastomas were prospectively collected between 2010 and 2015. RNA was extracted with the Nucleospin® TriPrep (Macherey-Nagel, Düren, Germany) and the QIASymphony RNA (Qiagen, Venlo, The Netherlands) kits according to the manufacturers' instructions. Affymetrix HG U133 plus 2.0 arrays were prepared and scanned according to the manufacturer's protocol and as reported previously [54]. Quality control and differential gene expression analyses were performed with R (v3.2.2). Based on principal component analysis (PCA) plots, 3 outliers were removed. Robust Multi-array Average (RMA) normalization was applied. Batch correction was performed with the 'sva' package. Differential expression was analyzed with the 'limma' package and heatmaps were created with the 'heatmap3' package (R).

Exploratory Gene Set Enrichment Analyses (GSEA) were performed after RMA-normalization [55] and batch correction, with the Partek® Genomics suite platform (v6.6) (Partek, St. Louis, MO, USA). Analyses were performed with the Broad Institute MySig libraries of curated gene sets C1—C7 version 5.0 [56], 1000 permutations and default additional parameters. An FDR threshold of 0.25 was applied as recommended [55].

miRNA Expression Analysis

RNA was isolated from the 76 fresh-frozen surgical samples of glioblastoma patients with the MiRNeasy Micro Kit (Qiagen). Expression profiling of 800 miRNA probes was performed with the nCounter® Human v2 miRNA Expression Assay (NanoString, Seattle, WA, USA) at The Ohio State University Nucleic Acid Core Facility. 250 ng RNA was used

per sample and conditions were set according to the manufacturer's instructions. RNA quality was insufficient for 4 samples. Data were processed with the Partek® Genomics suite platform (v6.6) by geometric mean normalization, average background subtraction and normalization to housekeeping genes. miRNA expression levels in glioblastomas in patients with and without seizures were analyzed with the 'limma' and 'heatmap3' package (R).

Class Prediction

Molecular subclassification (proneural, neural, classical, mesenchymal) was predicted by hierarchical clustering [3]. Microarray normalization, data filtering and analysis of inter-array homogeneity were performed as reported previously [3,57]. Affymetrix HG U133 plus 2.0 probesets were matched to 840 genes originally published for the classification of glioblastomas (http://tcga-data.nci.nih.gov/docs/publications/gbm_exp/). Relative gene expression values were calculated. Genes were then excluded for a median absolute deviation below 0.5 [3]. After filtering, 768 genes were used for the class prediction. The hierarchical clustering of samples was performed with cluster 3 software [58] with the agglomerative average linkage for the structure and 1 minus the Pearson's correlation for the distance metric [3].

qPCR Analyses

RNA for qPCR was available from the RNA extraction for miRNA expression analysis for 5 glioblastoma patients with epilepsy and 16 patients without epilepsy. RNA quality was checked by measuring of A260/280 and A260/230 values with Nanodrop. qPCR expression analyses were performed for HIF1A, SRF, VEGFA. Expression values were normalized to the average of 3 housekeeping genes (ACTB, GAPDH, GUSB).

Tissue Microarrays and Immunohistochemistry

Archival FFPE glioblastoma tumor tissues from a consecutive cohort of 286 patients treated in the UMCU between 2009 and 2013 were included on tissue microarrays (TMA's) as described previously [7]. Immunohistochemistry was performed, as described previously [7], with antibodies against STAT5b (phospho S731, Rabbit polyclonal, Abcam, Cambridge, UK), VEGF (Rabbit polyclonal, ThermoScientific, Waltham, MA USA), anti-NF- κ B p65 (phospho S276, Rabbit polyclonal, Abcam); anti-STAT3 (phospho Y705) (Rabbit monoclonal, Cell Signaling, Leiden, The Netherlands); anti-CEBP- β (Mouse monoclonal, Abcam); anti-SRF (Rabbit polyclonal, Abcam, and rabbit polyclonal, Sigma-Aldrich, St. Louis, MO, USA).

Protein expression evaluation was performed with blinding for the clinical data, and was supervised by a senior neuropathologist. The percentage of nuclear and/or cytoplasmatic staining was scored as: 0, negative; 1, 1–25% positive cells; 2, 26–50% positive cells;

3, 51–75% positive cells and 4, 76–100% positive cells. A mean expression score was computed per patient. Due to insufficient tissue quality on TMA, a variable number of tissues per staining could not be evaluated (n = 8–21).

Statistical Analyses

Expression analyses of individual mRNAs and miRNAs were performed with the ‘limma’ package in R (v3.2.2). To control for inflation of type I error by multiple testing, p-values were adjusted by default Benjamini-Hochberg procedure. Adjusted p-values < 0.05 were considered significant. GSEA was performed with the Partek® Genomics suite platform (v6.6). A recommended cutoff of $p < 0.05$ and false-discovery rate (FDR) < 0.25 was applied. All other analyses were performed with SPSS (v25, IBM, Armonk, NY, USA). A p-value < 0.05 was considered significant. Differential distributions of molecular subtypes across epilepsy and non-epilepsy patients were tested with a Chi-square test. Differences in RNA expression between patients with and without epilepsy were analyzed by independent samples t-test. Data distribution of protein expression was evaluated graphically and with a Kolmogorov-Smirnov test and differential expression was subsequently analyzed with a Mann Whitney U test.

RESULTS

Fresh-frozen tissue from 76 ‘*de novo*’ glioblastoma patients was included in this study. Baseline characteristics are shown in Table S1. Of these patients, 30 presented with epilepsy and 46 had different symptoms at presentation of the disease. mRNA expression analysis was performed for 73 patients, after quality control and removal of three outliers. miRNA expression analysis was performed for 72 patients, as four samples were removed due to insufficient RNA quality. Molecular classification could be assigned to 66/76 samples. TMA’s included archival fresh-frozen paraffin-embedded (FFPE) tissue from 286 consecutive glioblastoma patients. Details on this cohort are shown in Table S2.

Epileptogenic glioblastomas Show Downregulation of HIF1a/STAT5b Signaling

None of the individual mRNAs or miRNAs reached a significant association value after correction for multiple testing (Figure 1A,B). Exploratory gene set enrichment analyses (GSEA) were performed with use of the mRNA expression data and showed significant downregulation of 218 gene sets in the epilepsy subgroup compared to glioblastomas that did not present with epilepsy, with use of the Broad Institute MySig (MSigDB) libraries of curated gene sets C2 collection (curated gene sets, $p < 0.05$, false discovery rate (FDR) < 0.25). The top results are shown in Table 1, and full table is available in the supplementary material (Table S3). The majority of the associated gene sets are involved in hypoxia and HIF-1 α signaling. Additionally, a gene set containing STAT5 targets ($p <$

0.0001, FDR = 0.06) and gene sets involved in CEBP- β , STAT3 signaling and epithelial to mesenchymal transition (EMT) signaling ($p < 0.05$, FDR < 0.25) were downregulated in the epilepsy subgroup compared to patients without epilepsy.

GSEA with the MSigDB C3 collection containing motif gene sets showed, among others, downregulation of a gene set involved in CEBP- β signaling ($p < 0.05$, FDR < 0.25 , Table 1) and SRF signaling ($p < 0.05$, FDR < 0.25). Analysis with the MSigDB C7 gene set showed downregulation of multiple gene sets containing genes responsive to LPS stimulation in macrophages ($p < 0.05$, FDR < 0.25 , Table 1). qPCR experiments in a subset of fresh-frozen glioblastoma samples (epilepsy $n = 5$, no epilepsy $n = 16$) did not show significant differential expression of HIF1a, VEGF or SRF (Figure 2A). However, on a protein level, we observed a significant decrease in protein expression of nuclear phosphorylated STAT5b in the epilepsy subgroup (Mann-Whitney U test, $p = 0.004$, Figure 2B). The JAK/STAT5b pathway has been shown to closely correlate with hypoxia and HIF-1 α signaling in multiple cancers [20-23]. VEGFA and SRF protein expression did not differ between the two groups (Figures 2B and S1).

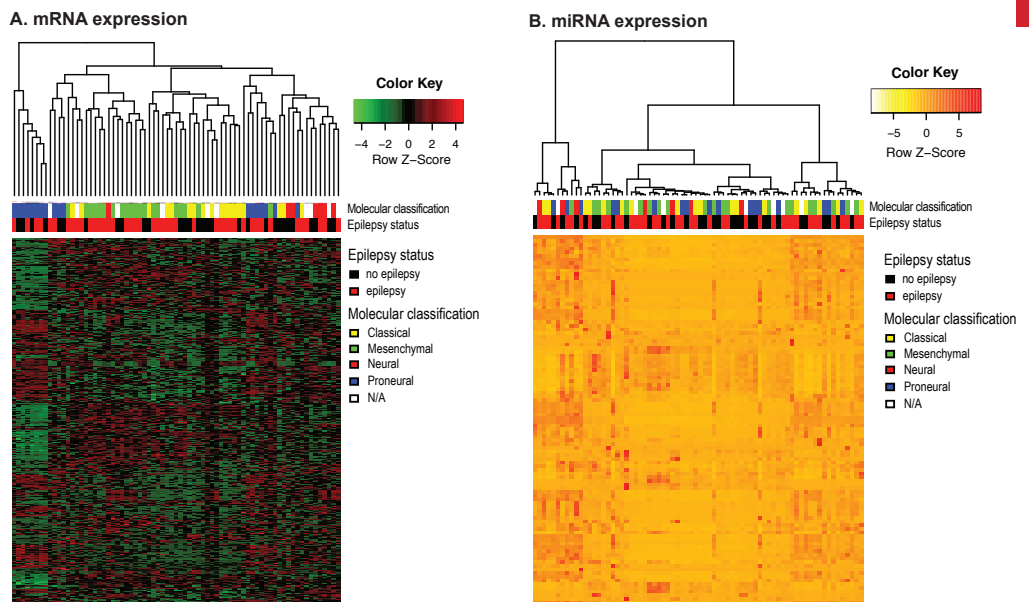


Figure 1 – Lack of correlation between glioblastoma-associated epilepsy and gene expression data. (A) Heatmap showing gene expression patterns of the 1000 RNA microarray probes with the highest standard deviation. Relative downregulation is shown as green, relative upregulation is shown as red, see color key. No differentially expressed genes were observed after correction for multiple testing (BH adjusted $p < 0.05$). (B) MiRNA expression patterns of the 100 probes with the highest standard deviation. 67 samples from our institute were included in this analysis. Relative miRNA downregulation is shown as white/yellow, and relative miRNA upregulation is shown as red, see color key. No differentially expressed miRNAs were observed after correction for multiple testing (Benjamini Hochberg adjusted $p < 0.05$).

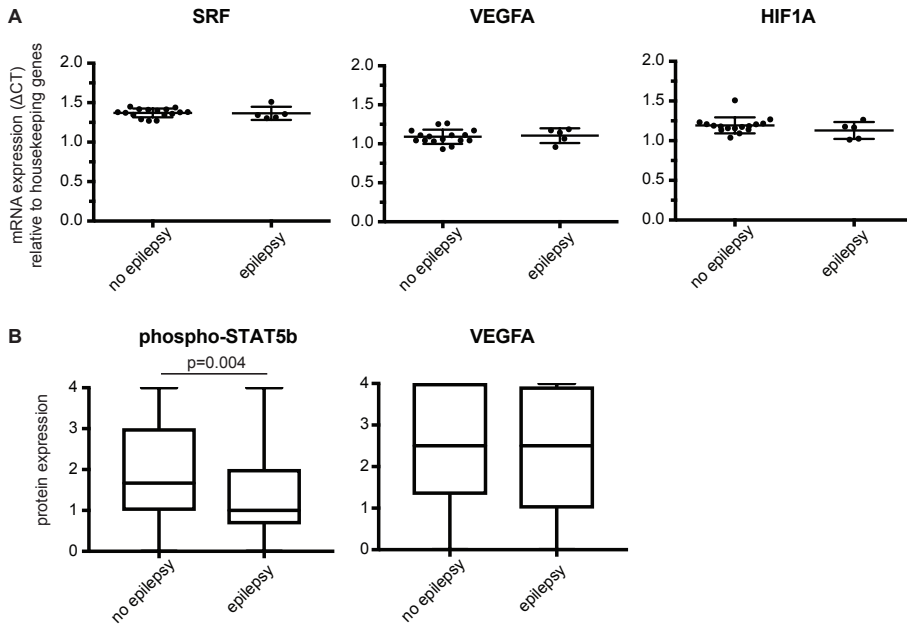


Figure 2 – Differential activation of STAT5b between epileptogenic and non-epileptogenic glioblastomas. (a) qPCR experiments showing mRNA expression (ΔCT) of SRF, VEGFA and HIF1A in glioblastoma patients with epilepsy ($n=5$) and without epilepsy ($n=16$). Graphs show mean \pm SD and expression values per patient. Expression values were normalized to the average of 3 housekeeping genes (ACTB, GAPDH, GUSB). There was no significant difference in mRNA expression between epilepsy and non-epilepsy samples (independent samples t-test, SRF: $p=0.9$, VEGFA: $p=0.76$, HIF1A: $p=0.23$). (b) Protein expression of phosphorylated STAT5b and VEGFA on glioblastoma samples included on a tissue microarray. STAT5b expression was significantly lower in patients that presented with epilepsy compared to glioblastoma patients with other presenting symptoms ($n=265$, Mann Whitney U test, $p=0.004$). VEGFA expression did not differ between the groups ($n=275$, Mann Whitney U test, $p=0.43$).

Table 1 – Gene set enrichment analysis with MSigDB collections.

Gene sets	NES	P-value	FDR
C2 collection – curated gene sets			
ELVIDGE_HIF1A_TARGETS_DN	-2.355	<0.0001	<0.0001
ELVIDGE_HYPOXIA_BY_DMOG_UP	-2.283	<0.0001	0.0007
ELVIDGE_HIF1A_AND_HIF2A_TARGETS_DN	-2.301	<0.0001	0.0007
ELVIDGE_HYPOXIA_UP	-2.259	<0.0001	0.0009
LEONARD_HYPOXIA	-2.285	<0.0001	0.001
FARDIN_HYPOXIA_11	-2.198	<0.0001	0.007
PID_HIF1_TFPATHWAY	-2.149	<0.0001	0.02
GROSS_HIF1A_TARGETS_DN	-2.136	<0.0001	0.02
GROSS_HYPOXIA_VIA_ELK3_AND_HIF1A_UP	-2.116	<0.0001	0.03
C3 collection – transcription factor targets			
V\$ROAZ_01	-1.69	0.03	0.11
V\$SRF_01	-1.71	0.02	0.13
CCAWWNAAGG_V\$SRF_Q4	-1.71	0.01	0.16
TTGCWCAY_V\$CEBPB_02	-1.73	0.004	0.18
GGGNRMNNYCAT_UNKNOWN	-1.62	0.006	0.20
KRCTCNNNNMANAGC_UNKNOWN	-1.77	0.013	0.25
C7 collection – immunologic signatures			
GSE14769_UNSTIM_VS_40MIN_LPS_BMDM_DN	-1.90	0.006	0.13
GSE37416_CTRL_VS_12H_F_TULARENSIS_LVS_NEUTROPHIL_DN	-1.90	0.006	0.15
GSE14769_UNSTIM_VS_80MIN_LPS_BMDM_DN	-1.91	0.008	0.17
GSE14769_UNSTIM_VS_60MIN_LPS_BMDM_DN	-1.91	0.006	0.21
GSE37416_CTRL_VS_3H_F_TULARENSIS_LVS_NEUTROPHIL_DN	-1.93	0.004	0.24

Gene sets are significantly downregulated in the epilepsy group compared to the patients without epilepsy. Cutoff values for significance were $p < 0.05$ and $FDR < 0.25$. Analyses were performed with MSigDB collections C1–C7. A subset of significant C2 results were displayed in this table. See supplementary Table S1 for full results with the C2 collection. NES: normalized enrichment score, FDR: false-discovery rate.

Epilepsy Does Not Correlate with a Mesenchymal Signature in glioblastomas

As described above, GSEA showed downregulation of, among others, gene sets involved in EMT, STAT3 and CEBP- β signaling in the epileptogenic glioblastomas. Based on these results, we further investigated the association of epileptogenic glioblastomas with mesenchymal transformation.

In the subgroup of patients without epilepsy a relatively larger percentage of tumors was classified as the mesenchymal subtype compared to the epilepsy group (40% vs. 25%), but this difference did not reach statistical significance (Chi-square test, $p = 0.48$, Figure 3A). In line with these results, no significant difference was observed in protein expression of phosphorylated NF- κ B p65, phosphorylated STAT3 and CEBP- β (Figure 3B), which are master transcriptional regulators of the mesenchymal gene signature in glioblastoma.

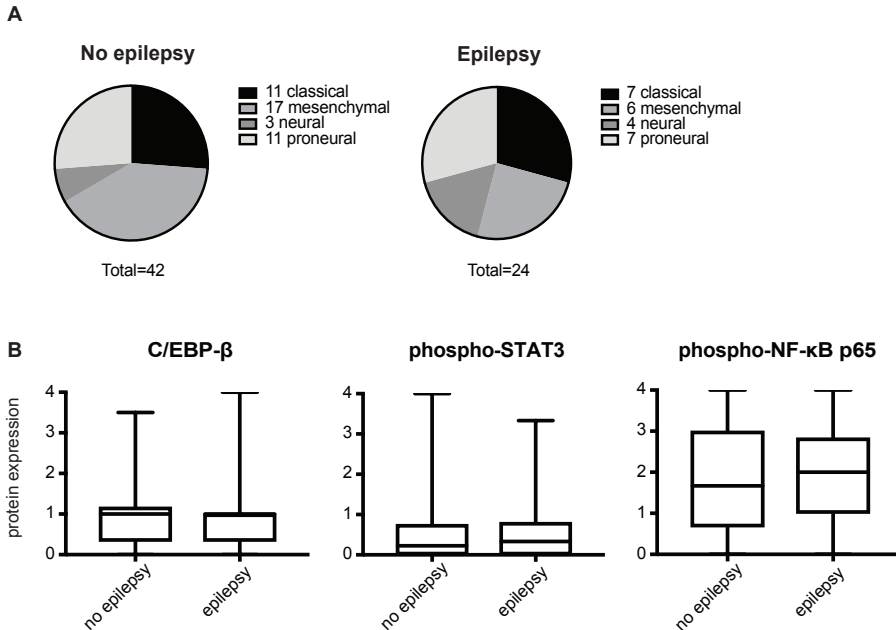


Figure 3 – Molecular subclassification and mesenchymal activation in epileptogenic glioblastomas. (a) Distribution of molecular glioblastoma subtypes in subgroup of patients with epilepsy ($n=24$) and without epilepsy ($n=42$), based on mRNA expression profile. There was no significant difference in subtype distribution (Chi-square test, $p=0.48$). (b) Protein expression of CEBP- β , phosphorylated STAT3 and phosphorylated NF- κ B p65 on glioblastoma tissues included on a tissue microarray. Mann Whitney U test did not show significant differences in protein expression between the epilepsy and non-epilepsy subgroups (CEBP- β : $n=266$, $p=0.81$, phosphorylated STAT3: $n=272$, $p=0.68$, phosphorylated NF- κ B p65: $n=278$, $p=0.56$). Boxes represent median and quartiles, whiskers show data range.

DISCUSSION

In our previous work, we observed that glioblastoma patients with epilepsy at the time of diagnosis have a significantly longer overall survival compared to patients that present with other symptoms. This prognostic effect was independent of anti-epileptic treatment and other important clinical characteristics [7].

Others have demonstrated that specific tumor biological effects are associated with epilepsy in glioma patients, such as neuronal excitation/inhibition disbalance and expression changes in the glutamate pathway [10-15]. Also, IDH1 mutation was linked to the risk of tumor-associated epilepsy and seizure prognosis [16, 17]. In our previous study, however, we found no correlation between epilepsy and IDH1 mutation in primary glioblastoma patients [7].

NF- κ B, CEBP- β and STAT proteins, including STAT3 and -5, are transcription factors that mediate a wide range of cellular cytokine responses in physiological and disease processes [24-26]. Previous studies have identified STAT3 and CEBP- β as principal regulators of the mesenchymal gene expression signature in glioblastoma [4, 27]. High expression of these mesenchymal markers has been associated with worse survival of glioblastoma patients [27]. Additionally, NF- κ B has been shown to drive mesenchymal transformation in glioma stem cells by induction of master transcription factors STAT3, CEBP- β and TAZ, which can subsequently contribute to resistance to radiation [5] and chemotherapy [28]. In our study, GSEA showed a downregulation of gene sets involved in epithelial to mesenchymal transformation (C2) and CEBP- β signaling (C3), suggesting a possible link between epileptogenic glioblastomas and molecular subclassification or mesenchymal transformation. Subsequent analyses could however not confirm this relationship. Although the epilepsy subgroup contained fewer tumors with the mesenchymal subtype, this was not a statistically significant difference. We also did not observe significant differences in protein expression of the key mesenchymal transcription factors NF- κ B p65, STAT3 and CEBP- β .

Hypoxia-inducible factors, such as HIF-1 α , contribute to the cell's response to hypoxia [29]. HIF-1 α is a major player in the oncologic signaling in glioblastoma. In hypoxic conditions, a mesenchymal shift mediated by HIF-1 α is induced in glioblastoma cells [30, 31]. Several of the key regulators of transcription involved in mesenchymal transformation (e.g., NF- κ B, CEBP- β) upregulate under hypoxic conditions in cancer cells [27, 32], and hypoxia activates the JAK2/STAT5b pathway in several types of cancer [20-23]. Also, crosstalk between HIF-1 α and STAT3 was reported, in different tumor types, including glioblastoma [33, 34]. Interest in STAT5 signaling in glioblastoma is growing, as multiple

studies have shown that STAT5b drives proliferation and invasion in glioma [35-38]. This may be, in part mediated by the oncogenic EGFRvIII variant [39-41].

In our study, we observed downregulation of multiple gene sets involved in HIF-1 α and hypoxia signaling in the epileptogenic glioblastomas. Additionally, STAT5 target genes seemed downregulated in this group. Interestingly, nuclear phosphorylated STAT5b protein expression was downregulated in the epileptogenic glioblastomas. Activated STAT5 proteins translocate to the nucleus [26], and serine 730 phosphorylation induces its intrinsic transcriptional activity [42]. We did not observe differential RNA or protein expression of HIF-1 α and its target VEGFA between the epileptogenic glioblastomas and tumors that did not cause epilepsy. These results indicate that epilepsy in glioblastoma patients more specifically correlates to decreased hypoxia/HIF-1 α /STAT5b signaling. Interestingly, STAT5b protein expression associated with glioblastoma patient survival in our population of patients [43].

Besides its role in tumor growth and carcinogenesis, HIF-1 α /STAT5b signaling could also be directly related to the epileptogenicity of the tumors, by altering the buffering and networking properties of the glial network. STAT5-null mice have indeed undetectable levels of connexin 32 [44], while connexin 43 (Cx43) mediates HIF-1 α in astrocytes [45]. High expression of connexin 43 has in turn been linked to both glioma-related epilepsy [46] and epilepsy due to mesiotemporal sclerosis [47], while this latter presents reduced levels of connexin 32. On the other hand, STAT5 is a negative regulator of xCT Expression and System _{x_c}-Activity [48]. The exploration of these potential correlations is beyond the scope of the present work but represents an interesting venue for future research. With respect to tumor epileptogenicity as well, our GSEA also showed decreased expression of gene sets involved in serum response factor (SRF) signaling in the epileptogenic tumors. SRF depletion has been associated with increased seizure frequency in a mouse model [49, 50]. Interestingly, SRF has also been linked to tumor invasion, proliferation, metastasis and resistance to therapy in different cancer types [51-53]. Its role in glioblastoma remains to be explored. In a subset of patients however, we did not observe differential SRF RNA expression between the epilepsy and non-epilepsy subgroups by qRT-PCR. Likewise, SRF protein expression was evaluated with two different antibodies on our tissue microarrays and did not associate with epileptogenicity. Hence, we could not confirm the association of SRF signaling with epileptogenic glioblastomas.

Our study presents some limitations. Not all results from the gene set enrichment analyses could be confirmed by other RNA or protein expression-based experiments. This discrepancy confirms the exploratory role of GSEA. The number of fresh-frozen tumor tissues available for confirmatory qRT-PCR experiments was somewhat limited. On the other hand, we included a large cohort of patients in the TMA analyses for our

confirmatory protein expression analyses. Yet, we cannot rule out that intratumoral tissue heterogeneity could alter these analyses as well. Fresh-frozen tumor specimens were all collected by an experienced neuro-oncological neurosurgeon (P.R.) from the vital tumor tissue during surgery. Due to ethical reasons, we were not able to include peritumoral brain tissue from the patients. Archival FFPE tissue was used for protein expression analyses on tissue microarrays and multiple tumor tissue regions per patient were included. To minimize this bias however, a combined protein expression score was computed per patient.

CONCLUSIONS

A reduced activity of the hypoxia/HIF-1 α /STAT5b signaling pathway is associated with epileptogenicity in glioblastomas. For the first time to our knowledge, these results provide biological insight in the favorable prognosis of tumor-associated epilepsy.

REFERENCES

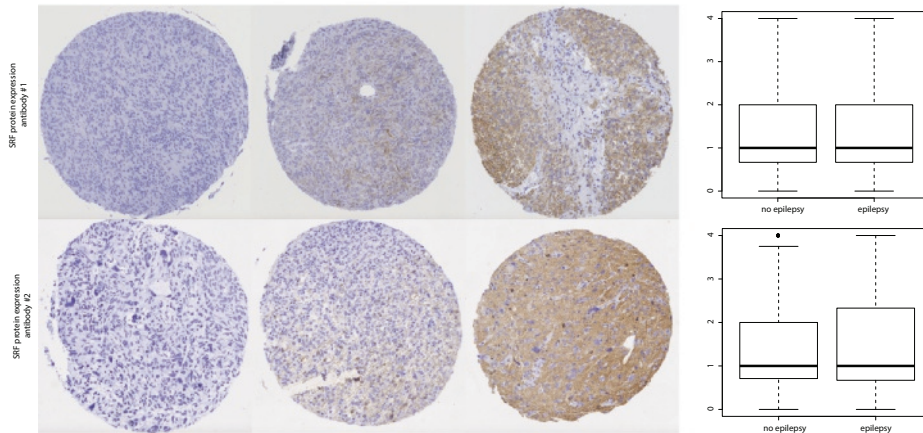
1. Stupp, R.; Taillibert, S.; Kanner, A.A.; Kesari, S.; Steinberg, D.M.; Toms, S.A. Maintenance Therapy With Tumor-Treating Fields Plus Temozolomide vs Temozolomide Alone for Glioblastoma: A Randomized Clinical Trial. *Jama* 2015, 314, 2535–2543.
2. Brennan, C.W.; Verhaak, R.G.; McKenna, A.; Campos, B.; Nounshmehr, H.; Salama, S.R. The somatic genomic landscape of glioblastoma. *Cell* 2013, 155, 462–477.
3. Verhaak, R.G.; Hoadley, K.A.; Purdom, E.; Wang, V.; Qi, Y.; Wilkerson, M.D. Integrated genomic analysis identifies clinically relevant subtypes of glioblastoma characterized by abnormalities in PDGFRA, IDH1, EGFR, and NF1. *Cancer Cell* 2010, 17, 98–110.
4. Carro, M.S.; Lim, W.K.; Alvarez, M.J.; Bollo, R.J.; Zhao, X.; Snyder, E.Y. The transcriptional network for mesenchymal transformation of brain tumours. *Nature* 2010, 463, 318–325.
5. Bhat, K.P.; Balasubramanian, V.; Vaillant, B.; Ezhilarasan, R.; Hummelink, K.; Hollingsworth, F. Mesenchymal differentiation mediated by NF-kappaB promotes radiation resistance in glioblastoma. *Cancer Cell* 2013, 24, 331–346.
6. Kerkhof, M.; Dielemans, J.C.; van Breemen, M.S.; Zwinkels, H.; Walchenbach, R.; Taphoorn, M.J.; Vecht, C.J. Effect of valproic acid on seizure control and on survival in patients with glioblastoma multiforme. *Neuro-oncology* 2013, 15, 961–967.
7. Berendsen, S.; Varkila, M.; Kroonen, J.; Seute, T.; Snijders, T.J.; Kauw, F. Prognostic relevance of epilepsy at presentation in glioblastoma patients. *Neuro-oncology* 2016, 18, 700–706.
8. Huppold, C.; Gorlia, T.; Chinot, O.; Gilbert, M.R.; Nabors, L.B.; Wick, W. Does Valproic Acid or Levetiracetam Improve Survival in Glioblastoma? A Pooled Analysis of Prospective Clinical Trials in Newly Diagnosed Glioblastoma. *J. Clin. Oncol.* 2016, 34, 731–739.
9. van Breemen, M.S.; Wilms, E.B.; Vecht, C.J. Epilepsy in patients with brain tumours: Epidemiology, mechanisms, and management. *Lancet Neurol.* 2007, 6, 421–430.
10. Dang, L.; White, D.W.; Gross, S.; Bennett, B.D.; Bittinger, M.A.; Driggers, E.M. Cancer-associated IDH1 mutations produce 2-hydroxyglutarate. *Nature* 2009, 462, 739–744.
11. Gao, X.; Wang, H.; Cai, S.; Saadatzaheh, M.R.; Hanenberg, H.; Pollok, K.E. Phosphorylation of NMDA 2B at S1303 in human glioma peritumoral tissue: Implications for glioma epileptogenesis. *Neurosurg. Focus* 2014, 37, E17.
12. Gao, X.; Wang, H.; Pollok, K.E.; Chen, J.; Cohen-Gadol, A.A. Activation of death-associated protein kinase in human peritumoral tissue: A potential therapeutic target. *J. Clin. Neurosci.* 2015, 22, 1655–1660.
13. Yuen, T.I.; Morokoff, A.P.; Bjorksten, A.; D'abaco, G.; Paradiso, L.; Finch, S. Glutamate is associated with a higher risk of seizures in patients with gliomas. *Neurology* 2012, 79, 883–889.
14. Robert, S.M.; Buckingham, S.C.; Campbell, S.L.; Robel, S.; Holt, K.T.; Ogunrinu-Babarinde, T. SLC7A11 expression is associated with seizures and predicts poor survival in patients with malignant glioma. *Sci. Transl. Med.* 2015, 7, 289ra86.
15. Rosati, A. Epilepsy in glioblastoma multiforme: Correlation with glutamine synthetase levels. *J. Neurooncol.* 2009, 93, 319–324.

16. Neal, A. IDH1 and IDH2 mutations in postoperative diffuse glioma-associated epilepsy. *Epilepsy Behav.* 2018, 78, 30–36.
17. Li, Y. IDH1 mutation is associated with a higher preoperative seizure incidence in low-grade glioma: A systematic review and meta-analysis. *Seizure* 2018, 55, 76–82.
18. Chen, H. Mutant IDH1 and seizures in patients with glioma. *Neurology* 2017, 88, 1805–1813.
19. Lee, J.W.; Norden, A.D.; Ligon, K.L.; Golby, A.J.; Beroukhi, R.; Quackenbush, J. Tumor associated seizures in glioblastomas are influenced by survival gene expression in a region-specific manner: A gene expression imaging study. *Epilepsy Res.* 2014, 108, 843–852.
20. Pak, S.H. Hypoxia upregulates Hsp90 α expression via STAT5b in cancer cells. *Int. J. Oncol.* 2012, 41, 161–168.
21. Joung, Y.H. Hypoxia activates the IGF-1 expression through STAT5b in human HepG2 cells. *Biochem. Biophys. Res. Commun.* 2007, 358, 733–738.
22. Joung, Y.H.; Lim, E.J.; Lee, M.Y.; Park, J.H.; Ye, S.K.; Park, E.U. Hypoxia activates the cyclin D1 promoter via the Jak2/STAT5b pathway in breast cancer cells. *Exp. Mol. Med.* 2005, 37, 353–364.
23. Lee, M.Y. Phosphorylation and activation of STAT proteins by hypoxia in breast cancer cells. *Breast* 2006, 15, 187–195.
24. Zhang, Q.; Lenardo, M.J.; Baltimore, D. 30 Years of NF-kappaB: A Blossoming of Relevance to Human Pathobiology. *Cell* 2017, 168, 37–57.
25. van der Krieken, S.E. CCAAT/enhancer binding protein beta in relation to ER stress, inflammation, and metabolic disturbances. *Biomed. Res. Int.* 2015, 2015, 324815.
26. Villarino, A.V. Mechanisms of Jak/STAT signaling in immunity and disease. *J. Immunol.* 2015, 194, 21–27.
27. Cooper, L.A.; Gutman, D.A.; Chisolm, C.; Appin, C.; Kong, J.; Rong, Y. The tumor microenvironment strongly impacts master transcriptional regulators and gene expression class of glioblastoma. *Am. J. Pathol.* 2012, 180, 2108–2119.
28. Bredel, M. Tumor necrosis factor-alpha-induced protein 3 as a putative regulator of nuclear factor-kappaB-mediated resistance to O6-alkylating agents in human glioblastomas. *J. Clin. Oncol.* 2006, 24, 274–287.
29. Carmeliet, P.; Dor, Y.; Herbert, J.M.; Fukumura, D.; Brusselmans, K.; Dewerchin, M. Role of HIF-1 α in hypoxia-mediated apoptosis, cell proliferation and tumour angiogenesis. *Nature* 1998, 394, 485–490.
30. Joseph, J.V.; Conroy, S.; Pavlov, K.; Sontakke, P.; Tomar, T.; Eggens-Meijer, E. Hypoxia enhances migration and invasion in glioblastoma by promoting a mesenchymal shift mediated by the HIF1 α -ZEB1 axis. *Cancer Lett.* 2015, 359, 107–116.
31. Talasila, K.M. The angiogenic switch leads to a metabolic shift in human glioblastoma. *Neuro-oncology* 2017, 19, 383–393.
32. Murat, A. Modulation of angiogenic and inflammatory response in glioblastoma by hypoxia. *PLoS ONE* 2009, 4, e5947.
33. Jung, J.E.; Lee, H.G.; Cho, I.H.; Chung, D.H.; Yoon, S.H.; Yang, Y.M. STAT3 is a potential modulator of HIF-1-mediated VEGF expression in human renal carcinoma cells. *FASEB J.* 2005, 19, 1296–1298.
34. Ganguly, D. The critical role that STAT3 plays in glioma-initiating cells: STAT3 addiction in glioma. *Oncotarget* 2018, 9, 22095–22112.
35. Alkharusi, A. Stimulation of prolactin receptor induces STAT-5 phosphorylation and cellular invasion in glioblastoma multiforme. *Oncotarget* 2016, 7, 79572–79583.

36. Gressot, L.V.; Doucette, T.A.; Yang, Y.; Fuller, G.N.; Heimberger, A.B.; Bögler, O. Signal transducer and activator of transcription 5b drives malignant progression in a PDGFB-dependent proneural glioma model by suppressing apoptosis. *Int. J. Cancer* 2015, 136, 2047–2054.
37. Liang, Q.C.; Xiong, H.; Zhao, Z.W.; Jia, D.; Li, W.X.; Qin, H.Z. Inhibition of transcription factor STAT5b suppresses proliferation, induces G1 cell cycle arrest and reduces tumor cell invasion in human glioblastoma multiforme cells. *Cancer Lett.* 2009, 273, 164–171.
38. Cao, S.; Wang, C.; Zheng, Q.; Qiao, Y.; Xu, K.; Jiang, T.; Wu, A. STAT5 regulates glioma cell invasion by pathways dependent and independent of STAT5 DNA binding. *Neurosci. Lett.* 2011, 487, 228–233.
39. Fan, Q.W. EGFR phosphorylates tumor-derived EGFRvIII driving STAT3/5 and progression in glioblastoma. *Cancer Cell* 2013, 24, 438–449.
40. Roos, A. EGFRvIII-Stat5 Signaling Enhances Glioblastoma Cell Migration and Survival. *Mol. Cancer Res.* 2018, 16, 1185–1195.
41. Latha, K.; Li, M.; Chumbalkar, V.; Gururaj, A.; Hwang, Y.; Dakeng, S. Nuclear EGFRvIII-STAT5b complex contributes to glioblastoma cell survival by direct activation of the Bcl-XL promoter. *Int. J. Cancer* 2013, 132, 509–520.
42. Park, S.H.; Yamashita, H.; Rui, H.; Waxman, D.J. Serine phosphorylation of GH-activated signal transducer and activator of transcription 5a (STAT5a) and STAT5b: Impact on STAT5 transcriptional activity. *Mol. Endocrinol.* 2001, 15, 2157–2171.
43. Robe, P.A., (University Medical Center Utrecht, Utrecht, The Netherlands). Personal communication, 2018.
44. Miyoshi, K.; Shillingford, J.M.; Smith, G.H.; Grimm, S.L.; Wagner, K.U.; Oka, T. Signal transducer and activator of transcription (Stat) 5 controls the proliferation and differentiation of mammary alveolar epithelium. *J. Cell Biol.* 2001, 155, 531–542.
45. Valle-Casuso, J.C. HIF-1 and c-Src mediate increased glucose uptake induced by endothelin-1 and connexin43 in astrocytes. *PLoS ONE* 2012, 7, e32448.
46. Dong, H. Complex role of connexin 43 in astrocytic tumors and possible promotion of glioma-associated epileptic discharge (Review). *Mol. Med. Rep.* 2017, 16, 7890–7900.
47. Collignon, F. Altered expression of connexin subtypes in mesial temporal lobe epilepsy in humans. *J. Neurosurg.* 2006, 105, 77–87.
48. Linher-Melville, K. Chronic Inhibition of STAT3/STAT5 in Treatment-Resistant Human Breast Cancer Cell Subtypes: Convergence on the ROS/SUMO Pathway and Its Effects on xCT Expression and System xc- Activity. *PLoS ONE* 2016, 11, e0161202.
49. Lösing, P.; Niturad, C.E.; Harrer, M.; zu Reckendorf, C.M.; Schatz, T.; Sinske, D. SRF modulates seizure occurrence, activity induced gene transcription and hippocampal circuit reorganization in the mouse pilocarpine epilepsy model. *Mol. Brain* 2017, 10, 30.
50. Kuzniewska, B. Adult Deletion of SRF Increases Epileptogenesis and Decreases Activity-Induced Gene Expression. *Mol. Neurobiol.* 2016, 53, 1478–1493.
51. Ohrnberger, S. Dysregulated serum response factor triggers formation of hepatocellular carcinoma. *Hepatology* 2015, 61, 979–989.
52. Qiao, J. SRF promotes gastric cancer metastasis through stromal fibroblasts in an SDF1-CXCR4-dependent manner. *Oncotarget* 2016, 7, 46088–46099.

53. Lundon, D.J.; Boland, A.; Prencipe, M.; Hurley, G.; O'Neill, A.; Kay, E. The prognostic utility of the transcription factor SRF in docetaxel-resistant prostate cancer: In-vitro discovery and in-vivo validation. *BMC Cancer* 2017, 17, 163.
54. Turkheimer, F.E.; Roncaroli, F.; Hennuy, B.; Herens, C.; Nguyen, M.; Martin, D. Chromosomal patterns of gene expression from microarray data: Methodology, validation and clinical relevance in gliomas. *BMC Bioinform.* 2006, 7, 526.
55. Subramanian, A.; Tamayo, P.; Mootha, V.K.; Mukherjee, S.; Ebert, B.L.; Gillette, M.A. Gene set enrichment analysis: A knowledge-based approach for interpreting genome-wide expression profiles. *Proc. Natl. Acad. Sci. USA* 2005, 102, 15545–15550.
56. Reich, M. GenePattern 2.0. *Nat. Genet.* 2006, 38, 500–501.
57. Wislet-Gendebien, S.; Poulet, C.; Neirinckx, V.; Hennuy, B.; Swingland, J.T.; Laudet, E. In vivo tumorigenesis was observed after injection of in vitro expanded neural crest stem cells isolated from adult bone marrow. *PLoS ONE* 2012, 7, e46425.
58. Eisen, M.B.; Spellman, P.T.; Brown, P.O.; Botstein, D. Cluster analysis and display of genome-wide expression patterns. *Proc. Natl. Acad. Sci. USA* 1998, 95, 14863–14868.

SUPPLEMENTARY FILES



Supplementary figure S1 – SRF protein expression does not correlate to glioblastoma-associated epilepsy. SRF protein expression on glioblastoma tissues included on a tissue microarray. Shown are examples of glioblastoma tissues with low, moderate and high SRF expression. Boxes represent median and quartiles, whiskers show data range. Upper panel: anti-SRF (rabbit polyclonal, Sigma, n=297, Mann Whitney U test p=0.63, lower panel: anti-SRF (Rabbit polyclonal, Abcam, n=290, Mann Whitney U test p=0.94).

Supplementary Table S1 – Baseline table fresh frozen tissues

Patient characteristics <i>n</i> (%)	Epilepsy 31 (40.7)	No epilepsy 45 (59.2)
Age (<i>mean ± SD</i>)	57.6 ± 10.9	63.4 ± 9.0
Gender (% <i>male</i>)	71	64.4
KPS <i>n</i> (%)		
< 70	4 (12.9)	7 (15.6)
≥ 70	27 (87.1)	38 (84.4)
Extent of surgery <i>n</i> (%)		
Biopsy	2 (6.5)*	2 (4.4)*
Debulking	31 (100)	45 (100)
Post-surgical treatment <i>n</i> (%)		
None	1 (3.2)	4 (8.9)
Monotherapy RT or TMZ	5 (16.1)	12 (26.7)
RT + TMZ	25 (80.6)	29 (64.4)

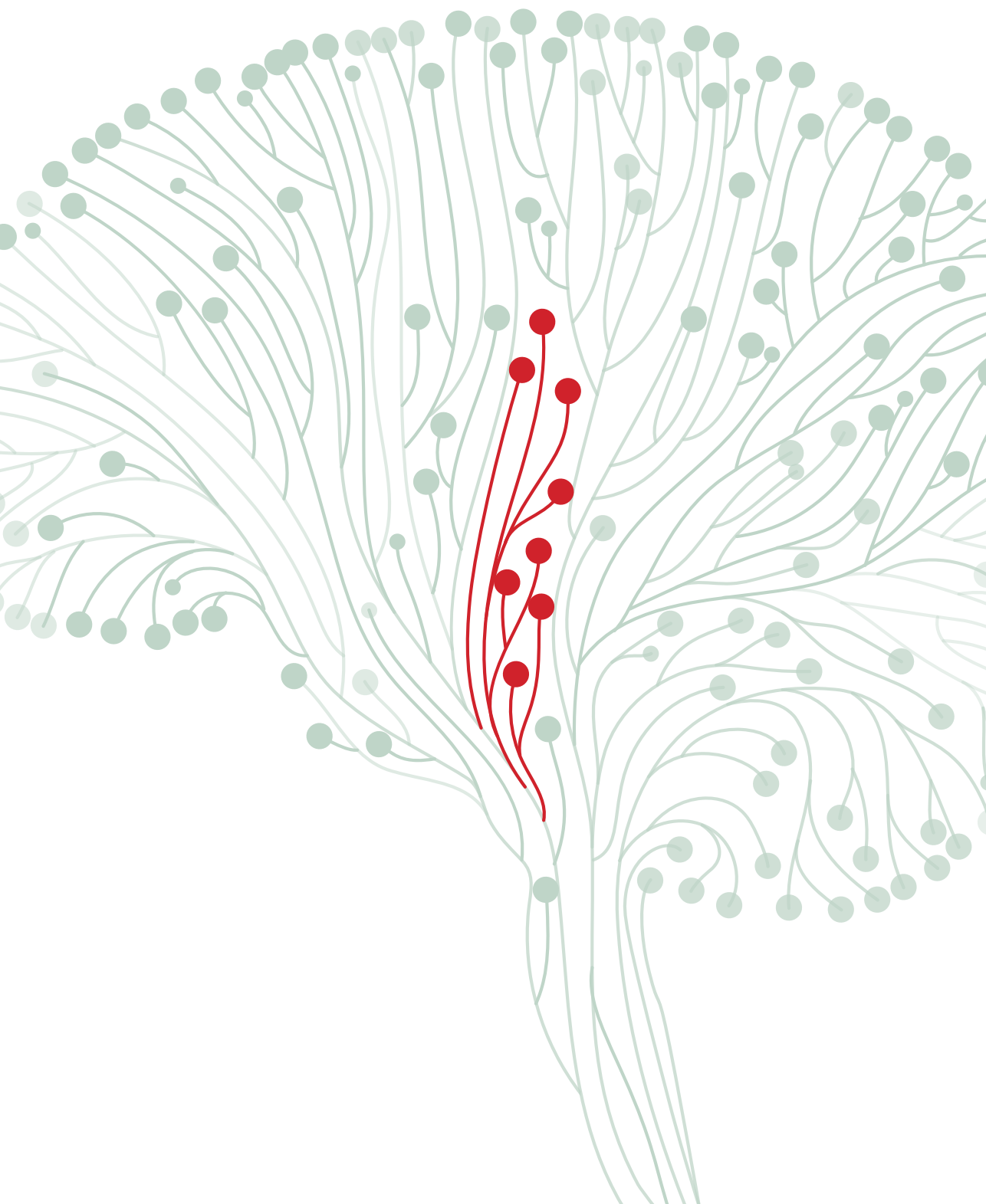
Abbreviations: KPS: Karnofsky performance score; RT: radiotherapy; TMZ: temozolomide. *4 patients received a biopsy first followed by debulking.

Supplementary Table S2 – Baseline table TMA cohort

Patient characteristics <i>n</i> (%)	Epilepsy <i>102 (35.7)</i>	No epilepsy <i>184 (64.3)</i>	Statistics
Age (<i>mean ± SD</i>)	57.8 ± 13.4	61.7 ± 12.0	Mann Whitney U test p=0.02
Gender (% <i>male</i>)	64.7	57.6	Chi-square p=0.24
KPS <i>n</i> (%)			
< 70	21 (20.6)	50 (27.2)	Chi-square p=0.23
≥ 70	80 (78.4)	134 (72.8)	
	<i>Missing: 1 (1)</i>		
Extent of surgery <i>n</i> (%)			
Biopsy	9 (8.8)	4 (2.2)	Fisher exact p=0.015
Debulking	93 (91.2)	180 (97.8)	
Post-surgical treatment <i>n</i> (%)			
None	9 (8.8)	27 (14.7)	Chi-square p=0.067
Monotherapy RT or TMZ	17 (16.7)	44 (23.9)	
RT + TMZ	76 (74.5)	111 (60.3)	
	<i>Missing: 2 (1.1)</i>		

Abbreviations: KPS: Karnofsky performance score; RT: radiotherapy; TMZ: temozolomide

Supplementary Table S3 – available at <http://www.mdpi.com/2072-6694/11/1/41/s1>





CHAPTER 6

Adverse prognosis of glioblastoma contacting the subventricular zone: biological correlates

Sharon Berendsen, Emma van Bodegraven, Tatjana Seute,
Wim G.M. Spliet, Marjolein Geurts, Jeroen Hendrikse,
Laurent Schoysman, Willemijn B. Huiszoon, Meri Varkila,
Soufyan Rouss, Erica H. Bell, Jérôme Kroonen, Arnab Chakravarti,
Vincent Bours, Tom J. Snijders & Pierre A. Robe.

PLoS One. 2019 Oct 11;14(10):e0222717.

ABSTRACT

Introduction: The subventricular zone (SVZ) in the brain is associated with gliomagenesis and resistance to treatment in glioblastoma. In this study, we investigate the prognostic role and biological characteristics of subventricular zone (SVZ) involvement in glioblastoma.

Methods: We analyzed T1-weighted, gadolinium-enhanced MR images of a retrospective cohort of 647 primary glioblastoma patients diagnosed between 2005-2013, and performed a multivariable Cox regression analysis to adjust the prognostic effect of SVZ involvement for clinical patient- and tumor-related factors. Protein expression patterns of a.o. markers of neural stem cellness (CD133 and GFAP- δ) and (epithelial-) mesenchymal transition (NF- κ B, C/EBP- β and STAT3) were determined with immunohistochemistry on tissue microarrays containing 220 of the tumors. Molecular classification and mRNA expression-based gene set enrichment analyses, miRNA expression and SNP copy number analyses were performed on fresh frozen tissue obtained from 76 tumors. Confirmatory analyses were performed on glioblastoma TCGA/TCIA data.

Results: Involvement of the SVZ was a significant adverse prognostic factor in glioblastoma, independent of age, KPS, surgery type and postoperative treatment. Tumor volume and postoperative complications did not explain this prognostic effect. SVZ contact was associated with increased nuclear expression of the (epithelial-) mesenchymal transition markers C/EBP- β and phospho-STAT3. SVZ contact was not associated with molecular subtype, distinct gene expression patterns, or markers of stem cellness. Our main findings were confirmed in a cohort of 229 TCGA/TCIA glioblastomas.

Conclusion: In conclusion, involvement of the SVZ is an independent prognostic factor in glioblastoma, and associates with increased expression of key markers of (epithelial-) mesenchymal transformation, but does not correlate with stem cellness, molecular subtype, or specific (mi)RNA expression patterns.

INTRODUCTION

Glioblastoma is the most malignant primary brain tumor, with a median prognosis of 15-20 months despite intensive treatment [1]. In many patients, glioblastoma cells invade the subventricular zone (SVZ) [2, 3]. This area represents a neurogenic zone in the adult brain and contains neural stem cells [4], which are suggested to play a role in gliomagenesis [4-6]. It is also a protective niche attracting tumor-initiating cells and allowing them to escape treatment [4, 7-11] and could thus favor tumor progression [12-14]. Furthermore, a more invasive and multifocal phenotype of tumors contacting the SVZ on MRI was reported [15].

Based on univariable statistics [14, 16, 17] or small to mid-size patient series [17, 18], the radiological involvement of the SVZ seems to associate with an adverse prognosis. Radiogenomics [19-23] and proteomics [24] studies have proposed potential associations between MRI characteristics and gene/protein expression profiles in glioblastoma. These studies have variably associated SVZ-contacting tumors with differential expression of several genes and gene expression signatures, involving glioma stem cell signaling, hypoxia, tumor vascularity, and invasion [19-26]. Simple radiological features might thus be informative of the tumor's biological characteristics.

In this paper, we aim to validate the prognostic role of glioblastoma involvement of the SVZ in a large, well-characterized cohort of 647 patients. Additionally, we analyze clinical and tumor biological factors that associate with this prognostic effect, to help further understand this relation.

MATERIALS AND METHODS

Ethics statement

This study was conducted following approval by the local ethical committee (METC Utrecht) and institutional review board (Biobank Research Ethics Committee Utrecht, protocols 16-229, 16-342, 16-348). Fresh-frozen samples were obtained following written informed consent. According to Dutch regulations, the need for informed consent was waived for the rest of this retrospective analysis.

Patient cohorts

A flowchart describing the cohorts in this study is included in Fig 1.

All adult patients (n=647) with histologically confirmed de novo supratentorial glioblastoma (WHO grade IV) diagnosed at the University Medical Center of Utrecht

(UMCU) between 2005-2013 were retrospectively included. Details on this cohort are provided in table 1, S1 Appendix and were published before [27]. Age, gender, Karnofsky performance status (KPS), tumor volume, surgery type and postoperative treatment were recorded. Complications within 30 days from surgery were recorded according to the Common Terminology Criteria for Adverse Events (CTCAE). Survival data (days from surgery) were retrieved from hospital records and community archives. IDH1 mutational status was not yet routinely determined in clinical practice at our center, and was available for 343/647 patients from a previous study [27]. SVZ contact was defined as direct contact of the T1-weighted, gadolinium-enhancing part of the tumor with the lateral ventricles, and as detailed in the supplementary methods (S2 Appendix). Tumor volume was measured as the volume of the contrast-enhancing lesion on the presurgical MRI scan with OsiriX software version 4.1.2 (Pixmeo, Bernex, Switzerland).

From these patients, 76 fresh-frozen surgical samples of *de novo* glioblastomas were prospectively collected between 2010 and 2015 for DNA, mRNA and miRNA analyses. SVZ status was unavailable for 5 of these patients.

In addition, we retrospectively collected archival tumor tissues for the consecutive 229 glioblastoma patients treated in the UMCU between 2005 and 2008. Tissue was available for inclusion in tissue microarrays (TMAs) for 220/229 patients. SVZ status was unavailable for 14 of these patients.

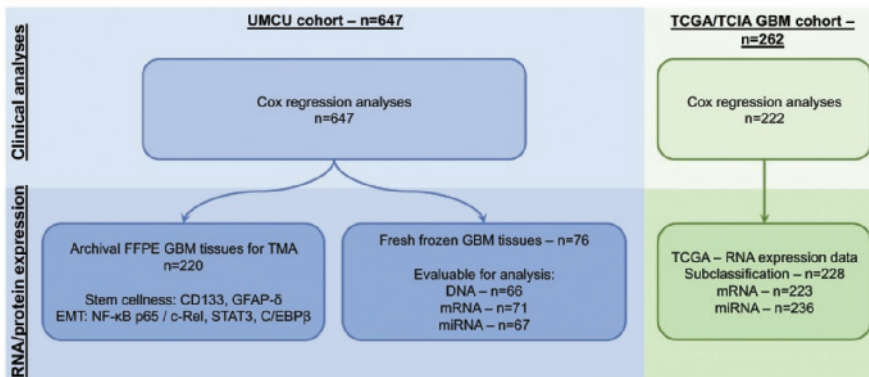


Figure 1 - Overview of study cohorts. Abbreviations: UMCU: University Medical Center Utrecht; FFPE: Formalin fixed paraffin embedded; GBM: glioblastoma; EMT: epithelial-mesenchymal transition; TCGA: The Cancer Genome Atlas; TCIA: The Cancer Imaging Archive.

Table 1 - Baseline table

Patient characteristics	SVZ contact	No SVZ contact	Statistical analysis
<i>n</i> (%)	371 (57.3)	240 (37.1)	
Age (<i>mean</i> \pm <i>SD</i>)	62.0 \pm 12.1	60.6 \pm 12.7	Independent t-test, <i>P</i> = 0.16
Gender (% <i>male</i>)	60.6	60.0	χ^2 test, <i>N.S.</i>
KPS <i>n</i> (%)			
< 70	112 (30.2)	50 (20.8)	χ^2 test, <i>P</i> = 0.01
\geq 70	256 (69.0)	189 (78.8)	
	Missing: 3 (0.8)	Missing: 1 (0.4)	
Tumor volume <i>cm</i> ³ (<i>median</i> (<i>IQR</i>))	46.8 (27.8-73.1) Missing: 6 (1.6)	16.8 (6.9-32.8) Missing: 3 (1.3)	Mann Whitney U test, <i>P</i> < 0.0005
Extent of surgery <i>n</i> (%)			Fisher exact test,
Biopsy	154 (41.5)	55 (22.9)	<i>P</i> < 0.0005
Debulking	217 (58.5)	185 (77.1)	
Post-surgical treatment <i>n</i> (%)			Fisher exact test,
None	97 (26.1)	34 (14.2)	<i>P</i> < 0.0005
Monotherapy	101 (27.2)	52 (21.7)	
RT + TMZ	171 (46.1) Missing: 2 (0.5)	152 (63.3) Missing: 2 (0.8)	
CTCAE complications grade 3-5 <i>n</i> (%)	62 (16.7)	25 (10.4)	χ^2 test, <i>P</i> =0.032
IDH1 mutational status <i>n</i> (%)			χ^2 test, <i>P</i> =0.21
R132H mutation	9 (2.4)	12 (5.0)	
Wild-type	183 (49.3) Missing: 179 (48.2)	139 (57.9) Missing: 89 (37.1)	

Legend: Missing SVZ status: 36 (5.6%). Abbreviations: KPS: Karnofsky performance score; SVZ: subventricular zone; IQR: interquartile range; RT: radiotherapy; TMZ: temozolomide.

mRNA and miRNA expression analysis

Processing of the fresh-frozen surgical samples-derived mRNA and miRNA samples and data was described previously [28]. Analyses are described in more detail in the supplementary methods (S2 Appendix). Microarray data are made publically available on the GEO platform (accession number GSE134783).

After omitting samples with missing MRI data or insufficient RNA quality, 71 RNA samples and 67 miRNA samples were evaluable for analysis. Gene expression analyses

were performed using the Partek suite built-in ANOVA pipeline, with an $FDR < 0.05$ threshold for significance. Exploratory Gene Set Enrichment Analyses (GSEA) were performed with use of the Broad Institute MySig libraries of curated gene sets C1 – C7 version 5.0 [29]. An exploratory false discovery rate (FDR) threshold of 0.25 was applied as recommended [30]. Molecular subclassification (proneural, neural, classical, mesenchymal) was predicted by hierarchical clustering, as described previously [28, 31]. Classes could be unequivocally assigned to 62 samples.

For the miRNA analyses, RNA was isolated with the MiRNeasy Micro Kit (Qiagen, Venlo, The Netherlands). Expression profiling of 800 miRNA probes was performed with the nCounter® Human v2 miRNA Expression Assay (NanoString Technologies, Seattle, USA) at The Ohio State University Nucleic Acid Core Facility.

Copy number analysis

DNA was extracted with sufficient quality from 67 fresh-frozen samples of our proprietary cohort of glioblastomas and processed on SNP6.0 Affymetrix chips according to manufacturer's recommendations. One outlier was removed after principal component analysis, and 66 samples were evaluable for analysis. Further details are described in the supplementary methods (S2 Appendix).

Tissue microarrays and immunohistochemistry

TMAAs were constructed including archival glioblastoma tissue from 220 patients, and were processed as reported previously [27]. Immunohistochemistry was performed, as described previously [27, 28] and in the supplementary methods (S2 Appendix), with antibodies against c-Rel, NF- κ B p65 (phospho-S276), STAT3 (phospho-Y705), anti-C/EBP β , anti-CD133 and anti-GFAP- δ .

Protein expression evaluation was evaluated with blinding to the clinical data, under supervision of a senior neuropathologist (WS). The percentage of nuclear and/or cytoplasmatic staining was scored on triplicate tumor cores as: 0, negative; 1, 1-25% positive cells; 2, 26-50% positive cells; 3, 51-75% positive cells and 4, 76-100% positive cells.

The percentage of positive GFAP- δ staining was calculated per sample. A mean staining score was computed per patient. Scores were analyzed with Mann Whitney U tests.

Analysis of TCGA/TCIA MRI and mRNA / miRNA expression data

Preoperative gadolinium-enhanced T1-weighted MRI scans from the The Cancer Genome Atlas (TCGA) glioblastoma patients were downloaded from The Cancer Imaging Archive (TCIA; September 2015) and assessed for SVZ contact as described above. Researchers

were blinded to the clinical data. A total of 222 patients could be included in the Cox regression analyses. Corresponding TCGA molecular classification and gene expression data were obtained for 228 and 223 patients, as described above and in the supplementary methods (S2 Appendix). Level 3 miRNA expression data from 236 glioblastomas was downloaded from the TCGA data portal (December 2015). MiRNA expression levels in glioblastomas with and without SVZ contact were analyzed with the 'limma' and 'heatmap3' package (R v3.2.2).

Survival analyses

Statistical analyses were performed with use of SPSS 25.0 (IBM, Armonk, USA). All statistical tests were two-sided, and a P value < 0.05 was considered statistically significant.

Kaplan-Meier curves were analyzed with the log-rank test. Cox regression was used for the survival analyses. The proportional hazards assumption of the Cox model was tested (details in supplementary methods (S2 Appendix)) [27]. Multivariable Cox regression was performed including the variables SVZ status, age, KPS, type of surgery, adjuvant treatment and a time-dependent variable for KPS. In a multivariable complete case analysis, 595 patients could be included. As a sensitivity analysis, multiple imputation was performed to include all 647 patients. Next, a Cox regression analysis was performed including the variables tumor volume, type of surgery, postoperative treatment, CTCAE grade 3-5 complications and time-dependent variables for KPS and tumor volume to explore underlying factors that could influence the observed prognostic effect. Missing values were imputed in this analysis.

Survival analyses with TCGA/TCIA data were performed as described above. Multivariable Cox regression was performed including age and KPS variables in the model. Multiple imputation based on these variables was performed for missing data, to include all 222 TCGA/TCIA-glioblastoma patients of which survival and MRI data was available.

RESULTS

SVZ contact is an independent prognostic factor in glioblastoma

SVZ status could not be determined for 36 patients (5.6%) of our cohort, due to unavailable MRI scans. Of the remaining 611 glioblastoma patients, 371 (57.3%) had an SVZ-contacting tumor on the preoperative MRI (Fig 2A-B). SVZ-contacting tumors were significantly associated with worse prognosis (median survival: 241 days from surgery; 95%CI: 203.6 to 278.4) compared to tumors without SVZ contact (median survival: 384 days; 95%CI: 338.9 to 429.1, log-rank test (Fig 2C; $P < 0.0005$), unadjusted HR:1.70; 95%CI:1.40 to 2.05, $P < 0.0005$, table 2). Multivariable complete case Cox regression

(n=595) with correction for age, preoperative KPS, type of surgery and adjuvant treatment showed that SVZ contact remained independently associated with worse overall survival (Adjusted HR: 1.57; 95%CI: 1.29 to 1.91; $P < 0.0005$; Table 2). Multiple imputation allowed for inclusion of all patients (n=647) in this multivariable analysis and did not alter the results (Adjusted HR: 1.50; 95%CI: 1.24 to 1.82; $P < 0.0005$). IDH1 mutational status was only available for a subset of the total cohort (n=343 of 647 patients) and did not correlate with SVZ contact (Chi-square test, $p = 0.21$, table 1). SVZ contact was also a negative prognostic factor in the TCGA/TCIA dataset both in univariable analyses (log-rank $P < 0.05$; Unadjusted HR: 1.43; 95%CI: 1.06 to 1.91; $P < 0.05$) and after correction for age and KPS (Adjusted HR: 1.37; 95%CI: 1.02 to 1.84; $P < 0.05$).

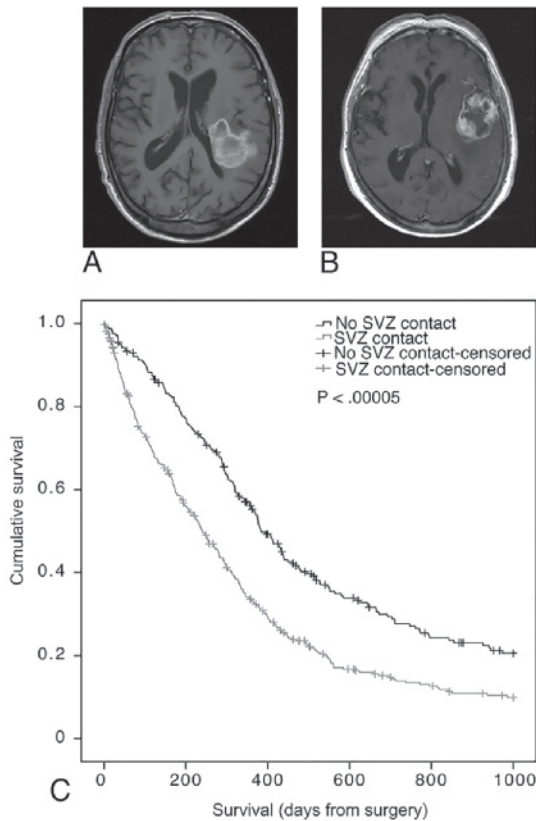


Figure 2 – SVZ involvement associates with glioblastoma patient survival. (A) Pre-operative T1-weighted MRI scan with gadolinium of patient (M, 1928) with glioblastoma contacting the SVZ. (B) Pre-operative T1-weighted MRI scan with gadolinium of patient (F, 1925) with glioblastoma not contacting the SVZ. (C) Association of tumor contact with the SVZ on glioblastoma patient survival. Kaplan-Meier plot of glioblastoma patients with a tumor contacting the SVZ (grey) and patients with a tumor that does not contact the SVZ (black). Patients with survival over 1000 days from surgery were censored. Survival was significantly different between the two groups (log-rank test, $P < 0.00005$).

Table 2 – Cox regression analysis – Prognostic model

Variable	Crude HR (95% CI)	P-value	Adjusted HR (95% CI)	P-value
SVZ contact	1.70 (1.40-2.05)	< 0.0005	1.57 (1.29-1.91)	< 0.0005
Gender (male)	1.05 (0.88-1.26)	0.57	-	-
Age	1.03 (1.03-1.04)	< 0.0005	1.01 (1.01-1.02)	0.002
KPS < 70	1.00		1.00	
KPS ≥ 70	0.44 (0.36-0.53)	< 0.0005	0.53 (0.37-0.74)	< 0.0005
KPS * time			1.002 (1.001-1.003)	0.003
Biopsy	1.00		1.00	
Resection	0.39 (0.33-0.47)	<0.0005	0.65 (0.53-0.80)	<0.0005
Adjuvant treatment				
None	1.00		1.00	
RT only	0.15 (0.11-0.19)	<0.0005	0.20 (0.15-0.26)	<0.0005
RT + TMZ	0.05 (0.04-0.06)	<0.0005	0.08 (0.06-0.11)	<0.0005

Abbreviations: HR: hazard ratio; KPS: Karnofsky performance score; SVZ: subventricular zone; RT: radiotherapy; TMZ: temozolomide.

Patient- and tumor-related clinical factors do not explain the prognostic effect of SVZ contact in glioblastoma

SVZ-contacting tumors exhibited larger tumor volumes compared to tumors without SVZ contact (Mann-Whitney U test, $P < 0.0005$, Table 1). Patients with a glioblastoma contacting the SVZ had a lower preoperative KPS (χ^2 -test; $P = 0.01$), underwent more biopsy procedures ($P < 0.0005$) and were less often treated with adjuvant chemoradiation ($P < 0.0005$). In addition, 16.7% of patients with an SVZ-contacting tumor experienced at least one CTCAE grade 3-5 complication in the 30-day postoperative period, compared to 10.5% of patients with a tumor without SVZ contact (χ^2 -test; $P < 0.05$, Table 1). No statistically significant difference in the prevalence of postoperative cerebral hemorrhage/ischemia, epilepsy, infection/meningitis, hydrocephalus or thrombosis. Patients with an SVZ-contacting tumor did more often experience metabolic complications, such as hyponatremia ($P = 0.005$), and hyperglycemia ($P < 0.05$).

After inclusion of these factors in the multivariable Cox model, SVZ contact remained a significant prognostic factor in glioblastoma patients (adjusted HR: 1.42; 95%CI: 1.13 to 1.77, $P < 0.01$, Table 3).

Table 3 – Cox regression analyses – Explanatory multivariable analysis

Variable	Crude HR (95% CI)	P-value	Adjusted HR (95% CI)	P-value
SVZ contact	1.70 (1.40-2.05)	< 0.0005	1.42 (1.13-1.77)	0.003
Age	1.03 (1.03-1.04)	< 0.0005	1.02 (1.01-1.02)	< 0.0005
KPS < 70	1.00		1.00	
KPS \geq 70	0.44 (0.36-0.53)	< 0.0005	0.56 (0.40-0.78)	0.001
KPS * time			1.002 (1.001-1.003)	0.002
Biopsy	1.00		1.00	
Resection	0.39 (0.33-0.47)	< 0.0005	0.58 (0.47-0.72)	< 0.0005
Adjuvant treatment				
None	1.00		1.00	
RT only	0.15 (0.11-0.19)	< 0.0005	0.18 (0.14-0.25)	< 0.0005
RT + TMZ	0.05 (0.04-0.06)	< 0.0005	0.08 (0.06-0.12)	< 0.0005
Tumor volume	1.002 (0.999-1.005)	0.13	1.009 (1.005-1.014)	< 0.0005
Tumor volume * time			1.000 (1.000-1.000)	< 0.0005
Complications grade CTCAE 3-5	0.55 (0.44-0.70)	< 0.0005	1.21 (0.94-1.55)	0.14

Abbreviations: HR: hazard ratio; KPS: Karnofsky performance score; SVZ: subventricular zone; RT: radiotherapy; TMZ: temozolomide.

SVZ contact, gene, and miRNA expression pattern

We analyzed the mRNA expression in 71 UMCU glioblastoma samples (39 (54.9%) with SVZ contact and 32 (45.1%) without SVZ contact) and 223 TCGA/TCIA samples (128 (57%) with SVZ contact and 96 (43%) without SVZ contact). The molecular subtype distribution of the glioblastomas [31] was not different between the groups in both the UMCU (Fisher's exact test, $P=1.0$) and TCGA/TCIA datasets (χ^2 -test, $P=0.11$, S1 Fig). After correction for multiple testing ($FDR<0.05$), no differentially expressed single gene was detected between the groups in both datasets (S2 and S3 Figs). Likewise, no miRNA was differentially expressed between the two groups in both UMCU and TCGA/TCIA cohorts (S4 and S5 Figs).

Exploratory GSEA with the C1 positional gene sets showed an enrichment of the chr9q34 gene set in tumors without SVZ contact ($P<0.001$, $FDR=0.038$) in the UMCU dataset and downregulation of gene sets corresponding to cytogenetic bands chr3q22–23, chr3p24–25, chr3q26–29 and chr19p12 ($P<0.01$; $FDR<0.25$) in tumors without SVZ contact in the TCGA/TCIA data (S1 Table). The DNA analysis of our samples did however not reveal any significant difference in copy number in any area of the genome between both groups ($FDR>0.5$ for all cytobands).

Tumors without SVZ contact also presented an increased activation of genes with promoter regions containing the motifs GTCNYYATGR (unknown target, $P < 0.001$, FDR=0.24) and GCGNNANTTCC ($P = 0.002$, FDR=0.23), which is an NF- κ B C-rel regulatory motif [32] in the UMCU cohort. Differential activation of genes containing these regulatory motifs was not confirmed in TCGA/TCIA tumors, which only showed an enrichment of genes upregulated by Bmi-1 knockdown in tumors without SVZ contact ($P = 0.004$, FDR=0.19). Bmi-1 is known to induce NF- κ B signaling in glioma cells [33].

Differential activation of proteins involved in (epithelial-) mesenchymal transformation in glioblastomas contacting the SVZ

Since neural stem cells are a core component of the SVZ, it can be hypothesized that their presence might explain the adverse prognostic effect of SVZ contact in glioblastomas. Also, activation of mesenchymal genes is associated with poor prognosis in glioblastoma patients [34]. This may not always be fully recapitulated by gene expression data. Therefore, we analyzed the protein expression patterns of neural stem cell markers CD133 [35] and GFAP- δ [36], and the activation of key markers of (epithelial-) mesenchymal transformation C/EBP- β , NF- κ B (P^{S536}-p65 and c-Rel) and STAT3 [34] (Fig 3) on FFPE tumor tissue obtained from a cohort of consecutive glioblastoma patients. Baseline characteristics of this cohort were comparable to the overall dataset. No differences in CD133 (n=141 evaluable tumors) or GFAP- δ (n=147) expression were observed between tumors with or without SVZ contact. In contrast, we observed increased nuclear expression levels of C/EBP- β (n=191, Mann Whitney U test, $P = 0.029$) and P^{Y705}-STAT3 (n=192, Mann Whitney U test, $P = 0.002$), but not of NF- κ B subunits P^{S536}-p65, or c-Rel in SVZ-contacting tumors.

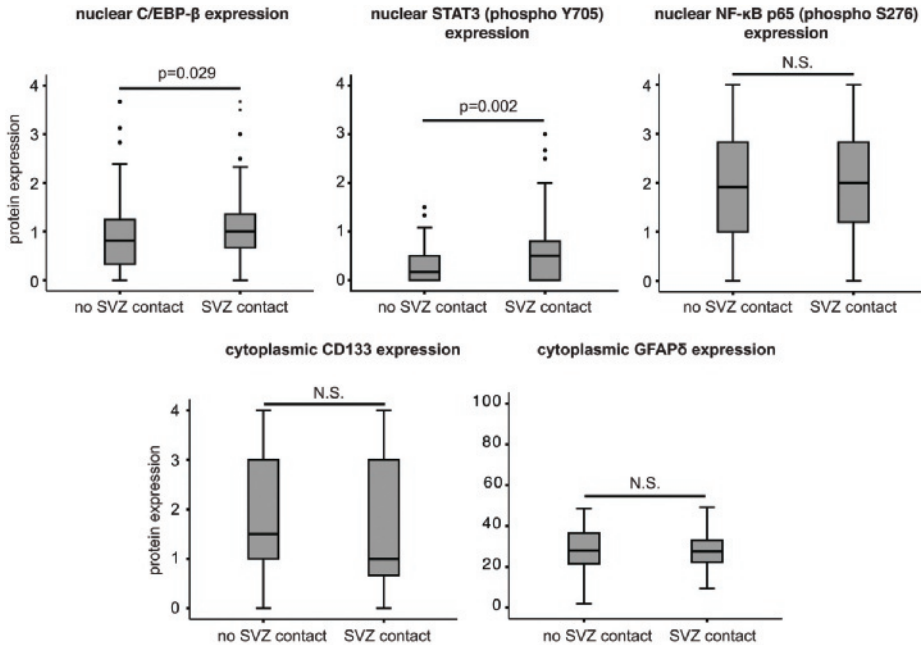


Figure 3 – SVZ involvement in glioblastoma correlates with increased protein expression of key markers of (epithelial-) mesenchymal transformation. Increased protein expression levels of (epithelial-)mesenchymal transformation markers C/EBP- β (Mann Whitney U test, $P = 0.029$) and P^{Y705}-STAT3 (Mann Whitney U test, $P = 0.002$), but not P^{S536}-p65, were observed in glioblastomas contacting the SVZ. No expression differences in stem cell markers CD133 or GFAP- δ were observed between tumors with or without SVZ contact.

DISCUSSION

In a large institutional cohort ($n=647$) and a cohort from the TCIA/TCGA repository ($n=222$), we show that contact between the gadolinium-enhancing, T1-weighted imaging core component of glioblastomas and the SVZ of the brain is an adverse prognostic factor, independent of other known prognostic factors age, preoperative KPS, surgery type and postoperative treatment [37]. These results considerably strengthen the associations found by others, who had explored this hypothesis with univariable survival models [14, 16, 17, 38-40] or smaller to mid-size cohorts [17, 18, 41-46], and may help define the prognosis of individual patients based on their preoperative MR imaging. A meta-analysis of these published series also showed a significant adverse prognostic effect of SVZ contact in glioblastoma patients [47], but these analyses were not corrected for the effects of other (clinical) factors, due to unavailable individual patient data. Our findings in multivariable analyses in two large cohorts, extend and validate these previous results [18, 43, 47], and point towards a true independent prognostic effect. Most importantly, we observed that this

prognostic effect was independent from tumor volume and postoperative complications. In a recent study of 35 glioblastoma patients it was shown that O-(2-[18F]fluoroethyl)-L-tyrosine (FET) PET scans can show SVZ infiltration of glioblastomas that is not visible on MRI scans, which is correlated to larger tumor volumes [48]. Further exploration of the correlations between SVZ contact on MRI, FET PET scans, tumor volume and prognosis of glioblastoma patients may further elucidate the biomechanical backgrounds of SVZ contact in glioblastoma.

Deep-seated tumors present an increased surgical risk [49], and are more likely to be biopsied rather than resected as compared to superficial glioblastomas. In our cohort, periventricular tumors were indeed more often biopsied than superficial ones. Tumor resection is known to improve survival in glioblastomas, as compared to biopsies [50, 51]. Aside from their potential lethal consequences, complications could also delay or prevent optimal post-operative adjuvant cytotoxic treatment. In our cohort as well, patients with an SVZ contacting tumor experienced more serious (CTCAE grade 3-5) complications. At our center, the main criterion for glioblastoma patients to come in consideration for adjuvant combined therapy is having a KPS score > 70. Our patients with a preoperative $KPS \geq 70$ and an SVZ-contacting tumor were however ultimately significantly less often allocated to chemoradiation (as opposed to less optimal monotherapies) after surgery than patients with a glioblastoma without SVZ contact (χ^2 -test, $P < 0.0001$), as a result of a decrease of KPS.

Given that SVZ-contact remained an independent prognostic factor in our multivariable survival analyses taking the type of surgery, post-operative complications and adjuvant treatment into account, other factors must contribute to the survival disadvantage of ventricular contact.

It has been suggested that SVZ-contacting glioblastomas present different biological characteristics than tumors without SVZ contact. Based on mRNA arrays, differential expression level of VEGF, HGF, CHI3L1, RAP2A, HES4, DLL3, PIR and HJURP, of several oncological transcriptomic (Notch, stem cell, hypoxia, angiogenesis and invasion) and inflammatory signatures have for instance variably been reported [16, 22, 25, 26]. An increased expression of mesenchymal markers (VEGF, HGF) was also observed by targeted q-RT PCR in SVZ-contacting tumors and differential expression of NOTCH1, CD133 and CHI3L1 was found between distinct periventricular regions [25]. A proteomic analysis of SVZ contacting tumors has also suggested a differential expression of vimentin, RBP1 and Lupus La, as well as an association with carbohydrate metabolism, blood coagulation, protease inhibitors and ECM pathways [24]. Our gene and miRNA expression analyses performed on proprietary samples and TCGA tumors, i.e. the largest cohorts analyzed to this end so far, could not replicate any of these results. In fact, even the findings of

miRNA (n=67) and gene expression (n=71) analyses on our proprietary samples could not be reproduced in the larger TCGA/TCIA cohorts. This underscores the exploratory value of gene expression analyses and GSEA when performed on small or intermediate-size cohorts and the importance to validate them with other techniques or on larger samples prior to drawing any conclusions.

Steed et al. also observed that proneural and neural tumors from the TCIA grew frequently closer (as measured by the distance to those structures) to the SVZ than mesenchymal and classical ones [52]. Using the same dataset however and our clinician-friendly definition of SVZ contact based on the enhancing tumor core rather than a complex image analysis algorithm, we did not find any association between molecular subtype and SVZ contact in this same TCGA/TCIA and our cohorts. Our results are in line with a recent report of similar analyses to explore this hypothesis with the TCGA/TCIA dataset [46].

A limitation of gene expression analyses is the dependence on the presence of sufficient tumor material, favoring the recruitment of samples from debulking surgeries rather than from needle biopsies. Both our proprietary fresh-frozen samples and the TCGA samples indeed consist of surgical debulking tumor samples, without any needle biopsy samples. Biopsies were however significantly overrepresented in SVZ-contacting glioblastomas (41.5% versus 22.9%, Table 1, $P < 0.0005$) in our consecutive patient cohort, and expression analyses may thus underrepresent the most aggressive/inoperable tumors. To minimize this bias, we also analyzed protein expression/activation patterns on TMAs that included the tumor tissues obtained from both biopsies and open surgeries of a subset of 220 consecutive patients. These analyses did not provide evidence for any association between SVZ contact and the expression of neural stem cell markers (CD133[35] and GFAP- δ [36]). This finding is congruent with a previous report [16], but contradicts another one based on microarray data [26].

Our gene set enrichment analyses suggested that SVZ contact could associate with increased NF- κ B activity in glioma. This was however not confirmed at a protein level, as nuclear phospho-p65 and c-Rel protein expression did not differ between groups. In contrast, our proteomic analyses showed higher activation of C/EBP- β and STAT3 signaling in tumors contacting the SVZ. These transcription factors are hallmarks of (epithelial-)mesenchymal transformation in glioma, which is associated with poor prognosis in glioblastoma [34, 53, 54], and might prevail in SVZ-contacting glioblastomas compared to tumors without SVZ contact. Further research is needed to establish whether these observations represent intrinsic biological properties of tumors contacting the SVZ or are regional effects mediated by the SVZ microenvironment.

Due to the retrospective nature of our study, some established prognostic factors such as MGMT methylation status, Mini Mental State Exam (MMSE) score and use of corticosteroids [36] could not be included in our Cox model, as these data were too often unavailable. In addition, the patients in our study were diagnosed based on the WHO 2007 Classification of Tumours of the Central Nervous System [55] and IDH1 mutational status was only available for a subset of the patients, as it was not yet evaluated in routine clinical care. However, in a subset analysis, an IDH1 mutation was found in only 21 (6.1%) of 343 glioblastoma patients, and did not correlate to tumor contact with the SVZ. Based on these observations and the other baseline characteristics, we expect that the study cohort and study results are representative for patients with glioblastoma, IDH1 wildtype, according to the new classification system [56].

Despite these shortcomings, our cumulative results show that contact with the SVZ correlates with increased expression of markers of epithelial-mesenchymal transformation of glioblastomas, and is a significant adverse prognostic factor in these tumors, independent of age, performance status, tumor volume, type of surgery, postoperative complications and adjuvant treatment. We found no correlations between SVZ contact and molecular subtype, distinct gene expression patterns, or markers of stem cellness.

REFERENCES

1. Stupp R, Taillibert S, Kanner AA, Kesari S, Steinberg DM, Toms SA, et al. Maintenance Therapy With Tumor-Treating Fields Plus Temozolomide vs Temozolomide Alone for Glioblastoma: A Randomized Clinical Trial. *JAMA*. 2015;314(23):2535-43. doi: 10.1001/jama.2015.16669.
2. Ellingson BM, Cloughesy TF, Pope WB, Zaw TM, Phillips H, Lalezari S, et al. Anatomic localization of O6-methylguanine DNA methyltransferase (MGMT) promoter methylated and unmethylated tumors: a radiographic study in 358 de novo human glioblastomas. *NeuroImage*. 2012;59(2):908-16. doi: 10.1016/j.neuroimage.2011.09.076.
3. Smith TR, Hulou MM, Abecassis J, Das S, Chandler JP. Use of preoperative FLAIR MRI and ependymal proximity of tumor enhancement as surrogate markers of brain tumor origin. *Journal of Clinical Neuroscience : Official Journal of the Neurosurgical Society of Australasia*. 2015;22(9):1397-402. doi: 10.1016/j.jocn.2015.02.029.
4. Sanai N, Alvarez-Buylla A, Berger MS. Neural stem cells and the origin of gliomas. *The New England Journal of Medicine*. 2005;353(8):811-22. doi: 353/8/811.
5. Wang Y, Yang J, Zheng H, Tomasek GJ, Zhang P, McKeever PE, et al. Expression of mutant p53 proteins implicates a lineage relationship between neural stem cells and malignant astrocytic glioma in a murine model. *Cancer Cell*. 2009;15(6):514-26. doi: 10.1016/j.ccr.2009.04.001.
6. Lee JH, Lee JE, Kahng JY, Kim SH, Park JS, Yoon SJ, et al. Human glioblastoma arises from subventricular zone cells with low-level driver mutations. *Nature*. 2018;560(7717):243-7. Epub 2018/08/03. doi: 10.1038/s41586-018-0389-3. PubMed PMID: 30069053.
7. Kroonen J, Nassen J, Boulanger YG, Provenzano F, Capraro V, Bours V, et al. Human glioblastoma-initiating cells invade specifically the subventricular zones and olfactory bulbs of mice after striatal injection. *International Journal of Cancer*. 2011;129(3):574-85. doi: 10.1002/ijc.25709.
8. Bao S, Wu Q, Sathornsumetee S, Hao Y, Li Z, Hjelmeland AB, et al. Stem cell-like glioma cells promote tumor angiogenesis through vascular endothelial growth factor. *Cancer Research*. 2006;66(16):7843-8. doi: 66/16/7843.
9. Lee P, Eppinga W, Lagerwaard F, Cloughesy T, Slotman B, Nghiemphu PL, et al. Evaluation of high ipsilateral subventricular zone radiation therapy dose in glioblastoma: a pooled analysis. *Int J Radiat Oncol Biol Phys*. 2013;86(4):609-15. Epub 2013/03/07. doi: 10.1016/j.ijrobp.2013.01.009. PubMed PMID: 23462418.
10. Goffart N, Kroonen J, Di Valentin E, Dedobbeleer M, Denne A, Martinive P, et al. Adult mouse subventricular zones stimulate glioblastoma stem cells specific invasion through CXCL12/CXCR4 signaling. *Neuro-Oncology*. 2015;17(1):81-94. doi: 10.1093/neuonc/nou144.
11. Goffart N, Lombard A, Lallemand F, Kroonen J, Nassen J, Di Valentin E, et al. CXCL12 mediates glioblastoma resistance to radiotherapy in the subventricular zone. *Neuro-Oncology*. 2017;19(1):66-77. Epub 2016/07/03. doi: 10.1093/neuonc/now136. PubMed PMID: 27370398; PubMed Central PMCID: PMC5193023.
12. Chen L, Chaichana KL, Kleinberg L, Ye X, Quinones-Hinojosa A, Redmond K. Glioblastoma recurrence patterns near neural stem cell regions. *Radiotherapy and Oncology : Journal of the European Society for Therapeutic Radiology and Oncology*. 2015;116(2):294-300. doi: 10.1016/j.radonc.2015.07.032.

13. Chen J, Li Y, Yu TS, McKay RM, Burns DK, Kernie SG, et al. A restricted cell population propagates glioblastoma growth after chemotherapy. *Nature*. 2012;488(7412):522-6. doi: 10.1038/nature11287.
14. Adeberg S, Konig L, Bostel T, Harrabi S, Welzel T, Debus J, et al. Glioblastoma recurrence patterns after radiation therapy with regard to the subventricular zone. *Int J Radiat Oncol Biol Phys*. 2014;90(4):886-93. Epub 2014/09/16. doi: 10.1016/j.ijrobp.2014.07.027. PubMed PMID: 25220720.
15. Lim DA, Cha S, Mayo MC, Chen MH, Keles E, VandenBerg S, et al. Relationship of glioblastoma multiforme to neural stem cell regions predicts invasive and multifocal tumor phenotype. *Neuro-Oncology*. 2007;9(4):424-9. doi: 15228517-2007-023.
16. Kappadakunnel M, Eskin A, Dong J, Nelson SF, Mischel PS, Liao LM, et al. Stem cell associated gene expression in glioblastoma multiforme: relationship to survival and the subventricular zone. *Journal of Neuro-Oncology*. 2010;96(3):359-67. Epub 2009/08/06. doi: 10.1007/s11060-009-9983-4. PubMed PMID: 19655089; PubMed Central PMCID: PMC2808508.
17. Chaichana KL, McGirt MJ, Frazier J, Attenello F, Guerrero-Cazares H, Quinones-Hinojosa A. Relationship of glioblastoma multiforme to the lateral ventricles predicts survival following tumor resection. *Journal of Neuro-Oncology*. 2008;89(2):219-24. Epub 2008/05/07. doi: 10.1007/s11060-008-9609-2. PubMed PMID: 18458819.
18. Jungk C, Warta R, Mock A, Friauf S, Hug B, Capper D, et al. Location-Dependent Patient Outcome and Recurrence Patterns in IDH1-Wildtype Glioblastoma. *Cancers*. 2019;11(1). Epub 2019/01/24. doi: 10.3390/cancers11010122. PubMed PMID: 30669568; PubMed Central PMCID: PMC6356480.
19. Gevaert O, Mitchell LA, Achrol AS, Xu J, Echegaray S, Steinberg GK, et al. Glioblastoma multiforme: exploratory radiogenomic analysis by using quantitative image features. *Radiology*. 2014;273(1):168-74. doi: 10.1148/radiol.14131731.
20. Diehn M, Nardini C, Wang DS, McGovern S, Jayaraman M, Liang Y, et al. Identification of noninvasive imaging surrogates for brain tumor gene-expression modules. *Proceedings of the National Academy of Sciences of the United States of America*. 2008;105(13):5213-8. doi: 10.1073/pnas.0801279105.
21. Gutman DA, Cooper LA, Hwang SN, Holder CA, Gao J, Aurora TD, et al. MR imaging predictors of molecular profile and survival: multi-institutional study of the TCGA glioblastoma data set. *Radiology*. 2013;267(2):560-9. doi: 10.1148/radiol.13120118.
22. Jungk C, Mock A, Exner J, Geisenberger C, Warta R, Capper D, et al. Spatial transcriptome analysis reveals Notch pathway-associated prognostic markers in IDH1 wild-type glioblastoma involving the subventricular zone. *BMC Med*. 2016;14(1):170. Epub 2016/10/27. doi: 10.1186/s12916-016-0710-7. PubMed PMID: 27782828; PubMed Central PMCID: PMC5080721.
23. Itakura H, Achrol AS, Mitchell LA, Loya JJ, Liu T, Westbroek EM, et al. Magnetic resonance image features identify glioblastoma phenotypic subtypes with distinct molecular pathway activities. *Science Translational Medicine*. 2015;7(303):303ra138. doi: 10.1126/scitranslmed.aaa7582.
24. Gollapalli K, Ghantasala S, Kumar S, Srivastava R, Rapole S, Moiyadi A, et al. Subventricular zone involvement in Glioblastoma - A proteomic evaluation and clinicoradiological correlation. *Sci Rep*. 2017;7(1):1449. Epub 2017/05/05. doi: 10.1038/s41598-017-01202-8. PubMed PMID: 28469129; PubMed Central PMCID: PMC5431125.

25. Denicoli E, Tabouret E, Colin C, Metellus P, Nanni I, Boucard C, et al. Molecular heterogeneity of glioblastomas; does location matter? *Oncotarget*. 2015. doi: 10.18632/oncotarget.6433.
26. Jamshidi N, Diehn M, Bredel M, Kuo MD. Illuminating radiogenomic characteristics of glioblastoma multiforme through integration of MR imaging, messenger RNA expression, and DNA copy number variation. *Radiology*. 2014;270(1):1-2. doi: 10.1148/radiol.13130078.
27. Berendsen S, Varkila M, Kroonen J, Seute T, Snijders TJ, Kauw F, et al. Prognostic relevance of epilepsy at presentation in glioblastoma patients. *Neuro-Oncology*. 2016;18(5):700-6. Epub 2015/10/01. doi: 10.1093/neuonc/nov238. PubMed PMID: 26420896; PubMed Central PMCID: PMC4827038.
28. Berendsen S, Spliet WGM, Geurts M, Van Hecke W, Seute T, Snijders TJ, et al. Epilepsy Associates with Decreased HIF-1 α /STAT5b Signaling in Glioblastoma. *Cancers*. 2019;11(1). Epub 2019/01/10. doi: 10.3390/cancers11010041. PubMed PMID: 30621209.
29. Reich M, Liefeld T, Gould J, Lerner J, Tamayo P, Mesirov JP. GenePattern 2.0. *Nature Genetics*. 2006;38(5):500-1. doi: ng0506-500.
30. Subramanian A, Tamayo P, Mootha VK, Mukherjee S, Ebert BL, Gillette MA, et al. Gene set enrichment analysis: a knowledge-based approach for interpreting genome-wide expression profiles. *Proceedings of the National Academy of Sciences of the United States of America*. 2005;102(43):15545-50. doi: 0506580102.
31. Verhaak RG, Hoadley KA, Purdom E, Wang V, Qi Y, Wilkerson MD, et al. Integrated genomic analysis identifies clinically relevant subtypes of glioblastoma characterized by abnormalities in PDGFRA, IDH1, EGFR, and NF1. *Cancer Cell*. 2010;17(1):98-110. doi: 10.1016/j.ccr.2009.12.020.
32. Xie X, Lu J, Kulbokas EJ, Golub TR, Mootha V, Lindblad-Toh K, et al. Systematic discovery of regulatory motifs in human promoters and 3' UTRs by comparison of several mammals. *Nature*. 2005;434(7031):338-45. doi: nature03441.
33. Jiang L, Song L, Wu J, Yang Y, Zhu X, Hu B, et al. Bmi-1 promotes glioma angiogenesis by activating NF-kappaB signaling. *PLoS One*. 2013;8(1):e55527. Epub 2013/02/06. doi: 10.1371/journal.pone.0055527. PubMed PMID: 23383216; PubMed Central PMCID: PMC3561301.
34. Bhat KP, Balasubramanian V, Vaillant B, Ezhilarasan R, Hummelink K, Hollingsworth F, et al. Mesenchymal differentiation mediated by NF-kappaB promotes radiation resistance in glioblastoma. *Cancer Cell*. 2013;24(3):331-46. doi: 10.1016/j.ccr.2013.08.001.
35. Singh SK, Hawkins C, Clarke ID, Squire JA, Bayani J, Hide T, et al. Identification of human brain tumour initiating cells. *Nature*. 2004;432(7015):396-401. doi: nature03128.
36. Roelofs RF, Fischer DF, Houtman SH, Sluijs JA, Van Haren W, Van Leeuwen FW, et al. Adult human subventricular, subgranular, and subpial zones contain astrocytes with a specialized intermediate filament cytoskeleton. *Glia*. 2005;52(4):289-300. doi: 10.1002/glia.20243 [doi].
37. Gorlia T, van den Bent MJ, Hegi ME, Mirimanoff RO, Weller M, Cairncross JG, et al. Nomograms for predicting survival of patients with newly diagnosed glioblastoma: prognostic factor analysis of EORTC and NCIC trial 26981-22981/CE.3. *The Lancet Oncology*. 2008;9(1):29-38. Epub 2007/12/18. doi: 10.1016/s1470-2045(07)70384-4. PubMed PMID: 18082451.
38. Adeberg S, Bostel T, König L, Welzel T, Debus J, Combs SE. A comparison of long-term survivors and short-term survivors with glioblastoma, subventricular zone involvement: a predictive factor for survival? *Radiation Oncology (London, England)*. 2014;9:95-717X-9-95. doi: 10.1186/1748-717X-9-95.

39. Matsuda M, Kohzuki H, Ishikawa E, Yamamoto T, Akutsu H, Takano S, et al. Prognostic analysis of patients who underwent gross total resection of newly diagnosed glioblastoma. *J Clin Neurosci*. 2018;50:172-6. Epub 2018/02/06. doi: 10.1016/j.jocn.2018.01.009. PubMed PMID: 29396060.
40. Nakagawa Y, Sasaki H, Ohara K, Ezaki T, Toda M, Ohira T, et al. Clinical and Molecular Prognostic Factors for Long-Term Survival of Patients with Glioblastomas in Single-Institutional Consecutive Cohort. *World Neurosurg*. 2017;106:165-73. Epub 2017/07/02. doi: 10.1016/j.wneu.2017.06.126. PubMed PMID: 28666913.
41. Jafri NF, Clarke JL, Weinberg V, Barani IJ, Cha S. Relationship of glioblastoma multiforme to the subventricular zone is associated with survival. *Neuro-Oncology*. 2013;15(1):91-6. Epub 2012/10/26. doi: 10.1093/neuonc/nos268. PubMed PMID: 23095230; PubMed Central PMCID: PMC3534420.
42. Young GS, Macklin EA, Setayesh K, Lawson JD, Wen PY, Norden AD, et al. Longitudinal MRI evidence for decreased survival among periventricular glioblastoma. *Journal of Neuro-Oncology*. 2011;104(1):261-9. doi: 10.1007/s11060-010-0477-1.
43. Mistry AM, Dewan MC, White-Dzuro GA, Brinson PR, Weaver KD, Thompson RC, et al. Decreased survival in glioblastomas is specific to contact with the ventricular-subventricular zone, not subgranular zone or corpus callosum. *Journal of Neuro-Oncology*. 2017;132(2):341-9. Epub 2017/01/12. doi: 10.1007/s11060-017-2374-3. PubMed PMID: 28074322; PubMed Central PMCID: PMC5771712.
44. Weinberg BD, Boreta L, Braunstein S, Cha S. Location of subventricular zone recurrence and its radiation dose predicts survival in patients with glioblastoma. *Journal of Neuro-Oncology*. 2018;138(3):549-56. Epub 2018/03/17. doi: 10.1007/s11060-018-2822-8. PubMed PMID: 29546530.
45. Woo P, Ho J, Lam S, Ma E, Chan D, Wong WK, et al. A Comparative Analysis of the Usefulness of Survival Prediction Models for Patients with Glioblastoma in the Temozolomide Era: The Importance of Methylguanine Methyltransferase Promoter Methylation, Extent of Resection, and Subventricular Zone Location. *World Neurosurg*. 2018;115:e375-e85. Epub 2018/04/22. doi: 10.1016/j.wneu.2018.04.059. PubMed PMID: 29678708.
46. Mistry AM, Wooten DJ, Davis LT, Mobley BC, Quaranta V, Ihrle RA. Ventricular-Subventricular Zone Contact by Glioblastoma is Not Associated with Molecular Signatures in Bulk Tumor Data. *Sci Rep*. 2019;9(1):1842. Epub 2019/02/14. doi: 10.1038/s41598-018-37734-w. PubMed PMID: 30755636; PubMed Central PMCID: PMC6372607.
47. Mistry AM. Clinical correlates of subventricular zone-contacting glioblastomas: a meta-analysis. *Journal of Neurosurgical Sciences*. 2017. doi: 10.23736/S0390-5616.17.04274-6.
48. Harat M, Malkowski B, Roszkowski K. Prognostic value of subventricular zone involvement in relation to tumor volumes defined by fused MRI and O-(2-[(18)F]fluoroethyl)-L-tyrosine (FET) PET imaging in glioblastoma multiforme. *Radiation Oncology (London, England)*. 2019;14(1):37. Epub 2019/03/06. doi: 10.1186/s13014-019-1241-0. PubMed PMID: 30832691; PubMed Central PMCID: PMC6398237.
49. Kongkham PN, Knifed E, Tamber MS, Bernstein M. Complications in 622 cases of frame-based stereotactic biopsy, a decreasing procedure. *The Canadian Journal of Neurological Sciences*. 2008;35(1):79-84.
50. Sanai N, Polley MY, McDermott MW, Parsa AT, Berger MS. An extent of resection threshold for newly diagnosed glioblastomas. *Journal of Neurosurgery*. 2011;115(1):3-8. doi: 10.3171/2011.2.JNS10998.

51. Brown TJ, Brennan MC, Li M, Church EW, Brandmeir NJ, Rakszawski KL, et al. Association of the Extent of Resection With Survival in Glioblastoma: A Systematic Review and Meta-analysis. *JAMA Oncology*. 2016;2(11):1460-9. Epub 2016/06/17. doi: 10.1001/jamaoncol.2016.1373. PubMed PMID: 27310651.
52. Steed TC, Treiber JM, Patel K, Ramakrishnan V, Merk A, Smith AR, et al. Differential localization of glioblastoma subtype: implications on glioblastoma pathogenesis. *Oncotarget*. 2016;7(18):24899-907. doi: 10.18632/oncotarget.8551.
53. Carro MS, Lim WK, Alvarez MJ, Bollo RJ, Zhao X, Snyder EY, et al. The transcriptional network for mesenchymal transformation of brain tumours. *Nature*. 2010;463(7279):318-25. Epub 2009/12/25. doi: 10.1038/nature08712. PubMed PMID: 20032975; PubMed Central PMCID: PMC34011561.
54. Cooper LA, Gutman DA, Chisolm C, Appin C, Kong J, Rong Y, et al. The tumor microenvironment strongly impacts master transcriptional regulators and gene expression class of glioblastoma. *The American Journal of Pathology*. 2012;180(5):2108-19. Epub 2012/03/24. doi: 10.1016/j.ajpath.2012.01.040. PubMed PMID: 22440258; PubMed Central PMCID: PMC3354586.
55. Louis DN, Ohgaki H, Wiestler OD, Cavenee WK, Burger PC, Jouvet A, et al. The 2007 WHO classification of tumours of the central nervous system. *Acta Neuropathologica*. 2007;114(2):97-109. Epub 2007/07/10. doi: 10.1007/s00401-007-0243-4. PubMed PMID: 17618441; PubMed Central PMCID: PMC1929165.
56. Louis DN, Perry A, Reifenberger G, von Deimling A, Figarella-Branger D, Cavenee WK, et al. The 2016 World Health Organization Classification of Tumors of the Central Nervous System: a summary. *Acta Neuropathologica*. 2016;131(6):803-20. Epub 2016/05/10. doi: 10.1007/s00401-016-1545-1. PubMed PMID: 27157931.

SUPPLEMENTARY FILES

S1 Appendix – The clinical dataset used in this study will be published online by PLOS One.

S2 Appendix – Supplementary methods

Assessment of SVZ contact on MRI

For the first series of MRI scans (n=86), direct contact of the contrast-enhancing part of the tumor with the lateral ventricles was assessed by a resident in radiology and an experienced neuroradiologist on preoperative gadolinium-enhanced T1-weighted MRI scans blinded to the clinical data. Based on the high interobserver agreement ($\kappa=0.78$), the remaining MRI scans were assessed by one observer.

Fresh-frozen tissue samples and mRNA expression analysis

76 fresh-frozen surgical samples of de novo glioblastomas were prospectively collected between 2010 and 2015. RNA was extracted with the Nucleospin® TriPrep (Macherey-Nagel, Düren, Germany) and the QIASymphony RNA (Qiagen, Venlo, The Netherlands) kits according to the manufacturers' instructions. Affymetrix HG U133 plus 2.0 arrays were prepared and scanned according to the manufacturer's protocol and as reported previously [1, 2]. Quality control and differential gene expression analyses were performed with R (v3.2.2). After quality control, 71 samples were evaluable for analysis. Batch correction was performed with the 'sva' package. Exploratory Gene Set Enrichment Analyses (GSEA) were performed after RMA-normalization [3] and batch correction, with the Partek® Genomics suite platform (Partek v6.6, St. Louis, MO, USA). Analyses were performed with the Broad Institute MySig libraries of curated gene sets C1 – C7 version 5.0 [4], 1000 permutations and default additional parameters. A FDR threshold of 0.25 was applied as recommended [3].

Class prediction

Molecular subclassification (proneural, neural, classical, mesenchymal) was predicted by hierarchical clustering [5]. Microarray normalization, data filtering and analysis of inter-array homogeneity were performed as reported previously [1, 5, 6]. Affymetrix HG U133 plus 2.0 probesets were matched to 840 genes originally published for the classification of glioblastomas (http://tcga-data.nci.nih.gov/docs/publications/gbm_exp/). Relative gene expression values were calculated. Genes were then excluded for a median absolute deviation below 0.5 [5]. After filtering, 768 genes were used for the class prediction. The hierarchical clustering of samples was performed with cluster3 software [7] with the agglomerative average linkage for the structure and 1 minus the Pearson's correlation for

the distance metric [5]. Classes were unequivocally assigned to 62/76 samples. Differential distributions were tested with Fisher's exact test.

miRNA isolation and expression analysis

Total RNA was isolated from 76 fresh-frozen surgical samples of glioblastoma patients with the MiRNeasy Micro Kit (Qiagen, Venlo, The Netherlands). Expression profiling of 800 miRNA probes was performed with the nCounter® Human v2 miRNA Expression Assay (NanoString Technologies, Seattle, WA, USA) at The Ohio State University Nucleic Acid Core Facility. Procedure details are available in the supplementary methods. 250ng RNA was used per sample and conditions were set according to the manufacturer's instructions. RNA quality was insufficient for 4 samples and SVZ status was not available for 5 patients, leaving 67 samples evaluable for analysis. Data were processed with the Partek® Genomics suite platform (Partek v6.6, St. Louis, MO, USA) by geometric mean normalization, average background subtraction and normalization to housekeeping genes.

Copy number analysis

Total DNA was extracted with sufficient quality from 67 fresh-frozen samples from our proprietary cohort of glioblastomas and processed on SNP 6.0 Affymetrix chips as recommended by the manufacturer. After discarding one outlier on the PCA analysis of the raw intensity data, copy number analysis was performed on 66 samples after batch correction using the circular binary segmentation algorithm of the Partek Suite (35 with SVZ contact and 31 without SVZ contact, Partek v6.6, St. Louis, MO, USA). Copy number data were compared between the two groups using Chi-square tests and FDR correction for multiple testing.

Analysis of TCGA RNA and miRNA expression data

Preoperative gadolinium-enhanced T1-weighted MRI scans from all available TCGA-glioblastoma patients (n=262) were downloaded from The Cancer Imaging Archive (TCIA; accessed September 2015), and the SVZ status of these patients was determined as described above, blinded to the clinical data. Clinical and MRI data from 222 glioblastoma patients was available for Cox regression analysis.

Molecular classification data was downloaded from the UCSC cancer genomics browser (September 2015) and was analyzed for 228 patients. Clinical data and Level 1 Affymetrix U133A mRNA microarray data were obtained from the TCGA data portal ([8], September 2015). Differences in molecular subtypes between the tumor groups were analyzed with a χ^2 -test. After quality control, microarray data from 223 patients were analyzed with R, as described above. Correction for batch effects and GSEA were performed as described above. Heatmaps were created with the 'heatmap3' package (R).

Level 3 miRNA expression data from 236 glioblastoma patients was downloaded from the TCGA data portal (December 2015). MiRNA expression levels in glioblastomas with and without SVZ contact were analyzed with the 'limma' and 'heatmap3' package (R).

Tissue microarrays, immunohistochemistry and scoring

Archival FFPE tumor tissues were retrospectively collected for a consecutive cohort of 229 glioblastoma patients treated in the UMCU between 2005 and 2008. Tissue was available for inclusion in tissue microarrays (TMAs) for 220/229 patients and was processed as reported previously [1, 9]. SVZ status was unavailable for 14 patients.

Histology of each specimen was reviewed under supervision of a senior clinical neuropathologist and marked on H&E stained sections. Immunohistochemistry was performed, as described previously [1], with antibodies against c-Rel (Mouse monoclonal, Santa Cruz Biotechnology, Dallas, TX, USA), NF- κ B p65 (phospho S276) (Rabbit polyclonal, Abcam, Cambridge, UK), STAT3 (phospho Y705) (Rabbit monoclonal, Cell Signaling, Leiden, The Netherlands), anti-C/EBP β (Mouse monoclonal, Abcam, Cambridge, UK), anti-CD133 (Rabbit polyclonal, Rockland, Limerick, PA, USA) and anti-GFAP δ (Rabbit polyclonal, Netherlands Institute for Life Sciences, Amsterdam, The Netherlands [10, 11]). Antigen retrieval was achieved by incubation in citrate buffer (NF- κ B p65, c-Rel, STAT3, C/EBP β and GFAP- δ) or EDTA buffer (CD133) during 12 minutes at 126°C (NF- κ B p65, c-Rel, STAT3, C/EBP β and CD133) or in a steamer for 30 minutes (GFAP- δ). Following incubation with the secondary antibody, the signal was developed with 3,3'-diaminobenzidine (DAB). Slides stained for GFAP- δ were incubated with anti-Rabbit Alexa 594 (Jackson ImmunoResearch, Ely, UK). Nuclear counterstaining was performed with hematoxylin or Hoechst (GFAP- δ staining). In order to block auto-fluorescence, slides were incubated for 5 minutes in Sudan Black and thereafter rinsed with 70% ethanol.

Protein expression evaluation was blinded to the clinical data and supervised by a senior neuropathologist. The percentage of nuclear and/or cytoplasmatic staining was scored as: 0, negative; 1, 1-25% positive cells; 2, 26-50% positive cells; 3, 51-75% positive cells and 4, 76-100% positive cells.

The GFAP- δ stained tissue was analyzed with fluorescent imaging. ImageJ was used to calculate the percentage of positive GFAP- δ staining per sample. Auto-fluorescent and necrotic areas were excluded from the analysis. A mean staining score was computed for each patient. Staining scores were analyzed with Mann Whitney U tests.

Survival analyses

Statistical analyses were performed with use of SPSS 25.0 (IBM, Armonk, NY, USA). Two-sided P-values < 0.05 were considered significant. Kaplan-Meier curves were analyzed with the log-rank test. Cox regression was used for the survival analyses. The proportional hazards (PH) assumption of the Cox model was checked with log-minus-log plots and time-dependent variables. Details on this procedure have been published in a previous study [9]. The PH assumption did not hold for the KPS and tumor volume variables, suggesting that the hazard function of these variables change over time. Therefore, the model was extended with time-dependent variables for KPS (KPS*time) and tumor volume (tumor volume*time). The PH assumption did not hold for the SVZ variable for patients with a long follow-up (>1000 days). The analyses were therefore restricted to a maximal follow-up of 1000 days after surgery.

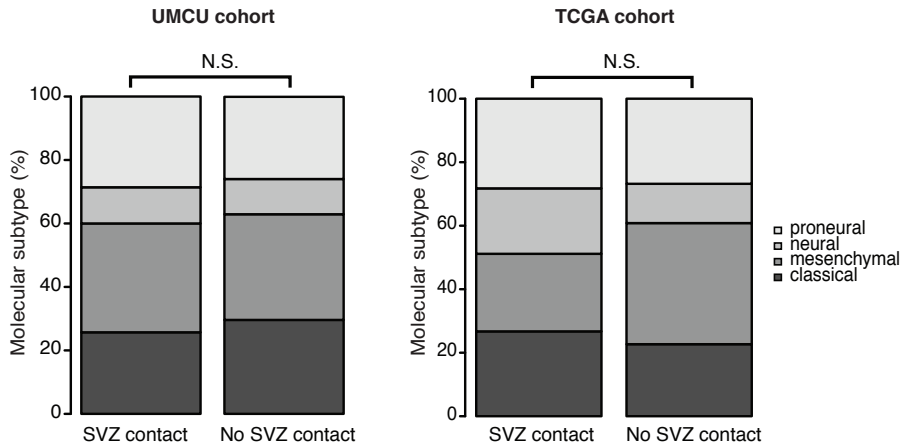
Univariable Cox regression was performed to assess the prognostic effect of tumor contact with the SVZ on glioblastoma patient survival. Next, multivariable Cox regression was performed including the following variables: SVZ status, age, KPS, KPS*time, tumor volume, tumor volume*time, surgery type, and post-surgical adjuvant treatment.

595 patients could be included in a multivariable complete case analysis. Multiple imputation was performed as a sensitivity analysis, allowing inclusion of all 647 patients.

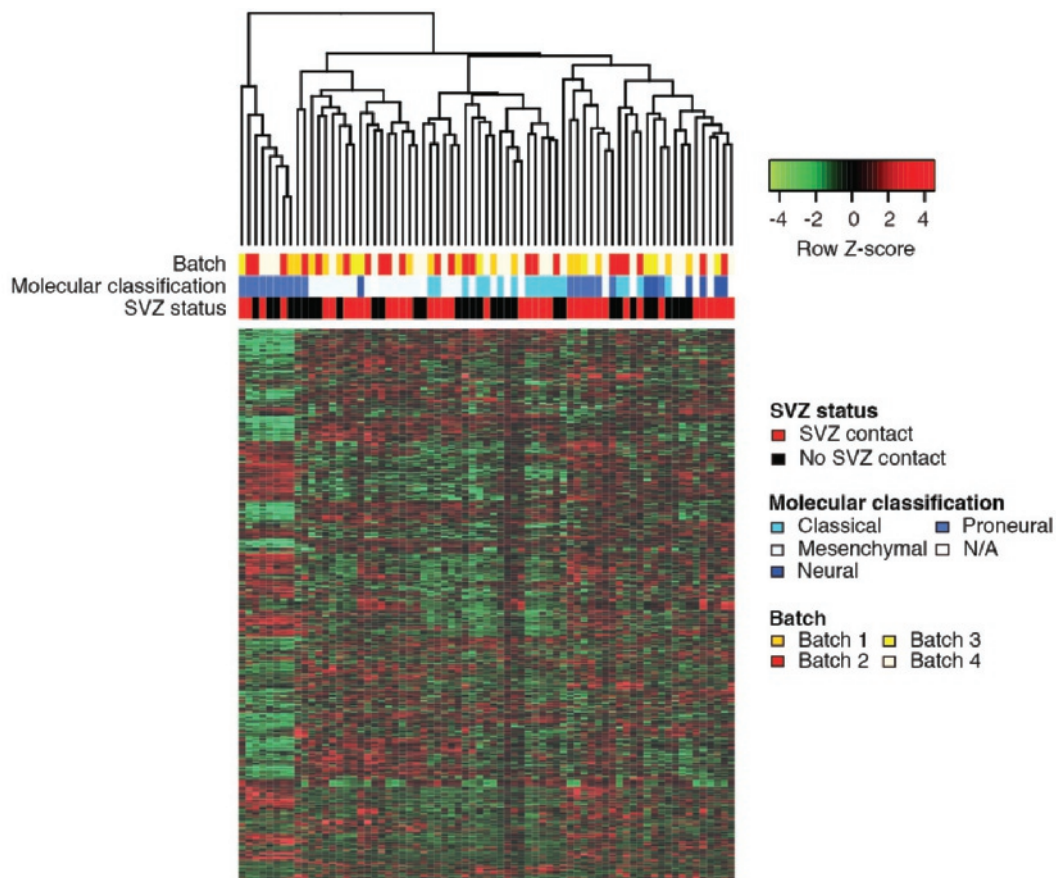
Survival analyses with TCGA data were performed as described above. Multivariable Cox regression was performed including age and KPS variables in the model. Multiple imputation was performed for missing data, to include all 222 patients of which survival and MRI data was available.

SUPPLEMENTARY REFERENCES

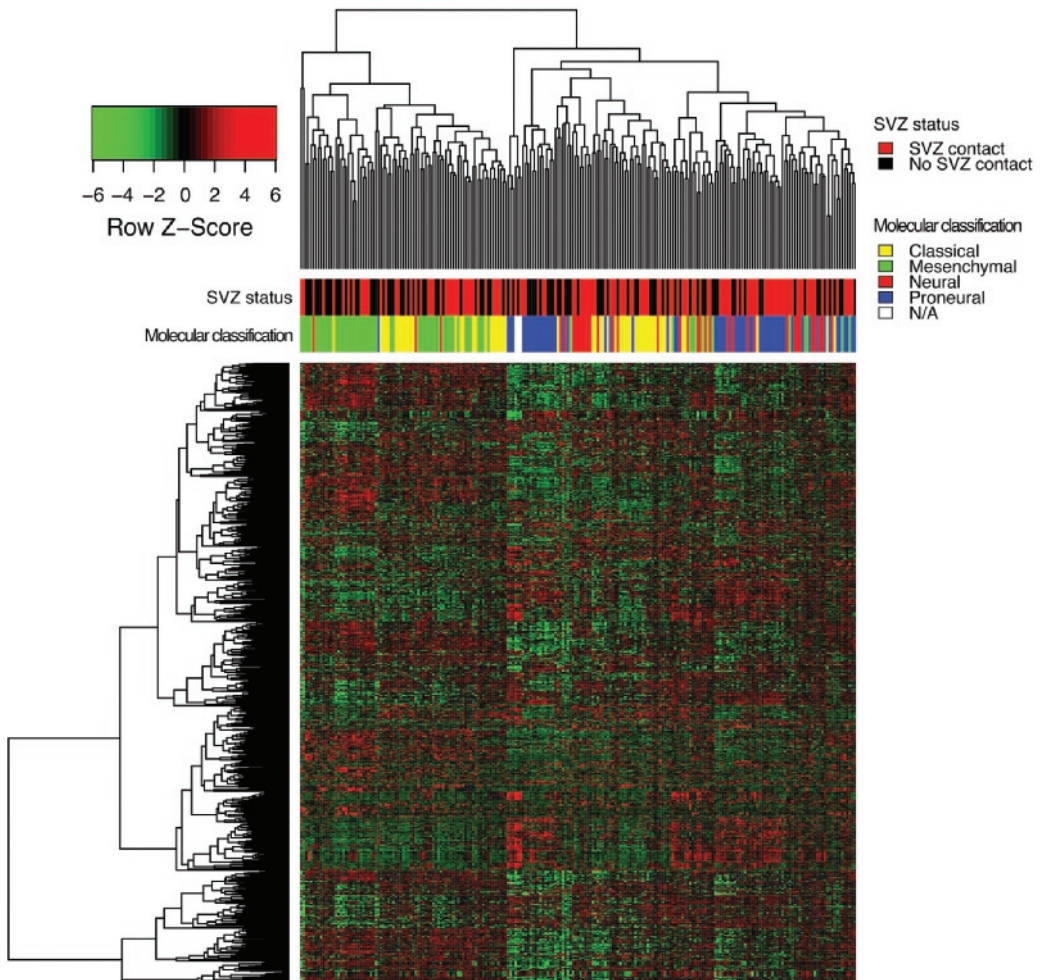
1. Berendsen S, Spliet WGM, Geurts M, Van Hecke W, Seute T, Snijders TJ, et al. Epilepsy Associates with Decreased HIF-1 α /STAT5b Signaling in Glioblastoma. *Cancers*. 2019;11(1). Epub 2019/01/10. doi: 10.3390/cancers11010041. PubMed PMID: 30621209.
2. Turkheimer FE, Roncaroli F, Hennuy B, Herens C, Nguyen M, Martin D, et al. Chromosomal patterns of gene expression from microarray data: methodology, validation and clinical relevance in gliomas. *BMC Bioinformatics*. 2006;7:526. doi: 1471-2105-7-526.
3. Subramanian A, Tamayo P, Mootha VK, Mukherjee S, Ebert BL, Gillette MA, et al. Gene set enrichment analysis: a knowledge-based approach for interpreting genome-wide expression profiles. *Proceedings of the National Academy of Sciences of the United States of America*. 2005;102(43):15545-50. doi: 0506580102.
4. Reich M, Liefeld T, Gould J, Lerner J, Tamayo P, Mesirov JP. GenePattern 2.0. *Nature Genetics*. 2006;38(5):500-1. doi: ng0506-500.
5. Verhaak RG, Hoadley KA, Purdom E, Wang V, Qi Y, Wilkerson MD, et al. Integrated genomic analysis identifies clinically relevant subtypes of glioblastoma characterized by abnormalities in PDGFRA, IDH1, EGFR, and NF1. *Cancer Cell*. 2010;17(1):98-110. doi: 10.1016/j.ccr.2009.12.020.
6. Wislet-Gendebien S, Poulet C, Neirinckx V, Hennuy B, Swingland JT, Laudet E, et al. In vivo tumorigenesis was observed after injection of in vitro expanded neural crest stem cells isolated from adult bone marrow. *PLoS One*. 2012;7(10):e46425. doi: 10.1371/journal.pone.0046425.
7. Eisen MB, Spellman PT, Brown PO, Botstein D. Cluster analysis and display of genome-wide expression patterns. *Proceedings of the National Academy of Sciences of the United States of America*. 1998;95(25):14863-8.
8. Brennan CW, Verhaak RG, McKenna A, Campos B, Nounshmehr H, Salama SR, et al. The somatic genomic landscape of glioblastoma. *Cell*. 2013;155(2):462-77. doi: 10.1016/j.cell.2013.09.034.
9. Berendsen S, Varkila M, Kroonen J, Seute T, Snijders TJ, Kauw F, et al. Prognostic relevance of epilepsy at presentation in glioblastoma patients. *Neuro-Oncology*. 2015. doi: nov238.
10. Roelofs RF, Fischer DF, Houtman SH, Sluijs JA, Van Haren W, Van Leeuwen FW, et al. Adult human subventricular, subgranular, and subpial zones contain astrocytes with a specialized intermediate filament cytoskeleton. *Glia*. 2005;52(4):289-300. doi: 10.1002/glia.20243.
11. van Strien ME, Sluijs JA, Reynolds BA, Steindler DA, Aronica E, Hol EM. Isolation of neural progenitor cells from the human adult subventricular zone based on expression of the cell surface marker CD271. *Stem Cells Translational Medicine*. 2014;3(4):470-80. Epub 2014/03/08. doi: 10.5966/sctm.2013-0038. PubMed PMID: 24604282; PubMed Central PMCID: PMC3973708.



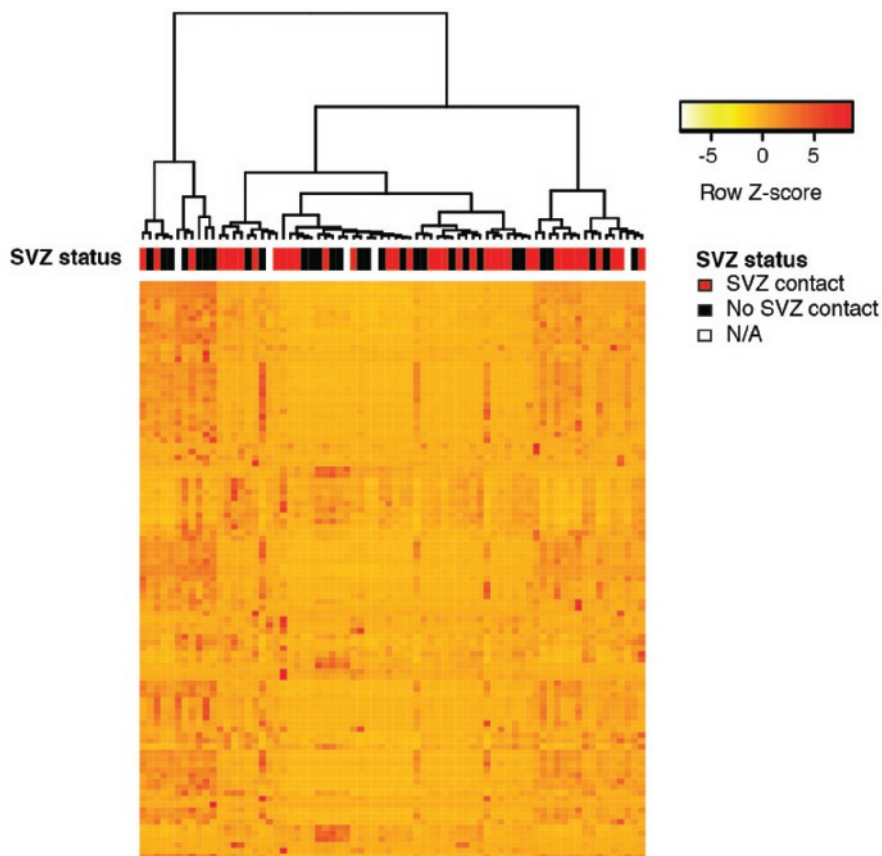
S1 Fig. Molecular classification. No significant difference in molecular subclass distribution was detected between SVZ contacting glioblastomas and tumors not contacting the SVZ in the UMCU cohort (Fisher's exact test, $P=1.0$) and the TCGA cohort (χ^2 -test, $P=0.11$).



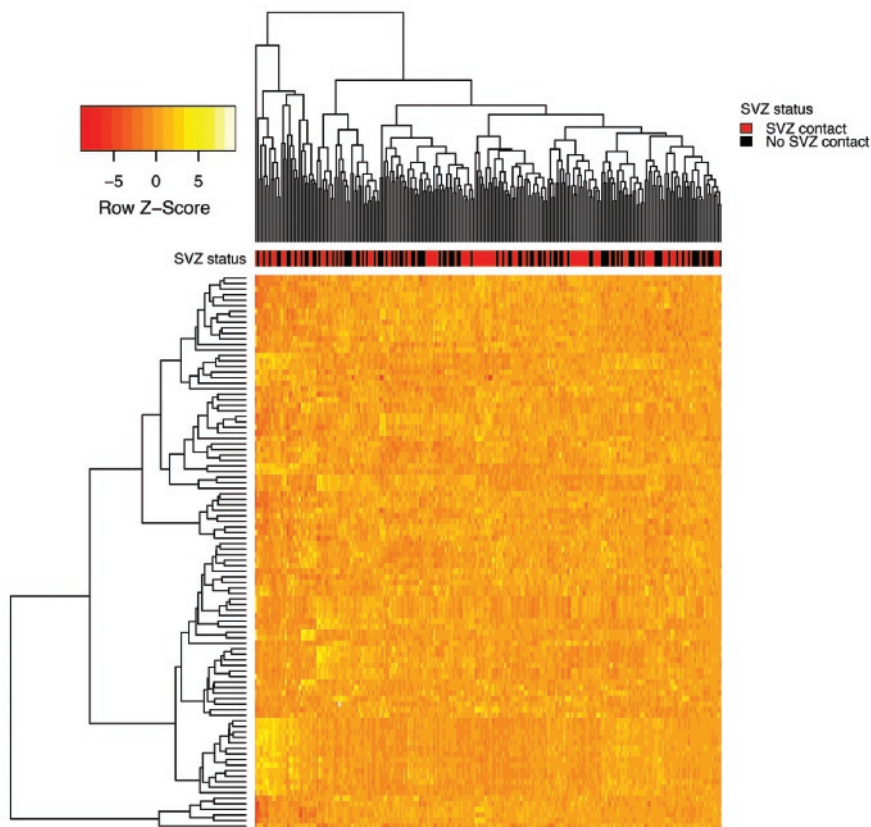
S2 Fig. RNA expression analysis UMCU cohort. Gene expression patterns of the 1000 RNA microarray probes with the highest standard deviation in the UMCU cohort. Gene expression patterns do not cluster to SVZ status or batch. No significantly differentially expressed genes were observed after correction for multiple testing ($FDR < 0.05$).



S3 Fig. RNA expression analysis TCGA cohort. Gene expression patterns of the 1000 RNA microarray probes with the highest standard deviation in the TCGA cohort. Gene expression patterns do not cluster to SVZ status or batch. No significantly differentially expressed genes were observed after correction for multiple testing ($FDR < 0.05$).



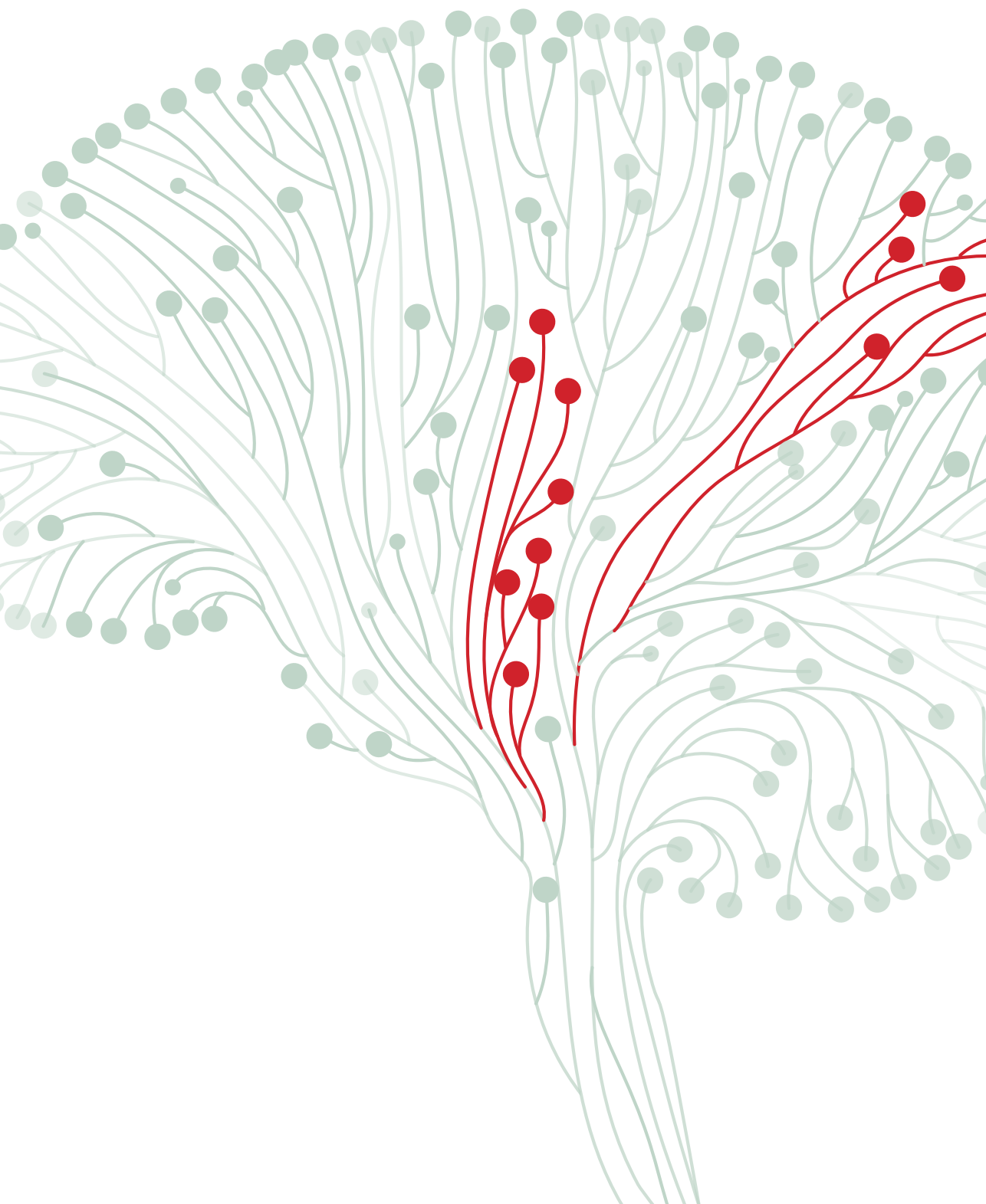
S4 Fig. MiRNA expression analysis UMCU cohort. MiRNA expression patterns of the 100 probes with the highest standard deviation in the UMCU cohort. 67 samples from our institute were included in this analysis. miRNA expression patterns did not cluster to SVZ status. No differentially expressed miRNAs were observed after correction for multiple testing ($FDR < 0.05$).



S5 Fig. MiRNA expression analysis TCGA cohort. MiRNA expression patterns of the 100 probes with the highest standard deviation in the TCGA cohort. miRNA expression patterns did not cluster to SVZ status. No differentially expressed miRNAs were observed after correction for multiple testing ($FDR < 0.05$).

S1 Table – Gene set enrichment analysis. Gene set enrichment in glioblastomas without SVZ contact compared to glioblastomas with SVZ contact. RNA expression data from the UMCU cohort (upper panel) and TCGA dataset (lower panel) was used. Abbreviations: ES: enrichment score; FDR: false discovery rate.

UMCU cohort				
MSigDB collection	Gene set	ES	P-value	FDR
C1 – positional gene sets	chr9q34	0.57	<0.001	0.038
C3 – motif gene sets	GCGNNANTTCC_UNKNOWN	0.37	0.002	0.229
<i>Transcription factor targets</i>	GTCNYYATGR_UNKNOWN	0.35	<0.001	0.239
TCGA cohort				
MSigDB collection	Gene set	ES	P-value	FDR
C1 – positional gene sets	chr3p24	-0.69	<0.001	0.070
	chr3q22	-0.68	0.006	0.092
	chr3q29	-0.65	0.006	0.113
	chr3q23	-0.73	0.004	0.118
	chr3q27	-0.63	0.006	0.127
	chr3p25	-0.54	0.006	0.134
	chr3q26	-0.53	0.004	0.182
	chr3q28	-0.66	0.016	0.184
	chr19p12	-0.65	0.018	0.217
C3 – motif gene sets	V\$PEA3_Q6	0.46	0.004	0.141
<i>Transcription factor targets</i>				
C6 – oncogenic signatures	BMI1_DN.V1_UP	0.48	0.004	0.185





CHAPTER 7

Glioblastomas within the subventricular zone are region-specific enriched for mesenchymal transition markers: an intratumoral gene expression analysis

Diana J.Z. Dalemans*, Sharon Berendsen*, Kaspar Draaisma,
Pierre A. Robe#, Tom J. Snijders#

* and #: these authors contributed equally.

Submitted.

ABSTRACT

Background: Involvement of the subventricular zone (SVZ) in glioblastoma is associated with poor prognosis and is suggested to associate with specific tumor-biological characteristics. The SVZ microenvironment can influence gene expression in glioblastoma cells in preclinical models. We aimed to investigate whether the SVZ microenvironment has any influence on intratumoral gene expression patterns in glioblastoma patients.

Methods: The publicly available Ivy Glioblastoma database contains clinical, radiological and whole exome sequencing data from multiple regions from en bloc resected glioblastomas. SVZ involvement of the various tissue samples was evaluated on MRI scans. In the tumors that contacted the SVZ, we performed gene expression analyses and gene set enrichment analyses to compare gene (set) expression in tumor regions within the SVZ to tumor regions outside the SVZ, within the same tumors. We also compared these samples to glioblastomas that made no contact with the SVZ.

Results: Within glioblastomas that contacted the SVZ, tissue samples within the SVZ showed enrichment of gene sets involved in (epithelial-)mesenchymal transition, NF- κ B and STAT3 signaling, angiogenesis and hypoxia, compared to the samples outside of the SVZ region from the same tumors ($P < 0.05$, $FDR < 0.25$). Comparison of glioblastoma samples within the SVZ region to samples from tumors that did not contact the SVZ yielded similar results. In contrast, we observed no differences when comparing the samples outside of the SVZ from SVZ-contacting glioblastomas with samples from glioblastomas that did not contact the SVZ at all.

Conclusion: Glioblastoma samples in the SVZ region are enriched for increased (epithelial-) mesenchymal transition and angiogenesis/hypoxia signaling, possibly mediated by the SVZ microenvironment.

INTRODUCTION

Glioblastoma is the most common primary malignant brain tumor. The prognosis is poor, with a median survival of about 15 months, despite intensive treatment [1].

The subventricular zone (SVZ), lining the walls of the lateral ventricles of the brain, has been of increasing interest in recent glioblastoma research. One key aspect of the SVZ is the neural stem cell niche it harbors. These astrocyte-like neural stem cells are hypothesized as the cells of origin of glioblastoma [2-4]. SVZ contact is associated with poor prognosis in glioblastoma patients. The underlying mechanisms of this adverse prognostic effect are possibly mediated by intrinsic tumor-biological characteristics. However, studies focused on exploring tumor-biological differences between glioblastomas with and without SVZ contact have shown inconclusive results [5-12]. In all previous gene expression studies on this subject, bulk tumor data was analyzed. Intratumoral heterogeneity, a known characteristic in glioblastoma, was not taken into account [13, 14]. It is proposed that the tumor microenvironment contributes to this intratumoral heterogeneity [15].

Hence, our study focused on exploring oncogenic signaling in patient glioblastoma samples within the SVZ microenvironment, to explore a possible influence of the SVZ microenvironment on glioblastoma gene expression. We made use of glioblastoma tissue samples from the publicly available Ivy Glioblastoma Atlas, which contains clinical, radiological and whole exome sequencing data from multiple regions from *en bloc* resected glioblastomas [16]. In the tumors that contacted the SVZ, we performed gene expression analyses and gene set enrichment analyses to compare gene (set) expression in tumor regions within the SVZ to tumor regions outside the SVZ, within the same tumors. We also compared these samples to glioblastomas that made no contact with the SVZ.

We hypothesized that gene expression in glioblastoma samples from within the SVZ region show unfavorable oncogenic signaling characteristics, as a possible effect from the SVZ microenvironment.

MATERIALS AND METHODS

Patient cohort and baseline characteristics

Patients were selected from the Ivy Glioblastoma Atlas, an online accessible database that contains clinical, genomic and histologic information on patients with glioblastoma (<http://glioblastoma.alleninstitute.org/>) [16]. Adult patients with a primary IDH wildtype glioblastoma were included. Subsequently, clinical features including gender, age, initial KPS, extent of resection, adjuvant radiotherapy and/or chemotherapy and survival

were collected. Also, molecular characteristics including EGFR amplification, MGMT methylation, PTEN status and molecular subtype (classical, mesenchymal, proneural and neural [13]) were collected. The baseline characteristics were compared between patients with SVZ-contacting glioblastoma and patients with glioblastoma without SVZ contact. Survival of patients with SVZ-contacting glioblastoma and patients with glioblastoma without SVZ involvement was compared with Kaplan-Meier curves and a log rank test.

MRI analysis and tissue block selection

SVZ involvement in glioblastomas was inspected on pre-operative T1-weighted post-contrast MRI images. SVZ contact was defined as contact of contrast-enhancing tumor with a lateral ventricle. The presence of SVZ contact was evaluated independently by two investigators (DJZD and SB), with blinding to the clinical and genomic data. In case of disagreement, a third investigator (TJS) gave the conclusive statement.

Along with the MRI scans, macroscopic images of *en bloc* resected tumors were available. The spatial orientation of the resected tumor was provided (i.e. anterior, posterior, lateral and medial side). The tumor tissue had been divided subsequently into multiple tissue blocks, for *in situ* hybridization and RNA expression analysis, as described in the original paper [16]. In this way, tissue blocks could be matched to their anatomical location on the MRI images and tissue blocks from the SVZ region were selected.

These selection processes resulted in three groups of samples for further analysis and comparison: (a) glioblastoma samples within the SVZ (*withinSVZ* samples), (b) samples outside of the SVZ from the same SVZ-contacting glioblastomas (*outsideSVZ* samples), and (c) samples from tumors without any SVZ contact (*noSVZcontact* samples).

RNA sequencing data selection

Sampling of tissue blocks for RNA sequencing is described in the original paper [16] and was based on anatomical structural features that are commonly seen by neuropathologists in glioblastoma tissue sections stained with hematoxylin and eosin (H&E). The major structural regions were Leading Edge, Cellular Tumor and Infiltrating Tumor. Leading Edge was defined as the outermost boundary of the tumor, where the ratio of tumor to normal cells is about 1-3/100. Cellular Tumor constitutes the major part of core, where the ratio of tumor to normal cells is about 100/1 to 500/1. Infiltrating Tumor is the intermediate zone between the Leading Edge and Cellular Tumor, where the ratio of tumor cells to normal cells is about 10-20/100[16]. In our study, only RNA sequencing data sampled by Cellular Tumor were included, as this yields the most tumor-specific data.

RNA sequencing data analysis

Detailed information on tissue processing, RNA isolation, sequencing, quality control and alignment was described previously[16]. Subsequent RNA sequencing analysis was performed with aligned files in bam format with R (version 3.5.2). Count matrices were generated with the GenomicAlignments package (version 1.18.1). Genes with low read counts were dropped and TMM normalization for library size was performed to eliminate composition biases between libraries (edgeR package, version 3.24.3). We performed differential expression analyses by fitting a linear mixed model, with the location of the sample as fixed effect and patient ID as random effect, with the dream (differential expression analysis for repeated measures) analysis from the variancePartition package (version 1.12.3). We used mixed models, as this analysis method allows for correction of gene expression correlations in tumor samples from the same patient. Genes with a p-value adjusted for multiple testing with Benjamini-Hochberg's False Discovery Rate (FDR) below 0.05 were considered to be significantly differentially expressed. A heatmap was constructed to visualize the most differentially expressed genes across tumor locations (gplots package).

Subsequently, we performed Quantitative Set Analysis for Gene Expression (qusage package) in order to identify differential enrichment of gene sets between the groups. The ggen function of the qusage package (version 2.16.1) allowed us to incorporate the linear mixed model with the location of the tissue sample as fixed effect and patient ID as random effect. This analysis was performed with the hallmark gene sets [17] from the Molecular Signatures Database. Enriched gene sets with a $P < 0.05$ and a false discovery rate (FDR) < 0.25 were considered significant. The results were visualized with pathway activity plots (qusage package).

RESULTS

The Ivy Glioblastoma Atlas contains a total of 41 glioblastoma patients of whom 34 had IDH1 wildtype primary glioblastoma (Figure 1). Due to absence of spatial orientation data of the tumor or absence of RNA sequencing data, eight patients were excluded (Figure 1). As a result, a total of 26 patients were included in our analysis (Figure 2).

Patients with SVZ-contacting glioblastoma did not differ significantly from patients with glioblastoma without SVZ contact with respect to age, initial KPS, extent of resection, treatment, PTEN status, MGMT methylation status, EGFR amplification status and EGFRvIII mutation status (Table 1). Median overall survival was shorter in patients with SVZ-contacting glioblastoma (442 days vs. 544 days in patients with glioblastoma without

SVZ contact), but this observation did not reach a statistically significant difference. (Table 1, supplementary figure 1).

Table 1 - Baseline characteristics

	SVZ (n=16)	Non-SVZ (n=10)	P-value
Gender <i>n</i> (%)			0.68
Male	7 (43.8%)	3 (30%)	
Female	9 (56.3%)	7 (70%)	
Age <i>mean</i> (SD)	62.1 (6.3)	60.2 (8.4)	0.51
Initial KPS <i>median</i> (IQR)	90 (28)	90 (20)	0.76
Extent of resection <i>n</i> (%)			0.35
Total	11 (68.8%)	9 (90%)	
Subtotal	5 (31.3%)	1 (10%)	
Chemo and/or radiotherapy <i>n</i> (%)			0.29
Both	14 (87.5%)	9 (90%)	
Only chemotherapy	0	1 (10%)	
Only radiotherapy	0	0	
None	2 (12.5%)	0	
PTEN <i>n</i> (%)			0.52
Loss	11 (68.8%)	7 (70%)	
Normal	2 (12.5%)	0	
Gain	1 (6.2%)	1 (10%)	
Missing	2 (12.5%)	2 (20%)	
MGMT Methylation <i>n</i> (%)			0.40
Yes	7 (43.8%)	2 (20%)	
No	9 (56.3%)	8 (80%)	
EGFR Amplification <i>n</i> (%)			1.0
Yes	8 (50.0%)	4 (40%)	
No	6 (37.5%)	4 (40%)	
Missing	2 (12.5%)	2 (20%)	
EGFR <i>vIII</i> <i>n</i> (%)			0.62
Yes	3 (18.8%)	3 (30%)	
No	11 (68.8%)	5 (50%)	
Missing	2 (12.5%)	2 (20%)	
Survival in days, <i>median</i> (IQR)	442 (119)	544 (137)	0.23

Abbreviations: SVZ: subventricular zone, SD: standard deviation, KPS: Karnofsky Performance Score, IQR: interquartile range, PTEN: phosphatase and tensin homolog, MGMT: O6-methylguanine–DNA methyltransferase, EGFR: epidermal growth factor receptor.

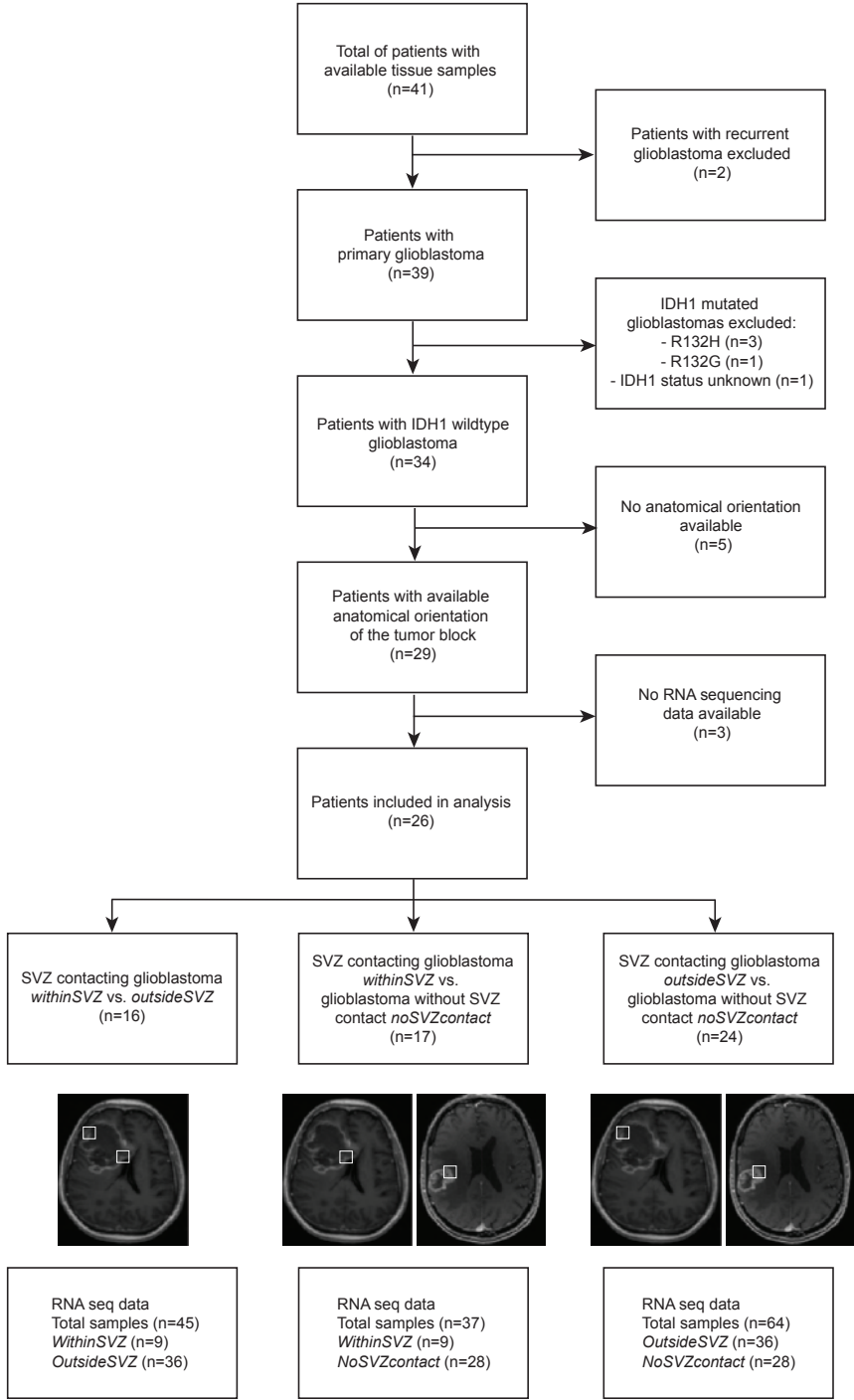


Figure 1 - Flowchart

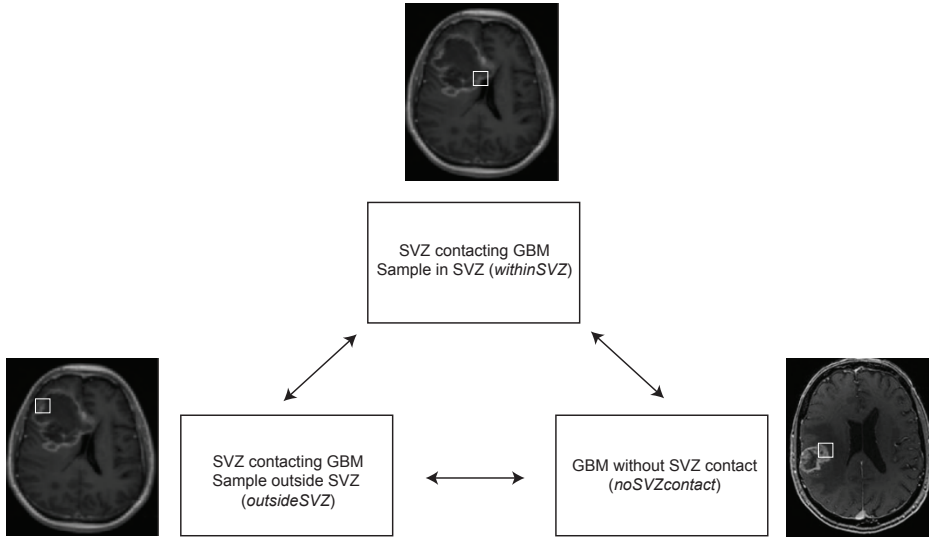


Figure 2 – analysis overview. In our study, we compare gene (set) expression between (a) glioblastoma samples within the SVZ (*withinSVZ* samples), (b) samples outside of the SVZ from SVZ-contacting glioblastomas (*outsideSVZ* samples), and (c) samples from tumors without SVZ contact (*noSVZcontact* samples).

Differential expression of oncogenic gene sets across tumor regions: intratumoral analysis

First, we analyzed RNA expression in all tumors with SVZ contact. Within the same tumors, we compared the *withinSVZ*-samples to the *outsideSVZ*-samples. In this analysis, 45 tumor samples (nine *withinSVZ*-samples and 36 *outsideSVZ*-samples) were included, from sixteen patients (Figure 1).

After adjustment for multiple testing, no single gene was significantly differentially expressed between tumor samples from within and outside of the SVZ (supplementary figure 2). Gene set expression analysis however, showed differential expression of 24 gene sets ($P < 0.05$, $FDR < 0.25$) (supplementary Table 1, Figure 3). In the *withinSVZ*-samples, we observed the most increased expression of gene sets involved in (epithelial-) mesenchymal transition, angiogenesis, and NF- κ B and JAK/STAT3 signaling compared to the *outsideSVZ*-samples from the same tumors (supplementary table 1).

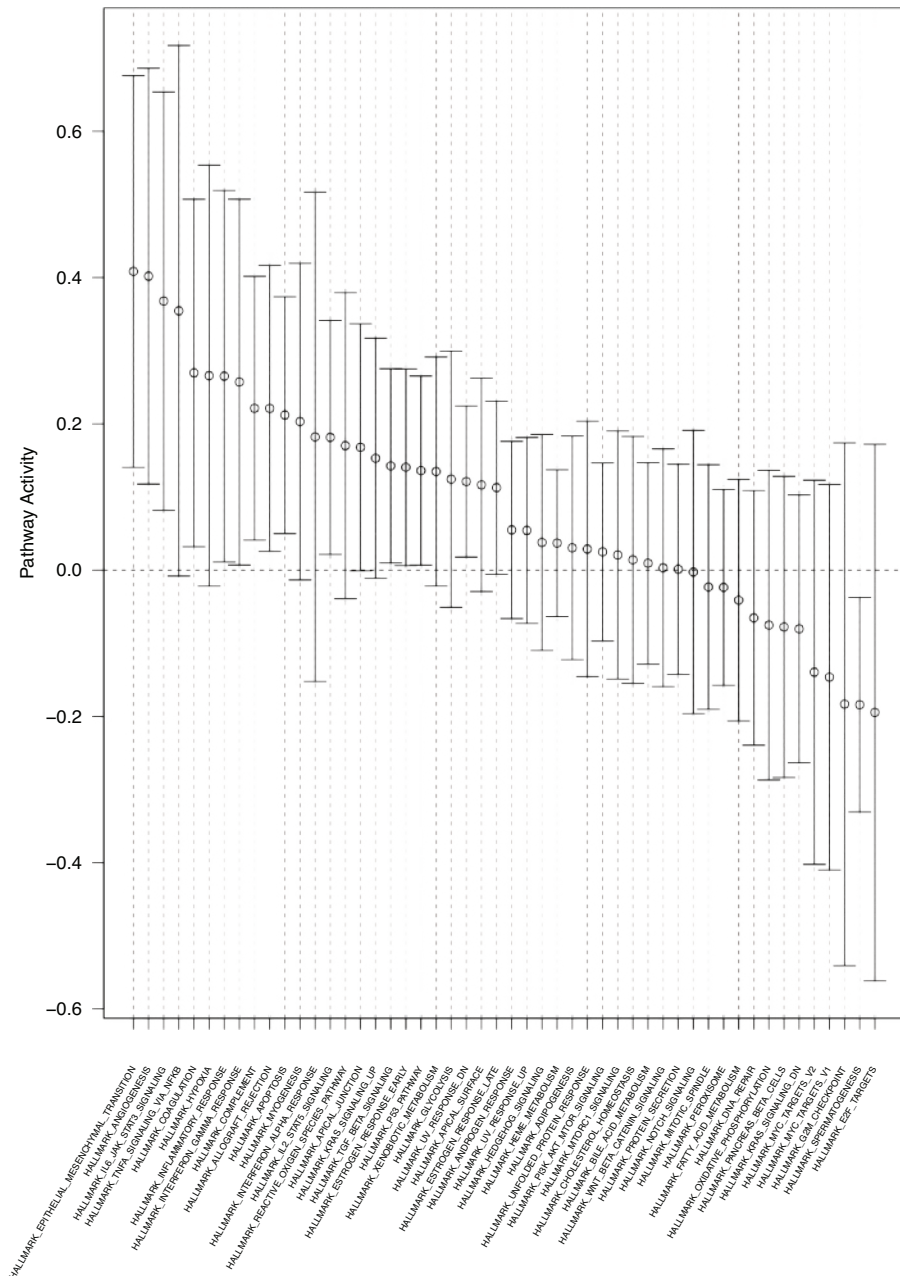


Figure 3 – Pathway activity plot of the within SVZ contacting glioblastoma (*withinSVZ*-samples vs. *outsideSVZ*-samples) analysis. Gene set expression analysis of the *withinSVZ*-samples vs. *outsideSVZ*-samples showed differential expression of 24 gene sets ($p < 0.05$, $FDR < 0.25$). The relative gene set activity (log fold change) is displayed on the y-axis. The 95% confidence intervals are represented by the horizontal bars. Most gene sets were upregulated in the *withinSVZ*-samples group, as shown by their positive log fold changes.

Differential expression of oncogenic gene sets in glioblastomas in the SVZ region: intertumoral analysis

In this analysis 37 tumor samples (nine *withinSVZ*-samples and 28 *noSVZcontact*-samples, Figure 2) from seventeen patients were included.

The only significantly differentially expressed gene between the *withinSVZ*-samples and the *noSVZcontact*-samples was DCAF4, which was downregulated in the *withinSVZ*-group (logFC= -1.50, adjusted P = 0.002). The separate expression values (log counts per million) of DCAF4 per sample are shown in supplementary figure 3. The results for the fifty genes with the lowest (unadjusted) p-values are shown in a heatmap (supplementary figure 4).

Gene set expression analysis showed differential expression of 27 gene sets ($P < 0.05$, $FDR < 0.25$, supplementary table 2, Figure 4). Again, we found relatively increased expression of gene sets involved in (epithelial-)mesenchymal transition, angiogenesis, and NF- κ B and JAK/STAT3 signaling in the *withinSVZ*-samples.

No difference in oncogenic signaling between glioblastoma samples from outside the SVZ and tumors without SVZ contact: intertumoral analysis.

In this analysis, 64 tumor samples (36 *outsideSVZ*-samples and 28 *noSVZcontact*-samples) were included, from 24 patients (Figure 1).

No significant differentially expressed genes between the *outsideSVZ*-samples and *noSVZcontact*-samples were found (adjusted p-values > 0.50 for all genes). The results for the fifty genes with the lowest adjusted p-values are shown in a heatmap (supplementary figure 5). No differential expression of gene sets (with an FDR less than 0.25) were found.

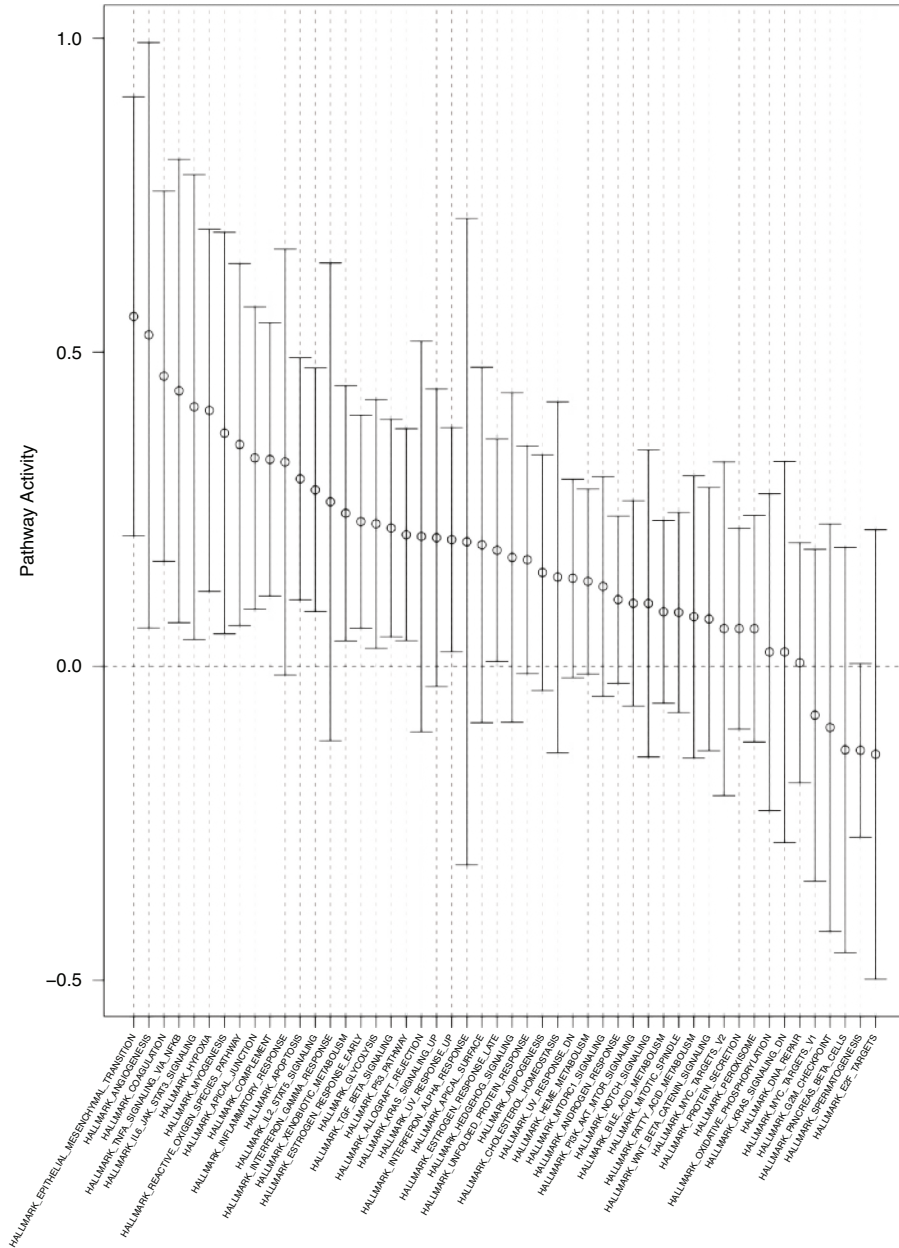


Figure 4: Pathway activity plot of the *withinSVZ*-samples vs. *noSVZcontact*-samples analysis. Gene set expression analysis of the *withinSVZ*-samples vs. *noSVZcontact*-samples showed differential expression of 27 gene sets ($p < 0.05$, $FDR < 0.25$). The relative gene set activity (log fold change) is displayed on the y-axis. The 95% confidence intervals are represented by the horizontal bars. Most gene sets were upregulated in the *withinSVZ*-samples group, as shown by their positive log fold changes.

DISCUSSION

With intra- and intertumoral gene expression analyses, we show that gene sets associated with mesenchymal transition are relatively upregulated in glioblastoma tissue in the SVZ region as compared to tumor tissue outside the SVZ region. To our knowledge, this is the first study in which gene expression in glioblastomas contacting the SVZ is regionally explored to this end so far. Our findings suggest that the SVZ microenvironment could influence oncogenic signaling in glioblastoma.

The differential expression of gene sets was more pronounced in the comparison of *withinSVZ*-samples versus *noSVZcontact*-samples, than in the comparison of different samples from the SVZ-contacting tumors (*withinSVZ* versus *outsideSVZ*), which could reflect a greater degree of similarity of the samples in the latter comparison. The comparison of *outsideSVZ*-samples from the SVZ-contacting tumors with *noSVZcontact*-samples from glioblastomas without SVZ contact showed no significantly different gene or pathway expression. This is in line with the hypothesis that the SVZ microenvironment could influence region specific gene expression in glioblastoma.

Few studies have focused on the interaction of the SVZ micro-environment and glioblastoma (stem) cells (GSCs) [18-20]. This is of particular interest, as the SVZ niche is believed to serve as a GSC reservoir which contributes to resistance to therapy. It is proposed that the microenvironment in the SVZ closely interacts with GSCs in order to establish this protective niche [18, 19, 21]. One study showed that GSCs in the SVZ appear to have an enhanced mesenchymal signature compared with their counterparts from the tumor [19]. These mesenchymal features, including a higher expression level of N-cadherin and vimentin, were shown to be upregulated by SVZ-released CXCL12. Moreover, inhibition of the CXCL12/CXCR4 signaling axis with AMD3100 (a CXCL12/CXCR4 antagonist) weakened the tumor's mesenchymal signature in the SVZ and increased the tumor's sensitivity to radiotherapy [19]. This correlation of mesenchymal activation in glioblastoma and resistance to radiotherapy (and chemotherapy) has been reported in other studies as well [22]. Another study found a similar predominance of the mesenchymal subtype in glioblastoma samples from the SVZ as compared to SVZ distant samples from the same tumor [20]. Moreover, in this study, isolated GSCs from the SVZ and GSCs from other tumor mass of the same glioblastoma showed different patterns of response to therapies [20].

In this light, our results provide further evidence to this SVZ region specific mesenchymal transition in glioblastoma. However, a deeper insight into the complex interaction between glioblastoma cells (and GSCs in particular) and the SVZ micro-environment is needed to unravel the mechanism behind this mesenchymal shift.

Besides the (epithelial-)mesenchymal transition signaling pathway, several other gene sets linked to aggressive growth of glioblastoma were relatively upregulated in the *withinSVZ*-samples group, including TNF- α -mediated NF- κ B activation, IL-6 induced STAT3 activation, TGF- β signaling, p53 signaling, KRas signaling, genes upregulated by reactive oxygen species, angiogenesis, hypoxia, coagulation, complement activation and inflammatory response. Activation of and interaction between several of these pathways has been linked to induction of (epithelial-)mesenchymal transition in glioblastoma as well [22-29]. For example, the mesenchymal subtype of glioblastoma is characterized by increased levels of NF- κ B signaling components and moreover, glioma sphere cultures of the proneural subtype can transform to a mesenchymal state under TNF- α -mediated NF- κ B activation [22]. Also, it has been demonstrated that STAT3 activation increases when initial proneural tumors experience a mesenchymal shift upon recurrence [30, 31]. Furthermore, STAT3 was shown to be highly expressed in glioblastoma stem cells (GSCs), which are tumor cells with self-renewing properties that contribute to tumor initiation and therapeutic resistance [32]. Finally, also hypoxia and reactive oxygen species could potentially induce mesenchymal transition in glioblastoma [26, 33].

The only significantly differentially expressed gene (DCAF4) was observed in the *withinSVZ*-samples vs. *noSVZcontact*-samples analysis. DCAF4 (DDB1 and CUL4-associated factor 4) encodes a WD (Trp-Asp) repeat-containing protein that interacts with the CUL4-DDB1 E3 ligase macromolecular complex. The CUL4-DDB1 ubiquitin ligase is involved in cell proliferation, survival, DNA repair and genomic integrity [34]. CUL4A demonstrated the potential to promote (epithelial-)mesenchymal transition through the activation of ZEB1 in breast cancer cells [35]. One study showed that overexpression of DCAF4L2, a paralog of DCAF4, could support (epithelial-)mesenchymal transition in colorectal cancer cells through activation of the NF- κ B pathway [36], and genetic variations in DCAF4 have been previously associated with leukocyte telomere length, keloid formation and lung cancer risk [37-39]. However, as we found a relative downregulation of DCAF4 in nearly all *withinSVZ*-samples, the relevance of this observation compared to increased expression of gene sets involved in (epithelial-) mesenchymal transition in tumor samples from the SVZ region remains unclear.

Our study has some technical limitations that should be considered. We relied on the availability of data from the comprehensive Ivy GBM Atlas. RNA sequencing data was not available for all tissue regions and spatial orientation of the tumor tissues was not clear in some cases. As a consequence, only a limited number of patients could be included in our analyses. Especially for the samples within the SVZ region, the number of available tumor samples was limited (nine samples from seven patients). Although the gene set expression results of our separate subanalyses are in line with each other, gene set analyses

in relatively small-sized cohorts should be regarded as exploratory, and must be validated in other studies prior to drawing any conclusions.

CONCLUSIONS

Glioblastoma tissues within the SVZ region show increased expression of gene sets involved in (epithelial-)mesenchymal transition, angiogenesis, and NF- κ B and JAK/STAT3 signaling, compared to tumor tissues from non-SVZ-regions, either from the same SVZ-contacting tumors or from glioblastomas that do not contact the SVZ. Our results suggest that the SVZ microenvironment could influence regional gene expression in glioblastoma, to induce (epithelial-)mesenchymal transition and possibly a more invasive glioblastoma phenotype.

REFERENCES

1. Stupp, R., et al., Effects of radiotherapy with concomitant and adjuvant temozolomide versus radiotherapy alone on survival in glioblastoma in a randomised phase III study: 5-year analysis of the EORTC-NCIC trial. *Lancet Oncol*, 2009. 10(5): p. 459-66.
2. Sanai, N., et al., Unique astrocyte ribbon in adult human brain contains neural stem cells but lacks chain migration. *Nature*, 2004. 427(6976): p. 740-4.
3. Alcantara Llaguno, S., et al., Malignant astrocytomas originate from neural stem/progenitor cells in a somatic tumor suppressor mouse model. *Cancer Cell*, 2009. 15(1): p. 45-56.
4. Lee, J.H., et al., Human glioblastoma arises from subventricular zone cells with low-level driver mutations. *Nature*, 2018. 560(7717): p. 243-247.
5. Berendsen, S., Adverse prognosis of glioblastoma contacting the subventricular zone: biological correlates. Accepted for publication in *PLoS one*, 2019.
6. Mistry, A.M., et al., Ventricular-Subventricular Zone Contact by Glioblastoma is Not Associated with Molecular Signatures in Bulk Tumor Data. *Sci Rep*, 2019. 9(1): p. 1842.
7. Jungk, C., et al., Spatial transcriptome analysis reveals Notch pathway-associated prognostic markers in IDH1 wild-type glioblastoma involving the subventricular zone. *BMC Med*, 2016. 14(1): p. 170.
8. Denicolai, E., et al., Molecular heterogeneity of glioblastomas; does location matter? *Oncotarget*, 2015.
9. Jamshidi, N., et al., Illuminating radiogenomic characteristics of glioblastoma multiforme through integration of MR imaging, messenger RNA expression, and DNA copy number variation. *Radiology*, 2014. 270(1): p. 1-2.
10. Kappadakunnel, M., et al., Stem cell associated gene expression in glioblastoma multiforme: relationship to survival and the subventricular zone. *J Neurooncol*, 2010. 96(3): p. 359-67.
11. Han, S., et al., Can lateral ventricle contact predict the ontogeny and prognosis of glioblastoma? *J Neurooncol*, 2015. 124(1): p. 45-55.
12. Gollapalli, K., et al., Subventricular zone involvement in Glioblastoma - A proteomic evaluation and clinicoradiological correlation. *Sci Rep*, 2017. 7(1): p. 1449.
13. Verhaak, R.G., et al., Integrated genomic analysis identifies clinically relevant subtypes of glioblastoma characterized by abnormalities in PDGFRA, IDH1, EGFR, and NF1. *Cancer cell*, 2010. 17(1): p. 98-110.
14. Sottoriva, A., et al., Intratumor heterogeneity in human glioblastoma reflects cancer evolutionary dynamics. *Proc Natl Acad Sci U S A*, 2013. 110(10): p. 4009-14.
15. Bonavia, R., et al., Heterogeneity maintenance in glioblastoma: a social network. *Cancer Res*, 2011. 71(12): p. 4055-60.
16. Puchalski, R.B., et al., An anatomic transcriptional atlas of human glioblastoma. *Science*, 2018. 11;360(6389): p. 660-663.
17. Liberzon, A., et al., The Molecular Signatures Database (MSigDB) hallmark gene set collection. *Cell Syst*, 2015. 1(6): p. 417-425.
18. Goffart, N., et al., Adult mouse subventricular zones stimulate glioblastoma stem cells specific invasion through CXCL12/CXCR4 signaling. *Neuro-oncology*, 2015. 17(1): p. 81-94.
19. Goffart, N., et al., CXCL12 mediates glioblastoma resistance to radiotherapy in the subventricular zone. *Neuro Oncol*, 2017. 19(1): p. 66-77.

20. Piccirillo, S.G., et al., Contributions to drug resistance in glioblastoma derived from malignant cells in the sub-ependymal zone. *Cancer Res*, 2015. 75(1): p. 194-202.
21. Kroonen, J., et al., Human glioblastoma-initiating cells invade specifically the subventricular zones and olfactory bulbs of mice after striatal injection. *International journal of cancer*, 2011. 129(3): p. 574-585.
22. Bhat, K.P., et al., Mesenchymal differentiation mediated by NF-kappaB promotes radiation resistance in glioblastoma. *Cancer cell*, 2013. 24(3): p. 331-346.
23. Conroy, S., et al., IL-8 associates with a pro-angiogenic and mesenchymal subtype in glioblastoma. *Oncotarget*, 2018. 9(21): p. 15721-15731.
24. Xie, T.X., et al., Constitutive NF-kappaB activity regulates the expression of VEGF and IL-8 and tumor angiogenesis of human glioblastoma. *Oncol Rep*, 2010. 23(3): p. 725-32.
25. Talasila, K.M., et al., The angiogenic switch leads to a metabolic shift in human glioblastoma. *Neuro Oncol*, 2017. 19(3): p. 383-393.
26. Joseph, J.V., et al., Hypoxia enhances migration and invasion in glioblastoma by promoting a mesenchymal shift mediated by the HIF1alpha-ZEB1 axis. *Cancer Lett*, 2015. 359(1): p. 107-16.
27. Magnus, N., et al., Coagulation-related gene expression profile in glioblastoma is defined by molecular disease subtype. *J Thromb Haemost*, 2013. 11(6): p. 1197-200.
28. Carro, M.S., et al., The transcriptional network for mesenchymal transformation of brain tumours. *Nature*, 2010. 463(7279): p. 318-25.
29. Cooper, L.A., et al., The tumor microenvironment strongly impacts master transcriptional regulators and gene expression class of glioblastoma. *Am J Pathol*, 2012. 180(5): p. 2108-19.
30. Phillips, H.S., et al., Molecular subclasses of high-grade glioma predict prognosis, delineate a pattern of disease progression, and resemble stages in neurogenesis. *Cancer Cell*, 2006. 9(3): p. 157-73.
31. Halliday, J., et al., In vivo radiation response of proneural glioma characterized by protective p53 transcriptional program and proneural-mesenchymal shift. *Proc Natl Acad Sci U S A*, 2014. 111(14): p. 5248-53.
32. Sherry, M.M., et al., STAT3 is required for proliferation and maintenance of multipotency in glioblastoma stem cells. *Stem Cells*, 2009. 27(10): p. 2383-92.
33. Singer, E., et al., Reactive oxygen species-mediated therapeutic response and resistance in glioblastoma. *Cell Death Dis*, 2015. 6: p. e1601.
34. Lee, J. and P. Zhou, DCAFs, the missing link of the CUL4-DDB1 ubiquitin ligase. *Mol Cell*, 2007. 26(6): p. 775-80.
35. Wang, Y., et al., CUL4A induces epithelial-mesenchymal transition and promotes cancer metastasis by regulating ZEB1 expression. *Cancer Res*, 2014. 74(2): p. 520-31.
36. Wang, H., et al., DCAF4L2 promotes colorectal cancer invasion and metastasis via mediating degradation of NFkappab negative regulator PPM1B. *Am J Transl Res*, 2016. 8(2): p. 405-18.
37. Mangino, M., et al., DCAF4, a novel gene associated with leucocyte telomere length. *J Med Genet*, 2015. 52(3): p. 157-62.
38. Hellwege, J.N., et al., Gene-based evaluation of low-frequency variation and genetically-predicted gene expression impacting risk of keloid formation. *Ann Hum Genet*, 2018. 82(4): p. 206-215.
39. Liu, H., et al., Functional variants in DCAF4 associated with lung cancer risk in European populations. *Carcinogenesis*, 2017. 38(5): p. 541-551.

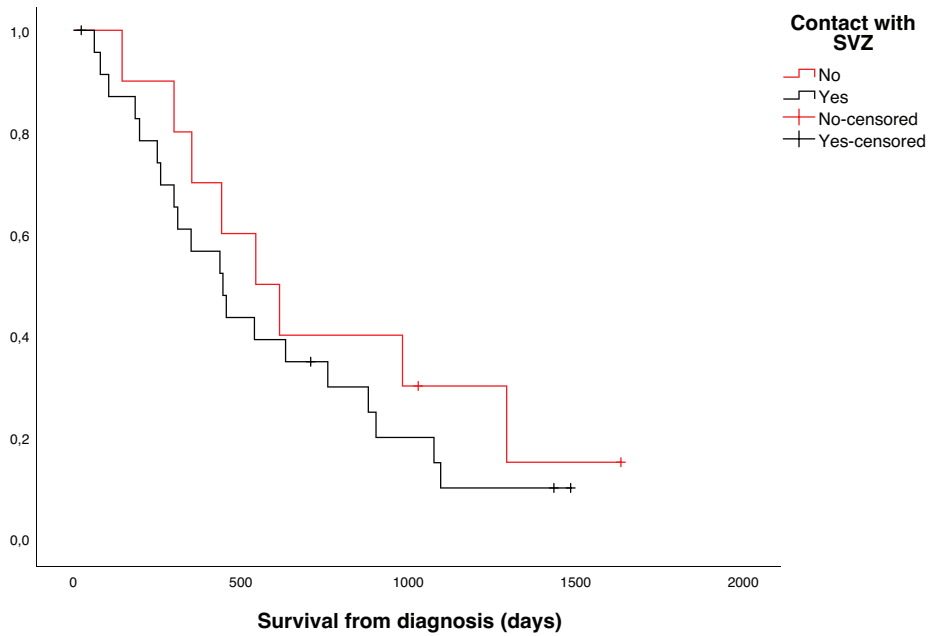
SUPPLEMENTARY FILES

Supplementary table 1 – Hallmark genesets in within SVZ-contacting glioblastoma (*withinSVZ*-samples vs *outsideSVZ*-samples) analysis with FDR<0.25 sorted by p-value. Most gene sets are upregulated in the withinSVZ-samples group, as shown by their positive log fold changes (logFC).

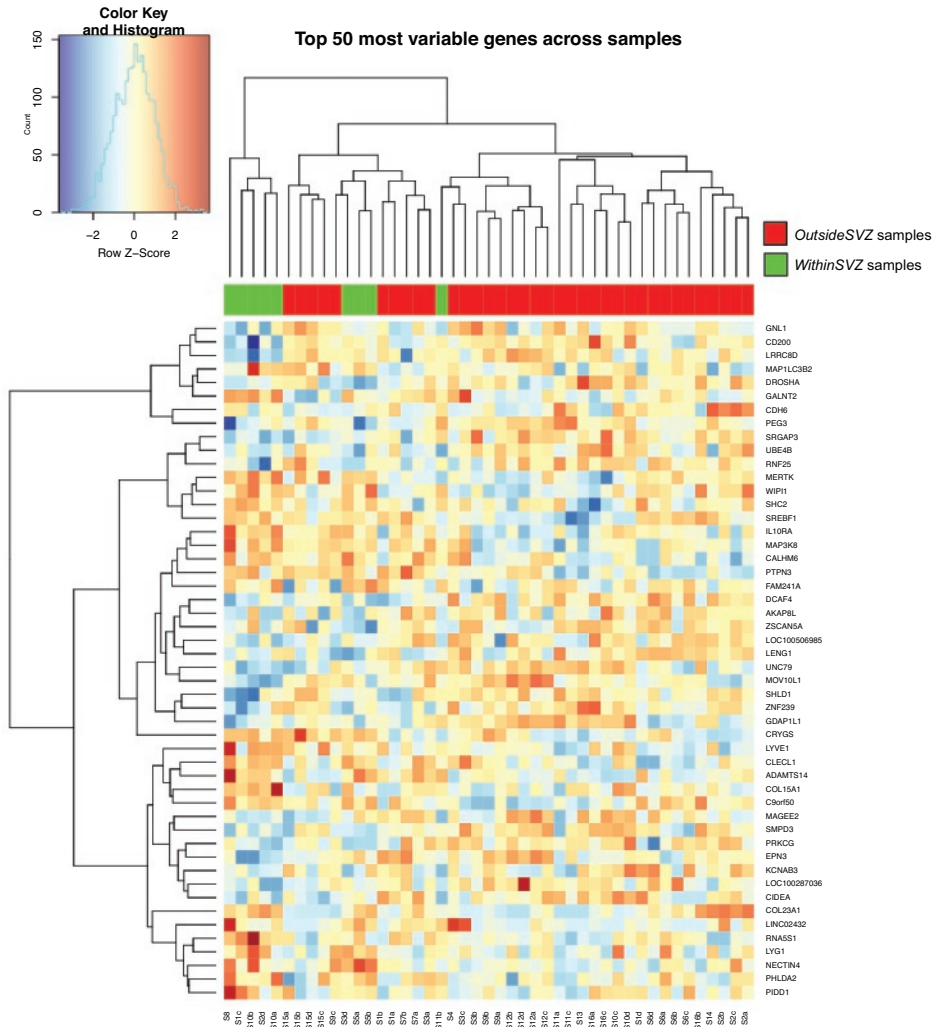
Pathway name	Log Fold Change	p-value	FDR
EPITHELIAL_MESENCHYMAL_TRANSITION	0.41	0.003	0.13
ANGIOGENESIS	0.40	0.006	0.13
APOPTOSIS	0.21	0.01	0.13
IL6_JAK_STAT3_SIGNALING	0.37	0.01	0.13
SPERMATOGENESIS	-0.18	0.01	0.13
COMPLEMENT	0.22	0.02	0.13
UV_RESPONSE_DN	0.12	0.02	0.13
ALLOGRAFT_REJECTION	0.22	0.03	0.13
COAGULATION	0.27	0.03	0.13
IL2_STAT5_SIGNALING	0.18	0.03	0.13
ESTROGEN_RESPONSE_EARLY	0.14	0.04	0.15
INFLAMMATORY_RESPONSE	0.27	0.04	0.15
INTERFERON_GAMMA_RESPONSE	0.26	0.04	0.15
P53_PATHWAY	0.14	0.04	0.15
TGF_BETA_SIGNALING	0.14	0.04	0.15
APICAL_JUNCTION	0.17	0.05	0.16
TNFA_SIGNALING_VIA_NFKB	0.35	0.06	0.16
ESTROGEN_RESPONSE_LATE	0.11	0.06	0.17
HYPOXIA	0.27	0.07	0.17
KRAS_SIGNALING_UP	0.15	0.07	0.17
MYOGENESIS	0.20	0.07	0.17
XENOBIOTIC_METABOLISM	0.13	0.09	0.21
REACTIVE_OXIGEN_SPECIES_PATHWAY	0.17	0.11	0.24
APICAL_SURFACE	0.12	0.12	0.24

Supplementary table 2 – Hallmark genesets in *withinSVZ*-samples vs *outsideSVZ*-samples analysis with FDR<0.25 sorted by p-value. Most gene sets are upregulated in the *withinSVZ*-samples group, as shown by their positive log fold changes (logFC).

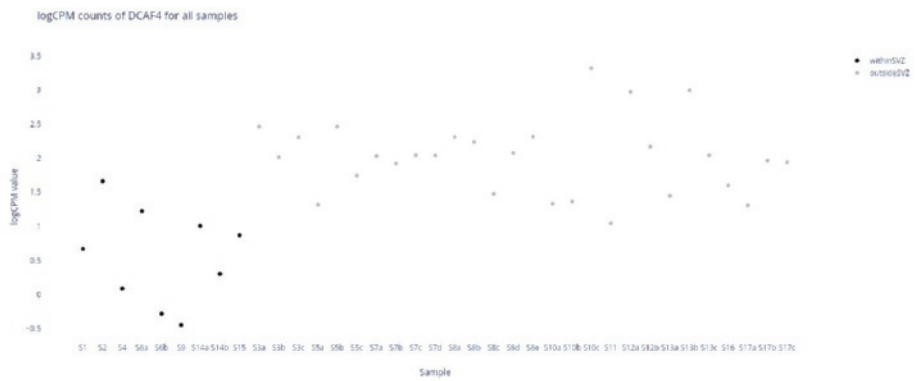
Pathway name	Log Fold Change	p-value	FDR
EPITHELIAL_MESENCHYMAL_TRANSITION	0.56	0.002	0.04
COAGULATION	0.46	0.002	0.04
APOPTOSIS	0.30	0.002	0.04
COMPLEMENT	0.33	0.003	0.04
IL2_STAT5_SIGNALING	0.28	0.005	0.05
HYPOXIA	0.41	0.006	0.05
APICAL_JUNCTION	0.33	0.007	0.05
ESTROGEN_RESPONSE_EARLY	0.23	0.008	0.05
TGF_BETA_SIGNALING	0.22	0.01	0.07
TNFA_SIGNALING_VIA_NFKB	0.44	0.02	0.08
MYOGENESIS	0.37	0.02	0.08
REACTIVE_OXIGEN_SPECIES_PATHWAY	0.35	0.02	0.08
XENOBIOTIC_METABOLISM	0.24	0.02	0.08
P53_PATHWAY	0.21	0.02	0.08
ANGIOGENESIS	0.53	0.03	0.08
IL6_JAK_STAT3_SIGNALING	0.41	0.03	0.08
GLYCOLYSIS	0.23	0.03	0.08
UV_RESPONSE_UP	0.20	0.03	0.08
ESTROGEN_RESPONSE_LATE	0.18	0.04	0.11
INFLAMMATORY_RESPONSE	0.33	0.06	0.14
SPERMATOGENESIS	-0.13	0.06	0.14
UNFOLDED_PROTEIN_RESPONSE	0.17	0.07	0.15
HEME_METABOLISM	0.14	0.07	0.16
UV_RESPONSE_DN	0.14	0.08	0.17
KRAS_SIGNALING_UP	0.20	0.09	0.18
ADIPOGENESIS	0.15	0.12	0.22
ANDROGEN_RESPONSE	0.11	0.12	0.22



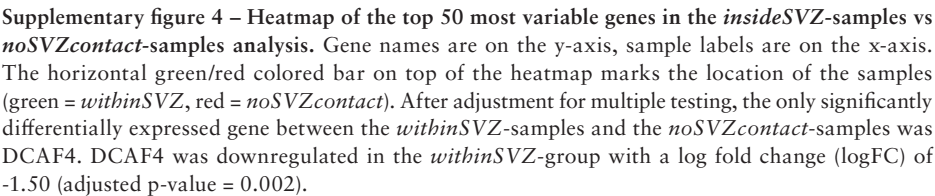
Supplementary figure 1 – Kaplan-Meier plot of patients with SVZ contacting glioblastoma vs. patients with glioblastoma without SVZ contact. Overall survival did not differ significantly between the groups, although a numerically shorter overall survival was observed in patients with SVZ-contacting glioblastoma.

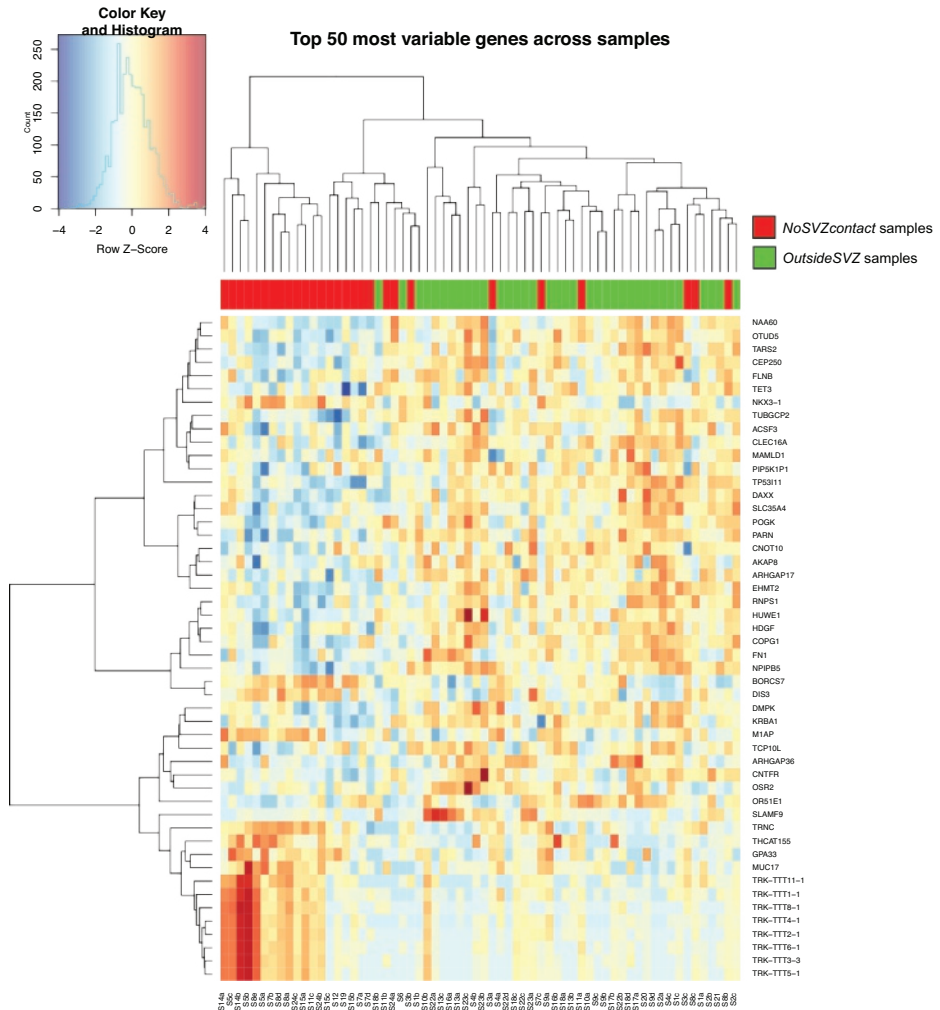


Supplementary figure 2 – Heatmap of the top 50 most variable genes in the within SVZ contacting glioblastoma (*withinSVZ*-samples vs. *outsideSVZ*-samples) analysis. Gene names are vertically placed, whereas sample names are horizontally placed. The horizontal green/red coloured bar on top of the heatmap marks the location of the samples (green = *withinSVZ*, red = *outsideSVZ*). After adjustment for multiple testing, no single genes were significantly differentially expressed between tumor samples from within and outside of the SVZ ($p < 0.05$).

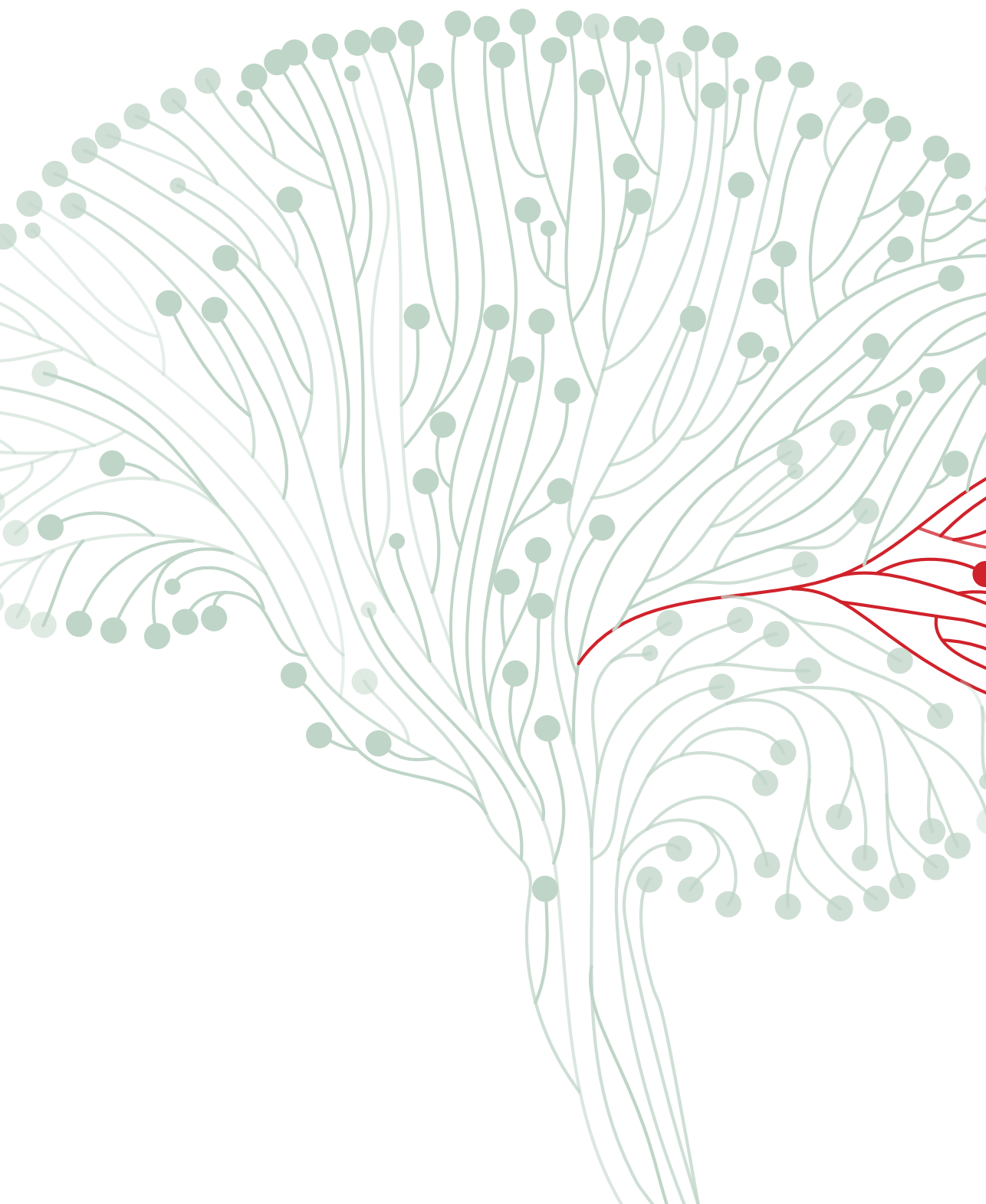


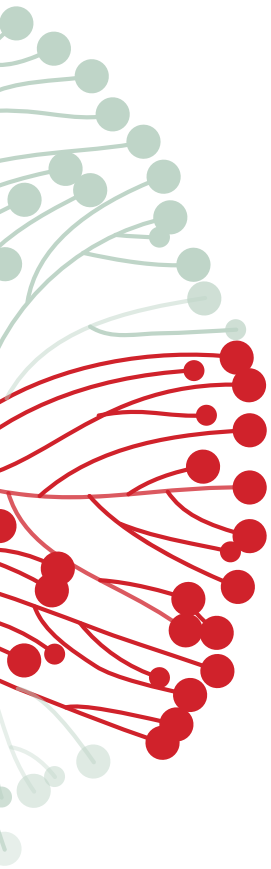
Supplementary figure 3 – logCPM counts of DCAF4 for all samples. Overall, DCAF4 showed lower expression values in *withinSVZ*-samples as compared to *noSVZcontact*-samples. DCAF4 was downregulated in the *withinSVZ*-group with a log fold change (logFC) of -1.50 (adjusted p-value = 0.002).





Supplementary figure 5 – Heatmap of the top 50 most variable genes in the *outsideSVZ*-samples vs. *noSVZcontact*-samples analysis. Gene names are on the y-axis, sample labels are on the x-axis. The horizontal green/red colored bar on top of the heatmap marks the location of the samples (green = *outsideSVZ*, red = *noSVZcontact*). After adjustment for multiple testing, no single genes were significantly differentially expressed between the two groups ($p < 0.05$).





CHAPTER 8

Fractal structure correlates with oxidative metabolic pathway gene expression signature in glioblastoma

Kai J. Miller, Sharon Berendsen, Tatjana Seute, Kirsten Yeom,
Melanie G. Hayden, Gerald A. Grant, Pierre A. Robe.

Published in: Translational Cancer Research 2017;6(6):1275-1282.

ABSTRACT

Background: Fractal structure is found throughout many processes in nature, and often arises from sets of simple rules. We examined MRI contrast enhancement patterns from glioblastoma patients for evidence of fractal structure and correlated these with gene expression patterns.

Methods: For 39 glioblastoma patients, volumetric T1-post-contrast MRI scans were obtained before surgical resection. We calculated the fractal dimension of each tumor's contrast enhancement using a box-counting (cubic scaling) approach. RNA expression microarray data from resected tissue were explored by gene set enrichment analysis (GSEA), and vascular endothelial growth factor (VEGF) expression was determined by immunostaining of resected tissue.

Results: We found robust evidence for fractal structure in the contrast enhancement pattern, with an average fractal dimension of 2.17 ± 0.10 , and a visually apparent split at 2.10. GSEA analysis showed a clear association between high fractal dimension ($\chi > 2.10$) and decreased gene expression in 6 gene sets (of 4,080), all 6 of which are linked to mitochondrial respiration/ATP production pathways. On a protein level, high fractal dimension was correlated with increased VEGF.

Conclusions: There is fractal structure in the volumetric enhancement pattern of glioblastomas. Variation in the fractal dimension, and therefore the complexity of contrast enhancement it reflects, is specifically associated with genetic correlates of a shift to glycolytic metabolism in tumor cells and VEGF. Drugs that restore oxidative metabolism have recently been identified as independent therapeutic agents as well as sensitizing agents for irradiation. Therefore, a radiogenomic marker of glucose metabolism, such as this fractal structure in enhancement, might help to guide individualized therapy.

INTRODUCTION

Fractals are structures that have the same general physical appearance when viewed over many scales of magnification [1]. There are many examples of fractals in nature and biology; some famous ones are snowflakes, coastlines, retinal vasculature, and Romanesco Broccoli [2-4]. Each fractal is associated with a fractal dimension, a statistical measure that quantifies how detail in a pattern changes with the spatial scale it is measured at [1]. In general, a higher fractal dimension implies a more complex structure. Sophisticated fractal structures can emerge from iterations of simple growth rules. For example, the complex branching structure of snowflakes results from a simple tradeoff between surface tension and heat diffusion [5]. This emergence of fractal structure may be of particular interest for those that study brain tumors—firstly because tumors emerge when a few genetic mutations change the rules for how cells behave with one another and grow, and secondly because blood vessels in the brain can develop in a fractal manner [6].

The term “radiogenomics” is used to describe the relationship between imaging findings and genomic changes, with the hope of inferring molecular properties without the need to obtain tissue surgically. These approaches have already established some direct links between imaging features and underlying molecular changes in brain tumors, particularly glioblastoma [7-11]. Recent molecular studies have found that there are genomic subtypes of brain tumors that confer different prognoses and different susceptibility to surgical, radiation-based, and medicinal intervention. If one can accurately infer underlying tumor biology from imaging rather than surgical specimen, conservative therapies may be initiated with less associated morbidity and at lower cost. Existing glioblastoma radiogenomic studies have examined the gross volumes of the tumors, contrast enhancement volumes, and qualitative shape [11], but quantitative metrics to describe the internal structure of the tumor have not yet been developed as markers.

We have devised a new way to quantitatively describe volumetric brain imaging using the fractal dimensionality of contrast enhancement. In glioblastoma tumors, gadolinium enhancement reflects the diminished blood-brain barrier integrity from abnormally permeable endothelial cell layers. This increased permeability is both a property of newly-formed small blood vessels, and also a result of circulating endothelial growth factors that induce constant remodeling of the tumor vasculature [12,13]. Therefore, quantifying the structure of enhancement in glioblastoma tumors may specifically inform us about a combination of both microvascular structure and angiogenic drive. The purpose of our study was to measure whether the large-scale structure of brain tumors exhibited fractal structure and to correlate these results with biological tumor characteristics.

METHODS

Patients

After institutional review board approval (approval number 09-420), we retrospectively identified a cohort of 42 patients, who presented to care at the UMC Utrecht from February 2010 to November 2012. Each of these underwent open resection of intracranial lesions that were histologically confirmed to be *de novo* WHO grade 4 glioblastoma. All patients provided an informed consent for the (anonymized) genetical/biological analyses of their tumor samples and the use of the relevant clinical/radiological information. Patients with both treatment-naïve MR imaging and fresh-frozen surgical tissue specimens available for molecular analysis were included in this study. Survival data, documented in days from surgery, were obtained from hospital records, and analyzed with Kaplan-Meier curves and log-rank testing.

Imaging

All patients had pre-operative gadolinium contrasted T1 MRI images with voxel resolution of $1 \times 1 \times 1 \text{ mm}^3$, and plainly visible contrast enhancing tumors. For each patient, a three-dimensional tumor boundary trace and contrast intensity threshold was manually identified by one investigator (Kai J. Miller), who was blinded to demographic, clinical, pathologic, and molecular data. For multifocal glioblastoma, all masses were traced, and the one with the largest volume was retained for further analysis.

Tumor enhancement fractal structure (illustrated in Figure 1)

For each tumor, a fractal dimension (Minkowski-Bouligand dimension/scaling exponent) using was calculated a 3D box-counting (cubic) approach [14,15]. Each T1 post-contrast tumor volume was thresholded at an intensity determined based upon a histogram of voxel contrast intensities of the isolated tumor as well as visual inspection of the MRI. The thresholded tumor volume was then parsed by cube-counting using a fixed grid scan, which determines the number of cubes, N , of edge length ℓ , needed to cover the thresholded volume. The fractal dimension, χ , is estimated from the relation $N \propto \ell^{-\chi}$, by performing a linear least-squares fit of $\log_2 N$ versus ℓ over a set fit range. The fit range was theoretically constrained on the lower end by voxel resolution, and on the upper end by tumor size. For stable fits, we chose the range $\ell = 2$ voxels to $\ell < \text{middle dimension of tumor bounding region}$, with interval steps of $\ell = 2^n$ (see supplemental comment on fitting). Prior to further examination, 3 patients were excluded from study because their tumor size was too small to estimate an acceptable fit range. One examiner (Kai J. Miller) determined natural split value of $\chi = 2.10$ from the histogram of fractal dimension values for the 39 patients included in the cohort, and a separate examiner (Pierre A. Robe) independently performed the molecular analyses. This natural split was confirmed appropriate by applying a Gaussian mixture model to the set of fit fractal dimensions, and drawing the fit threshold such that

all values below threshold have >90% chance of belonging to the lower fractal dimension group (this results in $\chi = 2.099$ before rounding as the tumor with the highest fractal dimension to belong to the lower group). Future studies, with larger cohorts, may further refine this threshold.

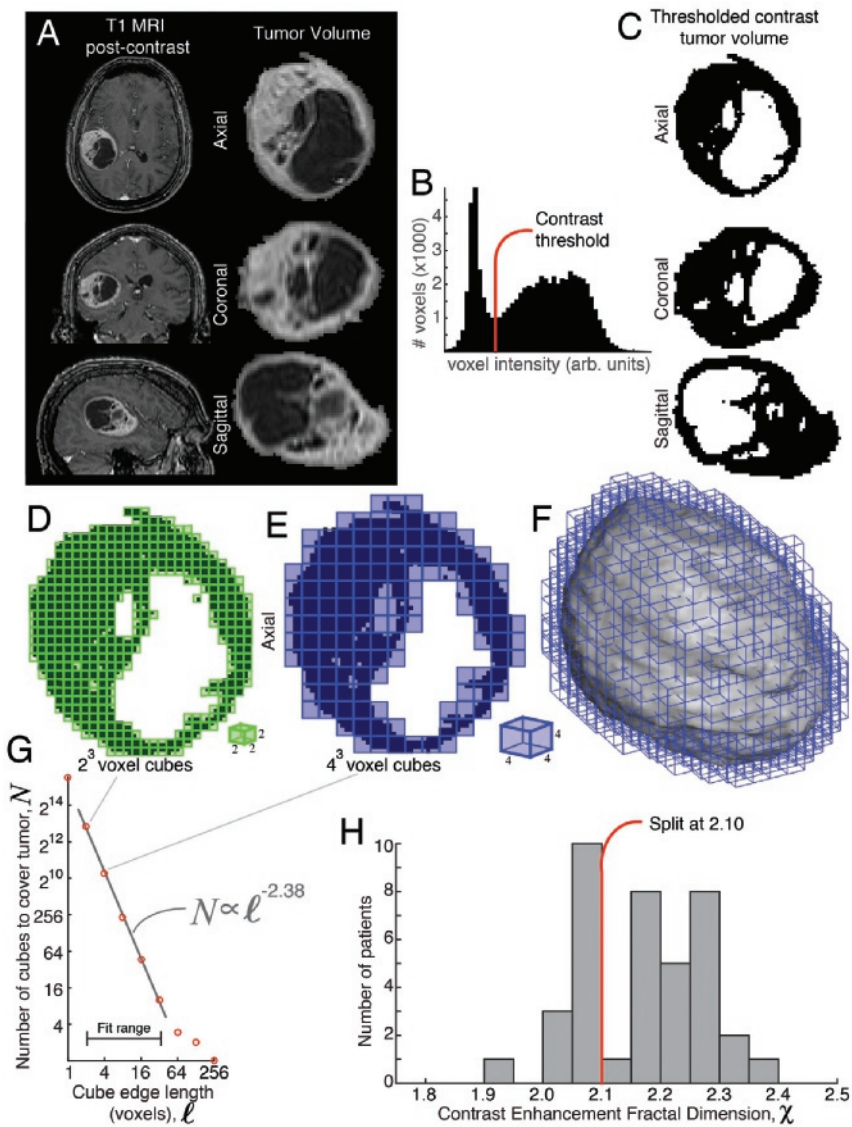


Figure 1 – Quantifying fractal dimensionality of contrast enhancement in glioblastomas. (A) Post-contrast T1 MRI scan shows an enhancing tumor of the left hemisphere (in-situ – left column; isolated – right column). (B) A contrast threshold is determined based upon a histogram of voxel contrast intensities of the isolated tumor as well as visual inspection of (A). (C) The thresholded tumor volume

Figure 2 - VPA does not increase histone acetylation activity in tumor tissue from glioblastoma patients (continued). from (A). (D) A volumetric box-counting (cubic scaling) method, which determines the number of cubes (N) of for each edge length (ℓ) needed to cover the thresholded volume. An axial section is shown here, with cubes of $\ell = 2$ voxels per edge. (E) As in (C), but with cubes of $\ell = 4$ voxels per edge. (F) Tumor surface shown from external perspective, with cubes of $\ell = 4$ voxels per edge. (G) The fractal dimension, χ , is estimated from the relation $N \propto \ell^{-\chi}$, by performing a linear fit of $\log_2 N$ versus $\log_2 \ell$ over a set fit range. (H) The set of fractal dimensions for our patient cohort ($n=39$) showed a natural split at $\sim\chi=2.10$. GSEA analysis showed a robust association between this split in fractal dimension and mitochondrial respiration/ATP production pathways ($p<0.05$, $FDR<0.15$).

Fresh-frozen tissue samples and mRNA expression analysis

Fresh-frozen surgical samples of glioblastoma patients were prospectively collected between February 2010 and November 2012. RNA was extracted with the Nucleospin® TriPrep kit (Macherey-Nagel, Bethlehem, PA, USA) to the manufacturer's instructions. Affymetrix HG U133 plus 2.0 array preparation and scanning were performed according to the manufacturer's protocol and as reported previously [16]. Exploratory gene set enrichment analyses (GSEA) were performed after RMA-normalization [17] and correction for batch effects, with the Partek Genomics suite platform (Partek® Genomic Suite 6.6). Analyses were performed with the Broad Institute MySig libraries of curated gene sets C2&C4, version 5.0 (17), 1,000 permutations and default additional parameters. A false discovery rate (FDR) threshold of 0.15 was chosen to be more stringent than the recommended threshold level of 0.25 for GSEA studies [17].

Vascular endothelial growth factor (VEGF) expression assessment (illustrated in Figure 2)

Based upon initial findings with the GSEA analysis that showed an association between fractal dimension of contrast enhancement and oxidative metabolism (Table 1), we decided to test the samples for VEGF expression. Formalin fixed, paraffin embedded tissue samples of 35 of the patients in our cohort were included in tissue microarrays. Construction and processing of tissue microarrays and methods on immunohistochemical staining have been reported in a previous study [18]. Rabbit polyclonal VEGF antibody was used for staining (1:100, Thermo Scientific, Waltham, MA, USA). Assessment of cytoplasmic VEGF expression was performed blinded to the clinical and imaging data. The VEGF expression was quantified as percentage of cytoplasmic staining, and scored by visual slide inspection: 0, no staining; 1, 1–25% of cells stain; 2, 26–50%; 3, 51–75%; 4, 76–100%. Images were obtained at 40× magnification using a Nanozoomer 2.0HT digital slide scanner (Hamamatsu Photonics, Hamamatsu City, Japan).

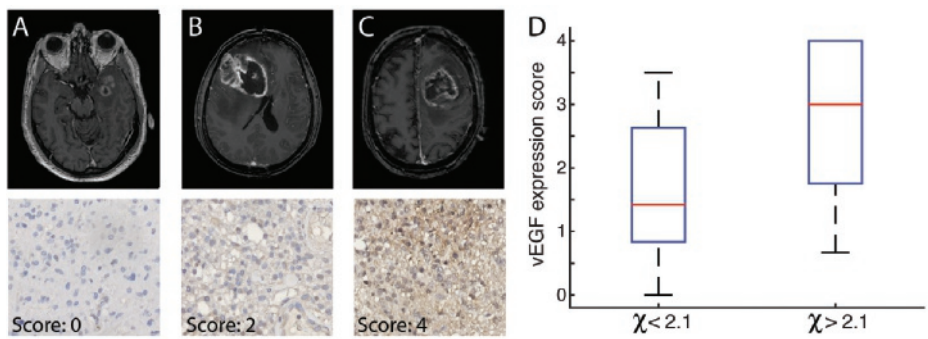


Figure 2 – Quantifying VEGF expression. (A-C) Example slides to illustrate VEGF expression-grading scores (A-0, B-2, C-4, magnified at 40x) are shown for 3 tumors, with corresponding axial MRIs. (D) Box-plot of VEGF expression score, sorted by fractal dimension. On each box, the central red mark is the median, the edges of the blue box are the 25th and 75th percentiles, and the black whiskers extend to the most extreme datapoints the algorithm considers to be not outliers.

Table 1 - GSEA associations with fractal exponent (split at $\chi=2.10$), all gene expression decreased with increasing fractal exponent (e.g. $\chi>2.10$, $p<0.001$).

Gene Set (MsigDB C2&C4 collections)	# Markers	Enrichment Score	FDR
Reactome respiratory electron transport	134	0.66	0.090
Reactome respiratory electron transport, ATP synthesis by chemiosmotic coupling & heat production by uncoupling proteins	169	0.65	0.099
Reactome citric acid cycle TCA cycle	47	0.73	0.106
Kegg citrate cycle TCA cycle	65	0.72	0.114
Reactome TCA cycle and respiratory electron transport	254	0.61	0.122
Mootha TCA	39	0.67	0.148

RESULTS

Note that in addition to these results, there is also a supplement, which contains a comment on the fitting, four supplemental figures (Figures S1–S4), and one supplemental table (Table S1).

Fractal structure of contrast enhancement in glioblastoma

We found robust evidence for fractal structure in the contrast enhancement pattern, with a fractal dimension of 2.17 ± 0.10 (Figure 1 and supplemental Figure S1— significantly different from 2.00, $P<10^{-9}$ by unpaired t-test). There was a significant correlation between fractal dimension and tumor-volume ($r=0.35$, $P=0.03$, t-test), contrast-enhancement-volume ($r=0.54$, $P=4\times10^{-4}$, t-test), and volumetric-fraction-of-tumor-enhancement ($r=0.35$,

$P=0.03$, t-test). However, there was no correlation between survival and fractal dimension ($P=0.75$, log-rank test, supplemental Figure S3). When comparing patients with tumors of fractal dimension above and below 2.1, prognosis did not vary between both groups, both in univariable and Cox multivariable analyses (taking age and KPS into account). Age, KPS and post-operative treatment do not vary between both groups (Table S1). All assessed tumors were IDH1 WT (25% of IDH data missing, evenly distributed between both groups). Tumor volumes were similar in both groups, and all tumors had a gross total resection.

Fractal dimension correlates with specific gene set expression pattern

Exploratory GSEA analysis showed a strong association between fractal dimension and mitochondrial respiration/ ATP production pathways (Table 1: all associations significant with $P<0.001$, at $FDR<0.15$). The gene set enrichment assay assesses correlations of a split parameter (in this case our measure of fractal dimension, split at visually-apparent and fit-confirmed threshold $\chi=2.10$, as illustrated in Figure 1H) with a large library of RNA expression gene clusters [MsigDB v5.0 C2&C4 curated gene set collections [17]]. This assessment was performed over 4,080 potential gene set pathways (Figure S2), and only 6 gene sets met significance threshold. All of these showed decreased gene expression for tumors with higher fractal exponent (e.g., $\chi>2.10$). The full set of 4,080 gene sets tested for is listed in supplemental <http://tcr.amegroups.com/public/addition/tcr/supp-tcr.2017.10.15.pdf>.

Higher fractal dimension is correlated with increased VEGF expression

Increased fractal dimension was correlated with increased VEGF expression ($r=0.45$, $P=0.006$, t-test). The split in fractal dimension at $\chi=2.10$ is associated with significant increase in VEGF expression (illustrated in the box-plot of Figure 2D, $P=0.01$, t-test).

DISCUSSION

The fractal dimension of approximately 2.15 that we observe in glioblastoma enhancement quantitatively describes a structure that is significantly more complex than a simple surface, such as a hollow sphere (also fractal, but with dimension 2), but less complex than some other volumetric structures with extensive branching, such as a broccoli (fractal with dimension 2.66) [19]. Interestingly, there is variation in the complexity of enhancement across tumors from different patients. Being able to quantitatively describe the internal structure of tumors in this way may be an important new tool. However, there is no a priori reason why glioblastoma tumors should have fractal structure at all—one can easily imagine other tumors, with plainly observable structural complexity at one particular level of magnification, which would be non-fractal. For example, metastatic adenocarcinomas

would not be expected to have self-similarity at different spatial scales. Instead, they would have well-defined, non-fractal, structure reflecting the glandular anatomy of the tissue of origin.

The fractal structures generated by mathematical simulation have infinite resolution, and the fractal fit can extend over an arbitrarily large range. However, real world phenomena have structure that can only be measured over a limited range—e.g., snowflakes only grow to a few millimeters and coastlines can't be measured in centimeters. Our measurements are no exception, and we were spatially limited in quantification of fractal structure on the on the upper end by the finite width of tumors at ~3–5 cm, and the lower end by MRI voxel edge length of 1 mm. In future studies, one might attempt to work around this lower limit by obtaining smaller voxel sizes with higher field magnets (e.g., 7T).

Because contrast enhancement reflects fragile neovascularization within the glioblastoma tumor, the fractal measurement may directly reflect microvascular structure and angiogenic drive, and indirectly reflect genetic expression profiles of the tumor. Indeed, a correlation between fractal structure and underlying tumor biology was found; increases in the fractal dimension of contrast enhancement correlate with decreased oxidative pathway gene set expression (a shift to glycolytic metabolism), with increased VEGF expression (Figure 2). We propose two potential explanations for this, one anaerobic and one aerobic. In the anaerobic case, one might presuppose that some of these glioblastoma tumors outgrow their blood supply, forcing them to undergo an ischemia driven glycolytic shift, while simultaneously releasing angiogenic factors like VEGF to induce rapid neovascularization. The correlation between increasing fractal dimension and increased tumor volume may suggest that larger tumors produce more ischemic drive for a glycolytic shift while releasing VEGF in an attempt to improve oxygen delivery. Conversely, there may be an aerobic explanation for our findings, independent of ischemic drive: many tumors show a distinct shift from mitochondrial oxidative phosphorylation to glycolysis for energy production, known as the “Warburg effect” (aerobic glycolysis) [20,21]. This involves a number of changes in genetic expression, such as stabilization of HIF-1 α , and increased expression of VEGF, GLUT1, and pyruvate dehydrogenase kinase. These changes encourage tumor growth by reducing reactive oxygen species levels, increasing ATP supply, and providing structural elements for new cell growth [20,21]. With this connection in mind, future studies may measure HIF-1 α and markers of metabolism using an acute frozen preparation of tumor tissue, before it is affected by ischemia at time of resection.

Predictive radiogenomic features in MRI that reflect molecular aberrations and subtypes of tumors would serve as a preliminary surrogate prior to invasive and expensive genomic tissue testing, and facilitate real-time translation/integration of genomic-based studies into the clinic. If our finding hints at a possible metabolic drive for vascularization during

tumor development, in response to the Warburg effect, it begs the question: does metabolic change drive neovascularization independent of ischemic drive to do so? Administration of an anti-VEGF agent for glioblastoma results in decreased volume of tumor enhancement, but increased glycolysis and increased tumor invasion [22]. This suggests that perhaps increased VEGF expression comes as a downstream effect of other glycolysis-associated changes that promote tumor growth, but that VEGF is not itself of direct benefit to the developing tumor. Conversely, inhibitors of pyruvate dehydrogenase kinase like dichloroacetate reverse the Warburg effect and potentiate formation of oxidating free radicals [23]. Dichloroacetate decreases tumor invasion [24], is safe for glioblastoma patients (based upon phase 1 FDA trial) [25], and is rapidly gaining popularity as an adjunct agent in glioblastoma therapy [24,26-28]. HIF-1 α is a transcription factor that increases transcription of VEGF, enzymes of glycolysis, and glucose transporters; many tumors exhibiting the Warburg effect have loss-of-function mutations in enzymes that degrade HIF-1 α [21]. Initiation of HIF-1 α translation is blocked the agent auraptene, which has been shown to inhibit glycolytic and mitochondrial metabolism, decrease cell motility, and inhibit VEGF-induced neovascularization [29]. Tumors with higher fractal dimension in enhancement structure may be selectively susceptible to administration of dichloroacetate, auraptene, and other emerging agents. Pending further exploration, this fractal-dimension measurement might help to non-surgically identify which patients would benefit from these agents.

CONCLUSIONS

Quantification of fractal structure in tumor enhancement is a new type of methodology for the emerging radiogenomic toolbox, and may be of direct clinical benefit if it can guide therapies without need for tissue sample. We observed fractal structure in the volumetric contrast enhancement pattern of glioblastoma tumors, with an average fractal dimension of approximately 2.15, but variation from ~2.0–2.3. Higher fractal dimension correlated specifically with decreased gene expression for oxidative metabolic pathways on GSEA analysis, and also correlated with increased VEGF expression by immunostaining. Together, these measurements suggest that increased fractal dimension of glioblastoma enhancement reflects a glycolytic shift in tumor, and may indicate which patients would benefit from emerging anti-glycolysis agents like auraptene and dichloroacetate.

REFERENCES

1. Mandelbrot BB. Self-affine fractals and fractal dimension. *Physica Scripta* 1985;32:257.
2. Mandelbrot BB. How long is the coast of Britain. *Science* 1967;156:636-8.
3. Green DG. Fractals and scale. 1993, self published.
4. Family F, Masters BR, Platt DE. Fractal pattern formation in human retinal vessels. *Physica D* 1989;38:98-103.
5. Ben-Jacob E, Goldenfeld N, Langer J, et al. Dynamics of interfacial pattern formation. *Phys Rev Lett* 1983;51:1930.
6. Risser L, Plouraboué F, Steyer A, et al. From homogeneous to fractal normal and tumorous microvascular networks in the brain. *J Cereb Blood Flow Metab* 2007;27:293-303.
7. Zinn PO, Mahajan B, Sathyan P, et al. Radiogenomic mapping of edema/cellular invasion MRI-phenotypes in glioblastoma multiforme. *PLoS One* 2011;6:e25451.
8. Gutman DA, Cooper LA, Hwang SN, et al. MR imaging predictors of molecular profile and survival: multi- institutional study of the TCGA glioblastoma data set. *Radiology* 2013;267:560-9.
9. Diehn M, Nardini C, Wang DS, et al. Identification of noninvasive imaging surrogates for brain tumor gene-expression modules. *Proc Natl Acad Sci U S A* 2008;105:5213-8.
10. Naeini KM, Pope WB, Cloughesy TF, et al. Identifying the mesenchymal molecular subtype of glioblastoma using quantitative volumetric analysis of anatomic magnetic resonance images. *Neuro Oncol* 2013;15:626-34.
11. Itakura H, Achrol AS, Mitchell LA, et al. Magnetic resonance image features identify glioblastoma phenotypic subtypes with distinct molecular pathway activities. *Sci Transl Med* 2015;7:303ra138.
12. Brasch R, Pham C, Shames D, et al. Assessing tumor angiogenesis using macromolecular MR imaging contrast media. *J Magn Reson Imaging* 1997;7:68-74.
13. Roberts HC, Roberts TP, Brasch RC, et al. Quantitative measurement of microvascular permeability in human brain tumors achieved using dynamic contrast-enhanced MR imaging: correlation with histologic grade. *AJNR Am J Neuroradiol* 2000;21:891-9.
14. Liebovitch LS, Toth T. A fast algorithm to determine fractal dimensions by box counting. *Physics Letters A* 1989;141:386-90.
15. Perret J, Prasher S, Kacimov A. Mass fractal dimension of soil macropores using computed tomography: from the box-counting to the cube-counting algorithm. *Eur J Soil Sci* 2003;54:569-79.
16. Artesi M, Kroonen J, Bredel M, et al. Connexin 30 expression inhibits growth of human malignant gliomas but protects them against radiation therapy. *Neuro Oncol* 2015;17:392-406.
17. Subramanian A, Tamayo P, Mootha VK, et al. Gene set enrichment analysis: a knowledge-based approach for interpreting genome-wide expression profiles. *Proc Natl Acad Sci U S A* 2005;102:15545-50.
18. Berendsen S, Varkila M, Kroonen J, et al. Prognostic relevance of epilepsy at presentation in glioblastoma patients. *Neuro Oncol* 2016;18:700-6.
19. Kapelner A, Schupack V, Golomshtok M, et al. Fractal Dimension of Broccoli. *The Physics Factbook*. 2002. Available online: <https://hypertextbook.com/facts/2002/broccoli.shtml>
20. Vander Heiden MG, Cantley LC, Thompson CB. Understanding the Warburg effect: the metabolic requirements of cell proliferation. *Science* 2009;324:1029-33.

21. Linehan WM, Rouault TA. Molecular pathways: fumarate hydratase-deficient kidney cancer—targeting the Warburg effect in cancer. *Clin Cancer Res* 2013;19:3345-52.
22. Keunen O, Johansson M, Oudin A, et al. Anti-VEGF treatment reduces blood supply and increases tumor cell invasion in glioblastoma. *Proc Natl Acad Sci U S A* 2011;108:3749-54.
23. Velpula KK, Bhasin A, Asuthkar S, et al. Combined targeting of PDK1 and EGFR triggers regression of glioblastoma by reversing the Warburg effect. *Cancer Res* 2013;73:7277-89.
24. Kumar K, Wigfield S, Gee HE, et al. Dichloroacetate reverses the hypoxic adaptation to bevacizumab and enhances its antitumor effects in mouse xenografts. *J Mol Med (Berl)* 2013;91:749-58.
25. Dunbar E, Coats B, Shroads A, et al. Phase 1 trial of dichloroacetate (DCA) in adults with recurrent malignant brain tumors. *Invest New Drugs* 2014;32:452-64.
26. Shen H, Hau E, Joshi S, et al. Sensitization of Glioblastoma Cells to Irradiation by Modulating the Glucose Metabolism. *Mol Cancer Ther* 2015;14:1794-804.
27. Shen H, Decollogne S, Dilda PJ, et al. Dual-targeting of aberrant glucose metabolism in glioblastoma. *J Exp Clin Cancer Res* 2015;34:14.
28. Michelakis ED, Sutendra G, Dromparis P, et al. Metabolic modulation of glioblastoma with dichloroacetate. *Sci Transl Med* 2010;2:31ra34.
29. Jang Y, Han J, Kim SJ, et al. Suppression of mitochondrial respiration with auraptene inhibits the progression of renal cell carcinoma: involvement of HIF-1 α degradation. *Oncotarget* 2015;6:38127.

SUPPLEMENTARY FILES

Supplemental comment on fitting

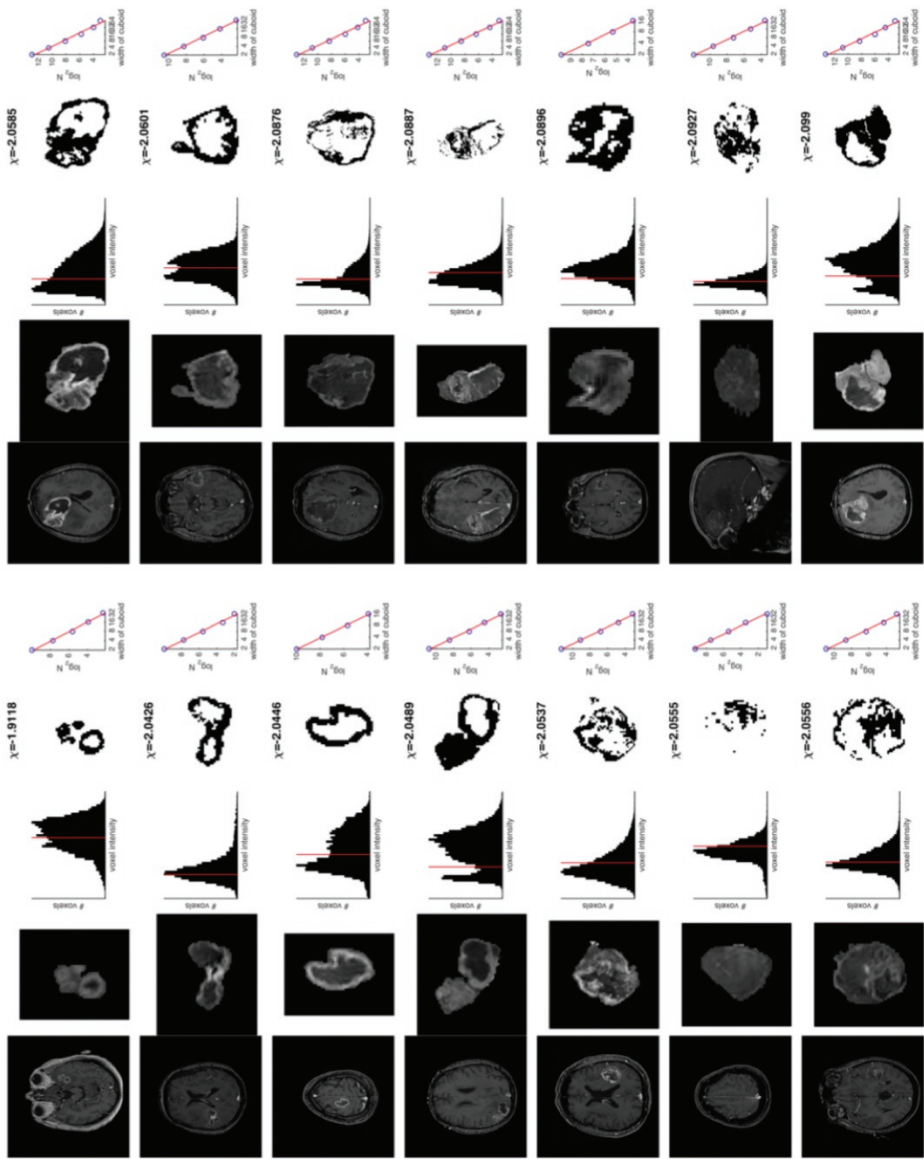
Prior to any calculation, we chose a set of steps to maximize the simplicity and stability of the scaling exponent fit, with as few assumptions as possible. Our technique for estimating the scaling exponent (fractal dimension) of each tumor is based upon a standard calculation to quantify the amount of “roughness in detail” for volumetric images at a variety of magnifications. As illustrated in Figure 1, cubes of various sizes are overlaid on the contrast-thresholded volume. This is an implementation of what is commonly called a “box-counting approach” [14,15].

We chose $\ell = 2$ voxels for the lower limit of cube size (instead of $\ell = 1$), so that the edge effect from thresholding across smooth contrast gradations is robust against the exact choice of threshold. To determine an upper limit for cube size, we fit each thresholded tumor contrast volume with a bounding box (rectangular cuboid). The upper limit for cube size was then set to the largest power of 2 less than the middle dimension of the bounding box. This ensured that cubes at the upper limit would still resolve at least some structure in the tumor, rather than simply a cube containing the whole tumor volume. We chose a fixed grid corresponding to the native volume of the MRI instead of several other potential alternatives. For example, if a grid corresponding to the principal axes of the tumor were preferred, then the MRI would have to be resliced—which introduces correlations when calculating the interpolation to new voxel space. In principle, a variable grid origin could be chosen for each cube size, but we defer this to future study.

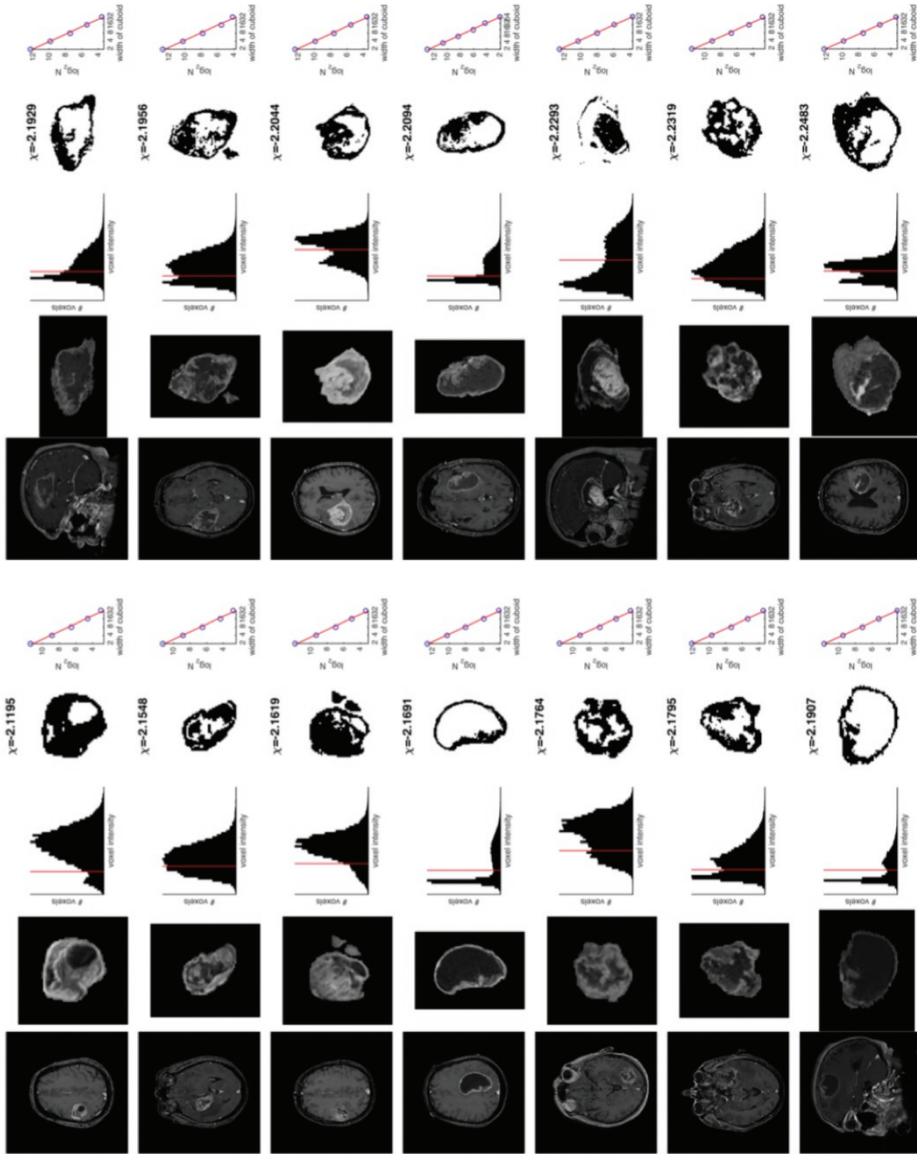
We chose cubes of edge length of edge length $\ell \propto 2^n$ voxels. Our reason for this was to have even density of points on the log-log plot, prior to least-squares fit. A common mistake when performing this type of fit would be to calculate the number of cubes needed to cover the thresholded volume with a linear density of points (e.g., $\ell \propto n$), and apply a global least squares fit. However, on a log-log plot, that assigns too much weight to the highest density of data points, at higher cube sizes, where the orientation of the principal axes of the tumor to the grid orientation, and relatively few number of cubes needed to cover the contrast, make the data noisiest. In future studies, with finer voxel resolution (from 7T scanners), we plan to employ more robust metrics to make these exponent fits [30].

SUPPLEMENTAL REFERENCES

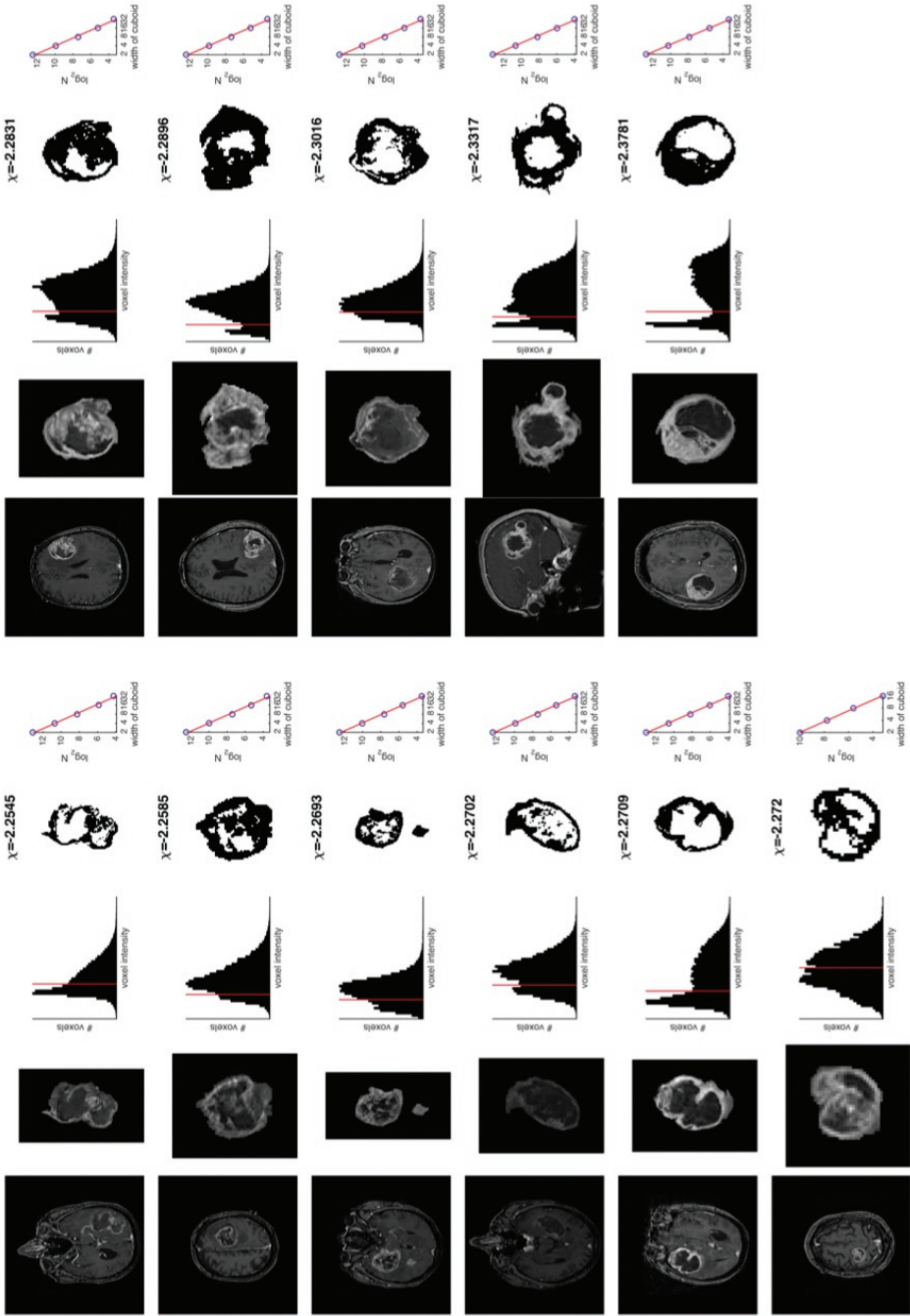
30. Clauset A, Shalizi CR, Newman ME.
Power-law distributions in empirical data.
SIAM Review 2009;51:661-703.



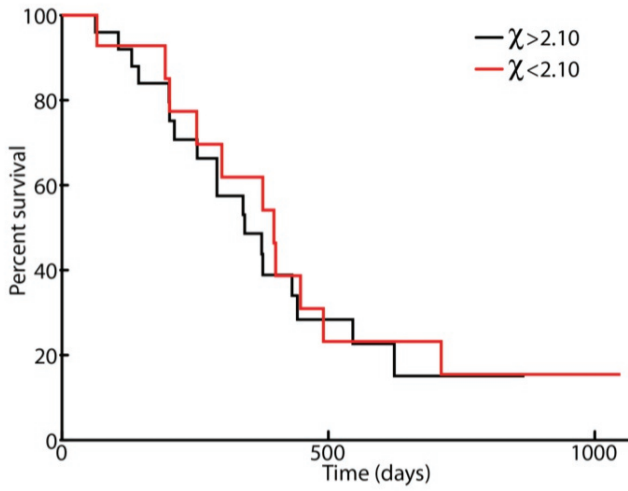
Supplemental figure S1 - (in 3 parts): Exponents for all tumors, sorted by estimated exponent, with representative cross-section, as in Figure 1 of the main text.



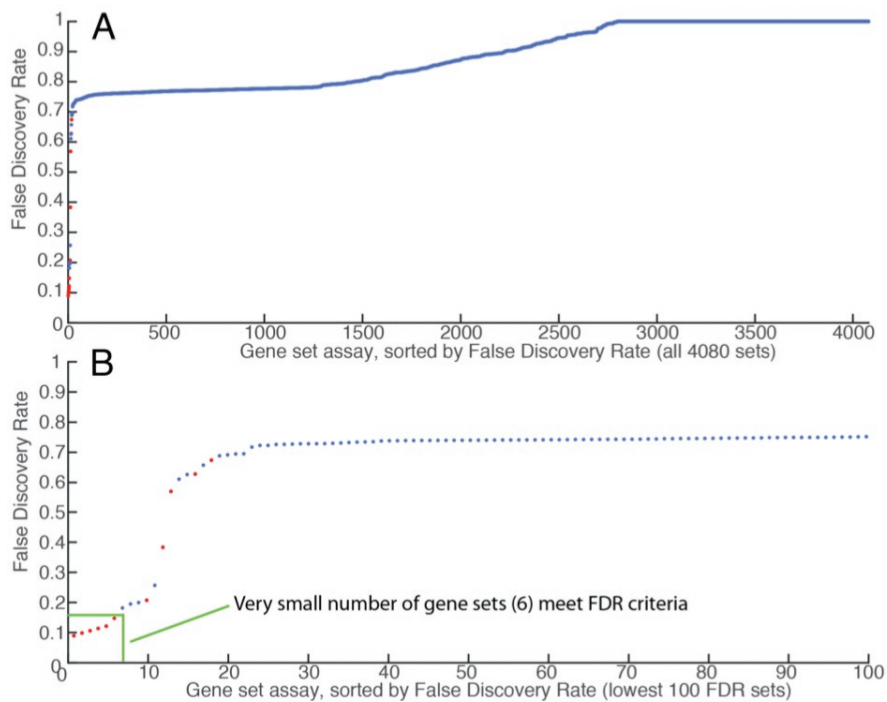
Supplemental Figure S1 (continued) – Exponents for all tumors, sorted by estimated exponent, with representative cross-section, as in Figure 1 of the main text.



Supplemental Figure S1 (continued) – Exponents for all tumors, sorted by estimated exponent, with representative cross-section, as in Figure 1 of the main text.



Supplemental Figure S2: Kaplan-Meier survival curve. There is no significant difference in survival for the $\chi = 2.10$ split.



Supplemental Figure S3: (A) Plot of estimate FDR for all 4080 gene sets, after sorting by FDR. (B) Plot of lowest 100 FDR gene sets. Note that only 6 gene sets meet criteria of $p < 0.001$ and $FDR < 0.15$. Red dot indicates $p < 0.001$. See <http://www.broadinstitute.org/cancer/software/gsea/wiki/index.php/FAQ> for further detail.

Table S1: Patient characteristics
available online at <http://tcr.amegroups.com/article/view/16581>





CHAPTER 9

General discussion & Recommendations

Sharon Berendsen, Tom J. Snijders & Pierre A. Robe.

In this thesis, prognostic factors in glioblastoma were explored with a translational approach. We analyzed clinical and radiological features for prognostic relevance and explored associations with underlying tumor biology. First, the focus lies on the prognostic role of epilepsy at diagnosis and anti-epileptic drug treatment in glioblastoma patients. Associated tumor biological alterations, and biological effects of anti-epileptic drugs are explored. Then, the observed correlations between radiologic features of glioblastomas and specific gene and protein expression signatures are described.

Since glioblastoma is both an oncological and neurological disease, both aspects are of relevance to the treatment options and quality of life of the patient. The translational approach in this thesis serves purposes for the oncological and neurological field, as will be further detailed below. Correlations between gene and protein expression signatures and clinical features (e.g. seizures, subventricular zone (SVZ) location) can provide insight in underlying tumor biology and oncogenic pathways, but can also aid in the quality of life of the patients, by increasing the understanding of neurological symptoms, such as epilepsy, and their treatment.

The research in this thesis contributes to knowledge of (1) tumor biology in glioblastoma, hopefully aiding in the development of more effective therapies, (2) prognostic factors in glioblastoma patients, which could aid patients and physicians in clinical decision making, tailoring of treatment, and reliable counseling of patients, (3) mechanisms of tumor-associated epilepsy and anti-epileptic drug treatment, allowing better clinical decision making in the treatment of glioblastoma patients who experience seizures, and possibly point the way towards more effective anti-epileptic drugs for glioma patients.

This thesis starts with an extensive analysis of the prognostic relevance and biological correlates of epilepsy at diagnosis and anti-epileptic drugs in glioblastoma patients. Multiple reports on *in vitro* experiments and early clinical data suggested anti-tumor properties and clinical benefit on survival for the anti-epileptic drug valproic acid in glioblastoma patients. In **chapter 2**, the preclinical and clinical evidence for this hypothesis, as was available at the start of this research project, is reviewed. This review formed the basis for the research presented in the following chapters.

Based on the HDAC inhibitory properties of valproic acid, we proceeded in **chapter 3** to explore the effects of VPA on histone acetylation in human glioblastoma samples. First, we confirmed that in our hands *in vitro*, VPA increased histone acetylation in an established glioma cell line and primary cell culture. Secondly, we analyzed the effects of VPA on histone acetylation in tumor samples from glioblastoma patients that were treated with this anti-epileptic drug at the time of their surgery. We did not observe any difference in the expression of acetylated histone H3 and H4 between tumor samples from patients that

were treated with valproic acid, and patients that experienced seizures and were not treated with any anticonvulsant at the time of their surgery. Although no serum drug levels were available for this retrospective analysis, these results suggest that dosages of valproic acid as currently used in clinical practice, are not sufficient to elicit HDAC inhibitory effects in the tumor of the patient. Prospective pharmacokinetic and functional studies should be performed to further explore this hypothesis, before additional *in vitro* studies on the mechanisms of VPA in glioma models are continued.

In a retrospective cohort study, we explored the prognostic relevance of valproic acid treatment in glioblastoma patients in **chapter 4**. In contrast to many previous papers, we did not find any difference in overall survival of glioblastoma patients who were treated with valproic acid at the time of surgery as compared to patients who did experience seizures, but were treated with other anti-epileptic drugs. These results are in line with the hypothesis we formed in **chapter 3**, that the valproic acid drug levels in the tumor are not sufficient to elicit sound anti-tumor effects. Consistent with our study, in a pooled analysis of multiple randomized controlled trials, no association between VPA use at baseline, progression free survival and overall survival in glioblastoma patients was observed [1]. Similarly, no survival benefit was observed from levetiracetam.

Although not evaluated in a randomized setting, the results of these studies advocate against addition of valproic acid to the current anti-tumor treatment regimens. Also, there seems no basis for treating of glioblastoma patients with prophylactic use of anti-epileptic drugs or selectively treating the glioblastoma patient with seizures with valproic acid.

In our study we did observe that the presence of epileptic seizures as a first symptom is a prognostic factor in glioblastoma and associates with prolonged survival. This association was independent of known other clinical prognostic factors, including tumor volume, suggesting that early diagnosis does not solely explain the prognostic effect. In order to further explore possible mechanisms that could explain the observed prognostic effect of epilepsy at diagnosis, we explored gene and protein expression patterns in tumor of patients with and without seizures at the time of diagnosis in **chapter 5**. We observed associations between epilepsy at diagnosis and decreased expression of gene sets involved in hypoxia/HIF-1 α , STAT5, CEBP- β and epithelial-mesenchymal transformation signaling. On a protein level, epileptogenic tumors were characterized by a significant downregulation of phospho-STAT5b, a target of HIF-1 α . HIF-1 α and STAT5b have prominent roles in oncologic signaling, proliferation and invasion in glioblastoma [2-6], but can also be linked to (tumor-related) epilepsy [7-9]. This presents a promising direction for further research in both oncogenic and epileptogenic signaling.

In this thesis, we proceed with the analysis of radiological characteristics of the glioblastomas and correlations with prognosis and tumor biology. In **chapter 6**, we showed in a large cohort study that SVZ-contacting glioblastomas associate with a worse prognosis compared to glioblastomas that do not contact the SVZ. This prognostic effect seems independent of other known clinical prognostic factors, and notably independent from tumor volume and the post-operative complication rate.

In a search to explore other factors that might contribute to this prognostic effect, underlying associations with tumor biology were explored. We observed increased expression of proteins involved in (epithelial-) mesenchymal transition in glioblastoma. Several key transcription factors (e.g. NF- κ B, CEBP- β and STAT proteins, including STAT3 and -5) have been identified as principal regulators of the mesenchymal gene expression signature in glioblastoma [10, 11]. High expression of these mesenchymal markers has been associated with worse survival of glioblastoma patients [11] as well as with resistance of the tumor to radiation [12] and chemotherapy [13]. Not only has constitutive activation of STAT3 been reported in glioblastoma cells, STAT3 also plays an important role in the tumor's microenvironment, contributing to evasion of immune responses [14, 15]. Surrounding brain tumors, reactive astrocytes expressing pSTAT3 were reported to gain self-renewal and pluripotent capacities (A. Iavarone, presented at the EANO Meeting 2019).

No differences in gene (set) expression, miRNA expression or molecular subtype distribution were observed in our cohort (n=71) nor in the larger validation cohort from the TCGA (n=223). These results were in line with a recent report in which a similar hypothesis was evaluated with the TCGA dataset [16]. In these studies, bulk tumor data were analyzed, not taking into account the known intratumoral heterogeneity in glioblastomas [17]. Based on our results and the knowledge from previous studies on the specific neural stem cell niche in the subventricular zone [18, 19], we questioned whether intratumoral gene expression patterns correlate with contact with the subventricular zone. In **chapter 7**, this is analyzed with multiple tumor samples from the same tumor. We observed increased expression of gene sets involved in (epithelial-) mesenchymal transition in glioblastoma tissues within the SVZ, as compared with tissue samples from outside of the SVZ, from the same tumors, and as compared to tumors that did not contact the SVZ.

Although our exploratory study is quite small, the results provide us with various insights. On a biological level, these distinct region-specific gene expression patterns might be influenced by the SVZ microenvironment. Our findings should be further evaluated and validated in larger cohorts. On a methodological level, these results strengthen the increasing evidence that advocates a different approach than bulk gene expression analyses: to evaluate multiple samples from the same tumor. Several studies have also shown the

advantage of single cell RNA sequencing in the analysis of intratumoral heterogeneity in glioblastoma [20]. Although gene expression data on multiple tumor samples from one tumor is more difficult and costly to obtain, it does provide more precise insights in intratumoral biological processes. In contrast, bulk gene expression analysis of only one sample per tumor might dilute or mask a true effect, seems very dependent on the exact intratumoral location, and might therefore require larger sample sizes. This might also be an explanation why no clear differences in gene (set) enrichment was seen between tumor with or without SVZ involvement in our study and in other reports [16].

The findings of region-specific, prognostically relevant, oncobiological processes in glioblastomas with SVZ contact may be used in the development of several potential therapeutic strategies. In several – relatively small – retrospective series, the effects of high dose irradiation of the SVZ region in glioblastoma patients have been explored and inconsistent associations with improved survival were reported [21-23]. With irradiation of the SVZ region, possible side-effects need to be considered. Irradiation of stem cell niches has been associated with increased neuro-cognitive deficits [24]. Targeted treatment of the glioma stem cell population is also an approach that is widely explored. In preclinical research many groups are currently searching for the most accurate markers for neural stem cells, to aid development of targeted treatments. Other approaches involve targeting of markers of mesenchymal transition, such as STAT3. Currently, one active phase I trial with a STAT3 inhibitor is registered (ClinicalTrials.gov Identifier: NCT01904123).

In **chapter 8**, we evaluate the complexity of the contrast enhancement pattern of glioblastomas on MRI by its fractal dimension and correlations with tumor biology and prognosis. Fractal dimensionality was found in the contrast-enhancement pattern of glioblastomas on MRI scans, and increases in the fractal dimension of contrast enhancement correlated with decreased oxidative pathway gene set expression (a shift to glycolytic metabolism) and increased VEGF expression. These biological changes might reflect an ischemic drive by tumors that outgrow their blood supply, or the “Warburg effect” (a shift from oxidative phosphorylation to glycolysis), which is seen in many tumors.

In our relatively small study, fractal dimensionality did not correlate with prognosis. Interestingly, others did find a correlation between fractional dimensionality of the MRI-based necrotic area in the glioblastoma and prognosis. In line with our results, gene ontology revealed increased expression of genes involved in, among others, angiogenesis and response to hypoxia in this study [25]. Although targeted inhibition of VEGF with bevacizumab did not result in prolonged survival in newly diagnosed glioblastoma patients or patients with recurrent tumors in randomized clinical trials [26, 27], preclinical evidence accumulates on multiple drugs that inhibit the Warburg effect in glioblastoma models [28-30]. Fractal dimensionality in glioblastoma might provide a non-surgical way to identify

patients that might benefit from such a targeted treatment. Other possible applications for MRI-based fractional dimensionality include distinction between glioblastoma and its mimics: primary central nervous system lymphoma [31] and brain metastases [32].

General methodological considerations

In this thesis, we analyzed correlations between clinical and radiological factors, prognosis and tumor biology with a consistent ‘triangular’ approach. In these studies, we combined exploratory ‘hypothesis-forming’ methods (such as gene set enrichment analyses (GSEA)) with other methods to support hypotheses (e.g. protein expression analyses). We show that clinical and radiological factors correlate with glioblastoma prognosis and distinct tumor biological features. This triangular approach has some potential advantages compared to more classical analyses. It might capture the interindividual clinical, biological and prognostic differences in glioblastomas better compared to more classical approaches in which correlations between either clinical factors and prognosis or biological factors and prognosis are explored. When analyses also take intratumoral heterogeneity into account (**Chapter 7**), these differences between tumors might be even more clearly captured. Eventually, this might provide solutions for the disappointing results in glioblastoma treatment development so far.

As mentioned above, some similar methodological approaches are applied in multiple chapters of this thesis. Certain considerations need to be taken into account with the interpretation of the results of these studies.

The clinical prognostic analyses in this thesis are based on a retrospective cohort, which has its possible limitations. Because of the retrospective nature of the study, missing data needs to be considered and addressed. In our studies, we could not apply the newest WHO classification system [33], because the IDH mutation screening was not yet performed in daily clinical practice, and was not available for a substantial part of the glioblastoma patients. We were able to perform a subset analysis, and found an IDH1 R132H mutation in only 21 (6.1%) of 343 glioblastoma patients. Based on these observations and the other baseline characteristics, we made the assumption that the study cohort and study results would be representative for patients with glioblastoma, IDH wildtype, according to the new classification system [33]. Future studies should however take the new classification system into account, and IDH-mutated glioblastomas should be excluded or analyzed separately, not only because of the evidence of a favorable clinical course [34, 35], but also because of the associations with epilepsy in lower grade gliomas [36, 37].

Furthermore, the retrospective nature of this the cohort studies did not allow for inclusion of some known prognostic factors in glioblastoma, such as MGMT methylation status, Mini Mental State Exam (MMSE) score and use of corticosteroids [38]. A next step in

this research would be to initiate a prospective prognostic study, in which all possible prognostic factors are prospectively collected, including epilepsy at presentation of the disease and tumor contact with the SVZ, with the aim to build a prognostic model for clinical use. Since accurate prognostic models for glioblastoma patients are still lacking [39, 40], such a model would be beneficial to guide individualized patient information and clinical decision making.

In several chapters in this thesis, gene (set) expression analyses are performed to unravel tumor biological features that potentially associate with the observed clinical (prognostic) effects. A few general considerations on these methods are in place, and are mostly already discussed in the separate chapters. Traditionally, differential expression analyses were performed between single genes. Although this can provide biological insight, this method does not inform the researcher on biological processes or pathways. Additionally, testing for groups of genes – in biological processes or pathways – poses a lower statistical multiple testing burden and can increase power to detect biologically relevant differences [41]. Several methods for gene set analyses have been developed so far, of which the gene set enrichment analysis (GSEA) method is among the most frequently used [42]. Knowledge on the statistical basis of the gene set analysis method is important to reduce the risk of drawing false-positive conclusions. There is a broad range of curated databases which can be used as a basis for gene set or pathway analyses. Consistent with the original paper by Subramanian [41], we performed GSEA with gene sets from the MSigDB database, which contains information from other large curated databases and is widely used. In comparison with other gene set analysis methods, GSEA showed relatively high power to detect small to moderate effect sizes [43]. As recommended in the study of Subramanian, phenotype permutation was applied which takes gene-gene interactions into account [41]. However, gene set enrichment analyses must be viewed as an exploratory approach to generate new hypotheses. Validation with other techniques is crucial, especially with low sample sizes. Indeed, in our studies, results from GSEA could not always be validated with qPCR or immunohistochemistry.

In our study cohort, we applied gene (set) expression analyses to RNA expression data obtained from one tumor sample per patient. During the past years, research groups are increasingly reporting on RNA expression analyses based on multiple tumor samples per patient, even at the level of single cells [20]. Although more costly and laborious, the clear advantage of this is that this approach takes intratumoral heterogeneity into account. Another consideration is the unavoidable mixture of different cell types in a bulk tumor sample used for RNA expression profiling. Single cell RNA sequencing allows the researcher to analyze the results classified by cell type.

Not only is the number of samples per tumor of relevance for the analysis, in **chapter 7** we also observe a correlation between gene expression signatures and the exact anatomical origin of the tumor samples, which might suggest that the tumors' microenvironment can also influence local gene expression. Therefore, more attention for the anatomical origin of the tumor samples used in expression analyses seems justified. The spatial transcriptomics method appears to be a promising technique for future analyses [44].

In our studies, we have made use of tissue microarrays to explore protein expression patterns in a large cohort of glioblastoma patients. Tissue microarrays are an appealing approach to perform high-throughput analysis of protein expression pattern in large cohorts. However, certain considerations should be taken into account when using this technique in glioblastoma research. We have previously noted the presence of intratumoral heterogeneity in glioblastomas, which is also an issue in analysis of protein expression patterns, especially because tissue microarrays generally contain only small (0.6 mm) samples of the tissue of interest.

In our studies, the selection of regions of interest to be included in the tissue microarrays were therefore selected by senior neuropathologists and we included tissue from at least three different regions from the tumor.

The immunohistochemical staining technique and interpretation of the staining require certain expertise and a trained eye. Manual scoring of the staining results is laborious and could prove subjective. However, a trained eye can identify the correct regions of tissue to score, and recognizes areas that should not be included (e.g. vascular proliferation, necrosis). Blinding to the study outcome is recommended and if feasible, scoring by independent reviewers to analyze interrater agreement. In recent years, several studies have reported on (semi-)automated scoring of immunohistochemical staining [45]. For certain antibodies that are used in experimental context, no clear references are available for the determination of cut-off scores, which is why a general descriptive approach was used in most of our analyses.

Recommendations based on this thesis

The work in this thesis allows me to present considerations for future research and recommendations for both the scientific field and the clinician.

Recommendations on future directions for the investigator:

- A prospective prognostic study will allow for the inclusion of all known possible prognostic factors, including epilepsy at diagnosis and tumor involvement of the SVZ. This approach can validate the observed prognostic effects of epilepsy at diagnosis and tumor involvement in the SVZ and potentially result in the development of

a prognostic model, which would be helpful to the clinical practice and aid with personalized patient information and clinical decision making.

- Integrated analysis of (a) clinicoradiological, (b) oncobiological and (c) prognostic aspects of a glioblastoma has the potential to offer insights beyond simple two-way correlations of such aspects.
- Further pharmacokinetic studies of valproic acid in glioblastoma patients and studies on the effective drug dose in glioblastoma tissue in the patient should be undertaken first, before further exploration of the underlying biological mechanisms of its antitumor effect (**Chapter 3**).
- In the search for underlying mechanisms of glioma-associated epilepsy, transcriptomic analyses of tumor samples from the infiltrating tumor boundaries might provide more insight. Also, the findings in **chapter 5** warrant further exploration of the hypoxia/HIF-1 α /STAT5 axis and SRF, which share associations with oncological signaling and (glioma-associated) epilepsy.
- Gene expression analyses of multiple tumor regions and their precise anatomical location should be considered more often in glioblastoma research. If feasible, single cell sequencing of multiple regions would be an ideal approach. As there is known intratumoral heterogeneity in glioblastoma, and the tumor's microenvironment possibly also influences regional gene expression, gene expression analyses from 'single samples' from unclear anatomical locations might dilute or bias relevant associations (**Chapter 7**).
- Glioblastomas that contact the SVZ are independently associated with worse survival and present increased expression of several targets involved in (epithelial-)mesenchymal transition (**Chapter 6**). This transcriptomic profile is specifically observed within the tumor region closed to the SVZ (**Chapter 7**). Antitumor therapies should therefore focus more on targeting (epithelial-)mesenchymal transition and/or the SVZ region.
- MRI-based fractal dimensionality might provide insight on the glioblastoma's metabolism (**Chapter 8**). Further validation of these observations is warranted. Eventually, this might prove a new non-surgical method to identify patients that might benefit from specific targeted treatment.

Recommendations for the clinician:

- Use of valproic acid, and levetiracetam, does not associate with overall survival in glioblastoma patients (**Chapter 4**), nor do we find evidence of histone deacetylase

inhibition by VPA in tumor samples of glioblastoma patients treated with the drug at time of their surgery (**Chapter 3**). These results of these studies advocate against addition of valproic acid to the current anti-tumor treatment regimens.

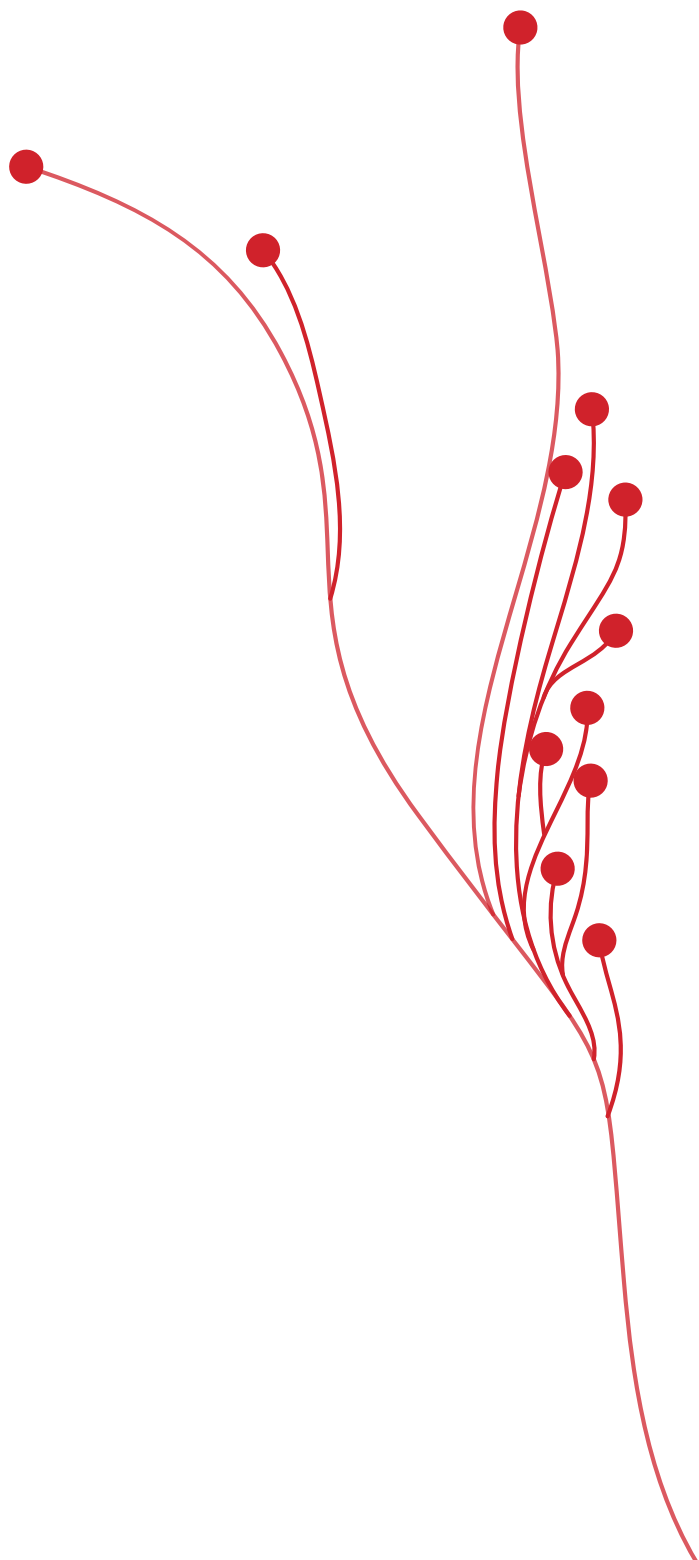
- Although SVZ contact and epilepsy at diagnosis are independent prognostic factors in glioblastoma patients (**Chapter 4 and 6**), these results are not yet suitable for usage in daily clinical practice yet. First, I would recommend validation in a prospective setting.

REFERENCES

1. Huppold, C., et al., Does Valproic Acid or Levetiracetam Improve Survival in Glioblastoma? A Pooled Analysis of Prospective Clinical Trials in Newly Diagnosed Glioblastoma. *J Clin Oncol*, 2016. 34(7): p. 731-9.
2. Joseph, J.V., et al., Hypoxia enhances migration and invasion in glioblastoma by promoting a mesenchymal shift mediated by the HIF1alpha-ZEB1 axis. *Cancer Lett*, 2015. 359(1): p. 107-16.
3. Talasila, K.M., et al., The angiogenic switch leads to a metabolic shift in human glioblastoma. *Neuro Oncol*, 2017. 19(3): p. 383-393.
4. Alkharusi, A., et al., Stimulation of prolactin receptor induces STAT-5 phosphorylation and cellular invasion in glioblastoma multiforme. *Oncotarget*, 2016. 7(48): p. 79572-79583.
5. Gressot, L.V., et al., Signal transducer and activator of transcription 5b drives malignant progression in a PDGFB-dependent proneural glioma model by suppressing apoptosis. *Int J Cancer*, 2015. 136(9): p. 2047-54.
6. Liang, Q.C., et al., Inhibition of transcription factor STAT5b suppresses proliferation, induces G1 cell cycle arrest and reduces tumor cell invasion in human glioblastoma multiforme cells. *Cancer letters*, 2009. 273(1): p. 164-171.
7. Valle-Casuso, J.C., et al., HIF-1 and c-Src mediate increased glucose uptake induced by endothelin-1 and connexin43 in astrocytes. *PLoS One*, 2012. 7(2): p. e32448.
8. Dong, H., et al., Complex role of connexin 43 in astrocytic tumors and possible promotion of glioma-associated epileptic discharge (Review). *Mol Med Rep*, 2017. 16(6): p. 7890-7900.
9. Linher-Melville, K., et al., Chronic Inhibition of STAT3/STAT5 in Treatment-Resistant Human Breast Cancer Cell Subtypes: Convergence on the ROS/SUMO Pathway and Its Effects on xCT Expression and System xc- Activity. *PLoS One*, 2016. 11(8): p. e0161202.
10. Carro, M.S., et al., The transcriptional network for mesenchymal transformation of brain tumours. *Nature*, 2010. 463(7279): p. 318-25.
11. Cooper, L.A., et al., The tumor microenvironment strongly impacts master transcriptional regulators and gene expression class of glioblastoma. *Am J Pathol*, 2012. 180(5): p. 2108-19.
12. Bhat, K.P., et al., Mesenchymal differentiation mediated by NF-kappaB promotes radiation resistance in glioblastoma. *Cancer cell*, 2013. 24(3): p. 331-346.
13. Bredel, M., et al., Tumor necrosis factor-alpha-induced protein 3 as a putative regulator of nuclear factor-kappaB-mediated resistance to O6-alkylating agents in human glioblastomas. *Journal of clinical oncology : official journal of the American Society of Clinical Oncology*, 2006. 24(2): p. 274-287.
14. See, A.P., et al., The role of STAT3 activation in modulating the immune microenvironment of GBM. *J Neurooncol*, 2012. 110(3): p. 359-68.
15. Wei, J., et al., Hypoxia potentiates glioma-mediated immunosuppression. *PLoS One*, 2011. 6(1): p. e16195.
16. Mistry, A.M., et al., Ventricular-Subventricular Zone Contact by Glioblastoma is Not Associated with Molecular Signatures in Bulk Tumor Data. *Sci Rep*, 2019. 9(1): p. 1842.
17. Sottoriva, A., et al., Intratumor heterogeneity in human glioblastoma reflects cancer evolutionary dynamics. *Proc Natl Acad Sci U S A*, 2013. 110(10): p. 4009-14.

18. Lee, J.H., et al., Human glioblastoma arises from subventricular zone cells with low-level driver mutations. *Nature*, 2018. 560(7717): p. 243-247.
19. Goffart, N., et al., Adult mouse subventricular zones stimulate glioblastoma stem cells specific invasion through CXCL12/CXCR4 signaling. *Neuro-oncology*, 2015. 17(1): p. 81-94.
20. Patel, A.P., et al., Single-cell RNA-seq highlights intratumoral heterogeneity in primary glioblastoma. *Science*, 2014. 344(6190): p. 1396-401.
21. Gupta, T., et al., Can irradiation of potential cancer stem-cell niche in the subventricular zone influence survival in patients with newly diagnosed glioblastoma? *J Neurooncol*, 2012. 109(1): p. 195-203.
22. Lee, P., et al., Evaluation of high ipsilateral subventricular zone radiation therapy dose in glioblastoma: a pooled analysis. *Int J Radiat Oncol Biol Phys*, 2013. 86(4): p. 609-15.
23. Elicin, O., et al., Relationship between survival and increased radiation dose to subventricular zone in glioblastoma is controversial. *J Neurooncol*, 2014. 118(2): p. 413-419.
24. Monje, M., Cranial radiation therapy and damage to hippocampal neurogenesis. *Dev Disabil Res Rev*, 2008. 14(3): p. 238-42.
25. Liu, S., et al., Relationship between necrotic patterns in glioblastoma and patient survival: fractal dimension and lacunarity analyses using magnetic resonance imaging. *Sci Rep*, 2017. 7(1): p. 8302.
26. Chinot, O.L., et al., Bevacizumab plus radiotherapy-temozolomide for newly diagnosed glioblastoma. *N Engl J Med*, 2014. 370(8): p. 709-22.
27. Wick, W., et al., Lomustine and Bevacizumab in Progressive Glioblastoma. *N Engl J Med*, 2017. 377(20): p. 1954-1963.
28. Xing, F., et al., The Anti-Warburg Effect Elicited by the cAMP-PGC1alpha Pathway Drives Differentiation of Glioblastoma Cells into Astrocytes. *Cell Rep*, 2017. 18(2): p. 468-481.
29. Lu, C.L., et al., Tumor cells switch to mitochondrial oxidative phosphorylation under radiation via mTOR-mediated hexokinase II inhibition--a Warburg-reversing effect. *PLoS One*, 2015. 10(3): p. e0121046.
30. Velpula, K.K., et al., Combined targeting of PDK1 and EGFR triggers regression of glioblastoma by reversing the Warburg effect. *Cancer Res*, 2013. 73(24): p. 7277-89.
31. Liu, S., et al., MR imaging based fractal analysis for differentiating primary CNS lymphoma and glioblastoma. *Eur Radiol*, 2019. 29(3): p. 1348-1354.
32. Petrujic, K., et al., Computational quantitative MR image features - a potential useful tool in differentiating glioblastoma from solitary brain metastasis. *Eur J Radiol*, 2019. 119: p. 108634.
33. Louis, D.N., et al., The 2016 World Health Organization Classification of Tumors of the Central Nervous System: a summary. *Acta Neuropathol*, 2016. 131(6): p. 803-20.
34. Noushmehr, H., et al., Identification of a CpG island methylator phenotype that defines a distinct subgroup of glioma. *Cancer Cell*, 2010. 17(5): p. 510-22.
35. Baysan, M., et al., G-cimp status prediction of glioblastoma samples using mRNA expression data. *PLoS One*, 2012. 7(11): p. e47839.
36. Neal, A., et al., IDH1 and IDH2 mutations in postoperative diffuse glioma-associated epilepsy. *Epilepsy Behav*, 2018. 78: p. 30-36.
37. Li, Y., et al., IDH1 mutation is associated with a higher preoperative seizure incidence in low-grade glioma: A systematic review and meta-analysis. *Seizure*, 2018. 55: p. 76-82.
38. Gorlia, T., et al., Nomograms for predicting survival of patients with newly diagnosed glioblastoma: prognostic factor analysis of EORTC and NCIC trial 26981-22981/CE.3. *Lancet Oncol*, 2008. 9(1): p. 29-38.

39. Woo, P., et al., A Comparative Analysis of the Usefulness of Survival Prediction Models for Patients with Glioblastoma in the Temozolomide Era: The Importance of Methylguanine Methyltransferase Promoter Methylation, Extent of Resection, and Subventricular Zone Location. *World Neurosurg*, 2018. 115: p. e375-e385.
40. Parks, C., et al., Can the prognosis of individual patients with glioblastoma be predicted using an online calculator? *Neuro Oncol*, 2013. 15(8): p. 1074-8.
41. Subramanian, A., et al., Gene set enrichment analysis: a knowledge-based approach for interpreting genome-wide expression profiles. *Proceedings of the National Academy of Sciences of the United States of America*, 2005. 102(43): p. 15545-15550.
42. Zyla, J., et al., Ranking metrics in gene set enrichment analysis: do they matter? *BMC Bioinformatics*, 2017. 18(1): p. 256.
43. Mathur, R., et al., Gene set analysis methods: a systematic comparison. *BioData Min*, 2018. 11: p. 8.
44. Stahl, P.L., et al., Visualization and analysis of gene expression in tissue sections by spatial transcriptomics. *Science*, 2016. 353(6294): p. 78-82.
45. Aeffer, F., et al., The Gold Standard Paradox in Digital Image Analysis: Manual Versus Automated Scoring as Ground Truth. *Arch Pathol Lab Med*, 2017. 141(9): p. 1267-1275.



APPENDICES

Nederlandse samenvatting

Curriculum vitae

List of publications

Dankwoord

NEDERLANDSE SAMENVATTING

Inleiding en rationale

Het glioblastoom is de meest voorkomende primaire maligne hersentumor. Ondanks uitgebreide behandelingen, is er nog geen genezing mogelijk en hebben patiënten een slechte prognose van ongeveer 12-16 maanden na de diagnose. Sommige patiënten overleven slechts enkele maanden en een minderheid overleeft tot enkele jaren. Ondanks onderzoek naar prognostische factoren, blijft het voor de arts lastig om de individuele prognose voor de patiënt te voorspellen. Het vooraf kunnen identificeren van glioblastoompatiënten met een relatief kortere of langere overleving zou erg nuttig zijn bij de klinische besluitvorming en patiëntgerichte informatieverstrekking. Daarnaast zouden prognostische factoren een associatie met onderliggende biologische eigenschappen van de tumor kunnen hebben, wat ons mogelijk kan helpen met het ontwikkelen van nieuwe behandelstrategieën. In dit proefschrift worden daarom verschillende klinische en radiologische factoren in glioblastoompatiënten onderzocht op hun prognostische waarde en associaties met tumorbiologische eigenschappen.

Glioblastomen, en andere diffuse gliomen (*World Health Organization (WHO)* graad II-IV), zijn progressieve tumoren die diffuus infiltreren in het omliggende hersenweefsel. In Nederland komt een glioblastoom voor bij 2.5 personen per 100,000 per jaar, met een mediane leeftijd van 61 jaar bij de diagnose. De huidige palliatieve standaardbehandeling voor glioblastoompatiënten, mits in voldoende klinische conditie, is chirurgie, gevolgd door een nabehandeling met radiotherapie en chemotherapie met adjuvante en concomitante temozolomide. Door het infiltrerende karakter van de tumor is een volledige resectie van alle tumorcellen onmogelijk. Daarnaast vertonen deze tumoren vaak een zekere mate van resistentie tegen anti-tumorbehandelingen. Ondanks veel wetenschappelijk onderzoek wereldwijd, blijven resultaten van studies naar nieuwe behandelmethoden teleurstellend.

Patiënten met een glioblastoom lijden zowel aan een oncologische als een neurologische ziekte. De tumor kan leiden tot specifieke neurologische klachten, vaak afhankelijk van de tumorlocatie, maar ook door verhoogde intracraniele druk. Veel patiënten krijgen te maken met neurologische uitvalsverschijnselen, cognitieve stoornissen en/of gedragsveranderingen. Daarnaast krijgt een deel van de glioblastoompatiënten te maken met epileptische aanvallen. In 30-40% van de patiënten is een epileptische aanval het eerste symptoom van de ziekte. Dit zorgt vaak voor een extra belasting op de kwaliteit van leven voor de patiënt. Het mechanisme achter tumor-geassocieerde epilepsie is nog niet geheel opgehelderd, maar uit de literatuur blijkt dat deze vorm van epilepsie vaker moeilijk te behandelen is en geassocieerd is met meer morbiditeit en mortaliteit. In enkele artikelen wordt gesuggereerd dat glioompatiënten met epileptische aanvallen een betere prognose hebben, echter wordt dit door anderen weer tegengesproken. Daarnaast is er

veel literatuur over een mogelijk anti-tumoreffect van het anti-epilepticum valproïnezuur en effecten daarvan op de overleving van glioblastoompatiënten.

Magnetic resonance imaging (MRI) heeft een belangrijke plaats in de diagnostiek en follow-up van het glioblastoom. Typische MRI kenmerken van een glioblastoom zijn het radiologisch grillige en heterogene aspect van de tumor, centrale necrose, contrastaankleuring als gevolg van de beschadigde bloedhersenenbarrière en omringend oedeem. Middels MRI kunnen verschillende aspecten van de tumor worden onderzocht, zoals de exacte locatie. Glioblastomen ontstaan voornamelijk in het supratentoriële gedeelte van de hersenen en kunnen in iedere hersenkwab voorkomen. Sommigen hebben een verband beschreven tussen glioblastomen en een locatie dicht bij de subventriculaire zone (SVZ) – een gebied aan de randen van de laterale ventrikels. Dit gebied is een specifieke niche voor neurale stamcellen en is steeds vaker de focus van glioblastoomonderzoek. Er is gesuggereerd dat glioblastomen kunnen ontstaan in deze regio, maar ook dat tumorcellen aangetrokken worden door deze omgeving en dat deze bijdraagt aan resistentie tegen anti-tumorbehandelingen. Daarnaast zijn er verschillende studies die een verband aantonen tussen glioblastomen die contact maken met de SVZ en een slechtere prognose.

In de afgelopen jaren is er veel vooruitgang geboekt op het gebied van moleculaire veranderingen in glioblastomen. Dit heeft onder andere geleid tot een herziening van het wereldwijde histologische classificatiesysteem voor diffuse gliomen, waarin nu ook genetische veranderingen in de tumor worden geïntegreerd. Voor de diagnostiek van glioblastomen is momenteel de belangrijkste bepaling de mutatiestatus van *isocitrate dehydrogenase 1 of 2* (IDH1 of IDH2). Aanwezigheid van een mutatie in dit gen is geassocieerd met een gunstigere prognose en komt bij een minderheid van de glioblastomen voor. Afwezigheid van een mutatie (IDH wildtype) is een typisch kenmerk van glioblastomen is zelfs bij gliomen met histologisch laaggradige kenmerken geassocieerd met een agressief beloop dat vergelijkbaar is met een glioblastoom (Hoofdstuk 1, figuur 2).

Uitgebreide analyses van DNA profielen, epigenetische veranderingen, gen- en eiwitexpressiepatronen in glioblastoomweefsels hebben geleid tot veel inzichten in de moleculaire kenmerken van deze tumoren. Door vele genetische en epigenetische veranderingen worden veel verschillende signaalcascades en biologische processen in glioblastomen verstoord. Voorbeelden van processen die frequent op verschillende niveaus verstoord zijn in glioblastomen zijn de EGFR, Rb, p53 en PI3K signaalcascades. Het blijkt ook dat er veel sprake is van intertumorale, maar ook intratumorale, heterogeniteit. Zowel tussen glioblastomen van verschillende patiënten als binnen dezelfde tumor zijn de moleculaire kenmerken van de tumorcellen zeer verschillend. Dit bemoeilijkt de ontwikkeling van gerichte therapieën. Eerdere studies hebben verschillende classificaties

van glioblastomen gemaakt op basis van genexpressie- of methyleringsprofielen. Sommige van deze subklassen zijn geassocieerd met een betere prognose.

Inmiddels zijn verschillende prognostische factoren bekend in glioblastoompatiënten, zoals mate van tumorresectie, nabehandeling met een combinatie van radiotherapie en adjuvante en concomitante temozolomide, leeftijd, klinische conditie (*WHO performance status* of Karnofsky performance score (KPS)), gebruik van corticosteroiden, MMSE score, tumorlocatie (unilobair of centraal/multilobair) en MGMT promotor hypermethylatie, IDH mutatie, geslacht en preoperatieve neurologische uitval. Prognostische modellen die op basis van deze factoren zijn ontwikkeld blijken echter nog niet accuraat genoeg voor gebruik in de klinische praktijk.

Dit proefschrift

In dit proefschrift onderzoek ik de associaties tussen klinische en radiologische factoren, prognose en tumorbiologie in glioblastomen. Deze aanpak kan bijdragen aan verdere kennis van de tumorbiologie in glioblastomen en aan ontwikkeling van nieuwe behandelstrategieën.

Initieel ligt de focus op de prognostische waarde van epilepsie en anti-epileptica in glioblastoompatiënten. In **hoofdstuk 2** wordt de tot dan toe bekende literatuur over de preklinische en klinische effecten van het anti-epilepticum valproïnezuur als anti-tumorbehandeling bij glioblastoompatiënten beschreven. Valproïnezuur is een bekende remmer van histondeacetylase (HDAC), wat tot directe en epigenetische veranderingen in genexpressie kan leiden. Verschillende effecten van valproïnezuur op biologische processen lijken bij te dragen aan remming van proliferatie van glioblastoomcellen, invasie en angiogenese *in vitro*. Verschillende case reports en retrospectieve patiëntenseries suggereren een gunstig effect van valproïnezuur op de overleving bij glioblastoompatiënten.

Vervolgens tonen wij in laboratoriumexperimenten in **hoofdstuk 3** aan dat HDAC remmer valproïnezuur, inderdaad zorgt voor toename van expressie van geacetyleerde histonen. Echter, in tumorweefsels van glioblastoompatiënten die ten tijde van de operatie met valproïnezuur werden behandeld, vonden wij deze effecten niet terug. Mogelijk is de huidige klinische dosering niet voldoende om deze effecten in het glioblastoomweefsel te bereiken.

In **hoofdstuk 4** analyseren wij de prognostische waarde van epileptische aanvallen – als eerste symptoom van de ziekte – en behandeling met anti-epileptica in glioblastoompatiënten. We tonen aan dat een epileptische aanval als eerste symptoom van de ziekte een gunstige prognostische factor is, en dat dit effect onafhankelijk is van andere klinische prognostische factoren, inclusief tumorvolume. Deze bevindingen suggereren dat een snellere diagnose bij patiënten met epileptische aanvallen niet volledig verklarend is voor het geobserveerde

prognostische effect. Binnen de groep met patiënten met epileptische aanvallen, zien wij tevens geen prognostisch effect van behandeling met valproïnezuur of levetiracetam.

In een poging om het prognostische effect van epilepsie bij diagnose in glioblastoompatiënten beter te begrijpen, exploreren we in **hoofdstuk 5** correlaties tussen epileptische aanvallen en tumorbiologie. We analyseren gen- en eiwitexpressieprofielen van glioblastoomweefsels van patiënten met en zonder epileptische aanvallen bij diagnose. Epileptische aanvallen blijken geassocieerd met verminderde expressie van sets van genen betrokken bij signalering door hypoxie/HIF-1 α , STAT5, CEBP- β en epitheliale naar mesenchymale transformatie. Op eiwitniveau vinden we ook verminderde expressie van gefosforyleerd STAT5b, wat ook een onderdeel van de HIF-1 α signaalcascade is. Zowel HIF-1 α als STAT5 hebben een prominente rol in tumorbiologische processen, zoals tumorcelproliferatie en invasie in glioblastomen, daarnaast worden deze factoren gelinkt aan (tumor-geassocieerde) epilepsie.

Vanaf **hoofdstuk 6** verleggen we de focus naar correlaties van radiologische factoren met tumorbiologie en prognose. In **hoofdstuk 6** tonen we in een groot retrospectief cohort aan dat glioblastomen die contact maken met de subventriculaire zone (SVZ) geassocieerd zijn met een slechtere prognose. Dit effect is onafhankelijk van andere klinische prognostische factoren, in het bijzonder van tumorvolume en postoperatieve complicaties. We analyseren gen- en eiwitexpressieprofielen van tumorweefsels en tonen aan dat glioblastomen die contact maken met de SVZ toegenomen expressie hebben van eiwitten die betrokken zijn bij (epitheliale naar) mesenchymale transformatie (CEBP- β and fosfo-STAT3). Hogere expressie van deze mesenchymale markers is geassocieerd met een slechtere prognose in glioblastoompatiënten en toegenomen weerstand van de tumor tegen behandelingen.

In deze studie werd genexpressiedata van een stukje van de tumor geanalyseerd. Hierdoor kon echter geen rekening worden gehouden met de bekende heterogeniteit binnen de tumor. Daarnaast is er literatuur waaruit blijkt dat de specifieke omgeving van de SVZ effecten kan hebben op genexpressie in de tumorcellen. In **hoofdstuk 7** analyseren we verschillende regio's binnen dezelfde tumor, om uit te zoeken of de SVZ regio geassocieerd is met specifieke genexpressieprofielen. We vinden dat sets met genen die betrokken zijn bij (epitheliaal naar) mesenchymale transformatie verhoogd tot expressie komen in de tumorweefsels uit de SVZ regio, vergeleken met tumorweefsels – van dezelfde tumor – buiten deze regio. We vinden vergelijkbare resultaten als we de tumorweefsels uit de SVZ regio vergelijken met tumorweefsels van tumoren die geen contact maken met de SVZ. Deze resultaten suggereren dat de omgeving van de SVZ specifieke effecten heeft op de regionale genexpressie in glioblastomen.

In **hoofdstuk 8** analyseren we een ander radiologisch kenmerk van glioblastomen – de fractionele dimensionaliteit – wat een maat is voor de complexiteit van een vorm.

Complexe vormen zoals ijskristallen of broccoli hebben bijvoorbeeld een hoge fractionele dimensionaliteit. In onze studie blijkt dat het contrastaankleuringspatroon van glioblastomen op MRI scans ook deze eigenschap heeft. In deze tumoren blijkt een relatief hogere fractionele dimensionaliteit geassocieerd met specifieke gen- en eiwitexpressiepatronen, met afgenomen expressie van genen betrokken bij oxidatieve fosforylatie en toegenomen expressie van het eiwit VEGF. Op basis van deze resultaten zou fractionele dimensionaliteit een marker kunnen zijn voor onvoldoende bloedtoevoer door de groeiende tumor, ofwel van het ‘Warburg’ effect, een verschuiving van oxidatieve fosforylatie naar glycolyse, een fenomeen dat bij veel verschillende tumoren wordt gezien.

Aanbevelingen

Het onderzoek in dit proefschrift draagt bij aan kennis van (1) tumorbiologie in glioblastomen, wat hopelijk van nut is bij het ontwikkelen van nieuwe behandelstrategieën, (2) prognostische factoren in glioblastoompatiënten, wat patiënten en artsen kan helpen in de klinische besluitvorming en geïndividualiseerde voorlichting van patiënten, (3) mechanismen van tumor-geassocieerde epilepsie en behandeling met anti-epileptica, waardoor een betere besluitvorming mogelijk is over de behandeling van glioblastoompatiënten met epileptische aanvallen.

Op basis van het onderzoek in dit proefschrift doe ik een aantal aanbevelingen voor toekomstig onderzoek en voor de klinische praktijk.

Aanbevelingen voor toekomstig onderzoek:

- Middels een prospectief prognostisch onderzoek zullen alle bekende prognostische factoren kunnen worden geëvalueerd, inclusief epilepsie bij diagnose en contact van de tumor met de SVZ. Hierdoor kunnen deze bevindingen worden gevalideerd en zal er een nieuw prognostisch model kunnen worden ontwikkeld voor gebruik in de klinische praktijk.
- Geïntegreerde analyses van (a) klinische en radiologische factoren, (b) tumorbiologie en (c) prognose kunnen potentieel tot meer inzichten leiden dan klassiekere benaderingen.
- Er dienen eerst verdere farmacokinetische studies naar valproïnezuur in glioblastoompatiënten te worden gedaan alvorens er verder onderzoek naar potentiële anti-tumoreffecten van dit middel wordt gedaan (**hoofdstuk 3**).
- Voor het verder analyseren van tumor-geassocieerde epilepsie zouden gen- en eiwitexpressieanalyses van de infiltrerende tumorrand een vervolgstap kunnen zijn. Daarnaast zijn de associaties met hypoxia/HIF-1 α /STAT5 en SRF (**hoofdstuk 5**) ook een interessante richting voor verder onderzoek.

- Bij genexpressieanalyses van glioblastoomweefsel moet meer aandacht zijn voor meerdere tumorsamples van dezelfde tumor en de exacte anatomische locatie van deze weefsels, gezien de bekende intratumorale heterogeniteit en mogelijke invloed van de omgeving op regionale genexpressie (**hoofdstuk 7**).
- SVZ contact is een onafhankelijke ongunstige prognostische factor in glioblastomen. Deze tumoren zijn geassocieerd met toegenomen expressie van genen en eiwitten betrokken bij (epitheliale naar) mesenchymale transformatie en tevens lijkt de SVZ omgeving ook mogelijk een invloed te hebben op deze regionale genexpressie (**hoofdstuk 6 en 7**). Nieuwe therapeutische mogelijkheden gericht op remming van de (epitheliale naar) mesenchymale transformatie of op de SVZ omgeving zouden moeten worden geëxploreerd.
- Fractionele dimensionaliteit van het contrastaankleuringspatroon van glioblastomen op MRI verschaft inzicht in het metabolisme van de tumor (**hoofdstuk 8**). Deze bevindingen moeten worden gevalideerd en zouden uiteindelijk kunnen bijdragen aan identificatie van patiënten die baat bij gericht behandelingen kunnen hebben.

Aanbevelingen voor de klinische praktijk:

- Het gebruik van valproïnezuur, en levetiracetam, is niet geassocieerd met een betere overleving bij glioblastoompatiënten (**hoofdstuk 4**). Daarnaast vinden wij geen bewijs voor effecten van HDAC remming door valproïnezuur in tumorweefsels van glioblastoompatiënten die hiermee werden behandeld (**hoofdstuk 3**). Op basis van deze studies is er derhalve geen basis voor het toevoegen van valproïnezuur aan huidige antitumorbehandelingen voor glioblastomen.
- Hoewel SVZ contact en epilepsie bij diagnose onafhankelijke prognostische factoren in glioblastoompatiënten zijn in onze studies, zullen deze bevindingen eerst moeten worden gevalideerd in een prospectieve setting, alvorens deze bevinding toe te passen in de klinische praktijk.

CURRICULUM VITAE

Sharon Berendsen is geboren op 22 maart 1988 in Rheden. Na afronding van haar gymnasiumopleiding aan het Olympus College te Arnhem, begon zij in 2006 aan de studie Scheikunde aan de Radboud Universiteit in Nijmegen. Nadat zij het Honours Programma en de Bachelor of Science in Nijmegen behaalde, vervolgde zij haar studie in Utrecht met het Selective Utrecht Medical Master (SUMMA) programma. In de loop van haar opleidingen ontwikkelde zij een interesse in de neurowetenschappen en neuro-



oncologie, wat leidde tot verschillende wetenschappelijke stages in het laboratorium van prof. dr. Pierre Robe. Na het behalen van haar artsendiploma in 2013 bleef zij betrokken bij de onderzoeksgroep van prof. dr. Robe en begon ze met haar promotieonderzoek in de neuro-oncologie, onder supervisie van prof. dr. P. Robe en dr. T.J. Snijders. Tijdens deze periode behaalde zij ook haar masterdiploma Clinical Epidemiology aan de Universiteit Utrecht. Verschillende projecten van haar onderzoek heeft zij in de afgelopen jaren mogen presenteren op nationale en internationale congressen. In 2018 is haar onderzoek beloond met de stimuleringsprijs van Stichting Stophersentumoren.nl.

In 2017 is zij begonnen met het specialisatietraject tot neuroloog in het UMC Utrecht, onder supervisie van prof. dr. J. Wokke, dr. T Seute en prof. dr. G.J. Biessels.

LIST OF PUBLICATIONS

Berendsen S., van Bodegraven E., Seute T., Spliet W.G.M., Geurts M., Hendrikse J., Schoysman L., Huiszoon W.B., Varkila M., Rouss S., Bell E.H., Kroonen J., Chakravarti A., Bours V., Snijders T.J., Robe P.A. Adverse prognosis of glioblastoma contacting the subventricular zone: biological correlates. *PLoS One*. 2019 Oct 11;14(10):e0222717.

Berendsen S., Frijlink E., Kroonen J., Spliet W.G.M., Hecke W., Seute T., Snijders T.J., Robe P.A. Effects of valproic acid on HDAC inhibition in vitro and in glioblastoma patient samples. *Neuro-Oncology Advances*, Volume 1, Issue 1, May-December 2019, vdz025.

Maas S.L.N., Draaisma K., Snijders T.J., Senders J.T., **Berendsen S.**, Seute T., Schiffelers R.M., van Solinge W.W., Ten Berg M.J., Robe P.A., Broekman M.L.D. Routine Blood Tests Do Not Predict Survival in Patients with Glioblastoma-Multivariable Analysis of 497 Patients. *World Neurosurgery*. 2019 Jun;126:e1081-e1091.

Berendsen S., Spliet W.G.M., Geurts M., Van Hecke W., Seute T., Snijders T.J., Bours V., Bell E.H., Chakravarti A., Robe P.A., Epilepsy Associates with Decreased HIF-1 α /STAT5b Signaling in Glioblastoma. *Cancers (Basel)*. 2019 Jan 4;11(1).

Dubois N., **Berendsen S.**, Henry A., Nguyen M., Bours V., Robe P.A., I-Kappa-B Kinase-epsilon Activates Nuclear Factor-kappa B and STAT5B and Supports Glioblastoma Growth but Amlexanox Shows Little Therapeutic Potential in These Tumors, *Cancer Translational Medicine* 2018;4(1):1–8.

Miller K.J., **Berendsen S.**, Seute T., Yeom K., Gephardt M.H., Grant G.A., Robe P.A., Fractal structure in the volumetric contrast enhancement of malignant gliomas as a marker of oxidative metabolic pathway gene expression, *Translational Cancer Research* 2017;6(6):1275-1282

Snijders T.J., **Berendsen S.**, Seute T., Robe P.A., Glioma-associated epilepsy: toward mechanism-based treatment. *Translational Cancer Research* 2017;6(Suppl 2):S337-S341

Berendsen S., Snijders TJ, Robe PA. Response to: “Prognostic relevance of epilepsy at presentation in lower-grade gliomas”. *Neuro Oncology*. 2016 Sep;18(9):1327-8.

Goffart N, Lombard A, Lallemand F, Kroonen J, Nassen J, Di Valentin E, **Berendsen S.**, Dedobbeleer M, Willems E, Robe P, Bours V, Martin D, Martinive P, Maquet P, Rogister B, CXCL12 mediates glioblastoma resistance to radiotherapy in the subventricular zone. *Neuro Oncology*. 2016 Jul 1.

Berendsen S, Varkila M, Kroonen J, Seute T, Snijders TJ, Kauw F, Spliet WG, Willems M, Poulet C, Broekman ML, Bours V, Robe PA, Prognostic relevance of epilepsy at presentation in glioblastoma patients. *Neuro Oncology*. 2016 May;18(5):700-6.

Berendsen S, Broekman M, Seute T, Snijders TJ, van Es C, de Vos F, Regli L, Robe P, Valproic acid for the treatment of malignant gliomas: review of the preclinical rationale and published clinical results, *Expert Opinion on Investigational Drugs*. 2012 Sep;21(9):1391-415.

DANKWOORD

Onderzoek doe je niet alleen. Ik heb dan ook veel mensen te bedanken die aan de totstandkoming van dit proefschrift hebben bijgedragen, en die ervoor hebben gezorgd dat ik met veel plezier kan terugkijken op mijn promotieperiode.

Ten eerste bedank ik alle patiënten, die ondanks de ernstige diagnose, toestemming hebben gegeven voor het gebruik van weefselmateriaal voor wetenschappelijk onderzoek. Zoals in de afgelopen jaren is gebleken, is het onderzoek naar tumorweefselkenmerken van individuele patiënten in glioblastomen van onschatbare waarde.

Beste prof. dr. Robe, beste **Pierre**, onze onderzoeksband begon al jaren voor mijn promotieonderzoek. Toen ik als masterstudent het plan had opgevat om onderzoek te gaan doen op het gebied van de neuro-oncologie en bij jou aanklopte, was ik zeer benieuwd wie ik aan de andere kant van de tafel zou treffen. Het bleek een bevlogen en altijd enthousiaste neurochirurg, die van alle markten thuis is. Ik sta nog steeds versteld van je uitgebreide kennis van alle facetten van het onderzoek. Er kwam geen techniek voorbij of jij wist er de details van, waarbij je me altijd nuttige tips kon geven om mijn experiment weer aan de praat te krijgen. Hoewel het voor mij, vooral in het begin, soms moeilijk was om de rode draad tussen je (vele) ideeën te blijven zien, werd het mij gaandeweg duidelijk dat jij deze richting van het onderzoek al vanaf het begin had voorzien.

Ik waardeer de altijd gezellige en open sfeer tijdens onze besprekingen enorm. Niet alleen dacht je mee over mijn onderzoeksprojecten, maar ook over de planning van mijn carrière. Ik ben je erg dankbaar voor alle bijzondere kansen die je me tijdens mijn promotieonderzoek hebt gegeven. Van onze besprekingen kwam ik altijd vol enthousiasme terug met nieuwe ideeën. Dat ik in ruil daarvoor heel wat uurtjes op het blauwe bankje in de stafgang heb vertoefd, wachtend op onze afspraak, neem ik graag voor lief. In de loop van de jaren heb je een mooi onderzoeksteam in Utrecht weten op te bouwen en ik hoop dat we in de komende jaren nog regelmatig samen kunnen werken aan toekomstige projecten.

Beste dr. Snijders, beste **Tom**, toen het onderwerp van mijn promotieonderzoek uit enthousiasme iets teveel begon uit te dijen (waarbij ik mijn toekomstige proefschrift al ‘random things in glioblastoma’ had genoemd), leek het mij een goed idee om wat meer focus aan te brengen. Het was voor mij een gouden greep om jou bij mijn onderzoek te betrekken als copromotor, niet in de laatste plaats vanwege de altijd goede sfeer en je scherpe woordgrappen. Je kan het onderzoek ontzettend goed overzien en logische vervolgstappen kristalhelder overbrengen, zelfs als het onderwerp niet je dagelijkse praktijk betreft. Jouw manier van meedenken over methodologische vraagstukken en klinische relevantie waren voor mij van grote meerwaarde. Daarnaast verlies je de algemene

ontwikkeling van je promovendi niet uit het oog ('minder passieve zinsconstructies', 'niet alles hoeft in een heatmap') en neem je ze daartoe zelfs mee op gevarieerde excursies (van Jazz cafés in New Orleans tot De Jeugd van Tegenwoordig in de Tivoli). We zijn nog steeds bezig met gezamenlijke onderzoeksprojecten en ik hoop dat we dit in de komende jaren verder kunnen uitbreiden.

Ik bedank de leden van de leescommissie, **prof. dr. E.M. Hol**, **prof. dr. A.M. May**, **prof. dr. M.J. van den Bent**, **prof. dr. T. Würdinger**, en **dr. F.S.S. Leijten**, voor de interesse in mijn proefschrift en de bereidheid om aan de leescommissie deel te nemen. Ook wil ik de leden van de oppositie hartelijk bedanken.

Jérôme, as a postdoc in the Robe lab, you've been no stranger to the trains between Liège and Utrecht. Even though you lived in Belgium, you were often the first to arrive in the lab in Utrecht. In the first year of my PhD project, you thought me every technique I needed to know, with endless kindness and patience. Thanks for everything! Now the project is officially 'almost finished.'

Rosalie, zo'n 1.5 jaar lang deelden wij een kantoor samen. Hoewel de focus in ons onderzoek op verschillende dingen lag, deelden we het lief en leed wat voorkomt in het leven van iedere promovendus. Met jouw sprankelende persoonlijkheid leidde dit vooral tot veel hilariteit onderling en mooie belevenissen, zoals het bezoek aan de congressen in Philadelphia en San Antonio. Ook minder leuke momenten en teleurstellingen konden we goed delen, en meestal lukte het dan weer te relativeren door het luisteren van 'Bewuste sabotage' van De Jeugd van Tegenwoordig. Bedankt voor de ontzettend leuke tijd en ik ben heel blij dat je helemaal op je plek bent bij de geriatrie!

Mijn verschillende kamergenoten en labgenoten door de jaren heen, **Wilma**, **Ajit**, **Jeroen**, **Niek**, **Nicolas** en **Dimphna**, dank voor jullie hulp en gezelligheid! **Marieke**, bedankt voor je altijd enthousiaste adviezen en hulp! **Elselien**, wat knap dat je juist in het neuro-oncologie onderzoek bent gestart. Dank je dat je alle projecten met veel enthousiasme oppakte, waardoor we het project in hoofdstuk 3 konden afronden. Dit alles zonder onze dagelijkse lunchmomentjes te missen, waarbij we met steeds extravagantere broodjes en beleg aankwamen. Heel veel succes met je eigen promotietraject bij het NKI! **Kaspar**, dank voor het delen van jouw kennis van RNA sequencing in hoofdstuk 7! Succes met het afronden van jouw promotieonderzoek. **Marjolein**, dank voor je mooie bijdrage aan dit proefschrift met de miRNA data. Heel veel succes in Rotterdam!

Emma, als verse promovendus kwam jij op het kantoor in het Stratenum terecht. Hoewel in het begin duizelingwekkende termen als *gene set enrichment analyse* en *heatmaps* je om de oren vlogen, heb je dit alles in sneltreinvaart opgepikt en geleerd. Niemand had kunnen

vermoeden dat je binnen korte tijd zelfs met plezier over je eigen R script zou vertellen. Je zegt altijd dat je hiervan veel van mij hebt geleerd, maar ik heb minstens zo veel van jou geleerd. De geheel eigen stijl waarmee jij met efficiëntie en precisie je projecten aanpakt, en zo je begeleiders in toom houdt, is indrukwekkend. Daarnaast heb je me alles geleerd wat ik moest weten, toen ik na 3 jaar onderzoek weer als arts op de afdeling aan de slag ging. Dank je voor de ontzettend leuke tijd en de mooie vriendschap die we hierdoor hebben opgebouwd! Ik ben heel blij dat je mijn paranymf wil zijn, en hoop dat we in de toekomst nog vele vette chardonnay samen zullen drinken, met of zonder laptop op het terras.

Onderzoekers in het Hol lab, en medeleden van de superawesomejournalclub, **Sophietje, Marjolein, Emma, Bart, Paul, Katherine**, dank voor alle gezelligheid, kritische vragen en voor jullie hulp!

Some research in this thesis is a result of valuable collaborations with colleagues from international laboratories. I wish to thank my colleagues from the department of Human Genetics from the University Hospital in Liège (BE). **Prof. dr. V. Bours**, thank you for supporting my research projects. **Catherine, Marie, Maria**, thank you for all your help with my experiments! **Laurent**, thank you for your valuable contribution to chapter 6. **Christophe**, thank you for your contribution to the classification of tumor samples. **Prof. dr. A. Chakravarti** and **dr. E.H. Bell** from the department of Radiation Oncology from The Ohio State University (USA), thank you for contributing your valuable work on miRNA's to my projects. **Dr. Kai Miller**, from the department of Neurosurgery from the Stanford University, thank you for introducing me to the intriguing concept of fractional dimensionality.

Naast mijn promotieonderzoek ben ik ook gestart met de specialisatie tot neuroloog. Ik wil **prof. dr. J. Wokke, dr. T. Seute** en **prof. dr. G.J. Biessels** graag bedanken voor de mogelijkheid om mijn onderzoek te combineren met deze klinische werkzaamheden. Dr. Seute, **Tatjana**, door mijn onderzoek kenden wij elkaar al lang voordat je de rol van opleider op je nam. Indrukwekkend hoe jij in de afgelopen jaren zo'n goed klinisch neuro-oncologieteam hebt weten samen te brengen! De term 'kwartje' waardig! Bedankt voor al je steun en interesse in mijn onderzoek. Alle collega's van de neurologie in het UMC Utrecht, en in het bijzonder de arts-assistenten, bedankt voor de goede sfeer, zowel op de werkvloer als bij alle borrels!

Alle collega's van het klinische neuro-oncologieteam, dank voor jullie niet aflatende interesse in mijn onderzoek en voor alle gezellige sociale programma's op congressen! **Wim Spliet en Wim van Hecke**, dank voor jullie eindeloze inzet voor de TMA's en de immuunhistochemische kleuringen, zonder wanhopig te worden (of dit te laten blijken).

In de loop van de jaren heb ik meerdere studenten mogen begeleiden. **Anne-Cécile**, **Josje**, **Meri** en **Nienke**, dank voor jullie inzet! Jullie hebben allen een bijdrage geleverd aan dit proefschrift en/of aan de kennis binnen onze onderzoeksgroep, en daarnaast heb ik ook veel van jullie geleerd. **Hema** en **Eva**, dank voor de prettige samenwerking tot nu toe en voor jullie eindeloze geduld om immunohistochemische kleuringen te beoordelen. Ik hoop dat onze projecten tot mooie resultaten zullen leiden! **Diana**, knap hoe jij in korte tijd zo'n ingewikkeld project hebt opgepakt en uitgevoerd! Dank voor je grote bijdrage aan hoofdstuk 7.

Albi en **Marja**, bedankt voor al jullie inspanningen om mijn onderzoeksbesprekingen in de drukke agenda van prof. Robe te plannen. **Marja**, bedankt voor het regelen van alle administratieve details rondom mijn promotie.

Annemieke, sinds de peuterspeelzaal hebben wij altijd aan elkaars zijde gestaan. We hebben uiteindelijk heel verschillende richtingen gekozen en hierom was het juist verfrissend om alle onderzoeksprikelen met je te bespreken. Nuchter als je bent, had je altijd goede adviezen. Bij hoogtepunten werd er traditiegetrouw een ijsje gegeten. Maar het allerbelangrijkst zijn natuurlijk alle mooie en gezellige momenten die we samen hebben beleefd in de afgelopen jaren en die ongetwijfeld nog gaan volgen! Voor mij was het vanzelfsprekend dat jij op 14 januari ook aan mijn zijde zou staan en ik ben heel blij dat je mijn paranimf wilt zijn!

Lieve **vrienden en (schoon)familie**, gedurende mijn hele promotieonderzoek zijn jullie altijd oprecht geïnteresseerd geweest in alle vorderingen van mijn onderzoek. Veel dank daarvoor! Nog dankbaarder ben ik voor alle gezamenlijke mooie en leuke momenten, waarop ik me even met iets anders kon bezig houden dan met het onderzoek!

Debbie en **Ronald**, jullie trots en enthousiasme over mijn onderzoek is hartverwarmend! Jullie zijn toppers!

Papa, het enthousiasme voor studeren en onderzoek heb ik niet van een vreemde. Al vanaf jonge leeftijd herinner ik me je enthousiaste verhalen over allerlei wetenschappelijke onderwerpen. Nog nooit heb ik iemand hier zo gepassioneerd over horen vertellen. Het is niet vreemd dat ik ook onderzoek ben gaan doen. **Mama**, samen met papa volgde jij al mijn stappen in studie en onderzoek op de voet. Jullie trots was altijd voelbaar. Daarnaast hield je ook goed in de gaten of ik ook genoeg leuke dingen naast het werk deed! Ik heb alles aan jullie te danken.

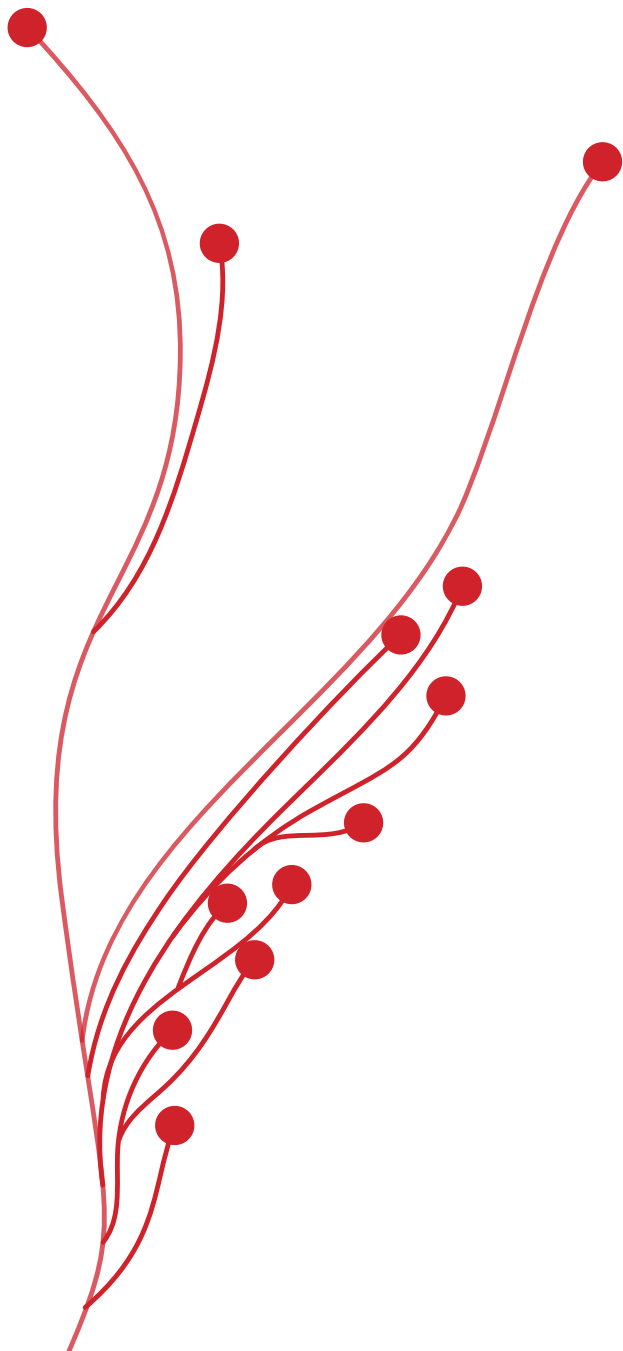
Lieve **Lennart**, tien jaar geleden zaten we samen in de trein naar Utrecht. Ik vertelde je over een afspraak die ik die dag had met een neurochirurg met wie ik misschien een onderzoeksproject zou gaan doen. Sindsdien heb jij dit hele onderzoeksavontuur

Dankwoord

aan mijn zijde gestaan. Je bent de beste supporter die ik me kan wensen. Jij was er bij alle hoogtepunten, bij alle interessante resultaten, geaccepteerde artikelen en mooie congresbezoeken. Je was ook er bij alle minder leuke momenten, bij alle mislukte experimenten, afwijzingen van tijdschriften, en deadlines waar tot diep in de nacht aan doorgewerkt moest worden. Met jouw humor en steun kon ik alles altijd weer snel relativiseren en kan ik alles aan. Buiten het werk om hebben we in de afgelopen tien jaar nog ontelbaar veel andere prachtige momenten samen meegemaakt. Zoals we altijd samen van avontuur in avontuur springen, van fantastische reizen tot het verbouwen van een huis (zonder enige kluservaring), kijk ik enorm uit naar ons grootste avontuur tot nu toe!

Liefs,

Sharon



UMC Utrecht



Universiteit Utrecht

ISBN 978-94-028-1854-3